SINGLE-CHANNEL PROPERTIES AND REGULATION OF CHLORIDE INTRACELLULAR CHANNEL PROTEINS

HARPREET SINGH

THESIS SUBMITTED FOR THE DEGREE OF DOCTOR OF PHILOSOPHY

THE UNIVERSITY OF EDINBURGH

NOVEMBER 2006

Declaration

I, Harpreet Singh, PhD candidate in Biomedical Sciences, declare that work presented in thesis has been composed solely by myself, except where indicated and that this work has not been submitted for any other degree or professional qualification.

Dedicated to my parents and teachers

Acknowledgements

I would like to thank my supervisors, Dr. Richard H. Ashley and Dr. Michael A. Cousin for their guidance and constructive advice throughout this project. I am grateful to Dr. Iain Rowe for his invaluable help and encouragement over the last three years. I am thankful to Prof. Mathew K. Mathew (NCBS, India) for providing me the initial launch pad into the field of ion channels. I would like to thank Linda W. Wilson for technical assistance with the confocal microscopy facility. I would like to thank all the members of Centre for Integrative Physiology for their tremendous support and friendship at every step. It was always very enjoyable to work with the members of membrane biology group.

I would like to thank my parents, Mrs. Harvinder Kaur and Capt. Sohan Singh, my brother Inderpreet and sisters Poornima and Fozia for their love, support and encouragement. I am thankful to Mrs. Prabhavathi and Mr. K.S. Ramanujam for their blessings. A very special person has made a remarkable change in my life and career, Shubha, thanks to her for being with me always. I know that she has suffered silently most of this time and had to overcome many difficulties alone. I hope that in the future I will be able to make it up.

I am grateful to all my friends from Chail Military School (Georgians) especially Arvind Gajraj, for encouraging me from all corners of the world. Special thanks to Sunil Kappanguntala, Bilal, Mrs and Mr Bharath Shetty, and many other friends from India for their continuous inspiring support. I am thankful to Chail Military

School (King George Royal Indian Military College) for making me a 'gentleman cadet'.

A very special thanks to the local people of Scotland for providing such a friendly environment. I have had a wonderful experience over the last three years in this beautiful country. The ever-smiling crowd of Edinburgh gave me a fresh reason to work every day with enthusiasm and dedication.

Last but not least, I would like to thank the College of Medicine and Veterinary medicine for a Faculty Scholarship, Universities UK for an Overseas Research Studentship (ORS), Dr. Kulvinder Singh Saini for a Saini travel grant and Arun (Georgian) from Texas for a travel grant, for supporting my PhD in UK. I could not have pursued a PhD without these funding bodies.

Finally, I am grateful to the almighty God for his love and blessings without whom none of this would have been accomplished.

List of abbreviations

A	absorbance
A	adenine
ATP	adenosine triphosphate
bp	base pair
BSA	bovine serum albumin
C-	carboxy
C	cytosine
cDNA	complementary DNA
°C	degree celsius
CFTR	cystic fibrosis transmembrane conductance regulator
CGN	cerebellar granular neurons
CLC	chloride channel
CLIC	chloride intracellular channel
CNS	central nervous system
cyt	cytoplasmic
DEPC	diethyl pyrocarbonate
DMEM	Dulbecco's modified Eagle's medium
DMSO	dimethyl sulphoxide
DNA	deoxyribonucleotide
dNTP	2'-deoxyribonucleoside 5'-triphosphate
DTT	dithiothreitol
ECL	enhanced-chemiluminescence

EDTA	ethylenediaminetetraacetic acid
EGTA	ethylene glycerol bis(β-aminoethyl ether)-N,N,N',N tetraacetate
ER	endoplasmic reticulum
FCS	foetal calf serum
G	guanidine
GABA	gamma-aminobutyric acid
GFP	green fluorescent protein
GST	glutathione S-transferase
GSH	reduced Glutathione
GSSG	oxidised Glutathione
h	hours
HCl	hydrochloric acid
HEPES	N-2-hydroxyethylpiperazine-n'-2-ethanesulfonic acid
HEK 293	human embryonic kidney cell line
His	histidine
HRP	horseradish peroxidase
H_2O	water
IAA	indanyloxyacetic acid
IgG	immunoglobulin G
IPTG	isopropyl-β-thiogalactopyranoside
kb	kilobase-pairs(s)
kDa	kiloDalton(s)
l	litre
λ	wavelength

LB	Luria-Bertani medium
M	molar
MCS	multiple cloning site
mins	minutes
mg	milligram
µg	microgram
µl	microlitre
µM	micromolar
mV	millivolts
N	amino
NCC27	nuclear chloride channel protein-27kDa
ng	nanogram
nm	nanomolar
NMDG	N-methyl-D-glucamine
ORF	open reading frame
p64	bovine chloride channel protein-64kDa
PBS	phosphate-buffered saline
PC12	pheochromocytoma cells
PCR	polymerase chain reaction
PMSF	phenyl methyl sulfonyl fluoride
pS	picoSiemens
PVDF	polyvinylidene difluoride
pmol	picomoles
RNA	ribonucleic acid

RNase	ribonuclease
Rpm	revolutions per minute
RT	room temperature
RVI	regulatory volume increase
RVD	regulatory volume decrease
RyR	ryanodine receptor
VSOAC	volume-stimulated osmolyte and anion channel
s	second(s)
SDS	sodium dodecyl sulphate
SDS-PAGE	sodium dodecyl sulphate polyacrylamide gel electrophoresis
SV	synaptic vesicle
T	thymine
TB	terrific broth
TPBS	Tween phosphate-buffered saline
TCA	trichloroacetic acid
TEMED	N,N,N,N',N-tetramethylenediamine
Tm	melting point
TMD	transmembrane domain
Tris	tris[hydroxymethyl]aminomethane
Triton X-100	octylphenyl-nonaoxyethylene
Tween-20	polyoxyethylene-sorbitan monolaurate
UV	ultraviolet
VDAC	voltage-dependant anion channel
VRAC	volume-regulated anion channel

vs	versus
wt	wild-type
v/v	volume per volume
w/v	weight per volume
w/w	weight per weight

Contents

List of figures

List of tables

Abstract

Chloride Intracellular Channel (CLIC) proteins are ubiquitous in multicellular organisms and often coexist in soluble and integral membrane forms. They can autoinsert into membranes to form molecular components of intracellular ion channels. Soluble CLICs are structurally similar to Ω-type glutathione-S-transferases (GSTs), but the structure of the membrane proteins remains elusive.

In this study, soluble, recombinant, human CLIC1, rat brain CLIC4 (p64H1) and human CLIC5A, a splice variant of p64 (CLIC5B), were expressed as cleavable His-tagged proteins and incorporated into voltage-clamped planar lipid bilayers. They inserted spontaneously with or without an intact His-tag to form redox-regulated ion channels. All showed well-defined sublevels with similar reversal potentials and ionic selectivities. Redox titration *in vitro* using a glutathione coupled buffer system led to a sequential reduction in conductance as oxidation progressed on the extracellular or "luminal" side. These changes were fully reversible, suggesting that intracellular redox potential may play a role in modulating CLIC channel activity. The channels were sensitive to the cysteine-reactive compounds NEM and DTNB. Furthermore, CLIC1 and CLIC4 activity was inhibited by their respective affinity-purified antibodies.

The putative pore forming region was identified based on previous work and CLIC channels appear to contain at least 4 subunits each with a single transmembrane domain (TMD). In this simple model, the luminal side of each subunit contains a single cysteine residue located just before the putative pore entrance. Consistent with these ideas, truncated proteins comprising the first 58 residues of CLIC1, or the first

61 residues of CLIC4 (sufficient in each case to contain the putative TMD), autoinserted into bilayers to form redox-sensitive ion channels and could be blocked by cysteine reactive compounds applied from the luminal side. The truncated proteins showed reduced conductances, and were non-selective between anions and cations.

CLIC5A was originally identified in an ezrin-containing cytoskeletal complex. The hypothesis that actin regulates the channel activity of CLICs was tested. Actin polymerisation on the cytosolic side (but not the luminal side) led to near-complete channel closure, restricting openings to minor substate levels of CLIC1 and CLIC5A (there was no effect on CLIC4). Addition of actin-destabilising agents such as latrunculin B and cytochalasin B inhibited or reversed the effect. CLIC1 also colocalised with F-actin in both HEK-293 cells and neuroblastoma cells (N2a). These studies indicated that CLIC5A and CLIC1 channel function may be regulated by the cortical actin cytoskeleton, providing a new mechanism to regulate localised ion flux in cells. Unusually, the interaction may be direct, without any intermediate or adapter protein.

CLICs also interact with dynamin I and cytoskeletal proteins *in vitro*. Additional *in vitro* studies were carried to map the CLIC binding site to the proline-rich domain (PRD) of dynamin I. This interaction also occurs *in vivo*, since dynamin I and CLICs form a complex in nerve terminals as previously shown by co-immunoprecipitation. In agreement, immunofluorescence studies in rat cerebellar granule cells showed significant co-localization between dynamin I and CLICs. The CLIC proteins showed distinct sub cellular localizations. CLIC1 and CLIC4 are also localised in

nerve terminals as shown by co-localization with the synaptic vesicle (SV) marker synaptophysin. The localisation of CLICs in nerve terminals and their interaction with dynamin suggests a possible role in SV recycling.

In summary, CLICs can form poorly-selective, oligomeric ion channels modulated by luminal GSH-dependent transthiolation and in some cases by actin polymerisation from the cytosolic side. The transmembrane domain can autoinsert, but is not enough to form channels identical to wild-type channels. These preliminary structure-function studies have provided an overview of the molecular mechanism of membrane CLICs. Discovery of regulatory mechanisms for CLICs may shed more light on their functional roles in cells during processes such as the cell cycle and apoptosis.

CHAPTER 1

INTRODUCTION

1.1 Ion Channels

All cells are surrounded by a semi-permeable plasma membrane, composed of a lipid-bilayer (Fig 1.1). Lipid bilayers are in the fluid state, and phospholipids diffuse rapidly in two dimensions within each leaflet of the membrane, leading to the fluid mosaic model of biological membranes (mosaic as it includes proteins, cholesterol, and other type of molecules besides phospholipids) (Singer and Nicolson, 1972). Along with phospholipids, cholesterol is embedded in the bilayer (Fig 1.1) and is a necessary component of eukaryotic biological membranes.

Cells derive their electrical properties from the plasma membrane, which facilitates the flow of charges by means of ion channels and transporters. Ion channels are found in the membranes of all cells ranging from prokaryotes to eukaryotes, and are essential for important physiological processes such as sensory transduction, nerve action potentials and muscle contraction (Hille, 1984). In the past decade, numerous crystal structures of ion channels have increased our understanding of gating and selectivity. In structural terms, ion channels are macromolecular protein tunnels that span the membrane bilayer, and allow the passage of charged ions through hydrophobic membranes, as shown in fig 1.1. As reiterated by Ashley (2003), a protein can be classified as an ion channel only if:

- It is able to adopt a structure compatible with a transmembrane, channel forming protein;
- It forms an ion channel when expressed in cells;

- It forms identical channels when incorporated as a pure protein into planar bilayers or liposomes; and
- Ion transport is altered when critical pore-forming regions are modified.

Unlike membrane transporters such as carriers and pumps, the flow of ions through ion channels across the cell membrane is passive and follows an electrochemical gradient. The turnover rate of an ion channel can be as high as 10^8 / sec.

More than 340 human genes are thought to encode ion channels (www.ensembl.org/Homo_sapiens/index.html), and they have diverse functional roles in for example cell proliferation, nerve and muscle function, hormone secretion, learning and memory, salt and water balance, fertilization, cell death, and regulation of blood pressure (Ashcroft, 2000). Because of their important functional roles, their membrane localisation, their structural heterogeneity and the restricted tissue expression of certain channel types, ion channels are attractive targets for drug therapy.

1.2 Tracing the history of ion channels

The concept of ion channels can be traced back to 1791 when Galvani showed that electricity could trigger a biological response in a frog's leg. In 1890, Ostwald proposed that the electrical signals measured in living tissue could be due to ions passing through cell membranes. In the early 1900s, Hermann and Bois-Reymond's students were able to conclude that nerve and muscle cells are capable of exhibiting a

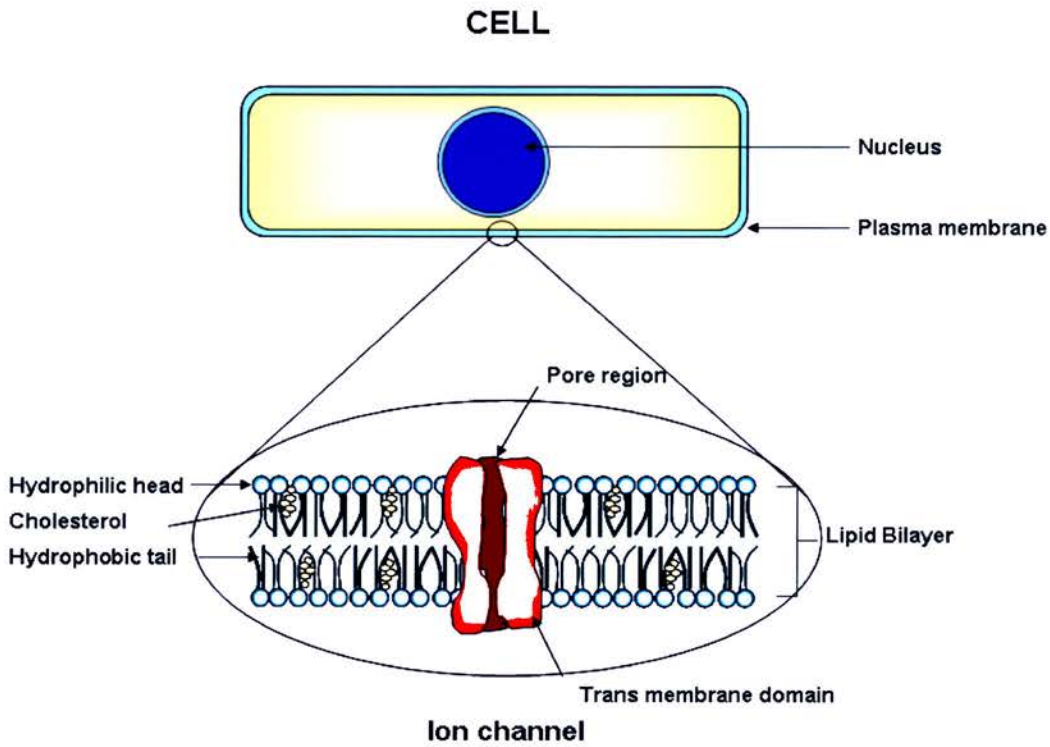

Fig 1.1. Ion channel in the cell membrane. Cell pores or ion channels are present in all cell membranes. Cholesterol is an important constituent of mammalian cell membranes, changing their mechanical properties and hence their motions. The pore-forming region of an ion channel is normally selective for specific ions.

"self propagating wave of negative charge which advances in steps along the tissue". Bernstein first proposed the ionic theory, the Nernst equation and the assumption of a semi-permeable membrane surrounding nerve and muscle cells. He postulated that the concentration difference in potassium ion concentrations across the cell membrane could account for the presence of the membrane potential. Hodzkin and Katz showed that sodium ions were responsible for the formation of the action potential, and found a relationship between the amount of sodium outside the neuron and the amplitude of the action potential. By the 1940s Hodgkin, Huxley and Katz had explained the resting potential and the action potential in terms of the movement of specific ions (K^+, Na^+, and Cl^-) through pores in the cell membrane (Chapter 2, Hille, 1985).

In 1971, Hille measured the mobilities of several species of ions other than sodium to gain information about ion channel structure and the mechanism of ion permeation, while Tien, Montal and Mueller progressively developed the planar bilayer technique to functionally reconstitute single ion channels (especially antibiotic channels) *in vitro* (Benz et al., 1975). Although the bilayer technique had already been used to demonstrate and study cellular ion channels (e.g. by Miller and others), in 1976 Neher and Sakmann invented cellular patch-clamping, referred to as the single most important development in ion channel research in the last half of the 20^{th} century (Neher and Sakmann, 1976). In 1980 it was noticed that slight suction improved the seal by two orders of magnitude, into the gigaohm range, the so-called 'gigaseal', permitting excellent single-channel current resolution in many cells *in vivo* (Hamill et al. 1981). More recently, in 1998, the first high-resolution, crystal structure of a

selective ion channel, the KscA potassium channel from the bacterium *Streptomyces lividans*, was revealed by Mackinnon's group (Doyle et al., 1998), another landmark discovery.

1.3 Nomenclature of ion channels

The nomenclature of ion channels is not as systematic as it is for other proteins. Initially various components of membrane permeability were identified by their kinetics, pharmacology, and response to ionic substitution. A kinetic model for ion channels is often expressed as a mathematical component, in which it is assumed that each component of the model corresponds to a type of a channel, and the putative channels are given the same names as the permeability components. Hodgkin and Huxley (1952) recognised sodium, potassium and leakage currents in the giant squid axon. Based on this, present day Na^+ and K^+ channels are universally accepted as the corresponding ionic components in axons. This rational approach fails when the ions involved are not completely known or when one type of ions is involved in different kinetic components. These discrepancies have led to nomenclatures such as A, B, C and so on, for permeability components in molluscan ganglion cells (Adams at al., 1980) or qi, si and x_1 in cardiac purkinje cells (McAllister et al., 1975). Also, channels are often named after anatomical regions, or activators or inhibitors (including neurotransmitters), or their cellular localisations.

Class	Examples
Voltage-gated channels	Na^{+}, K^{+}, and Ca^{2+}channels.
Extracellular ligand-gated channels	nAChR channels, GABA and glycine receptors.
Intracellular ligand-gated channels	ATP-K, ASICs, SK and BK channels.
Mechanosensory and volume-regulated channels	CLC channels and VRACs.
Miscellaneous channels	gramicidins, porins and gap junctions

Table. 1.1 Classification of ion channels on the basis of regulation. Classifying ion channels on the basis of regulation is most commonly used. Some examples are given for each class of the channel.

1.4 Classification of ion channels

Ion channels can be classified on the basis of various aspects such as sequences, molecular structures and evolutionary history etc. Classification on the basis of amino acid sequences and phylogenetic relationships is the most appropriate and logical way of classifying ion channels. Most channels can be divided into three major groups on the basis of their selectivity, as anion (ClCs), cation (K^+) and non-selective channels. The most widespread is the classification based on channel regulation as summarised in table 1.1. Harte and Ouzounis (2002) classified ion channels from 32 entire genome sequences from Archaea (6), Bacteria (23) and Eukaryotes (3) into 13 distinct groups on the basis of their structural, functional and physiological properties. The groups were, neurotransmitter-gated channels, ionotropic glutamate-activated cationic channels (both extracellular ligand-gated), cyclic nucleotide-gated (CNG), voltage-gated potassium, voltage-gated sodium, voltage-gated calcium, voltage-gated chloride (CLC), inward rectifier potassium, two-pore potassium, prokaryotic potassium channels, ATP-gated purinergic (P2X), degenerin/amiloride-sensitive sodium epithelial (ASC) and large-conductance mechanosensitive channels.

1.5 Ohm's law

The electrical properties of ion channels were deduced from electrical measurements by following specific principles. The most important is Ohm's law which defines a relation between current, voltage and conductance. Conductance is a measure of the

ease of flow of current between two points and is measured in Siemens (S, formerly called mho) and is defined by Ohm's law in simple conductors:

$$I = gE \qquad [1]$$

where, I (current) equals the product of conductance (g) and difference in voltage between two electrodes (E, $E = \Delta V = V_2 - V_1$, where V is voltage). The reciprocal of conductance is resistance (R) and is measured in ohms (Ω). Hence Ohm's law can be written as:

$$E = IR \qquad [2]$$

If Ohm's law is tested on an ion channel, current in the pores goes to zero at E_{Cl} and not at 0 mV, where E_{Cl} is obtained from the Nernst equation which can be written (for monovalent ions):

$$E_{Cl} = (RT/F) \ln [Cl]_o/[Cl]_i = 2.303\ RT/F\ (\log_{10}[Cl]_o/[Cl]_i)V \qquad [3]$$

where R is the gas constant, F is Faraday's constant, T is absolute temperature and [Cl] is the concentration of ions, outside (o) (extracellular) and inside (i) (intracellular).

Due to the electrochemical gradient Ohm's law can be rewritten as:

$$I_{Cl} = g_{Cl}(E-E_{Cl}) \quad [4]$$

where the electromotive force is $E_{Cl,}$ and the net driving force on Cl^- ions is now $E-E_{Cl}$ and not E. This equation is suitable for linear current-voltage relationships, but not all channels show linear current-voltage relationships (Hille, 1984).

1.6 Selectivity of channels

For electrical excitability, ion channels should be selective for specific ions, but no channel is perfectly selective. The Na^+ channels of axons are fairly permeable to ammonium ions, and anion channels are often selective for various anions. Ionic selectivity can be measured by measuring the zero current potential for the channels. With ions A^+ on the outside and B^+ on the inside, the zero current potential is also called the biionic potential. If both ions have the same valency and no other permeant ion is present, then the permeability ratio P_A/P_B is defined by the equation:

$$Er = RT/F \ln (P_A [A]_o/P_B [B]_i) \quad [5]$$

where the zero current potential is called reversal potential (Er), since at Er, the current reverses sign. It is the simplest form of an expression derived from diffusion theory by Goldman (1943) and Hodgkin and Katz (1949) (Chapter 1, Hille, 1984).

1.7 Chloride channels

For more than 50 years, the study of ion channels has been dominated by proteins involved in neuronal function, which ignored Cl^- channels. However, in the past decade, work on Cl^- channels attracted unaccustomed attention. Chloride is the most ubiquitous aqueous ion on earth. Therefore, anion channels are often called chloride channels, even though they may be permeable to other anions. All living organisms have evolved membrane transport and various ion channel proteins, to exploit Cl^- towards varied physiological ends. The leakage channels in giant squid axon ignored as experimental irritants (Hodgkin and Huxley, 1952), were largely mediated by chloride channels. Now it is known that these leakage channels play diverse functional roles from regulation of blood pressure, muscle tone, cell volume control for synaptic transmission and cellular excitability (Maduke at el., 2000).

Chloride currents were recognized electrophysiologically long ago (Hodgkin and Huxley, 1952) but an understanding of their molecular arrangement has only begun to emerge recently. The first chloride channel to be cloned was the voltage-gated Cl^- channel from an electric fish (Jentsch et al., 1990), which was followed by the discovery of an abundant, widespread, and ancient molecular family of Cl^- channels. Like other ion channels, Cl^- channels were predicted to function in the plasma membrane or in the membranes of intracellular organelles. Patch-clamp studies have revealed a variety of anion channels that differ in their single-channel conductance, selectivity and regulatory mechanisms.

1.8 Classification of Cl^- channels

Cl^- channels may be classified according to their localisation, single-channel conductance or mechanism of regulation, but such classification schemes are ambiguous as the same channel may reside on the plasma membrane and intracellular membranes, or their regulation mechanisms may overlap. Classification on the basis of their molecular structure is most logical, however the large variety of biophysically identified Cl^- channels are not yet matched to a similar number of known Cl^- channel genes.

Cl^- channels can be broadly classified on the basis of their physiological role into 1) Ligand-gated Cl^- channels; 2). Intracellular calcium-activated Cl- channels; 3). cAMP-gated Cl^- channels; 4). G protein-activated Cl^- channels; 5) mechanical stretch-activated Cl^- channels and 6) cell-swelling related Cl^- channels (Nilius and Droogmans, 2003). On the basis of their sequences, Cl^- channels can also be grouped as 1). glycine and GABAα receptors; 2) CFTR; 3) CLC family; and 4). CLIC family. Recently a new family of Cl^- channels, bestrophins were found on the membranes of retinal cells (Sun et al., 2002). VDAC (the mitochondrial voltage-dependent anion-selective channel) is poorly selective for anions over cations and forms a transmembrane β-barrel (Forte et al., 1987).

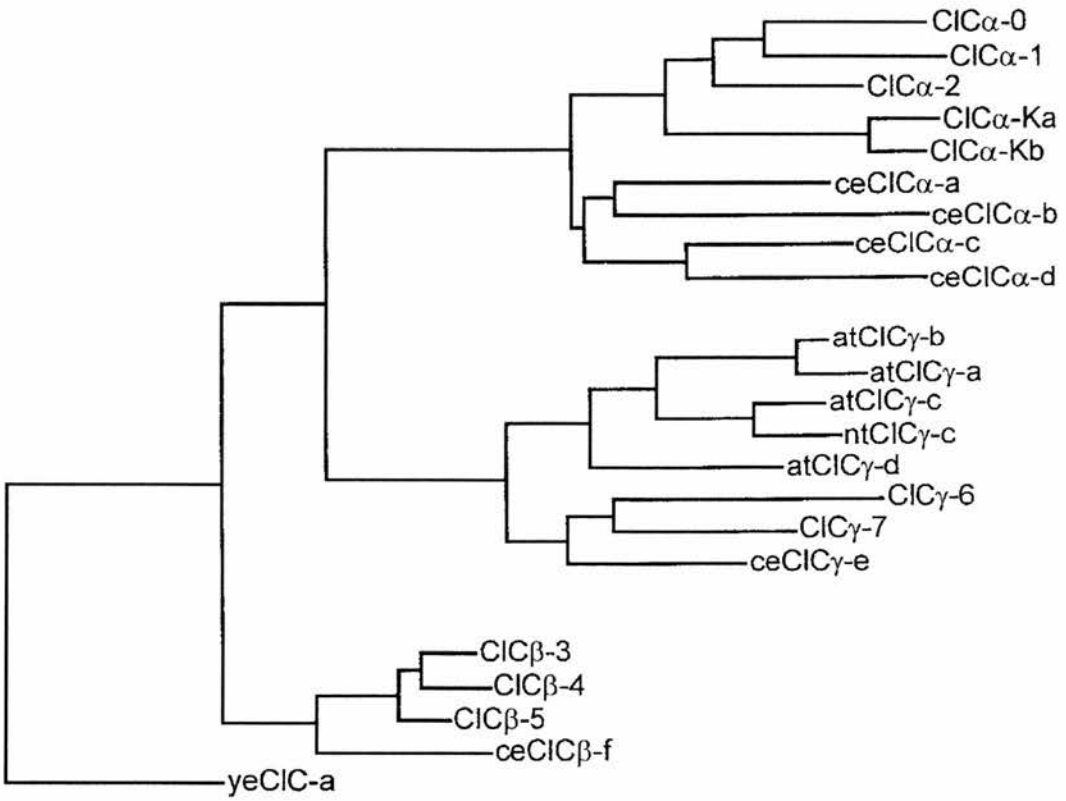

Fig 1.2. Organisation of CLC superfamily. Phylogenetic tree of selected CLC genes (derived by clustal analysis). Invertebrate genes are annotated with prefixes such as "ce" (*C.elegans*), "ye" (*S.cerivisiae*), "at" (*A. thaliana*) and "nt" (*N. tabacum*) (Maduke et al. 2000).

1.8.1 Chloride channel proteins (CLC family)

CLC proteins were originally discovered in *Torpedo* electroplax (Miller, 1982), and identified by expression cloning of the voltage-gated Cl^- channel ClC-0 from the electric organ of *Torpedo marmorata* (Jentsch et al., 1990, Bauer et al., 1991). Members of CLC are present in prokaryotes and eukaryotes. Nine different CLC genes have been identified in mammals and they fall into three subfamilies (Fig 1.2) (Maduke et al., 2000).

The recently identified crystal structure of CLC channels gives a definitive picture of topology (Fig 1.3). An X-ray structure of two prokaryotic CLC Cl^- channels from *Salmonella enterica serover typhyimurium* and *Escherichia coli* at 3.0 Å and 3.5 Å, respectively revealed two identical pores, each being formed by a separate subunit contained within a homodimeric membrane protein (Dutzler et al., 2002). Bacterial CLCs are composed of 18 helices, most of which do not entirely span the membrane (Fig 1.3).

The individual subunits are composed of two repeated halves, which span the membrane in opposite orientations. This anti-parallel architecture defines a selectivity filter in which Cl^- ions are stabilised by electrostatic interactions with α-helix dipoles and by chemical coordination with nitrogen atoms and hydroxyl groups. The dimer containing two largely independent pores has been established in α- subfamily of ClCs but not in other ClC channels.

A).

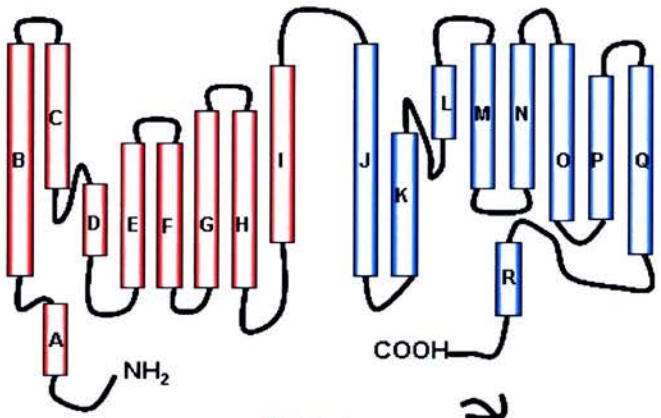

B).

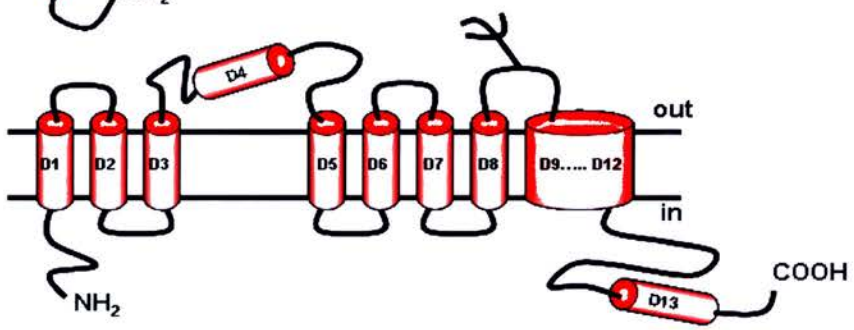

C).

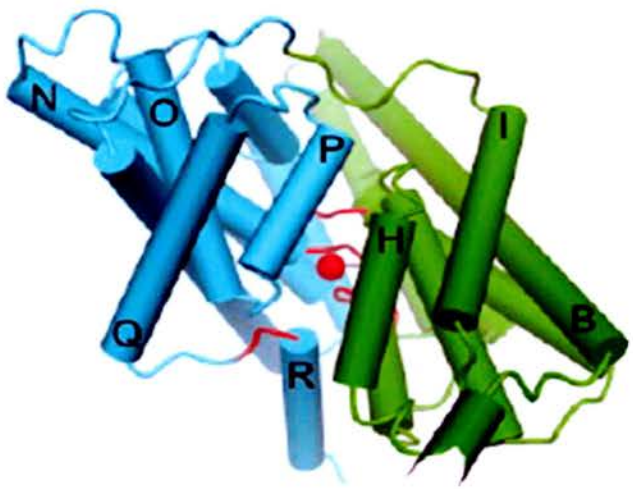

Fig 1.3 Toplogy model of ClC and structure of StClC. (A) The α-helices (A-R) of StClC are drawn as cylinders. The two halves of the subunit are represented as red and blue (redrawn from Dutzler et al. 2002). (B) Membrane topology of ClC on the basis of biochemical studies. The broad hydrophobic region between D9 and D12 is difficult to investigate experimentally (redrawn from Jenstch, 1996). (C) View of the StClC subunit viewed from within the plane of the membrane. The α-helices are drawn as cylinders, loop regions as cords, with the selectivity filter is shown in red and Cl^- ion is a red sphere.

ClC-ec1 from *Escherichia coli* actually lacks a continuous transmembrane pore, and is a Cl^-/H^+ transporter (Dutzler et al., 2002). Within each subunit is a buried prominent active site or anion-coordinating region occupied by a Cl^- ion. The most widely-studied ClC channels, ClC-0 and ClC-1 are voltage-dependant, but not all ClC channels are strictly voltage-dependant, and there is a lack of knowledge about the structural details of channel gating. ClC-2 can be activated by hypotonicity, low extracellular pH and hyperpolarisation (Furukawa et al., 1998).

The ubiquitous expression of ClC channels confirms the importance of these proteins in cells. CLC channels can be found in all phyla from prokaryotes to eukaryotes. However, certain organisms such as *Helicobacter pylori* completely lack the gene for CLCs, suggesting that they are not strictly needed for life and this is supported by a knock out (KO) model of the single yeast CLC gene, which yields viable cells (Jenstch et al., 1999). The central role of ClC-0 and ClC-1 is the excitability of muscle or muscle-derived tissues is well established, and CIL-Kb certainly provides a major salt resorption pathway in mammalian kidneys. ClC-2 and ClC-3 are sensitive to changes in osmolarity (Jenstch et al., 1999). ClC-Ka and ClC-Kb are exclusively found in the kidney, and ClC-3, ClC-4, ClC-5, ClC-6 and ClC-7 have been shown to be localised to the membrane of intracellular organelles such as lysosomes and endosomes (Günther et al., 1998; Stobrawa et al., 2001; Konark et al., 2001). ClC-5 was also shown to be involved in acid transport by intracellular vesicles (Günther et al., 1998).

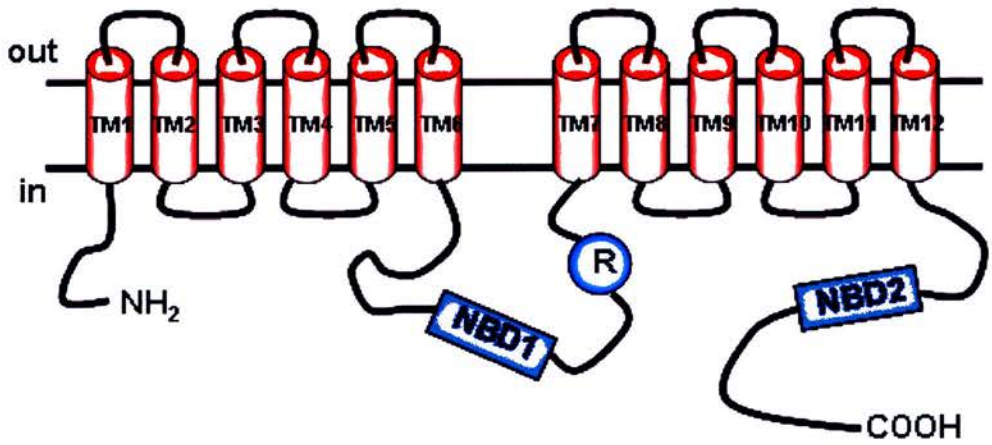

Fig 1.4. Membrane topology of CFTR channels. CFTR is an integral membrane protein consisting of a single polypeptide chain of 1480 amino acids, and has 12 TM domains arranged in two separate groups. It has two nucleotide-binding domains (NBD) and an R-domain (redrawn from Jentsch, 1996).

1.8.2 CFTR- Cystic fibrosis transmembrane conductance regulator

CFTR was the first anion channel to be identified by positional cloning (Riordan et al., 1989). The gene for CFTR emerged from the search for the cystic fibrosis (CF) locus and yielded a sequence, that of an ATP-binding cassette (ABC) transporter, with a tandem repeat of a transmembrane domain of six putative transmembrane helices (TMD) and a nucleotide binding fold (NBF), linked by a regulator domain containing numerous phosphorylation sites. The ion channel functions of CFTR were established by comprehensive experimentation (Sheppard and Welsh, 1999). CFTR is now known to be a voltage-independent anion channel, which requires the presence of hydrolysable nucleoside triphosphates for efficient activity.

CFTR has 12 TM segments arranged in two separate blocks and two nucleotide binding folds as shown in fig 1.4. It also has a regulatory (R)-domain, which is absent in ABC transporters and contains various consensus sites for phosphorylation by protein kinase A and C, and is thought to regulate the function of the channel (Nilius and Droogmans, 2003).

CFTR is expressed in the apical membranes of epithelia of intestine, airways, secretory glands, bile ducts and epididymis. A splice variant is also found in cardiac muscle, where its function is unknown. The localisation of the protein depends on the interaction with apical PDZ proteins via the carboxy-terminal PDZ-interacting domain of CFTR. CFTR is crucial for a number of transepithelial transport processes, as evident from the pathophysiology of CF patients, who show severe

impairments of epithelial salt and fluid secretion as well as reabsorption. CFTR has (with ClC channels) additional intracellular roles, in establishing the low pH in the biosynthetic compartments of the trans-Golgi network and in endosomes, as suggested by reduced acidification rates of these organelles in CF cells. CFTR forms a small (5-8 pS) anion channel which is highly-selective for Cl^- ions, and opening of the CFTR channel requires phosphorylation by protein kinase A, making it susceptible to regulation by cyclic AMP. CFTR activation appears to be a multiple step process that requires the activity of protein kinase C, PKA, and a high ATP/ADP ratio to achieve maximal activity (Nilius and Droogmans, 2003).

In earlier studies of CF, it was noted that the activation properties of Na^+ and Cl^- channels were altered in CF epithelia. The first channel suggested to be regulated by CFTR was the outwardly-rectifying Cl^- channel (ORCC) (Guggino, 1993) which comprises of one or more unidentified anion channels. ENaC is another candidate for CFTR interaction (Kunzelmann et al., 1997).

1.8.3 Ligand-gated anion channels

Glycine and GABA receptors were the first family of Cl^- channels to be discovered, and they belong to the ligand-gated receptor channel superfamily (LGIC) (Betz, 1990). LGIC superfamily members are assembled as pentamers to form an ion channel. They share both structural and primary sequence homology and evolved from a common ancestor receptor subunit (Betz, 1990). Each subunit of the LGICs consists of a large N-terminal domain of ~ 200 amino acids, 4 putative TMDs and a

short extracellular C-terminus. The N-terminus contains a conserved motif, the Cys loop. TMD3 and TMD4 are linked by a cystolic loop of variable length. These features are common to glycine receptors (Vannier and Triller, 1997), nicotinic acetylcholine receptors (Lindstrom, 1995), GABA receptors and ionotropic serotonin receptors (Maricq et al., 1991).

GABA receptor channels consist of six α-isoforms, three each of β and ρ-subunits, and one δ-subunit. Glycine receptors have four different α-subunits and one β-subunit. This diversity is increased further by alternate mRNA splicing of some of these subunits. Both GABA and glycine receptor channels have multiple conductance levels in the range of 10-90 pS. These channels are poorly-selective for Cl^- and in addition both channel types are significantly permeable to bicarbonate, and the resulting intracellular acidification may be important for modulating synaptic activity (Jentsch et al., 2002).

1.8.4 Ca^{2+}-activated Cl^- channels (CaCCs)

Cl^- channels activated by intracellular calcium are found in many cell types, like excitable cells, including neurons, cardiac and smooth muscle cells, and in non-excitable cells such as epithelial, endothelial and also in blood cells. In neurons and muscle cells, CaCCs may modulate excitability. In olfactory receptor cells, CaCCs play an important role in signal transduction as they are activated by Ca^{2+} entering through cGMP-activated channels. In epithelial cells they play an important role in

transepithelial transport. Some Cl^- channels are also dependant on extracellular calcium (Jentsch et al., 2002).

The salient features of CaCCs are very similar in the various cell types. They are activated in a voltage-dependant manner by an increase in Ca^{2+}, due to the binding of Ca^{2+}. CaCCs are characterised by their poor selectivity and a small single-channel conductance (0.5-5pS) (Evans and Marty, 1986). They show outward rectification, activate slowly at positive potentials and deactivate at negative potentials. Activation is faster at higher Ca^{2+} concentrations and at stronger depolarisations. In general, the proteins that are thought to form CaCCs are characterised by a precursor of approximately 125 kDa, consisting of 900-940 amino acids. This precursor is cleaved to form heterodimers of approximately 90 and 35 kDa. The most likely topology is a 4-5 TMD with an extracellular glycosylated N terminus, containing conserved cysteines and an intracellular (for 5 TMD) or extracellular (for 4 TMD) C-terminus.

1.8.5 Swelling-activated Cl^- channels

Volume regulation in response to external and internal osmolic changes is extremely important for cells. Some cells in the proximal gastrointestinal tract and kidneys are exposed to significant changes in extracellular osmolarity. Cell volume regulation is also required during growth and cell division. To regulate their volumes, cells have evolved various ion and organic transport proteins that are activated upon cell swelling or shrinkage. In regulatory volume increase (RVI) and regulatory volume decrease (RVD), Cl^- concentration is strictly maintained. It is accepted that the

volume-stimulated osmolyte and anion channel (VSOAC) is responsible for the electrogenic flow of chloride and the passive efflux of osmolytes (Jentsch et al., 2002).

Cell swelling induces a characteristic anion-selective whole-cell conductance in every vertebrate cell type. This current is called $I_{Cl,swell}$, which displays outward rectification, lacks time-dependant activation upon depolarisation, and shows variable inactivation at holding potentials above +40 mV. Various candidates such as Mdr (P-glycoprotein), pI_{Cln}, and ClC-3, have been reported to mediate $I_{Cl,swell}$ but none of these could be confirmed (Nilius and Droogrmans, 2003).

1.8.6 Bestrophins

Bestrophins were originally defined as a family of over 20 related sequences in the *Caenorhabditis elegans* genome with no homology to any proteins of known function. The first mammalian bestrophin was identified as the protein product of the gene responsible for autosomal dominant vitelliform muscular dystrophy (VMD), also known as Best disease (Sun et al., 2002; Marmorstein et al., 2002). It is homologous to at least 3 other proteins encoded within the human genome, 4 in the *Drosophila* genome and 20 in the *Caenorhabditis elegans* genome.

The first direct evidence for bestrophins as chloride channels was established from whole-cell recordings from the transiently transfected HEK 293 cells. It was demonstrated that two human, one *Drosophila* and one *C. elegans* bestrophin

produce a chloride conductance with a distinct I/V relationship and ion selectivity. The chloride current conferred by wild type human bestrophin (hBest1) is rapidly inactivated by sulphydryl-reactive reagents, whereas cysteineless hBest1 is resistant to this inactivation. They oligomerise to form tetramers or pentamers and the Cl^- conductance observed upon expression of hBest1 is calcium-sensitive. Human bestrophins hBest3 and hBest4 are 668 and 474 amino acids in length. All four hBests show between 55% and 66% sequence identity with the conserved N-terminus and minimal homology within the C-terminal domain.

The human bestrophin is sensitive to intracellular calcium and is coupled physically and functionally to the protein phosphatase PP2Ac and its structural subunit PR65. Patients carrying mutations in Bests have a decreased light peak in the electroculogram (Hartzell et al., 2005).

In addition to the Cl^- channels discussed above and apart from the CLIC family, which will be discussed separately, a few more Cl^- channels have been reported such as VDAC (Voltage dependant anion-selective channel and MCLC (Cl^- channel in rat)).

VDAC is found in the outer mitochondrial membranes of numerous species ranging from fungi to mammals. VDAC is believed to be involved in the transport of metabolic intermediates across the mitochondrial membrane, in addition to anions. The molecular mass of VDAC proteins ranges from 30 to 32 kDa and they are believed to span the membrane several times. VDAC channels are important for

mitochondrial function and can be regulated by polyanions, cellular constituents such as NADH, and Bcl-xl, Bax and Bak. These channels play an important role in mitochondrial events leading to apoptosis (Blachly-Dyson and Forte, 2001).

MCLC was cloned by homology to the *Saccharomyces cerevisiae* MID1 gene encoding a stretch-activated channel as probe for a rat cDNA library. Its gene encodes a protein of 541 amino acids with four putative transmembrane domains. The mRNA of MCLC is expressed abundantly in the testis and moderately in spleen, liver, kidney, heart, brain and lungs. MCLC is localised to the cytoplasm and nucleus and in intracellular compartments including endoplasmic reticulum and the Golgi apparatus in transiently transfected CHO-K1 cells. They form anion channels in lipid bilayers (Nagasawa et al., 2001; Li and Weinman, 2002).

1.9 Function and Biological roles of Cl^- channels

On the basis of location, Cl^- channels can be divided into plasma membrane channels and intracellular channels.

1.9.1 Plasma membrane channels

Plasma membrane Cl^- channels serve a variety of physiological functions including cell volume regulation and ionic homeostasis, transepithelial transport, and regulation of electrical excitability. Cl^- channels regulate the pH of the cytoplasm and cell volume with a close interplay between various ion transporters, including pumps,

cotransporters and other ion channels. They are also required for the transport of salts and fluid across many epithelia. Another important function is to regulate membrane electrical excitability. Cl^- channels are often found in conjunction with active cation transport systems, where Cl^- serves as a counter ion to the transported cation. In osteoclasts, Cl^- channels carry bicarbonate ions, to counter the hydrogen ion accumulation that occurs during bone resorption (Jentsch et al., 2002; Nilius and Droogmans, 2003; Suzuki et al., 2006).

1.9.2 Intracellular Cl^- channels

Anion channels are required for the passage of anionic substrates such as phosphates and sulphates out of degradative as well as biosynthetic compartments, e.g., lysosomes and Golgi apparatus respectively. They are also implicated in organellar volume regulation, for example mitochondria which are subjected to volume changes related to the metabolic state of the cell. Chloride conductance is also required in the acidification of intracellular organelles such as endosomes in the *trans*-Golgi network. Intracellular K^+, Cl^- and water efflux resulting in cell shrinkage have been implicated in the regulation of apoptosis (Jentsch et al., 2002; Ashley, 2003).

The impact of chloride channels has been shown on diverse cellular functions by elucidating their contribution to several diseases and by knock-out mouse models. An increasing volume of data has shown the strong relationship between Cl^- channels and some genetic diseases, which have been observed clinically.

Cystic fibrosis (CF) is the most frequent monogenetic fatal genetic disease in caucasians. The symptoms rise due to defects in transepithelial transport, leading to an accumulation of mucus in pancreatic ductules and in the airways, increased susceptibility to infection, and infertility in males due to blockage of the vas deferens and reduced fertility in females. Physiological studies indicate that the underlying molecular defect may be a cyclic AMP-regulated Cl^- channel of airway epithial cells (Li et al., 1988). In total 300 different mutations associated with CF have been described, with the most common being ΔF508 (deletion of phenylalanine at position 508), a mutation that leads to incomplete retention of CFTR protein in the Golgi, preventing its translocation to the plasma membrane. The misfolding of the mutant form of the CFTR is temperature-sensitive and some of the mutant protein manages to localise to the plasma membrane, where it displays normal Cl^- channel activity in cells grown at lower temperature (Du et al., 2005). Surprisingly, CFTR KO models have a much less severe phenotype.

Various inherited genetic disorders have been ascribed to mutations in glycine receptor subunits (Shiang et al., 1993). Missense mutations in the human α1 glycine receptor cause dominant hyperekplexia. A common characteristic is an exaggerated startle reflex, a stereotypic response involving facial grimacing, the hunching of shoulders, flexure of arms, and the clenching of fists in response to an unexpected stimulus. Mutations in the α6 subunit of the glycine and GABA receptors subunits cause inherited diseases, both in human and in animal models (Olson et al., 1999).

Autosomal dominant myotonia congenital (Thomsen's disease) and the autosomal recessive myotonia (Becker myotonia) in humans have been closely linked to mutations in CLC-1 (Jentsch et al., 2005). Mutation in CLC-kb results in Bartter's III disease which is a syndrome defined by low blood pressure, hypokalemic alkalosis and hypercalciuria. It can be explained by defective electrolyte reabsorption due to decreased basolateral Cl^- conductance which causes inhibition of the apical NKCC2 (Na -K -Cl- Cotransporter 2) (Maduke et al., 2000).

CLC-2 KO mice show a severe degeneration of photoreceptors. CLC-3 KO mice show a severe degeneration of the hippocampus and the retina with complete loss of photoreceptors after 4 weeks. Mutation in CLC-5 induces Dent's disease, an X-linked disorder with low molecular weight proteinuria, hypercalciuria, hyperphosphaturia, kidney stones, nephrocalcinosis and rickets. The current model postulates that the disruption of CLC-5 limits proton entry, which results in vesicular acidification, inhibiting normal endocytosis in the proximal tubule, and preventing reabsorption of protein. Mutation in the CLC-7 gene induces severe osteopetrosis and also retinal degeneration (Konark et al., 2001). CLC-7 is localised in the late endosomal and lysosomal compartments of osteoclasts. The phenotype of osteopetrosis in CLC-7 deficient mice is due to osteoclasts failing to reabsorb bone because they cannot acidify the extracellular resorption lacuna (Maduke et al., 2000; Jentsch et al., 2002; Nilius and Droogmans, 2003).

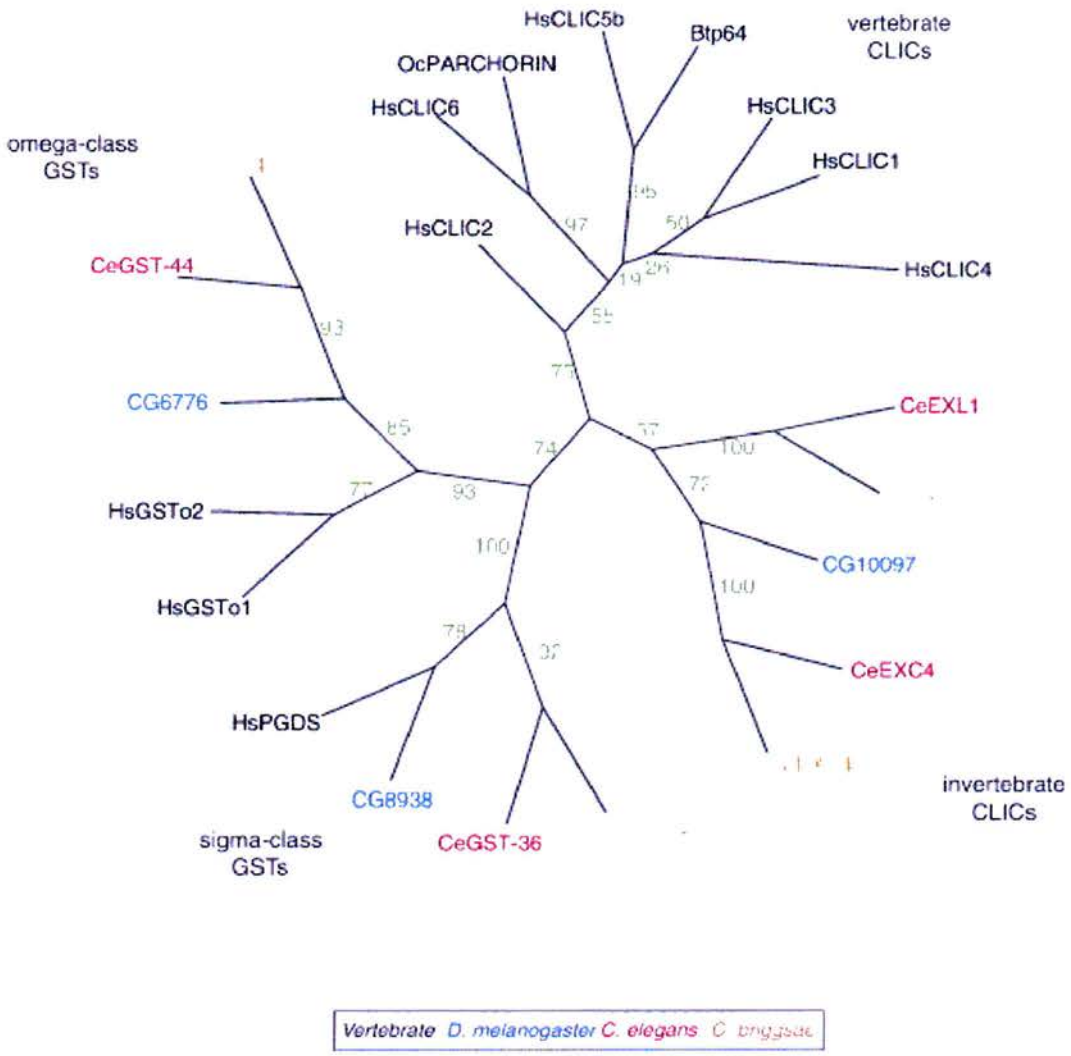

Fig 1.5. Classification of CLICs and GSTs (Berry & Hobert, 2006). Phyologenetic tree of CLIC and GST protein sequences from vertebrates (black), *Drosophila* (blue), *C. elegans* (red), and *C. briggsae* (orange). The number associated with each internal branch is the local bootstrap probability.

1.10 Chloride Intracellular channels (CLICs)

A new family of ion channel proteins has been recognised recently and was named ChLoride Intracellular Channel (CLIC) proteins (Heiss and Poustka, 1997; Edwards, 1999). p64 (CLIC5B) is the founder member of the CLIC family, isolated from octyl-glucoside (OG) solubilisates of bovine tracheal apical epithelium and kidney cortex microsomal membrane vesicles. They were affinity-purified taking advantage of their binding to the chloride channel blocker indanyloxyacetic acid 94 (IAA 94) (Landry et al., 1989).

The common features of CLIC family members are:

a). they are present in cytosol as well as in membranes;

b). they are low molecular weight proteins, between 23 kDa and 34 kDa except for p64 (49kDa) and CLIC6 (65 kDa);

c). they are highly conserved between vertebral species;

d). they share weak homology to omega class GSTs (Dulhunty et al. 2001);

e). the membrane forms show intracellular localisations, and

f). they probably have a single putative transmembrane domain (PTMD).

Each member of the CLIC family has its own salient features such as different single channel properties, tissue distribution pattern or subcellular localisation, regulatory mechanisms and different associated or interacting proteins. So far, several CLIC genes have been identified in vertebrates and invertebrates, which are distantly related to omega-GSTs (Fig 1.5). CLICs have been shown to play roles in diverse

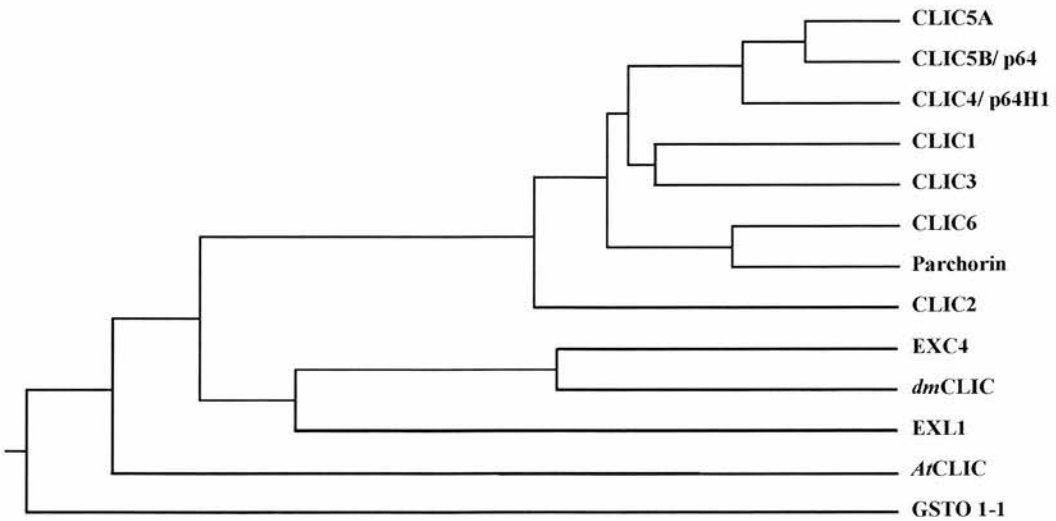

Fig 1.6. Phylogenetic tree of CLIC proteins (using clustal analysis). Vertebral CLIC1 (CAG46868), CLIC2 (CAA03948), CLIC3 (CAG46863), CLIC4/p64H1 (CAG38532), CLIC5A (CAI21031), CLIC5B/p64 (AAA02561), CLIC6 (Q96NY7), Parchorin (BAA94345) and GSTO 1-1 (P78417); Invertebral CLIC proteins, EXC4 (AAQ75554), EXL1 (O45405), and *dm*CLIC (AAF48326); and plant orthologue *At*CLIC (AAF98403) were analysed with the clustal method to draw the phylogenetic tree.

processes including bone resorption (Schlesinger et al., 1997), regulation of cell motility (Ronnov-Jessen et al., 2002), tubulogenesis (Berry et al., 2003), β-amyloid induced neurotoxicity (Novarino et al., 2004), and p53-mediated apoptosis (Fernandez-Salas et al., 1999; Fernandez-Salas et al., 2002; Suh et al., 2004; Suh et al., 2005). Human CLIC1, CLIC4, CLIC5A, CLIC5B, and rabbit parchorin can bind to a 133-amino acid domain within AKAP350 through the last 120 amino acids in their conserved carboxyl termini (Shanks et al., 2002). *Xenopus* homologues of CLIC1 and CLIC4 were isolated and were shown to be well-conserved throughout chordate evolution, but poorly conserved in invertebrates (Shorning et al., 2003). The phylogenetic tree of vertebral and invertebral CLICs is shown in fig 1.6. CLIC1, CLIC4 and CLIC5 were identified in spermatozoa (Myers et al., 2004), and have distinct localisations. CLIC1 was shown to co-purify with PP1γ2 and was localised to the acrosomal region. CLIC4 was confined to the anterior perimeter of the sperm head whereas CLIC5 was predominantly located in the post-acrosomal region of the sperm head. CLIC4 and CLIC5 were also localised to the flagellum, mainly in the principle piece. CLIC proteins contain consensus sequences for tyrosine phosphorylation and Src-homology domain type 2 (SH2)-binding domains.

Sequence alignments (by the clustal method) of CLIC proteins with Ω-GST and percentage homology is summarised in fig 1.7. The mammalian CLICs show around 50% homology to each other. They show structural homology to Ω-GSTs though they have weak sequence (approximately 15%) homology. Individual percentage homology and divergence are summarised in fig 1.7b.

1.10.1 p64 (CLIC5B)

The first identified member of the CLIC family was bovine p64, originally isolated and purified from bovine kidney with IAA-94 affinity chromatography (Landry et al., 1987; Landry et al., 1989). Bovine p64 was cloned and found to be a 428 amino acid protein with a hydrophobic N-terminal domain (Landry et al. 1993). p64 was also isolated from solubilised skeletal muscle sarcolemma (Weber-Schurholz et al., 1993).

The subcellular distribution and targeting of p64 was investigated in detail in kidney tissues, clonal cell lines (including Pancl cells, a human cancer cell line devoid of endogenous p64) (Redhead et al., 1992) and *Xenopus* oocytes (Redhead et al., 1997). Confocal and electron microscopy studies showed that p64 was localised to the membranes of large (0.5-1.0 μm) dense-core secretory vesicles (Chuang et al., 1999). Recombinant p64 never appears to enter the plasma membrane of cells as shown in *Xenopus* oocytes (Landry et al., 1993), where it was targeted to a specific class of intracellular vesicles (Redhead et al., 1997). The N-terminal domain functions as a positive targeting signal directing p64 to its final destination. In contrast, the C-terminal domain acts as a negative targeting signal that prevents the expression of p64 in the plasma membrane (Redhead et al., 1997).

Electrophysiological studies revealed three distinct types of ion channels when microsomes were reconstituted into asolectin (partially purified soybean phosphatidylcholine, PC) bilayers, with increasing conductances and decreasing Cl^-:

A).

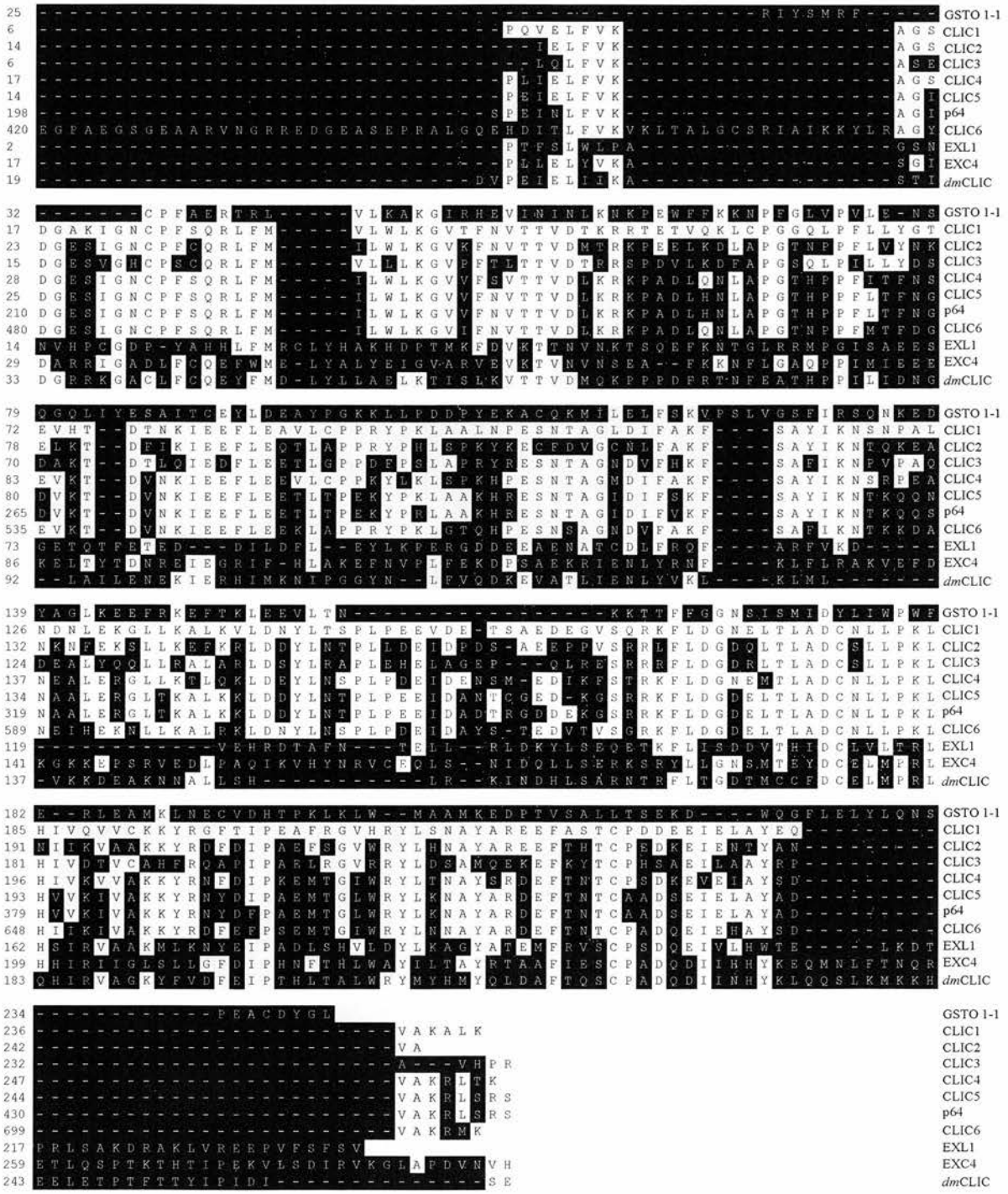
GSTO 1-1
CLIC1
CLIC2
CLIC3
CLIC4
CLIC5
p64
CLIC6
EXL1
EXC4
dmCLIC

B).

Percent Identity

Divergence

	1	2	3	4	5	6	7	8	9	10	11		
1		13.7	14.5	12.3	15.8	14.9	15.8	14.5	11.3	11.6	13.3	**1**	GSTO 1-1
2	265		59.3	50.4	66.4	62.7	61.8	62.2	19.3	19.1	20.3	**2**	CLIC1
3	227	53.6		47.5	63	64.2	61.3	62.6	20.6	20.6	25.5	**3**	CLIC2
4	347	72.7	78.1		47.9	49.2	49.2	47	17.8	16.1	20.3	**4**	CLIC3
5	214	42	44.2	79.3		74.1	70.8	70.4	18.1	20.9	24.1	**5**	CLIC4
6	237	45.7	45	74.8	24.8		90.8	69.3	19.3	18.7	23.9	**6**	CLIC5
7	244	49.7	49.6	78.7	33.3	7.1		46	18.5	16.6	23.5	**7**	p64
8	232	47.7	43.9	77.6	32.4	31.7	74.2		17.6	17.9	22.7	**8**	CLIC6
9	339	222	194.9	211	221	198	203	217		23.1	22.3	**9**	EXL1
10	315	199	193.3	216	200	197	219	194.7	169		35.8	**10**	EXC4
11	261	191.9	144.3	188.6	160.3	146.9	163.1	162.2	191.1	100.5		**11**	*Dm* CLIC
	1	**2**	**3**	**4**	**5**	**6**	**7**	**8**	**9**	**10**	**11**		

Fig 1.7 Sequence alignment of GSTO1-1 and CLIC proteins. A).Vertebrate and invertbrate CLICs were aligned by the clustal method. Three invertebrate CLICs (EXC-4, EXL-1 and *dm*CLIC) were aligned with human CLIC proteins. All the sequences were compared to CLIC1. Residues that differ from CLIC1 are shown as white on black. B). Sequence pair distance of CLICs using the clustal method.

K^+ selectivities (Landry et al., 1989). IAA-94 could inhibit channels from sarcolemmal proteins (Weber-Schurholz et al., 1993) and not microsomal channels. p64 expressed in HeLa cells appeared to be strongly anion-selective, rectifying, phosphatase-activated and inhibited by DNDS (4, 4'-dinitrostilbene-2-2'-disulphonic acid) and calixarene (Edwards et al., 1998).

Functional characterisation of p64 revealed that channel activity is regulated by $p59^{fyn}$, a member of the src family of tyrosine kinases (Edwards & Kapadia, 2000). Tyrosine 33 was identified as the necessary amino acid residue for SH2 binding. It was shown that phosphorylation of p64 (by Fyn kinase itself or by unidentified tyrosine kinase) had a positive effect on p64 channel activity by enhancing the Cl^- efflux rate. Thus, activation of p64 channel activity by $p59^{fyn}$ requires the presence of Fyn tyrosine kinase and phosphorylation of p64 at tyrosine 33. However, it is not clear whether phosphorylation of p64 is sufficient, or whether subsequent binding of phosphorylated p64 to Fyn-SH2 is important for its activation (Edwards & Kapadia, 2000).

1.10.2 CLIC1

Rat brain p64H1 was the first homologue of p64 to be identified (Howell et al., 1996) and characterised (Duncan et al., 1997), but its human (Edwards, 1999) and murine (Ferenandez-Salas et al., 1999) homologues were named CLIC4 rather than CLIC0. Human CLIC1 was cloned serendipitously from a monocytoid blood cell line on

screening for PKC-activated genes (Valenzuela et al., 1997). It was also designated as NCC27 (nuclear chloride channel of 27 kDa molecular mass) (Valenzuela et al., 1997), and p64CLCP. Northern blot analysis showed wide distribution of its mRNA in various cells and cell lines (Valenzuela et al., 1997). The gene for CLIC1 was located to 6p22.1-p21.2. (Chromosome 6), encoding 241 amino acids (molecular mass of 27.8 kDa) with a pI of 4.85. It shares about 60% homology with the C-terminal region of bovine p64 (CLIC5B) (fig 1.7).

CLIC1 was shown to be present as both soluble and integral membranous forms in the cells (Valenzuela et al., 1997). It was localised principally to the nucleus and nuclear membrane in Chinese hamster ovary (CHO) cells (Valenzuela et al., 1997), the brush border of renal proximal tubule (Tulk and Edwards, 1998), the cytosol of trophoblast but not in the nucleus (Berryman and Bretscher, 2000), nuclear membrane in human hepatocellular carcinoma (HCC) cells (Huang et al., 2004), and small vesicles surrounding osteoclast nuclei (Schaller et al., 2004). CHO cells transfected with CLIC1 revealed increased levels of Cl^- channel activity by patch-clamp recording (Valenzuela et al., 1997). The conductance of CLIC1-associated channels was Cl^--dependant (Tonini et al., 2000) and was 21 pS with a Km of about 40 mM. Antibodies recognizing FLAG-epitopes at either the N- and C-terminus of CLIC1 inhibited its channel activity when added to the external surface of the N-terminal tagged protein or the cytoplasmic face of the C-terminal tagged protein (Tonini et al., 2000). This was the first experiment to reveal that CLIC1 spans the membrane an odd number of times and some of its C-terminal sequence lies in the cytoplasmic side.

Currents could also be recorded from non-transfected cells following nuclear membrane fragmentation during the G2/M phase of mitosis (Valenzuela, 2000). CLIC1 could be reversibly inhibited by 10 μM IAA-94, unlike IAA affinity-purified p64 related channels. CLIC1 proteins were shown to form channels *in vitro* in the absence of detergents by two independent groups (Tulk et al., 2000; Tulk et al., 2002; Harrop et al., 2001). Purified, solubilised CLIC1 proteins were monomeric and showed channel-like activity in asolectin liposomes in the absence of detergents (Tulk et al., 2000; Tulk et al., 2002; Warton et al., 2002). They failed to form channels without acidic lipids in PC liposomes (Tulk et al., 2002). The single-channel conductance was however inconsistent between various groups, 67 or 160 pS in symmetrical 150 or 300 mM KCl respectively (Tulk et al., 2000; Warton et al., 2002), well above the limiting conductance of about 20 pS in CLIC1 transfected cells (Tonini et al., 2000).

The oxidised form of CLIC1 was shown to form an ion channel but reduced CLIC1 failed to insert into bilayers (Littler et al., 2004). In the same study it was shown that cysteine 24 (C24) and C59 were essential for channel activity. Channels obtained from strongly oxidised proteins were presumably oligomerised before insertion. Similarly residues equivalent to Cys 59 are not conserved in all CLIC family members and hence this effect is limited to CLIC1 only. This variation between conductances and differences in channels formed under various redox conditions are addressed in Results chapter 4. The channels were inhibited by pre-treatment with reduced or oxidised glutathione or alkylation with N-ethyl maleimide (NEM).

Sub-nuclear relocalization of CLIC1 was induced by insulin, and hence CLIC1 was shown to be a novel downstream effector of insulin signalling in human hematopoietic cells (Saeki et al., 2004). It was shown that beta-amyloid (Abeta) protein (Aβ) stimulation of neonatal rat microglia specifically increases CLIC1 protein expression and in turn increases the functional expression of CLIC1-mediated chloride conductance. CLIC1 protein expression in microglia increased after 24 hr of incubation with $A\beta_{25-35}$ (and $A\beta_{1-42}$) simultaneously with the production of reactive nitrogen intermediates and of tumor necrosis factor-alpha (TNF-alpha) (Novarino et al., 2004). The CLIC-blocker IAA-94 prevented the apoptosis of neurons co-cultured with Aβ-treated microglia. Knocking down CLIC1 expression by siRNA prevented TNF-α release induced by Aβ stimulation. This provided a direct link between Aβ-induced microglial activation and CLIC1 functional expression.

The crystal structure of the soluble form of CLIC1 (1.4Å) (Harrop et al., 2000) revealed a glutaredoxin fold typical of the omega class GSTs (Board et al., 2000; Dulhunty et al., 2001), a putative GSH α/β N-terminal binding domain, and an all α-helical C terminal domain (fig 1.8a). Hence, CLIC1 must undergo a major structural rearrangement to unfold and insert into the membranes to form functional channels. CLIC1 was also shown to undergo a reversible transition from a monomeric to a non-covalently linked dimeric state mediated by a C24-C59 intramolecular disulfide bond (Littler et al. 2004).

CLIC1 and CLIC2 were shown to interact with sedlin in a yeast-two-hybrid system.

A). CLIC1

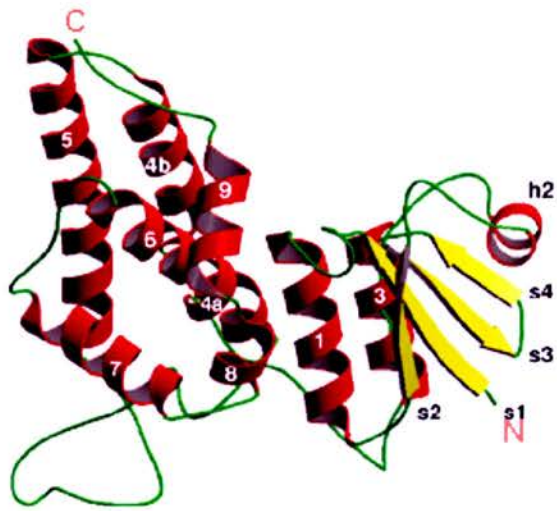

B). CLIC4

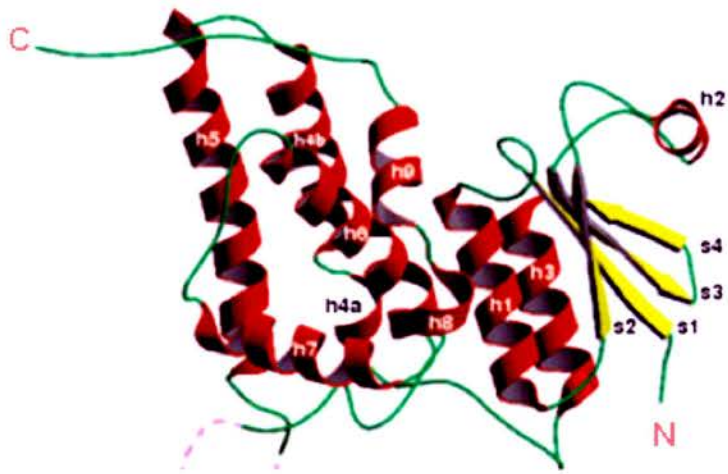

Fig 1.8. Crystal structures of soluble CLIC1 and CLIC4 proteins. Crystal structure of soluble CLIC1 (Harrop et al., 2001) and CLIC4 (Littler et al., 2005) proteins showed that they have 4 β-strands (yellow in CLIC1) and 10 α-helices. The putative trans-membrane domain is in the N-terminus region and it comprises of an α-helix and a β-strand in the soluble form. In CLIC4 the last two residues of the wild-type CLIC4 were replaced by a 16 residue peptide that promoted crystallisation.

This interaction of membranous proteins might be important for either functioning of TRAPP (transport protein particle) complex or the proper targeting and functioning of CLICs. It was further indicated that the region between 138 and 201 of CLIC1 was sufficient to bind sedlin in *vitro* and *in vivo* by co immunoprecipitation (Fan et al., 2003).

Transgenic mice lacking CLIC1 appear to be essentially normal apart from increased weight, splenomegaly, and mild thrombocythaemia. This result shows that in mammalian cells expressing multiple CLIC proteins, some or all of their functions may be redundant (Qiu, 2003).

1.10.3 CLIC2

CLIC2 was identified during transcriptional analysis of the IP2 (incontinentia pigmenti) region Xq28 (Rogner et al., *1996*) of the human X chromosome, as a potential candidate gene for a number of diseases linked to this region. It is 27.8 kDa, comprises of 243 amino acids having a pI of 5.24 (Heiss and Poustka., 1997) and the predicted protein is 60% identical to CLIC1. CLIC2 is expressed in foetal liver, adult skeletal muscle and spleen (Heiss and Poustka., 1997; Rogner et al., 1996). Five orthologs of CLIC2 were shown in *Canis familiari* (Dog), *Rattus norvegicus* (Rat), *Galus gallus* (chicken), *Drosophila melanogaster*(fruit fly) and *Anopheles gambiae* (mosquito). CLIC2 is down-regulated in radioresistant oesophageal sublines (Fukuda et al., 2004). Recently it has been shown that CLIC2 is one of the few physiological regulators of native cardiac ryanodine-sensitive Ca^{2+}-release channels RyR2

channels (Board et al., 2004). Recombinant CLIC2 increased [^{3}H]ryanodine-binding to native and purified RyR channels, enhanced the substate activity of individual channels and increased gating events associated with RyRs (Dulhunty *et al: 2005*). It inhibited RyR activity only when added to the *cis* (cytosolic) but not to the *trans* (luminal) side of RyR channels. CLIC2 was also shown to decrease the ATP-activation of RyR2 channels. It further depressed channel activity in the presence of 100 μM cytoplasmic Ca^{2+}, and the action of CLIC2 on RyR2 channels did not depend on modifying the redox state of the channels. It was shown that CLIC2 have the potential to prevent Ca^{2+} store depletion in the heart (Dulhunty et al., 2005).

1.10.4 CLIC3

CLIC3 is present on chromosome 9 at loci 9q34.3, and contains 236 amino acids, with a calculated mass of 26.7 kDa and a pI of 6.34. Human CLIC3 was isolated during a yeast two-hybrid screen using the cytoplasmic tail of extracellular signal-regulated kinase 7 (ERK7), a member of a mitogen-activated protein (MAP) kinase family (Qian et al., 1999). It was also identified with 30 regulated kruppel-like factor 6 (KLF6) growth suppressive target genes by microarray (Reeves et al., 2003). CLIC3 is approximately 49% and 61% identical to CLIC1 and CLIC2, respectively. It has a conserved transmembrane domain, N-terminal and central phosphorylation sites and an N-terminal N myristoylation site. Northern blot analysis has revealed expression of a 1.15 kb transcript in placenta, heart and lungs. It is also expressed at much lower levels in skeletal muscle, kidney, and pancreas, but could not be detected in brain. CLIC3 was also shown to interact and co-localise with ERK7 in nucleus but

it is not a substrate for ERK7. CLIC3 is expressed in the cytoplasm and hence it is predicted to function independently of ERK7.

Over-expression of CLIC3 in LTK cells (murine fibroblasts) resulted in an increase in whole-cell anionic currents. On reducing the concentration of extracellular Cl^- from 152.5 mM to 22.5 mM, outward currents at positive potentials were reduced (Qian et al., 1999). CLIC3-related channel activity was not examined in detail. CLIC3 must have been miscloned because it lacked the predicted N-terminal region (Qian et al. 1999) and hence this raises doubts about the identity of the channels recorded from cells transfected with a recombinant version of the defective protein (Qian et al., 1999). The nuclear localisation signal KKYR is not present in CLIC3, but it could be transported into the nucleus along with other proteins such as ERK7. The functional consequences of the interaction between CLIC3 and ERK7 are not yet clear. CLIC3 was recently shown to be localised to the cytoplasm, nucleus and membranes of syncytiotrophoblast and villous cytotrophoblast cells (Money et al., 2006).

1.10.5 CLIC4 (p64H1)

Amongst several CLIC family members, the biological activity of CLIC4 has been studied most extensively. CLIC4, also called mtCLIC, HuH1 and p64H1, was the first homologue of p64 to be identified (Howell et al., 1996) and cloned (Duncan et al., 1997) as a potential p64 homologue and candidate for the intracellular anion channel co-localised with brain ER ryanodine-sensitive Ca^{2+}-release channels

(Ashley, 1989). CLIC4 was mapped to chromosome 1p36.11 which encodes a predicted protein of 253 residues with a calculated mass of 28.6 kDa and a pI of 5.42 (for the human isoform).

CLIC4 lacks a signal sequence, like other family members, and is distributed as both a soluble and an intracellular membrane protein (Duncan et al., 1997; Edwards, 1999; Fernandez-Salas et al., 1999). It is expressed in a wide range of tissues and is highly-conserved across species. In addition to brain and kidney, CLIC4 mRNA is ubiquitously expressed in many other mammalian tissues including lung, liver, skeletal muscle, testis and skin (Duncan et al., 1997; Edwards, 1999; Chuang et al., 1999; Fernandez-Salas et al., 1999; Berryman & Bretscher, 2000; Berryman & Goldenring, 2003). The intracellular localisation of CLIC4 varies considerably among different cell lines and tissues (Edwards, 1999; Berryman & Goldenring, 2003), plasma membrane and intracellular organelles (including inner mitochondrial membranes) (Fernandez-Salas et al., 2002), caveolae and trans-Golgi network (Edwards, 1999), endoplasmic reticulum (Duncan et al., 1999), and large dense-core vesicles (Chuang et al., 1999). CLIC4 was also shown to form complexes with β-actin, tubulin, dynamin I, 14-3-3 isoforms, and other unidentified proteins (Edwards, 1999; Suginta et al., 2001; Shanks et al., 2002) and cytoplasmic CLIC4 has been shown to co-localise with A-kinase anchoring proteins (AKAPs) in specific cellular microdomains, including centrosomes and the cortical actin cytoskeleton. It translocates into the nucleus by multiple stress inducers, possibly by means of an internal nuclear localisation signal 199KVVAKKYR206 (Suh et al., 2004).

CLIC4 isologues are highly-conserved in vertebrates ranging from fish to mammals. CLIC4 is expressed during embryogenesis of *Xenopus laevis* and it is developmentally regulated (Shorning et al., 2003). In mammalian cell lines, increase in the gene expression of CLIC4 is linked to the differentiation of murine keratinocytes (Fernandez-Salas et al., 2002) and adipocytes (Kitamura et al., 2001) as well as TGF-β1-mediated transdifferentiation of fibroblasts into myofibroblasts (Ronnov-Jessen et al., 2002). Increased or reduced expression of CLIC4 induces apoptosis in various cell types. These results indicate that CLIC4 is involved in both keratinocyte differentiation and carcinogenesis (Fernandez-Salas et al., 1999; Fernandez-Salas et al., 2002; Chen et al., 2004; Suh and Yuspa, 2005). However, the functional role of CLIC4 in differentiating keratinocytes is not known. It has not been studied how the subcellular localisation of CLIC4 (including phosphorylated CLIC4) contribute towards differentiation or apoptosis.

A number of studies have been carried out to determine the channel properties of CLIC4. Patch-clamp studies of CLIC4-associated plasma membrane channel activity in transfected human embryonic kidney (HEK-293) cells revealed an association of CLIC4 with anion channel activity (Proutski et al., 2002). The single-channel conductance in choline Cl^- (300 mM choline Cl^- in the pipette and 140 mM choline Cl^- in the bath) was around 1 pS. This channel activity was abolished by an antibody directed against an epitope fused to the C-terminus of CLIC4, or by an anti-CLIC4 antiserum that cannot recognise the N-terminus, added from the cytoplasmic side (Proutski et al., 2002). Reconstitution of microsomal membrane vesicles containing recombinant CLIC4 into bilayers showed a 10 pS channel (Duncan et al.,

1999). The reason for the difference between these two conductances was not clear. This has been addressed in results section in chapter 4.

The structure of a soluble form of human CLIC4 (fig 1.8b), crystallised with a short random C-terminal extension, is similar to CLIC1 (Littler et al., 2005; Harrop et al., 2001), as predicted by modelling CLIC4 onto CLIC1 (Ashley, 2003). Like soluble CLIC1, CLIC4 is monomeric and has an Ω-glutathione-S-transferase (GST) fold. There is no Cys residue equivalent to Cys 59 of CLIC1 in CLIC4 which rules out the possibility of the formation of an intramolecular disulphide bond (Cys24- Cys59) (Littler et al., 2005). Later, another group has shown a trimeric organization for CLIC4 (Li et al., 2006).

1.10.6 CLIC5 (CLIC5A)

The gene for CLIC5 was mapped to chromosome 6p21.1-p12.1 based on similarity between the sequence of CLIC5 and chromosome 6 clone RP3-447E21 (Berryman and Bretscher, 2000). The primary RNA transcript of the clic5 gene is subjected to alternative splicing at the first exon to give rise to two distinct mRNAs that encode CLIC5A and CLIC5B (p64).

CLIC5 was isolated from extracts of placental microvilli as a component of a multimeric complex consisting of several cytoskeleton proteins (Berryman and Bretscher, 2000). Human CLIC5 was pulled down with actin and other proteins from human placenta by actin-binding regions of the C-terminal domain of the AKAP

ezrin (Berryman and Bretscher, 2000). The cDNA of CLIC5 encodes a predicted protein of 251 residues with a calculated mass of 28K and pI of 5.44. CLIC5 is 76%, 52%, 66% and 63% identical to CLIC4, CLIC3, CLIC2 and CLIC1, respectively. CLIC5 is 91% identical to residues 197-437 of bovine p64. By northern blot analysis, CLIC5 was shown to be expressed as a major 6.4 kb transcript and, minor 3.8 and 2.3 kb transcripts, in heart and skeletal muscles, with moderate levels in kidney, lung and placenta. It has a highly conserved hydrophobic domain in the N-terminus region and 3 conserved tyrosines involved in nuclear internalization signal motifs.

CLIC5 associates with the microvillus cytoskeleton, either binding to actin directly or to ezrin-associated actin or other ezrin-bound proteins (Berryman and Bretscher, 2000). Immunoflourescence microscopy has demonstrated the highest expression of CLIC5 on the apical surface of trophoblast epithelium (Berryman and Bretscher, 2000). In human JEG 3 choriocarcinoma cells, CLIC5 was localised to the apical region where it also co-localised with ezrin in microvilli (Berryman et al., 2004). It was further shown that the predicted TMD along with the C terminus is required for microvillar localisation of CLIC5 (Berryman et al., 2004). Anion transporting activity associated with CLIC5A (Berryman et al., 2004) was not convincing as the efflux rate was very low for an ion channel and it failed to form channels in transfected JEG3 cells. This may be due to low expression of CLIC5 or exclusion of the protein from the plasma membrane, or may be due to lack of a specific stimulus for activation of the channels.

1.10.7 CLIC6 (Parchorin)

CLIC6 is present in the conserved gene cluster ACD21 [i.e., AML (Acute Myeloid Leukemia)/CLIC/DSCR-1 (Down Syndrome Candidate Region 1-like) like], whereas CLIC4 and CLIC5 are present within ACD1 and ACD6, respectively, according to their chromosomal localizations (Strippoli et al., 2002). Phylogenetic analysis of the ACD family suggests that the ACD segment on human chromosome 21 is the most ancient. CLIC6 is localised to loci 21q22.12 and encodes 704 amino acids (73 kDa) with a pI of 4.23 (Griffon et al., 2003). CLIC6 was also called CLIC1L as a partially predicted DNA in the initial annotation of chromosome 21 sequence (Hattori, 2000). CLIC6 is the longest identified member of the CLIC family. The high level of amino acid conservation between human CLIC6 and parchorin suggests the rabbit protein is the orthologue of human CLIC6. CLIC6 is widely expressed in water secreting cells, endocrine cells, astrocytes, and Purkinje cells. It is also expressed in placenta, pancreas, liver and brain (Nishizawi et al., 2000; Mizukawa et al., 2002; Griffon et al., 2003).

Parchorin (the rabbit orthologue of CLIC6) exists mainly in the cytosol in COS7 cells, and is translocated to the apical membrane fraction when acid secretion is activated. Its cDNA was first cloned from rabbit choroid plexus (Nishizawa et al., 2000). It was identified as a 120 kDa protein and hence called pp120 (Urshidani et al., 1999). It was highly enriched in tissues associated with water transport, including **par**ietal cells and **chor**oid plexus, and hence named parchorin. Immunohistochemically, parchorin was shown to be present in the ducts of

lachrymal parotid, submandibular, mammary glands, pancrease, prostate, testis and various other tissues. Expression of parchorin increases in rabbits with lactating mammary glands and in pregnant rabbits (Mizukawa et al., 2002). The wide distribution and changes in expression level of parchorin suggest that it plays an important role in multiple cellular processes.

CLIC6 differs from previously-described CLICs (CLIC1-5) in two essential features, it is significantly longer than other members (704 amino acids and 637 amino acids respectively compared to an average of 271± 80 for other CLICs) and the first exon contains a 408 nucleotide GC rich segment (76% GC), which encodes 14 copies of the AEGPAGDSVD consensus decapeptide repeat. The mouse orthologue of CLIC6 is expressed in brain, stomach, lung, kidney, testis, eyes and in the embryo. CLIC6 was also shown to be expressed in mouse E14.5 digestive tract and was predicted to have a role in Down's syndrome gastrointestinal abnormalities (Reymond et al., 2002). In Cos7 and MDCK cells, CLIC6 was shown to be localised to the cytoplasm and perinuclear structures. Voltage-clamped oocytes injected with CLIC6 and transiently transfected MDCK cells fail to show any novel currents. This may be attributed to an intracellular localisation, a requirement for additional subunits, an absence of ligand or complete absence of channel formation (Friedli et al., 2003). Yeast two-hybrid screens have shown that the C-terminal tails of dopamine D_2-like receptors, D_2R, D_3R and D_4R bind to CLIC6. Co-expression of CLIC6 with myc D_3R resulted in co-localisation of both proteins at the plasma membrane in HEK293 cells. However, CLIC6 did not show channel-like activity or chloride-efflux when chloride sensitive fluorophore MQAE was used to monitor the intracellular concentration of

Cl^- by spectrofluorimetry in CHO cells stably-expressing various combinations of Xpress/His-CLIC6, D_2R and D_3R (dopamine-receptors) (Griffon et al., 2003).

1.10.8 Invertebrate CLICs

1.10.8.1 *Dm*CLIC

Drosophila has a single CLIC-like gene which is present on the X chromosome (12C5-6) (www.flybase.org). Mutant flies created by P-element insertion have a 60-70% shorter lifespan than wild type flies and demonstrate a dosage-dependent hypersensitivity to oxidative stress (Berryman & Tanda, 2005).

1.10.8.2 *C. elegans* CLICs

Two orthologs of CLICs identified in *C. elegans* are *exc4* and *exl1* (exc4 like). They encode EXC-4 and EXL-1, respectively. EXC4 is a 33.7 kDa protein containing 290 amino acids and has a pI of 6.35. EXL-1 is 28 kDa protein, which is 238 amino acids long with a pI of 4.32. EXC-4 is required at the luminal membrane of the excretory cell to establish tubular architecture following development (Berry et al. 2003). In the absence of exc4 worms show a cystic malformation in the unicellular excretory canals.

Recently, the putative transmembrane domain and a minimal region required for insertion and functioning of EXC-4 and CLICs were mapped using an *in vivo* assay

in *C. elegans* (Berry and Hobert, 2006). The first 66 amino acids of the N-terminus region containing the putative transmembrane domain were shown to be key determinants of localisation and function of EXC-4. The expression of EXC-4 and EXL-1, and their localisation, overlap in intestinal cells. These proteins localize to lysosomal membranes and to the luminal membrane of the intestine.

1.10.9 CLICs in plants

The flow of ions and electrical signals control various processes involved in the growth of plants, and in adaptation to frequently changing environmental conditions. These processes depend on the combined action of receptors, ion channels and pumps. At present, most of the ion channels cloned in *Arabidopsis* sp. rely essentially on sequence homologies with animal channels. The shaker-like K^+ channel family is the only ion channel which is well characterised, at the molecular and physiological levels in plants.

Chloride is most dominant anion in plants and is involved in many physiological processes in plant cells. It is transported across the plasma membrane and endomembranes of plant cells. *Arabidopsis thalaiana* chloride intracellular channel (At-CLIC), which is a homolog of CLIC1, was identified and cloned recently (Elter et al., 2004). HEK293 cells transfected with At-CLIC showed an increased plasma membrane chloride conductance. At-CLIC is 26% identical to human CLIC1. GFP chimeras of At-CLIC have shown membrane localisation in HEK293 cells.

1.11 Ion channels in Planar Lipid Bilayers

Artificial lipid bilayers are common tools for the study of the molecular mechanisms of ion transport properties of cell membranes. Single-channel recording with artificial planar lipid bilayers has been applied to various types of channel proteins in order to study their physiological and pharmacological properties. This technique facilitates the measurement of the properties of intracellular ion channels. It provides the flexibility to change the channel environment by changing the experimental conditions such as the concentration of ions in aqueous solution, lipid contents in the membranes and redox potential, etc.

Planar lipid bilayers capable of ion channel insertion can be produced either by the painting technique (Mueller et al., 1962), or from lipid monolayers spread at the air buffer interface (Montal and Mueller, 1972). Lipids are generally suspended in a solvent like n-decane at appropriate concentrations for painting bilayers. These bilayers are thinned to an appropriate capacitance and monitored either by microscope and/or by capacitance measurement. The lipid bilayer is very thin (~50 Å) and the light reflected from the front and rear liquid/membrane interfaces undergoes destructive interference so that the membrane reflects no or very little light and thus it appears black. For this reason the planar bilayer is referred to as a "black membrane" or BLM (black lipid membrane). The two aqueous compartments separated by the lipid film are defined as *cis* and *trans* compartments. The electrodes (Ag^{2+}/AgCl) in both chambers are connected through 3M KCl agar bridges, to minimise the junction potentials. Both chambers are provided with stirring facilities.

A).

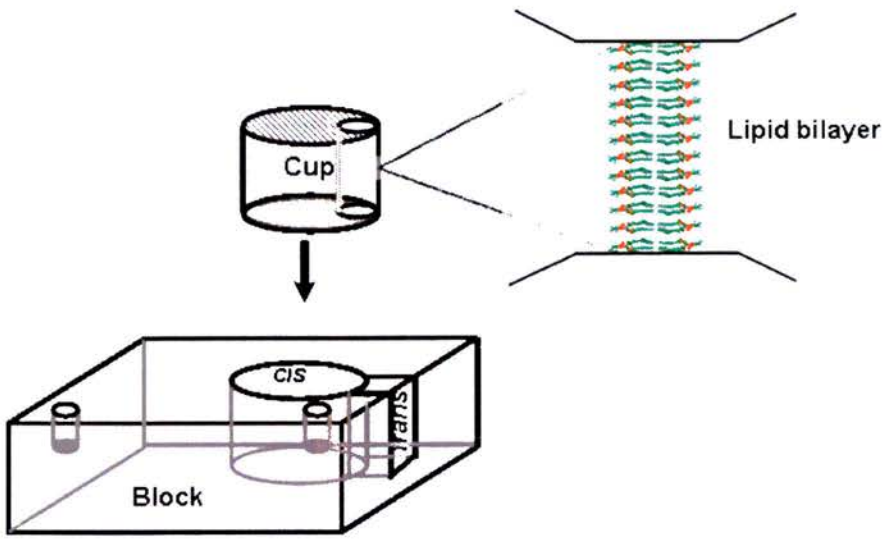

B).

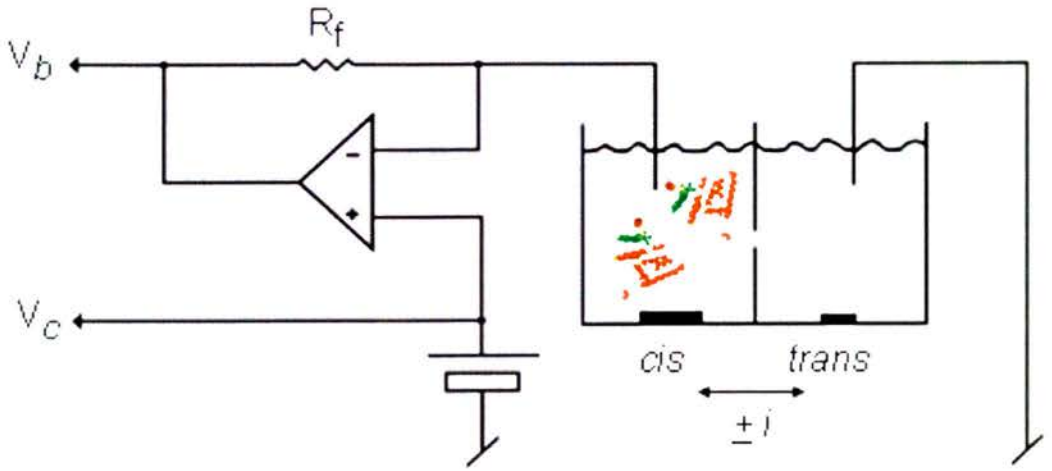

$\Delta V = V_c - V_b = iR_f : i = \Delta V/R_f$

Fig 1.9. Channel reconstitution. (A) The block contains a chamber (*trans*) where a cup containing a well (*cis*) fits inside the cavity. The face of the cup contains a small hole (~300 μm in diameter) where lipids suspended in n-decane are painted. In addition to the chamber, the block also contains two small wells which are filled with electrolyte solution and provide a means of coupling the *cis* and *trans* chambers to the amplifier through agar bridges and Ag^{2+}/AgCl electrodes. (B) CLIC proteins were always added to the *cis* chamber which is voltage-clamped at a given potential (V_c) relative to the *trans* chamber, which is grounded, by using an operational amplifier (opamp) configured as a current-to-voltage convertor. When the channel opens the opamp attempts to keep potentials at its non-inverting (+) and inverting (-) inputs the same, i.e., set to V_c by adjusting the output or backoff potential (V_b) applied to the feedback resistor R_f (10 GΩ). Channel blockers, modifiers and antibodies were added as required (figures redrawn from Ashley, 1995).

The schematic representation of the bilayer system and the basic circuit diagram of the negative feedback voltage-clamp mechanism is shown in fig 1.9.

1.12 Aims of the project

Over the past decade, extensive work related to the molecular and biochemical characterisation of CLICs has been carried out. The soluble structures of CLIC1 and CLIC4 are known, and they show remarkable similarities. A number of homologues have also been identified since the discovery of p64 and CLIC4 (p64H1). However, the molecular basis of the cellular localisation and functions of CLICs are not yet clear. Also, although purified proteins appear to form anion channels in artificial membranes, their single-channel properties have been inconsistent between different groups.

The main aims of this project were to express and purify selected soluble mammalian CLIC proteins, and reconstitute them in planar lipid bilayers to investigate and compare the ion channel functions of these novel autoinserting ion channel proteins, including detailed studies of their conductance and selectivity. Very limited information was available at the outset of the project on the regulation and modulation of CLIC channels, and this will be addressed in subsequent chapters. In addition, regulation of channel activity by cytoskeletal actin was investigated.

The known redox-sensitivity of the channels was also investigated and it was discovered that the channels are tightly-regulated by the external redox potential in

the presence of physiological glutathione buffers. This work was extended by carrying out preliminary patch-clamp studies on CLIC-transfected HEK-293 cells. Finally, these structure/function studies were extended by reconstituting truncated versions of CLIC1 and CLIC4 in an effort to identify the pore-forming region of the proteins.

CHAPTER 2

MATERIALS AND METHODS

2.1 General reagents

Chemicals used in the laboratory were of the highest grade and purchased from Sigma-Aldrich Company Ltd. (Dorset, UK), except where otherwise stated.

2.1.1 Molecular biology reagents

Abcam Limited, Cambridge UK

Agarose

Amersham Biosciences Ltd, Bucks, UK

Benzamidine sepharose™ 4B fast flow beads

Glutathione sepharose™ 4B beads

Membranes for Western blotting and ECL detection kit

Bioline Ltd. London UK

Covalent non-isotopic chemiluminescent reagent

Eppendorf, Cambridge UK

The Perfectprep® Gel Cleanup Kit

Fermentas

Restriction enzymes

Helena Biosciences Europe, Sunderland, Tyne & Wear, UK

Hyperladder^{Tm} I quantitative DNA ladder

Merck Biosciences Ltd., Beston, Nottingham, UK

Mowiol 4-88 reagent

MWG Biotech AG, Ebersberg, Germany

PCR Primers, Sequencing of DNA

New England Biolabs, Herts, UK

Restriction enzymes

Pharmacia Biotech, Cambridge, UK

Deoxyribonucleotide triphosphates

Promega Ltd., Southampton, UK

Restriction enzymes, T4 DNA ligase, DNA Polymerase

QIAGEN Ltd. Dorking Surrey, UK

QIAprep® HiSpeed^{TM} Plasmid Midi Kit

Ni-NTA Agarose

Roche, Lewes, East Sussex, UK

Dpn I, Complete protease inhibitor tablets

2.1.2 Antibodies

Molecular Probes Inc., Eugene, OR, USA

Donkey Anti-Goat IgG (H+L), Alex Fluor 488 (anti-rabbit) and 568 (anti-mouse).

Santa Cruz Technologies

Anti-Dynamin I antibodies (sc 6-402)

2.1.3 Lipids

Sigma Aldrich Chemical Company, Dorset, UK

Soybean lecithin (Type IV)

Avanti Polar Lipids, Albama, USA

Diphytanoylphosphatidylcholine (DPhPC),

Palmitoyl-oleoyl phosphatidylcholine (POPC),

Palmitoyl-oleloyl phosphatidylethanolamine (POPE),

Palmitoyl-oleoyl phosphatidylserine (POPS) and Cholesterol.

2.1.4 Culture media

Difco Laboratories Surrey UK

All media components for bacterial cell culture. Media were prepared according to standard recipes (Sambrook et al., 1989), except where indicated.

GIBCO BRL, Life technologies, Paisley UK

All reagents and media for mammalian cell culture, DMEM, MEM, FCS and Trypsin-EDTA.

2.1.5 Bacterial strains

DH5α *supE44ΔlacU169 (Φ80 lacZΔM15) hsdR17recA1 endA1 gyrA96 thi-1 relA1*

BL21 (DE3) *hsdS gal (λcIts857ind1Sam7nin5 lacUV5-T7gene1)*

2.2 Standard DNA manipulations

Protocols used for various experiments were as described (Sambrook et al., 1989). These included extraction of nucleic acids (2.2.1 and 2.2.2), nucleic acid preparation (2.3), agarose gel electrophoresis (2.3.7) and restriction endonuclease digestion (2.2.5).

Isolation of high quality plasmid DNA from *E.coli* cell lysate is used for many clinical and laboratory based applications. The alkaline lysis method is used for isolating plasmid DNA as it is a fast, reliable and relatively clean way to isolate DNA from cells. It depends on the unique property of the plasmid DNA to rapidly anneal after denaturation which allows it to be separated from chromosomal DNA.

2.2.1 Miniprep alkaline lysis

Individual bacterial colonies were inoculated, using a sterile pipette tip, into 5 ml LB medium containing a suitable selective marker (antibiotic), and incubated at 37°C with 250 rpm shaking overnight. An aliquot of 1.5 ml of each culture was transferred into a 1.5 ml micro centrifuge tube, and centrifuged in a table-top centrifuge at 8000 rpm for 1 min. The LB broth was completely aspired from the pellet, which was resuspended by vortexing in 250 µl of solution I (10 mM Tris-EDTA, 0.1 mg/ml RNase A, pH 8.0). After 5 min incubation at room temperature, 250 µl solution II (0.2 M NaOH, 1% SDS) was added, and the solutions were mixed by inverting 3-4 times. Within 5 minutes of this, 300 µl of solution III (3 M KOH, 5 M acetic acid) was added, and the solutions were mixed by inverting for 3-4 times. The solutions were centrifuged at 12000 rpm for 10 min, and the supernatant was transferred to fresh tubes, to which 400 µl of chloroform was added. These were vortexed and spun at 12000 rpm for 1 min. The upper aqueous phase of the supernatant was transferred to a fresh tube. An equal volume of ice cold isopropanol was added to precipitate the DNA. The mixture was spun at 12000 rpm for 10 min at 4°C. The supernatant was discarded and the pellet was washed in 200 µl of ice cold 70% ethanol and centrifuged at 12000 rpm for 5 min at 4°C. The pellet was air-dried and resuspended in 50 µl of Tris-EDTA buffer.

2.2.2 Midi preparation

Midipreparation of DNA (with a maximum yield of 200 µg) was carried out using the QIAprep® HiSpeed™ Plasmid Midi Kit according to the manufacturer's instructions.

2.2.3 Quantification of DNA

The accuracy and precision of DNA quantification is a critical factor for efficient use of the DNA samples in various applications. UV absorbance spectroscopy is reliable and the fastest method of DNA quantification. A 1/200 dilution of the DNA sample was prepared and its' absorbance measured at 260 and 280 nm using a UV spectrophotometer. Purity was assessed using the ratio of A260/A280; an ideal ratio of 1.8 indicated pure dsDNA, whereas lower ratios were indicative of contamination with other nucleic acids or proteins (Sambrook et al., 1989). To calculate the concentration, where an OD 260 of 1 indicates DNA at a concentration of 50 µg/ml, the following formula was used:

$$[\text{DNA}]\ (\mu g/ml) = \text{OD260} \times 50\ \mu g/ml \times \text{dilution factor} \qquad [1]$$

2.2.4 PCR (Polymerase Chain Reaction)

PCR is a technique to enzymatically amplify the DNA (Mullis et al., 1986) without using any living system. A small amount of DNA can be amplified exponentially,

which is used for various applications such as cloning of genes, diagnostics of genetic diseases etc.

PCR for gene amplification and site directed mutagensis was performed on an Applied Biosystems GeneAmp PCR system 9700 PCR machine. General conditions are listed here, and the concentrations used for specific constructs are listed in appendices.

2.2.4.1 Standard PCR conditions

PCR was generally carried out in 50 µl reactions, containing 10 ng of template DNA, 1 U of Pfu DNA Polymerase (Promega), 1X reaction buffer (Promega), 0.2 mM each of dNTPs (Promega) and 25 pmols each of forward and reverse primers (MWG Biotech). Reactions were generally run for 30 cycles, using annealing temperatures appropriate to the primers calculated Melting temperature (Tm) (assessed using the formula Tm = 4x (G+C) + 2x (A+T)) and extension phases according to length of the amplicon, approximately 2 min per kb.

2.2.4.2 Site-Directed Mutagensis (SDM)

In site-directed mutagenesis, a mutation is generated in a specific site of the DNA molecule. It is based on the principle of PCR that after the first cycle the template and the molecule containing the target mutation will be at equal concentration. The molecule containing the target mutation will outnumber the original template after 25

cycles in the ratio of 8 million to 1. The template DNA molecule can be digested by Dpn I which cleaves only the methylated DNA.

Mutations in the targeted DNA were generated by using two overlapping primers containing the desired mutations (Chen and Przybyla, 1994).

The target ORF present in the pHis-8 vector was used as a template (10 ng) in a 50 µl reaction mixture containing 25 pmol each of forward and reverse primers containing the desired mutations, 3 U of Pfu polymerase (Promega), 1X buffer (Promega) and 0.2 mM dNTPs (Promega). A 5 min denaturing hold at 95°C was followed by 25 cycles of 30 s at 95°C (for denaturation), 30 s at the specified annealing temperature and 5-7 min for DNA extension at the calculated temperature. A final extension of 7 min was carried out. Samples were collected after 12 cycles and digested with Dpn I at 37°C for 1 hr. The positive constructs were transformed into bacteria. The ORF was recloned into a new vector to avoid unwanted mutations in the vector.

2.2.5 Restriction digestion

Restriction digestion, also known as DNA fragmentation, uses restriction enzymes to digest DNA into shorter fragments at specific nucleotide sequences. Digested DNA can be used for cloning or analytical purposes.

DNA (0.2-1 μg) was digested by restriction endonucleases to generate compatible ends for designated vectors, in 30 μl reactions containing 2-5 U of the respective restriction enzyme (Promega, Roche, Fermentas, NEB) in the appropriate buffer (Promega, Roche, Fermentas, NEB) diluted to 1x with DEPC water. Reaction mixtures were incubated at the optimum temperature (generally 37°C) for 1-4 hr. Where two restriction enzymes were used, the digestion reactions were performed sequentially.

2.2.6 Gel purification

DNA bands were excised from agarose gel stained with ethidium bromide and purified using the DNA- binding Perfectprep™ Gel Cleanup Kit (Eppendorf), according to the manufacturer's instructions. DNA was eluted in the smaller recommended volume of 30 μl.

2.2.7 DNA agarose gel electrophoresis

DNA agarose gels were prepared by mixing 1% (w/v) agarose powder in 1XTBE (45 mM Tris-borate 1 mM EDTA) and heating until the agarose was dissolved (the percentage of agarose gels was varied depending on the size of the DNA). The agarose was cooled before adding 0.5 μg/ml ethidium bromide, poured into moulds and allowed to set at room temperature. DNA samples were mixed 1:1 with loading buffer (75 mM Tris-HCl pH 7.6, 30% (v/v) glycerol, 1.25 mg/ml bromophenol blue) and loaded into the wells along with suitable DNA standard ladders. Electrophoresis

was carried out at 150 V using a Biorad PowerPac 3000, in a Biorad Mini-PROTEAN® 3 cell buffer tank containing 1XTBE. Gels were examined on a UVP GelDoc UV transillumination.

2.2.8 Phosphatase treatment

To prevent re-ligation and to reduce the probability of false positives, phosphate groups were removed from the cut ends of vectors using Calf intestine alkaline phosphatase (Helena Biosciences) 1 U/pmol end of vector, in 50 mM TrisHCl pH 8.5, 5 mM $MgCl_2$. pmol ends were calculated from the following equation:

$$\text{pmol ends (linear double stranded DNA)} = (ugDNA/kbDNA) \times 3.04 \qquad [2]$$

Reaction mixtures were incubated at 37°C for 10 min and treated with a DNA-binding Perfectprep™ Gel Cleanup Kit (Eppendorf) to remove the alkaline phosphatase, according to the manufacturer's instructions. DNA was eluted in the smaller recommended volume of 30 µl.

2.2.9 Ligation

DNA ligation with T4 Ligase enzyme is a useful tool to generate recombinant DNA sequences. Digested products can be ligated together to form new plasmids which can be amplified and overexpressed in different systems.

The gel purified inserts and alkaline phosphatase digested vectors were ligated in a 10 µl reaction containing 1 U of T4 DNA ligase (NEB), 1X T4 ligase buffer (NEB), with vector and insert in the ratio of 1:3. The molar mass ratios were calculated using the following formula:

ng of vector required = [ng vector x insert size (kb)/ vector size (kb)] x molar ratio of insert [3]

The concentrations of vector and insert DNA were estimated by A_{260} measurements. The ligation reactions were incubated at 16°C overnight, and terminated by incubation at 65°C for 10 min.

2.3 Competent cells

Competent cells are those bacterial cells which can accept extra chromosomal DNA or plasmid. Competent cells for both BL21 RIL and DH5α strains were prepared using the standard protocol (Doyle, 1996) involving $MgSO_4$, Ca^{2+} salts and rubidium which increase rate of cell growth and transformation efficiency (Hanahan, 1983).

Cells were seeded from a glycerol stock stored at -70°C, into 5 ml of LB media (10 g bacto-tryptone, 5 g yeast extract, 10 g NaCl, made up to 1 L with distilled water, pH 7.4 with NaOH) and grown at 37°C overnight with shaking at 250 rpm. 1 ml of this culture was added to 250 ml of fresh LB media (with 20 mM filter sterilised $MgSO_4$) and grown with 250 rpm shaking at 37°C to an OD of ~0.4-0.6 at 600 nm. Cells were

pelleted by centrifuging for 5 min at 5000 g (Beckman Avanti J-25, JL 16.250 rotor) at 4°C in a sterile container. Harvested cells were resuspended in 100 ml of transformation buffer 1 (TFB1) (30 mM potassium acetate, 10 mM $CaCl_2$, 50 mM $MnCl_2$, 100 mM $RbCl_2$, 15% (v/v) glycerol, pH 5.8) and incubated on ice for 5 min. Cells were harvested as before and then resuspended in $1/25^{th}$ culture volume of TFB2 containing 10 mM MOPS, 75 mM $CaCl_2$, 100 mM $RbCl_2$, 15% (v/v) glycerol, pH 6.5 and incubated on ice for 15-60 min. 200 µl aliquots were transferred into sterile 1.5 ml eppendorf tubes. Tubes were flash frozen in a mixture of dry ice/isopropanol or liquid nitrogen and stored at -70°C.

2.4 Transformation of chemically competent *E.coli*

Both competent cell strains DH5α for DNA amplification and BL21 RIL for protein expression were transformed by the same method (Doyle, 1996).

Chemically competent *E.coli* cells were removed from storage at -70°C and thawed on ice. 10 ng of plasmid DNA was added to 200 µl of competent cells, and the mixture was incubated on ice for 20 min. Subsequently, cells were heat-shocked at 42°C for exactly 45 s, and incubated on ice for 2 min. 500 µl of LB medium was added and mixed. After incubation for 30 min at 37°C, 200 µl of cells were plated onto selective agar containing the appropriate antibiotic and incubated overnight at 37°C.

2.5 Analysis of transformants

2.5.1 Colony PCR

Single colonies were picked with a sterile pipette tip and resuspended in a PCR mixture containing appropriate concentrations of dNTPs, polymerase buffer, primers and polymerase. Standard protocols were followed for the PCR reaction (2.2.4.1) and positive colonies were analysed further by restriction digestion and DNA sequencing.

2.5.2 Analysis by restriction digestion

Restriction digestion was performed to ensure that recombinant vectors had been made and the DNA fragment had been inserted in the correct orientation. In most cases two enzymes, one for known vector site and the other for unique insert site were used for digestion. The enzymes were also chosen so that they would produce fragments of appropriate size which would indicate whether or not the DNA fragment had inserted into the vector in the correct orientation. In each reaction 10 µl of the miniprep DNA was used. The results were analysed by running digested DNA on an agarose gel.

2.5.3 Sequencing

When PCR is used to amplify a fragment of DNA for cloning or site directed mutagensis, the polymerase can make errors, introducing mutations into the sequence. The error frequency depends on the polymerase used, for Pfu the error

frequency is 1 x 10^{-6}/bp/duplication (Cline, Braman et al. 1996). All the plasmids were sequenced by MWG, Germany and for this the DNA was prepared following their instructions. 1 µg of DNA was precipitated using 0.5 volumes of 7.5 M ammonium acetate and 2 x volumes of 100% ethanol at -20°C for 20 min. The DNA was pelleted by centrifugation at 12000 rpm for 15 min, followed by washing with 70% (v/v) ethanol and centrifugation at 12000 rpm for 5 min. The pellet was air dried before being posted to Germany for sequencing.

2.6 Glycerol stocks

Glycerol stocks were made to store bacteria containing the desired plasmid. They were prepared by picking up a single colony of transformed bacteria with a sterile pipette tip and grown overnight in 5 ml of LB medium containing antibiotic. This culture was reseeded in fresh media and grown at 37°C with 250 rpm shaking until mid-exponential phase (OD 600= 0.6). 10% (v/v) sterile glycerol was added, and cells were aliquoted into sterile 2 ml screw cap tubes and flash frozen in a mixture of dry ice/isopropanol or liquid nitrogen.

2.7 Expression and purification of fusion proteins in *Escherichia coli*

The recombinant plasmid which contains a gene under control of the *lac* promoter was transformed into *E.coli* strain BL21 RIL (2.4). All the constructs are based on the *lac* promoter; hence IPTG (isopropyl-β-thiogalactopyranoside) was required to induce the expression of fusion protein. IPTG is a non metabolisable compound that

performs the same role as the natural inducer, allolactase. It binds to the lactose receptor molecule, preventing its binding to the promoter region which allows polymerase to bind and transcribe the gene of interest.

2.7.1 His-tagged proteins

A glycerol stock of bacteria containing the suitable plasmid was scraped with a sterile pipette tip and inoculated into 15 ml of LB media, with suitable antibiotic, and incubated overnight in an orbital shaker at 37°C at 250 rpm. The overnight grown culture was inoculated into one litre of Terrific Broth (TB) (900 ml TB base, 100 ml 10X PBS, 50 mg/ml kanamycin) and incubated in an orbital shaker for 4 hrs at 37°C (OD600 ~ 0.6). Then the culture was induced with 0.25 mM of IPTG and further incubated at 20°C for 6 hrs for protein expression.

The culture was then spun at 5000 g (Beckman Avanti J-25, JL 16.250 rotor) for 15 min at 4°C. The pellet was scraped into a glass beaker and resuspended in a buffer containing 150 mM NaCl, 20 mM Tris-HCl (pH 8.0), 1 mM DTT or 5 mM β-Mercaptoethanol (β-ME) for sonication. Lysozyme (1 small sterile tip per litre) was added to the suspended pellet and sonicated (preferably pulsed mode dismembranator, 0.5 sec on/0.5 sec off, 5-10 duty cycles of 30s each, on ice, Soniprep 150). Cell debris was pelleted at 28000 g (Beckman Avanti J-25, JA 20 rotor) for 50 min at 4°C and carefully decanted while retaining the supernatant.

For each litre of induced cells 2.5 ml of Ni-NTA resin slurry (Qiagen) was used. The Ni-NTA was spun at 1000 g for 5 min prior to use to give 1.25 ml of packed beads. The bacterial supernatant and beads were mixed and incubated at 4°C for 60 min on a rotating shaker to take up octa His tagged proteins onto the nickel beads. The mixture was then poured into disposable columns fitted with frits (Biorad) and allowed to drain at 4°C. Unbound proteins were allowed to flow through by gravity. The beads were washed with 5 volumes of 20 mM imidazole in a buffer containing 150 mM NaCl, 20 mM Tris-HCl (pH 8.0), 1 mM DTT or 5 mM β-ME. His tagged proteins bound to Ni-NTA beads were eluted with 250 mM imidazole in 150 mM NaCl, 20 mM Tris- HCl (pH 8.0) and 1 mM DTT or 5 mM β-ME, until the normal bright blue colour of nickel beads reached the bottom of the resin and the greenish/brown colour was washed off. The eluate (approximately 2.5 ml/litre) contained the His-tagged protein. The his-tag was cleaved by adding thrombin (5 μg/ml) to the eluted proteins and incubating at 4°C overnight. This step was combined with dialysis to remove the imidazole from the eluted proteins.

Dialysis was carried out in Seamless cellulose tubing (Sigma) against 1 litre of buffer containing 150 mM NaCl, 20 mM Tris-HCl (pH 8.0) and 1 mM DTT or 5 mM β-ME. Dialysis tubing was prepared according to manufacturer's instructions and stored in PBS with 0.1% Sodium azide. Dialysed proteins were incubated with 12.5 μl benzamidine sepharose 4B beads to remove thrombin, and Ni NTA resin was re-added to mop up any uncleaved fusion proteins. The purified proteins were stored at -80 °C in aliquots of 10 μl each.

2.7.2 GST-tagged proteins

The Proline rich domain (PRD) of Dynamin I was GST tagged and purified by glutathione-sepahrose beads. Glycerol stocks of bacteria containing the required plasmid were scraped with a sterile pipette tip and inoculated into 5 ml of LB media with suitable antibiotic and incubated overnight in an orbital shaker at 37°C. The overnight grown culture was inoculated into 250 ml of LB media with a suitable antibiotic and incubated on an orbital shaker at 250 rpm for 2-3 hr at 37°C until the optical density at 600 nm reached ~ 0.6-0.8. Then the culture was induced with 1 mM of IPTG and further incubated at 37°C for 3-4 hr for protein expression.

The culture was then spun at 5000 g for 15 min at 4°C. Supernatant was poured off and the pellet was resuspended in 20 ml of Saline Tris-EDTA (STE) buffer (10 mM Tris-HCl, 150 mM NaCl, 1 mM EDTA pH 8.0). The suspension was spun at 5000 g for 15 min in a 50 ml falcon tube. The supernatant was discarded and the semi-dry pellet was frozen at -70°C overnight. The -70°C pellet was resuspended in 40 ml of ice cold STE buffer with 1 mM PMSF and 7 µg/ml leupeptin (to inhibit proteases). 4 mg of lysozyme (for 250 ml culture volume) was added, and the suspension was incubated on ice for 30 min. During this incubation, 3 ml glutathione–Sepharose 4B beads (Amersham) were washed with 20 ml of PBS and 20 ml T-PBS (0.1% (v/v) tritonX-100 in PBS) followed by PBS. The beads were resuspended in 1 ml of PBS. The bacterial suspension was incubated a further 10 min with 1 mM DTT and 4.5 ml of 10% (v/v) triton X-100 on ice and samples were freeze-thawed 3 times in liquid nitrogen. The suspension was then sonicated for 6 cycles of 30 s on ice with a 30 s

break in-between each sonication. DNAse was added (10 μg/ml) and incubated on a rotating shaker for 30 min at 4°C. The lysate was spun at 20000 g (Beckman Avanti J-25, JA 20 rotor) for 15 min at 4°C. The supernatant was incubated with the beads for 1 hr (or overnight) at 4°C. The beads were spun at 500 g for 5 min and the supernatant was discarded. The beads were then washed with PBS five times, 1.2 M NaCl once and twice with PBS. The beads were then resuspended in PBS to give 50% (w/v) slurry and stored in a fridge at 4°C until required.

The GST-fusion protein glutathione sepharose complex was washed and resuspended in 1% (v/v) TritonX-100 in PBS. The slurry was poured onto a disposable type column with a frit (Biorad) and allowed to settle at 4°C. The column was washed twice with two column volumes of 1% (v/v) TritonX-100 in PBS and two column volumes of 150 mM NaCl in 50 mM Tris-HCl pH 8.0. The GST fusion protein was eluted with 1 column volume of 20 mM glutathione in 150 mM NaCl in 50 mM Tris-HCl pH 8.0.

2.8 FPLC

FPLC was carried out according to the manufacturer's instructions using Sephadex-200 in a 30 ml column. Strong reducing conditions were maintained by using 2 mM DTT in all the buffers for CLIC1 and CLIC4, and 5 mM β-mercaptoethanol in all the buffers for CLIC5A.

General principle involved in FPLC is, as the solute passes down the chromatographic bed its migration depends upon the bulk flow of the mobile phase and on the Brownian motion of the solute molecules. Separation in gel filtration depends on the different abilities of the various sample molecules to enter pores that contain the stationary phase. Very large molecules never enter the stationary phase and move faster as compared to smaller molecules that can enter large pores. Proteins are eluted in the order of decreasing molecular size. Monomers were stored and used for various studies. This ruled out the contamination of preformed oligomers in bilayer incorporation or contamination of full length proteins in truncated constructs of CLIC1 and CLIC4.

2.9 Estimation of protein concentrations

The estimation of concentrations of purified proteins needed to be determined for several applications for which three methods were followed.

2.9.1 Calculated absorbance

Absorbance assays, used for estimations of protein amounts are fast, reliable and they do not require any additional reagents or incubations. The relationship between absorbance and protein concentration is linear. Proteins in solutions absorb UV light with absorbance peaking at 280 and 200 nm. Aromatic amino acids give a peak at 280 nm and peptide bonds result in a peak at 200 nm. The concentrations of protein can be calculated from following formula:

concentration (mg/ml) = (1.55 x A280) - 0.76 x A260) (Stoscheck CM. 1990) [4]

2.9.2 Bradford method

The Bradford method is a fast and sensitive way to measure the protein concentration. The Bradford assay is based on an absorbance shift in comassie dye when bound to arginine and hydrophobic amino acids present in the proteins (Bradford, 1976). These dye mixtures are available commercially and can be used directly without filtration. A standard curve was generated using known concentrations of Bovine Serum Albumin (BSA, 120 mg/ml), the concentration of which was calculated from its absorbance at 280 nm (A280 1% (w/v) = 6.60). Samples were made using BSA concentrations ranging from 0-80 µg per sample made up to a final volume of 100 µl. Samples were mixed with 1 ml of Bradford's reagent and vortexed briefly. The absorbance at 595 nm of the samples relative to a blank was measured. These measurements were used to plot a standard curve of protein concentration vs. absorbance at 595 nm. Unknown protein samples were measured in duplicate with different volumes and concentrations were obtained graphically using the absorbance values at 595 nm.

2.9.3 Lowry method

The Lowry method was used to measure the protein concentrations of eluted proteins from beads (Peterson, 1977; Stoscheck, 1990). In alkaline conditions Cu^{2+} ions form

a complex with peptide bonds in which they are reduced to monovalent ions. Monovalent Cu^{2+} ions and the radical groups of tyrosine, tryptophan, and cysteine react with Folin's reagent to produce an unstable product that becomes reduced to molybdenum/tungsten blue.

Protein standards were prepared using BSA ranging from 0 to 100 µg/sample. To each of these 50 µl of 10% (w/v) sodium deoxycholate was added and the samples were vortexed. Proteins were precipitated by adding 1ml trichloroacetic acid (TCA) and vortexed. Samples were centrifuged at 14000 g for 2 min in a microfuge and the supernatant was removed. 1 ml of solution A (100 µl of 4% (w/v) $CuSO_4.5H_2O$ and 10 ml of 200 mM Na_2CO_3, 100 mM NaOH, 7 mM sodium tartarate and 1% (w/v) SDS) was added, followed by vortexing. 100 µl of Folin's reagent (1:1 dilution H_2O: Folin reagent, Solution B) was added and each sample was vortexed immediately. The samples were then incubated at room temperature for 1 hour. The absorbance was measured at 750 nm. The BSA standards were used to plot a standard curve, which was used to determine the protein concentration of the fusion protein samples. All samples were assayed in triplicate.

2.10 Sodium dodecyl sulphate – polyacrylamide gel electrophoresis (SDS-PAGE)

Proteins from cell lysate and tissue homogenate were separated by SDS-polyacrylamide gel electrophoresis (SDS-PAGE) using the BioRad Protein3 mini-gel system according to the manufacturers instructions. Gels were poured with a 10% or

12% resolving gel from 40% (w/v) acrylamide/bis-acrylamide (37.5:1) solution in 375 mM Tris-HCl pH 8.8, 0.1% (w/v) SDS, 0.1% (w/v) ammonium persulphate and 0.05% (v/v) N,N,N',N'-Tetramethylethylenediamine (TEMED) and 4% (w/v) stacking gel (125 mM Tris-HCl pH 6.8, 0.1% (w/v) SDS, 4% (w/v) acrylamide, 0.1% (w/v) bis-acrylamide, 0.05% (w/v) ammonium persulphate and 0.1% (v/v) TEMED). The gel running buffer contained 125 mM Tris-HCl pH 8.3, 1 M glycine and 0.01% SDS. Sample proteins were dissolved in equal volumes of 2X Laemmli sample buffer (Laemmli, 1970) to give final concentrations of 1% (w/v) SDS, 5% (v/v) glycerol, 1.25% (v/v) mercaptoethanol, 62.5 mM Tris-HCl pH 6.8 and 1% (w/v) bromophenol blue. Protein samples and prestained Kaleidoscope molecular weight markers (BioRad) were loaded onto the gel and electrophoresed at 150 V using a Biorad PowerPac 300 for 60-90 min. Once run, the gels were removed from the apparatus and either stained with Coomassie blue (stained for 1 hr with 40% (v/v) acetic acid, 20% (v/v) methanol and 0.004% (w/v) Coomassie brilliant blue and then destained overnight with 40% (v/v) acetic acid, 20% (v/v) methanol) or transferred for Western blotting. Destained gels were dried onto filter paper using a heated bed gel drier at 65°C for 45 min (BioRad).

2.11 Protein transfer and immunoblotting

2.11.1 Wet transfer

The proteins separated on SDS-PAGE gels were transferred to Hybond-P polyvinylidene difluoride (PVDF) membranes (0.45 μm pore size) (Amersham

Biosciences) for subsequent immunoblotting experiments with a BioRad Mini transfer electrophoretic transfer cell according to the manufacturer's instructions. The SDS-PAGE gels were equilibrated in transfer buffer (25 mM Tris, 192 mM glycine, 0.01% (w/v) SDS, 20% (v/v) methanol) for 20 min. PVDF membranes were used because of their improved handling characteristics and higher signal to noise ratio compared to conventional nitrocellulose membrane. PVDF membranes were pre-activated with 100% methanol for 2 min, followed by washing in distilled H_2O for 5 min and equilibrated in transfer buffer for 5 min. The gel and PVDF membranes surrounded by Whatman 3MM paper and fibre pads were assembled in a holder cassette and air bubbles were removed which would otherwise inhibit efficient protein transfer. The cassettes were placed in a transfer tank together with an ice pack to prevent overheating during transfer, and the tank was filled with transfer buffer. The proteins were transferred for 60 min at 100 V in a Biorad PowerPac 300. Transfer efficiency was routinely assessed by noting the intensity of the transferred prestained molecular weight markers. In addition the reversible stain Ponceau-S was used to stain the PVDF membrane (0.5% (w/v) Ponceau-S red, 1% (v/v) acetic acid for 1 min, de-stained in H_2O to the desired contrast) or Coomassie brilliant blue.

2.11.2 Immunoblotting

After transfer, the membranes were immunoblotted with desired antibodies raised against the protein of interest. Membranes were washed in Tween 20-Phosphate buffered saline (T-PBS: 0.05% (v/v) Tween-20, 150 mM NaCl, 10 mM Tris-HCl pH 7.4) to remove the transfer buffer and then blocked for 60 min with agitation at room

temperature or overnight at 4°C in 5% (w/v) low fat skimmed milk powder (Marvel) in T-PBS. The membranes were then incubated with primary antibody diluted to an appropriate concentration in blocking buffer for at least 60 min with agitation at room temperature. The unbound primary antibody was removed with 2 x 30 sec washes and 3 x 5 min washes of T-PBS. Membranes were then incubated for 60 min with an appropriate HRP (Horseradish peroxidase) conjugated secondary antibody also diluted in blocking buffer. The membranes were washed as before.

The bound HRP was visualised by incubation with Enhanced Chemiluminescence (ECL) substrate solution for 1 min and exposure to medical X-ray film (Konica) with a typical exposure time of 15 s to 2 min in a darkroom. Equal volumes of ECL solution 1 (100 mM Tris-HCl pH 8.5, 2.5 mM Luminol, 0.4 mM coumeric acid) and solution 2 (100 mM Tris-HCl pH 8.5, 0.019% (v/v) H_2O_2) were combined to make substrate solution. The film was developed in a Konica SRX-101A X-ray developer. When necessary, membranes were probed with more than one antibody by stripping previous antibodies from the membrane by incubation with agitation for 30 min in stripping buffer (62.5 mM Tris/HCl pH 6.8, 2% (w/v) SDS and 100 mM β-mercaptoethanol (β-ME)) at 50°C. Then after several washes in T-PBS, the membrane was reprobed as described above. Membranes which had been stripped showed no reaction with ECL after incubation with secondary antibody, showing that the entire primary antibody had been removed.

2.11.3 Dot Blotting

PVDF membranes were preactivated with methanol for 2 min and washed with dH_2O. Membrane was air dried and appropriate concentrations of protein samples were dotted on it. After drying, the proteins were fixed by 5 mins incubation in methanol and washed with T-PBS. The membrane was then blocked, immunoblotted and exposed for Western blotting.

2.12 Preparation of affinity-purified anti-CLIC antibodies

Recombinant CLIC1 and CLIC4 were subjected to SDS-PAGE and electrophoretically transferred to PVDF membranes. Membrane strips containing the proteins were blocked with 5% (w/v) non-fat milk in PBS, washed 3 x 5 min in PBS, and incubated overnight at 4°C with rabbit anti-CLIC antiserum raised to soluble, properly folded full length CLIC1 or full length CLIC4. After extensive washing in PBS containing 0.05% (v/v) Tween-20 followed by PBS alone, specifically bound antibodies were eluted with 100 mM glycine (pH 2.5), immediately readjusted to a pH of 8.0 with a precalibrated amount of Tris base, and stored in small aliquots at -70°C. Western blotting with ECL detection was carried out. When assessed by immunoblotting against pure protein standards, the affinity –purified anti-CLIC1 and anti-CLIC4 pAbs could detect a minimum of 0.1 ng CLIC1 and 10 ng CLIC4, respectively, and only showed measurable cross reactivity when the protein concentrations were increased to at least 1 μg. Protein concentrations were

determined by absorbance measurements using calculated extinction coefficients, or by the micro Bio-Rad procedure, using appropriate standards.

2.13 Preparation of synaptosomes

Synaptosomes are isolated nerve terminals without a nucleus. They are the simplest system containing all the necessary proteins for synaptic vesicle recycling (Nicholls, 1993). Synaptosomes are functional for up to 6 hours after preparation, hence it is important to minimise the time taken between extraction of the rat brain and homogenisation, and synaptic vesicle purification. No more than two rats were sacrificed at once to minimise the time between dissection and homogenisation. Crude P2 synaptosomes were sufficient for biochemical procedures but Percoll synaptosomes were used to isolate synaptosomes from the myelin and mitochondria.

2.13.1 Crude synaptosomes (P2)

Crude P2 synaptosomes were isolated and prepared from at least two month old Sprague-Dawley rats. Rats were killed by stunning and cervical dislocation. Rat forebrain was rapidly dissected and isolated in ice cold 1X sucrose/EDTA solution (0.32 M sucrose, 1mM EDTA, 5mM Tris pH 7.4), and swirled to remove excess blood. The forebrain was transferred to a clean polycarbonate detergent free tube containing 9 ml 1 X sucrose/EDTA solution and minced with scissors. This was then homogenised (Teflon coated, 30 ml homogenisor (Wheaton)) with at least six up and down strokes at 700 rpm. The homogenates were pooled and spun at 1075 g (Sorval

RC 26 plus with SS-34 rotar) for 10 min at 4°C. The red-tinted white loose pellet containing red blood cells, mitochondria and other debris was resuspended in 1X sucrose/EDTA and spun at 1075 g for 10 min at 4°C. The supernatant was added to supernatant (S1) from the earlier fraction stored on ice. This was spun at 20200 g for 30 min at 4°C to pellet the synaptosomes. The supernatant (S2) was discarded and the pellet (P2) was resuspended in minus Ca Krebs (118.5 mM NaCl, 4.7 mM KCl, 1.18 mM $MgSO_4$, 10 mM glucose, 1 mM Na_2HPO_4, 20 mM HEPES, pH 7.4 adjusted with saturated Tris base) and centrifuged for a further 10 min at 20200 g at 4°C. The pellet (P2) was resuspended in minus Ca Krebs buffer to an appropriate concentration. The concentration was measured by Bradford assay.

2.13.2 Percoll purified synaptosomes

Percoll synaptosomes were prepared by the standard method after Dunkley et al. (1986). Percoll gradients were prepared a night before the preparation of synaptosomes and stored at 4°C. 3 ml each of 23% (v/v) percoll (23 ml percoll, 25 ml 4X sucrose/EDTA, 52 ml dH_2O, pH 7.4) was pipetted into the tube and 3 ml each of 10% (v/v) (10 ml Percoll, 25 ml 4X sucrose/EDTA, 65 ml dH_2O, pH 7.4) and 3% (3 ml Percoll, 25 ml 4X sucrose/EDTA, 72 ml dH_2O, pH 7.4) Percoll was carefully layered on top respectively, in the order of 23% (v/v), 10% (v/v) and 3% (v/v) using a peristaltic pump.

The S1 synaptosomes were prepared as described in 2.13.1. The supernatants were combined and layered onto the Percoll gradients (2-3 ml/gradient). The Percoll

gradients were spun at 4°C for 12 min at 15000 g. By using a pipette aid with attached cut off yellow tip, the myelin layer between 10% (v/v) and 3% (v/v) gradients was removed. The synaptosome layer and 23% (v/v) and 10% (v/v) percoll layers carrying synaptosomes were removed into a fresh cold centrifuge tube and diluted with ice cold sucrose/EDTA. The synaptosomes were centrifuged at 4°C for 40 min at 15000 g. The supernatant was carefully poured off without losing any of the synaptosomal pellets. The pellet was resuspended in the minus Ca Krebs (118.5 mM NaCl, 4.7 mM KCl, 1.18 mM $MgSO_4$, 10 mM glucose, 1 mM Na_2HPO_4, 20 mM HEPES and adjusted a pH 7.4 with saturated Tris base) and spun at 4°C for 10 min at 15000 g. Synaptosomes were aliquoted in a small volume (10 ml) of Krebs solution. Protein concentrations were estimated by using Bradford method.

2.14 GST-fusion protein pull down assay

To identify *in vitro* binding partners of the PRD of Dynamin I, a GST pull down assay was performed. PRD was fused to glutathione S-transferase (GST) and coupled to glutathione sepharose beads. These beads can then be incubated with synaptosome lysates or proteins of interest. Binding partners of the protein or the proteins in the complex binding to the fusion protein can be extracted and identified.

ProbeQuant G-50 columns (Amersham) were used for GST-pull down assays. The synaptosomal pellet was resuspended in 200 µl of ice cold lysis buffer (25 mM Tris, 150 mM NaCl, 1 mM EGTA, 1 mM EDTA, 20 µg/ml leupeptin, 1mM PMSF, 1mM $ZnSO_4$, 1% Triton X-100, 1 protease inhibitor tablet per 25 ml lysis buffer, pH 7.4).

The resuspended pellet was incubated on ice for 15 min with periodical vortexing after 5 min. Lysates were spun at 13000 rpm at 4°C for 5 min and 175 µl of the supernatant was added to pre-prepared ProbeQuant G-50 columns containing the washed GST fusion protein coupled to GSH beads. GSH beads and lysate were incubated with rotation for 1 hr at 4°C.

Fusion protein columns were prepared by washing ProbeQuant G-50 columns with distilled water. GST fusion protein bead slurry (20-300 µl) was added to each column and columns were unplugged, and spun at 2800 rpm for 10 s. Beads were washed with chilled 500 µl lysis buffer and spun for further 10 s at 2800 rpm at 4°C. The tubes were then replugged and 50 µl of lysis buffer was added to the beads, and stored at 4°C until further use.

After incubation with lysate the columns were unplugged and spun at 2800 rpm for 10 sec at 4°C to remove the unbound proteins. The beads were washed three times with 500 µl of lysis buffer, once with lysis buffer containing 500 mM NaCl, once again with 500 µl lysis buffer and finally with 500 µl of 20 mM Tris pH 7.4. Columns were replugged and 30 µl of 1X sample buffer (67 mM Tris, 2 mM EGTA, 67 mM SDS, 9.3% glycerol, 12 % β-mercaptoethanol and bromophenol blue) was added. The columns were vortexed and boiled for 5 min. Samples were eluted into fresh 1.5 ml eppendorfs by spinning the unplugged columns at 14000 rpm for 10 min. Eluted samples were stored at -20°C until further use.

2.15 Immunoprecipitation of synaptosome proteins

Immunoprecipitation is a powerful technique to determine *in vivo* interactions of a protein of interest. The antibody for the desired protein is bound to an insoluble matrix (Protein G covalently linked to Sepharose beads) and the protein is extracted from a cell lysate. The desired protein is immunoprecipitated along with the complex containing direct and indirect interactors from the cell lysate.

Synaptosomes were prepared using a standard protocol (2.13.2). 500 µl of synaptosomal solution (percoll 2 mg/ml) was incubated in a water bath at 37°C, and lysed in 200 µl of ice cold lysis buffer (1% (v/v) Triton-X 100, 25 mM Tris HCl pH 7.4, 150 mM NaCl, 1 mM EGTA, 1 mM EDTA, 20 µg/ml leupeptin, 1 mM PMSF, 40 µM cyclosporine A, 1 mM Zn_2SO_4, complete protease inhibitor tablet (1:25 ml)) with incubation for 15 min on ice and occasionally vortexing. The lysate was spun at 13000 g in a microfuge at 4°C for 5 min and the supernatant was collected. For equal volume (175 µl) of BSA (50 mg/ml) was added to the supernatant and mixed by vortexing. 2 µl of antibodies were added to the samples, and incubated for 1 hr at 4°C.

Protein G beads (25% (v/v) slurry in PBS with 0.02% (w/v) sodium azide) were gently vortexed to resuspend the beads. 200 µl of the protein-G bead slurry were added to a plugged spin column. The columns were unplugged and spun into a 2 ml tube at 4°C for 10 s at 2800 g. The beads were washed with 500 µl of chilled lysis buffer. All the columns were replugged, and 50 µl of lysis buffer was added.

The antibody sample solution was added to the plugged spin columns containing freshly washed protein-G beads and further incubated for 60 min, rotating at 4°C. Spin columns were unplugged and placed inside the eppendorf tubes and spun at 4°C for 10 s at 2800 g. The beads were washed twice with 400 µl ice cold lysis buffer. The beads were further washed with ice cold lysis buffer containing 500 mM NaCl and then with lysis buffer again. The beads were finally washed with ice cold 20 mM Tris-HCl (pH 7.4). The columns were plugged and 50 µl of 1X SDS sample buffer was added to the beads, which were vortexed and boiled for 5 min. The samples were collected in fresh eppendorf tubes by spinning at 13000 g for 5 min, and then frozen until run on the gel.

2.16 *In vitro* binding assay

To determine whether the two proteins interact directly, an *in vitro* binding assay is used. One of the proteins of interest is bound to the insoluble matrix (GSH beads) and is incubated with a purified target protein to determine if they interact directly.

The assay was carried out using the ProbeQuant G-50 columns, which were washed with PBS, blocked in PBS + 0.1% Triton X-100 and washed in PBS again. Beads were resuspended to make a 50% (v/v) slurry. 40 µl of the slurry was added to the columns. The binding assay was carried out in binding buffer (20 mM HEPES, 1 mM DTT, 150 mM KCl, 0.05% (v/v) Tween20, pH 7.4). The concentration of the protein with the GST tag was kept constant (200 nM) and the concentration of the other protein was serially diluted from 500 µM to 25 µM.

Proteins were incubated in the binding assay buffer with blocked GHS beads with rotation for 2 hr at 4°C. Beads were washed after 2 hr in a similar manner to the GST pull down assay (2.15) five times with 400 µl of binding buffer. The bound proteins were then eluted in 40 µl of 1X sample buffer and stored at -20°C until further analysis.

2.17 CLIC oligomerization

Oligomerization of recombinant CLIC proteins was carried out by incubating them in 5 mM H_2O_2 for 60 min at room temperature. Oxidized samples were run on SDS PAGE in a sample buffer without any reducing agent.

2.18 Cell culture

HEK 293 cells (a transformed human embryonic kidney cell line) and stably transfected CLIC1 HEK-293 and CLIC4 HEK-293 cells were cultured in Dulbeccos modified eagle medium (DMEM) (Gibco BRL) supplemented with 10% (v/v) foetal calf serum (Gibco BRL), in 25 ml sterile flasks. Cells were passaged every 3-4 days at approximately 70-80% confluency. To passage the cells, the old medium was removed and discarded into bleach. Cells were washed briefly by adding 5 ml of HBSS (Gibco BRL) + 0.1% (w/v) EDTA, 0.5 ml Trypsin-EDTA was added to the cells and they were incubated at room temperature for 2 min. The back of the flask was tapped gently to detach the cells, which were resuspended in 2 ml DMEM + 10% (v/v) FCS by triturating slowly 5-10 times using a 1ml Gilson tip. For plating

on coverslips or new 25 cm^2 flasks, cells were diluted 24x (i.e. to 1 ml of cells add 3 ml DMEM + 10% (v/v) FCS) and triturated gently, 5 ml of the cell suspension was required for 25 ml flasks, typically 2 ml was seeded into each well of a 6 well plate (or 35 mm dish) containing approx 4x 12 mm coverslips. For stable cell lines, fresh Zeocin (200 µg/ml) was included in growth media.

2.19 Freezing HEK-293 cells for storage in liquid nitrogen

Cells were passaged in the normal way, centrifuged at 1000 g for 5 min, and resuspended in 1-2 ml growth medium; and resuspended again in growth medium containing 10% (v/v) DMSO. Cell suspensions were aliquoted into freezer ampoules (1ml/ampoule i.e., 1 x 10^6 cells/ml) and placed in an insulated box (Mr. Frosty). The Frosty box was incubated in a -70°C freezer overnight so that the cell suspension cooled at -1°C/min. Next day, the ampoules were transferred into liquid nitrogen.

2.20 Removal of cells from frozen liquid nitrogen stocks

The cells were defrosted at 37°C as quickly as possible and transferred into 25 ml flasks. Growth media (DMEM) with 10% (v/v) FCS (total 5 ml) was added very slowly to the cells to dilute the DMSO. The medium was changed completely to remove the DMSO and non-settled cells after 24 hours. Cells were then cultured as described earlier.

2.21 Primary culture of rat cerebellar granule neurons

Primary cultures of rat cerebellar granule neurons were prepared by Dr. M. A. Cousin and Dr G. J. Evans (Tan et al., 2003). The cerebellum of 7 day old Sprague-Dawley rats was extracted and minced using a McIlwan tissue chopper. The chopped tissue was then incubated with trypsin to dissociate the cells. After trypsinisation, soybean trypsin inhibitor (SBTI) was added to inhibit the trypsin and DNase was added to prevent the cell solution becoming viscous. Cells were pelleted and resuspended in 1.5 ml of buffer containing SBTI and DNase. The cells were triturated using sterile pipettes of decreasing bore size to fully dissociate the cells. The cell suspension was then layered onto Earle's balanced salt solution (EBSS, 10% (w/v) BSA, $MgSO_4$) and centrifuged to remove debris. The pellet was resuspended in 2 ml culture media containing Minimal Essential Medium (MEM) containing Earle's Salts plus 10% (v/v) foetal calf serum, 25 mM KCl, 2 mM glutamine, 30 mM glucose, 100 U/ml penicillin and 100 µg/ml streptomycin. The volume of the suspension was then adjusted to give 2.5 x 10^6 cells per 100 µl. 100 µl of suspension was seeded onto poly D lysine coated coverslips, and the coverslips were then incubated (5% (v/v) CO_2) at 37°C for an hour before a further 2-3 ml of culture media was added to each well.

After 24 hr of seeding, the media was replaced with 2 ml of culture media supplemented with 10 µM cytosine arabinoside, which inhibits cell division and prevents the growth of other cell types present in culture, such as astrocytes, multiplying.

2.22 Calcium phosphate transfection of DNA

Cells were transfected using the calcium phosphate transfection protocol. Rat cerebellar granular neurons were transfected 6 days after culturing, whereas HEK-293 cells were transfected after 3 days. Media was removed from the wells and stored in a 50 ml tube at 37°C with a loose lid in the incubator. Cells were washed twice with 2 ml MEM (Modified Eagle's medium)/DMEM (Dulbecco's MEM) (Gibco BRL) and incubated with serum-free medium (MEM/DMEM) at 37°C in 5% (v/v) CO_2 for 1 hr. Transfection solution was prepared by mixing 22.5 µl of 2X HeBS (300mM NaCl, 10mM KCl, 5 mM $Na_2HPO_4.12H_2O$, 60 mM D-Glucose, 5mM HEPES (free acid) and ddH_2O to make upto 180 ml (pH 7.14)), 2.25 µl of 2.5 M $CaCl_2$, 5.75 µg DNA and made up to 45 µl with sterile ddH_2O. 22.5 µl of the transfection solution was added drop wise to the cells in each well. The DNA was dispersed by mixing the media and agitating the wells. Cells were incubated for 30-40 min at 37°C in 5% (v/v) CO_2 incubator. The transfection media was removed and cells were washed twice with serum-free media. The conditioned culture media was replaced, and the cells were analysed between 1-5 days after transfection.

2.23 Immunofluorescence

Cells were cultured on coverslips in 6 well plates to 70% confluency (± transfection). The media was removed and the cells were washed with PBS for 3 min at room temperature. Cells were fixed in 4% (w/v) buffered paraformaldehyde (stored in aliquots at -20°C), washed twice with PBS and then incubated for 10 min in PBS

with 50 mM NH_4Cl for 10 min to quench any autofluorescence. Cells were washed twice with PBS and permeabilised by adding 2 ml of 0.1% (v/v) Triton X-100 in PBS, followed by two washes in PBS. Cells were incubated with primary antibodies (1:500 with 0.2% (v/v) fish skin gelatine in PBS) at room temperature for 1 hr. The cells were then washed with PBS thrice and incubated with secondary antibodies (1:500 with 0.2% (v/v) fish skin gelatine in PBS) at room temperature for 1 hr. The cells were washed with PBS thrice and mounted with mowiol. Optionally, nuclei were stained with 4'-6-diamidino-2-phenylindole (DAPI) (1:10,000) during the second last wash after secondary antibody treatment.

2.24 Confocal laser scanning microscopy

Cells fixed with formaldehyde on glass coverslips and mounted in Mowiol, were imaged with a Zeiss LSM Axioscope 510 confocal laser scanning microscope. CLICs were stained with Alexafluor-488 and other proteins were stained with Alexafluor-568.

2.25 Planar lipid bilayer studies

Planar lipid membranes (Black lipid membrane, BLM) were formed at room temperature (20°C) from several different lipids, including purified soybean lecithin (Type IV, Sigma), diphytanoylphosphatidylcholine (DPhPC), palmitoyl-oleoyl phosphatidylcholine (POPC), palmitoyl-oleloyl phosphatidylethanolamine (POPE), palmitoyl-oleoyl phosphatidylserine (POPS) and cholesterol (Avanti polaris). Stock

solutions of lipids were prepared at a concentration of 50 mg/ml and kept at -70°C. The working solution was air-dried prior to resuspending in n-decane. The lipid bilayer forming-solution contained the desired lipids at a concentration of 25 µg total lipid/µl in n-decane. BLMs were cast across a 300 µm diameter hole drilled in a polystyrene partition separating two solution filled chambers designated *cis* and *trans*. The outline of the aperture was primed with the lipid solution and air dried prior to bilayer formation to improve membrane stability. Using Ag^{2+}/AgCl2 electrodes and agar salt bridges (3M KCl), the *cis* chamber was voltage clamped by an Axopatch 200-B amplifier, and the *trans* chamber was grounded, minimising and offsetting liquid junction potentials. After thinning spontaneously to a capacitance of at least 250 pF, bilayers were bathed in 500 mM KCl *cis* vs. 50 mM KCl *trans* (all the solutions contained 10 mM TrisHCl, pH 7.4 and 1 mM DTT, unless otherwise specified), and up to 25 ng/ml (~1 nM) proteins were stirred into the *cis* chamber.

Transmembrane currents normally appeared within 10 min and were digitally recorded. Background (leakage) currents were less than 10 pS. Concentrated salt solutions were stirred into the relevant chamber as required, or the contents were changed by perfusion (at least 10 volumes). Unless otherwise specified, reagents were added to both chambers. Currents are labelled as positive or negative following the standard convention (i.e., positive currents represent net cation flux from *cis* to *trans*). To check whether the observed channel-like activity was (net) anionic or cationic, the K^+ ionophore valinomycin was incorporated into test bilayers in an ionic gradient (500 mM *cis* KCl *vs.* 50 mM *trans* KCl). The upwards openings of channels

at positive holding potentials were observed as net cation flux from the *cis* to *trans* chamber.

2.26 Whole-cell recordings

HEK-293 cells and stably-transfected CLIC1 HEK-293 and CLIC4 HEK-293 cells were used within 48 hours of plating. Cells were removed and re-equilibrated in bath solution containing 135 mM NMDG Cl, 1 mM $CaCl_2$, 10 mM glucose and 10 mM HEPES-KOH (pH 7.2) for 30 min at room temperature. Borosilicate glass pipettes (GC 150 F-7.5 1.5 mm O.D x 0.86 mm I.D (Harvard apparatus)) were pulled (Sutter instruments) (Heat 653, pull 0, velocity 40, time 220) and fire-polished to a final resistance of 5-7 MΩ (in 150 mM KCl). Pipettes were filled with 130 mM NMDG Cl, 1 mM $CaCl_2$, 1 mM $MgCl_2$, 5 mM EGTA, 10 mM glucose, and 10 mM HEPES-KOH (pH 7.2). Osmolarities were adjusted with 1 M mannitol as required. The bath electrode was connected through an agar salt bridge and junction potentials were corrected as a routine. The bath solution was changed by perfusion (10 volumes). Whole-cell and single-channel currents were digitally recorded and analysed using pClamp 8 software (Axon instruments).

2.27 Single-channel analysis

Single-channel currents were filtered at 50 Hz (8-pole, low pass Bessel type response) and analyzed using pClamp 8 software (Axon Instruments) and pStat (SPSS). Channel amplitudes were measured by fitting amplitude histograms to

Gaussian distributions. Salt concentrations were corrected for activity using standard tables, and (relative) anion permeabilities (P) were calculated from the Nernst equation adapted for bi-ionic conditions:

$$P_{anion}/P_{Cl} = a\,[Cl]_{cis}/a[anion]_{trans} \times \exp(-zFEr/RT) \quad [5]$$

where, a is the activity coefficient of the relevant salt, Er is the reversal or equilibrium potential, R is the gas constant, T is the temperature in Kelvin, F is Faraday's constant and z =-1 (chloride anion charge). Relative anion *vs.* cation permeabilities were calculated from the following form of the Goldman-Hodgkin-Katz (GHK) voltage equation:

$$P_{anion}/P_{cation} = \{n \times \exp(Er/k)-1\}/\{n - \exp(Er/k)\} \quad [6]$$

Where n is the *cis/trans* salt activity ratio and k=RT/F (26 mV). The redox or half-cell (E_{redox} or E_{hc}) potential of the buffer pair 2GSH/GSSG (2 reduced glutathione molecules equilibrated with oxidised glutathione in a reaction involving the transfer of 2 protons and 2 electrons) was calculated from:

$$E_{redox} = E^0 - RT/2F \times \ln([GSH]^2/[GSSG])\ mV \quad [7]$$

where E^0 (-240 mV) is the standard redox potential. We took account of the experimental pH 7.4 by including a pH dependant correction of:

$$(7.4\text{-}7.0) \times 2.3(RT/F) = -24 \text{ mV} \quad [8]$$

CHAPTER 3

EXPRESSION AND PURIFICATION OF CLIC PROTEINS

3.1 Introduction

Expression of recombinant proteins in prokaryotes and eukaryotes is frequently used to study the structure and function of proteins, to prepare proteins for reconstitution and to generate specific antibodies. Over-expression of proteins in *E.coli* can give very high yields and the expression can be regulated easily, making this prokaryotic system useful if the expressed protein folds correctly.

Many plasma membrane channels have been cloned and studied in detail, in contrast very little is known about Chloride Intracellular Channel (CLIC) proteins. CLICs exist as soluble proteins, which is advantageous for expression and purification. Rat brain CLIC4 (p64H1, or p64H1 homologue 1), also known as mtCLIC, was the first CLIC to be identified by homology to p64 and was cloned (Howell et al., 1996; Duncan et al., 1997). Later on, other p64 homologues were identified and named as CLICs. Invertebrate CLICs, such as EXC-4 and EXL-1 (Berry et al., 2003), were reported to be involved in various cellular mechanisms along with vertebral CLICs (Ashley, 2003; Suh et al., 2005). In order to carry out biochemical and electrophysiological studied of CLIC proteins, it was necessary to over express and purify them.

This chapter will provide a description of the over-expression and purification of various CLIC proteins. All the CLICs and their mutants were cloned into pHis8 (Jez et al., 2000) and transformed into *E.coli* BL21 (DE3) cells for overexpression. Ni^{2+}-affinity chromatography was used to purify the proteins. CLICs were also cloned into

pEGFP-N2 and pEYFP-N2 vectors to make GFP/YFP-tagged proteins for localisation studies.

Size-exclusion chromatography was performed on the CLIC proteins to remove oligomers and other contaminants from the purified proteins. The columns were calibrated with standard proteins, as reported in section 3.6. Purified CLICs were used for biochemical assays and single-channel studies in bilayers. It has been shown that CLICs can form oligomers *in vitro*. The oligomerisation properties of CLIC1, CLIC4 and CLIC5A were investigated. Purified full-length CLIC1 and CLIC4 were also used for the affinity-purification of anti-CLIC1 and anti-CLIC4 antibodies, respectively, from anti-sera. Anti-CLIC antibodies were affinity-purified and their specificity and cross-reactivities was tested. They were used for biochemical analysis, imaging, and electrophysiology.

3.2 Cloning of full length CLICs

The vector used for cloning and protein expression was pHis8 (Appendix I), a modified pET-28a (+) vector with additional histidines to increase the efficiency of purifications. The pHis8 vector encodes an N terminal octa-His tag (Jez et al., 2000) and a thrombin cleavage site along with the promoter and translational start site for the bacteriophage T7 gene10, MCS, the T7 terminator and a gene encoding aminoglycoside phosphotransferase (APH[3']-II) for kanamycin resistance.

A). Over expression and purification of full length CLICs

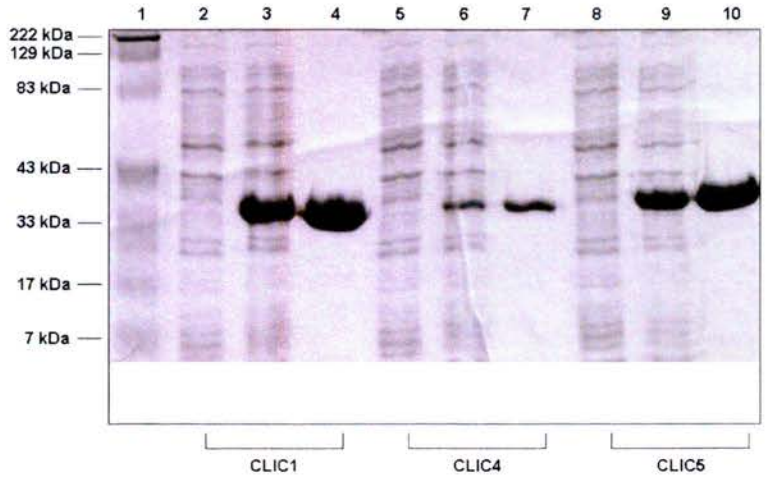

B). Over expression and purification of truncated CLICs

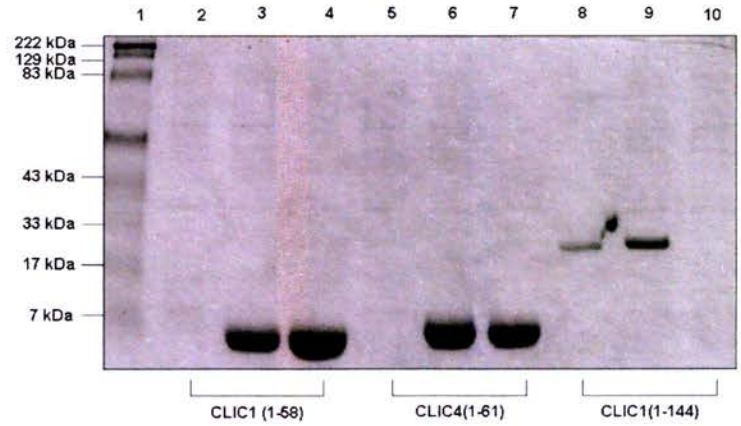

Fig 3.1. Overexpression and purification of CLIC proteins. Full-length and truncated CLICs were overexpressed as his-tagged proteins and purified by Ni-affinity columns (Chapter 2, 2.7.1). (A). Coomassie blue stained 10% (w/v) SDS-PAGE of recombinant CLIC1, CLIC4 and CLIC5A proteins. 10 µl cells were lysed and boiled for 5 min for both uninduced and induced samples, and 5 µl of the post-column eluates were loaded on the gels. (B). Coomassie blue stained gel of truncated CLIC1 and CLIC4 proteins. Lane 1. Markers, 2-4. Uninduced, induced and purified short CLIC1 (1-58), 5-7. Uninduced, induced and purified truncated CLIC4 (1-62), 8-10. Purified, induced and uninduced truncated CLIC1 (1-144). 5 µl cells were lysed and boiled for 5 min for both uninduced and induced samples, and 5 µl of post-column eluates were loaded on the gels.

Human CLIC1 (cDNA clone MGC:74817 IMAGE:5585323, MRC GeneService) was inserted into pHis8 vector (Appendix I.1) using primers (MWG) ACG GAT CCA TGG CTG AAG AAC (forward) and ATC TCG AGT TAT TTG AGG GCC (reverse), incorporating the restriction sites for *NcoI* and *XhoI* respectively (underlined). Full length rat brain CLIC4 in pHis8 was already available (R H Ashley, unpublished work). Human CLIC5A (cDNA clone MGC:53405 IMAGE:4611102, MRC Geneservice) was cloned into pHis8 using primers (MWG) TAG GAT CCA TGG CAG ACT CGG (forward) and ATC TCG AGT CAG GAT CGG CTG (reverse), with restriction enzyme sites for *NcoI* and *XhoI*, respectively. The constructs were sequenced with T7 forward and reverse primers (MWG sequencing facility).

3.3 Site-directed mutagenesis of CLICs

All the site-directed mutageneses were carried out by QuikChange PCR (Methods 2.2.4.2). CLIC1 C24A was made by using the primers GAT TGG GAA CGC CCC ATT CTC CCA GAG ACT (forward) and CAG ACT CAG GGA GAA TGG GGA GTT CCC AAT (reverse) in pHis8. The N-termini of CLIC1 and CLIC4 were prepared by introducing a stop codon by Quikchange PCR. In CLIC1, the stop codon was introduced at position 58 (C58STOP) by using the primers GTG CAG AAG CTG TGA CCA GGG GGG (forward) and CAC GTC TTC GAC ACT GGT CCC CCC (reverse). CLIC4 was truncated at position 61 (K61STOP) by using the primers CTG AAA AGG TAG CCT GCA CAT CTG (forward) and GAC TTT TCC ATC GGA CGT GTA GAC (reverse). The N-terminus of both CLICs included a single

cysteine residue at the beginning of the transmembrane domain (TMD) and the complete putative TMD. CLIC1 was truncated at position 144 by using primers GACAATTACTTATGATCCCCCCTCCCAG (forward) and CTGGGAGGGGGGA TCATAAGTAATTGTC (reverse). Inserts were recloned into a fresh pHis8 vector and constructs were verified by sequencing (MWG). Proteins were over-expressed with an Octa his tag and purified by Ni affinity chromatography.

3.4 CLIC GFP/YFP constructs

In order to study the localisation and functional role of CLICs *in vivo*, GFP and YFP tagged constructs of CLIC1 and CLIC4 were made. CLIC1 was cloned into pGFP-N2 (Appendix I.3) and pEYFP-N2 (Appendix I.4), by generating a suitable insert using the primers GGC AAG CTT ATG GCT GAA GAA C (forward) and TAT GGA TCC CCT TTG AGG GCC TTT GC (reverse), with enzymes sites for *Hind* III and *BamH* I. Similarly, CLIC4 was cloned into pGFP N2 and pYFP N2 by using the primers GGT AAG CTT ATG GCG CTG TCG AT (forward) and TAT GGA TCC TTG GTG AGT CTTTTG GC (reverse), incorporating enzyme sites for *Hind* III and *BamH* I. These constructs were transfected into HEK 293 and cerebellar granule neurons (CGNs).

3.5 Over-expression and purification of CLICs

Soluble Octa-His tagged fusion proteins were expressed in *E.coli* (DE3) cells and purified from cell lysates by Ni^{2+} NTA affinity chromatography (Methods 2. 7.1).

A). FPLC of standard proteins

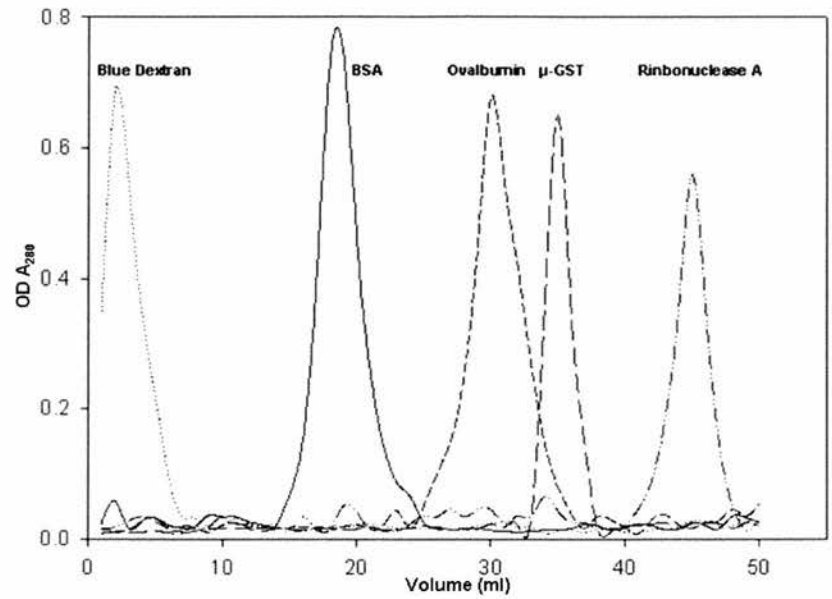

B). Calibration curve

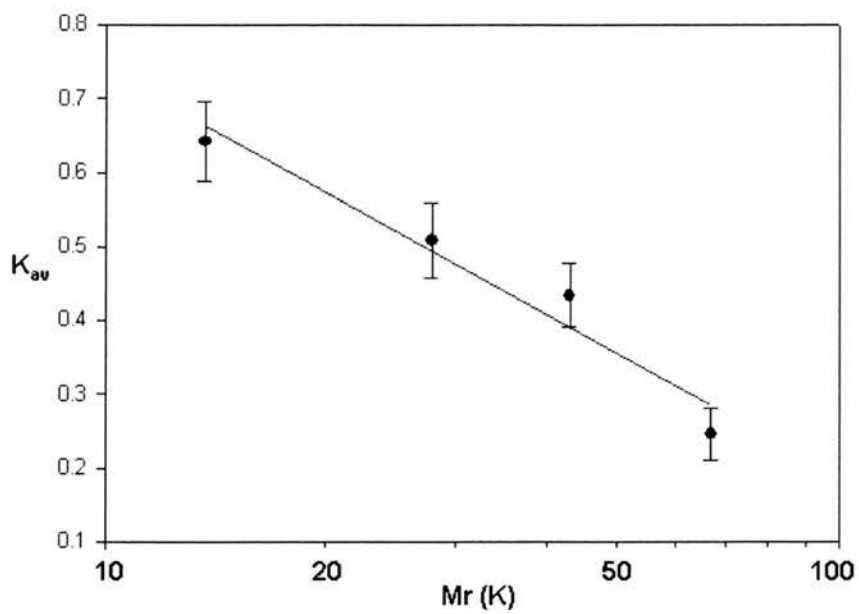

Fig 3.2. FPLC Column calibration. The FPLC column (24 ml, Superdex S-200) was calibrated prior to use and total volme (V_t) was measured by bromophenol blue. (A). Calibration of FPLC column with standard proteins; blue dextran for V_o, BSA (Mr = 67K), ovalbumin (Mr = 43K), μ-GST (Mr = 27K) and ribonuclease A (Mr =1 3.7K). (B). Calibration curve. K_{av} was calculated as shown in the text.

Non-specifically bound proteins were removed by extensive washing of the Ni^{2+}-beads with 150 mM NaCl, 30 mM imidazole and 20 mM Tris Cl (pH 8.0). Proteins were eluted using 150 mM imidazole in 150 mM NaCl containing 20 mM Tris Cl (pH 8.0). All the solutions contained a stoichiometric excess of DTT (5 mM). CLIC5A formed oligomers even with 2 mM DTT, hence, 2 mM β-mercaptoethanol was used in all the solutions while purifying and storing the protein. All the proteins were thrombin-cleaved unless otherwise stated to remove the His-tag, leaving 8 linker residues (Sequence: GGLVPRGS) before the initiating methionine. Dialysis was carried out overnight to remove the imidazole. The thrombin was removed by adding benzamidine Sepharose beads during dialysis. Fresh Ni-NTA beads were added to remove the cleaved His tags and any uncleaved proteins. The yields of CLIC1, CLIC4 and CLIC5A were 4.4 ± 0.75 mg/l culture medium (mean ± SD, n=25), 4.0 ± 0.68 mg/l culture medium (mean ± SD, n=22), and 5.0 ± 0.80 mg/l culture medium (mean ± SD, n=5) (Fig 3.1), respectively. The yield of short CLIC1 (1-58) was 2.5 ± 0.50 mg/l (mean ± SD, n=5), truncated CLIC1 (1-144) 2.8 ± 0.55 mg/l (mean ± SD, n=5), and short CLIC4 (1-62) 2.5 ± 0.65 mg/l (mean ± SD, n=9) (Fig 3.1).

3.6 Size-exclusion chromatography

Some of the CLIC proteins were subjected to size-exclusion chromatography to remove dimers and oligomers. The medium sized (30 ml) columns were packed with a 75% (v/v) slurry of Superdex 200, and washed with 0.2M NaOH, and then H_2O prior to use and stored in 20% (v/v) ethanol. The column was standardised with

A). Size-exclusion chromatography of CLIC1

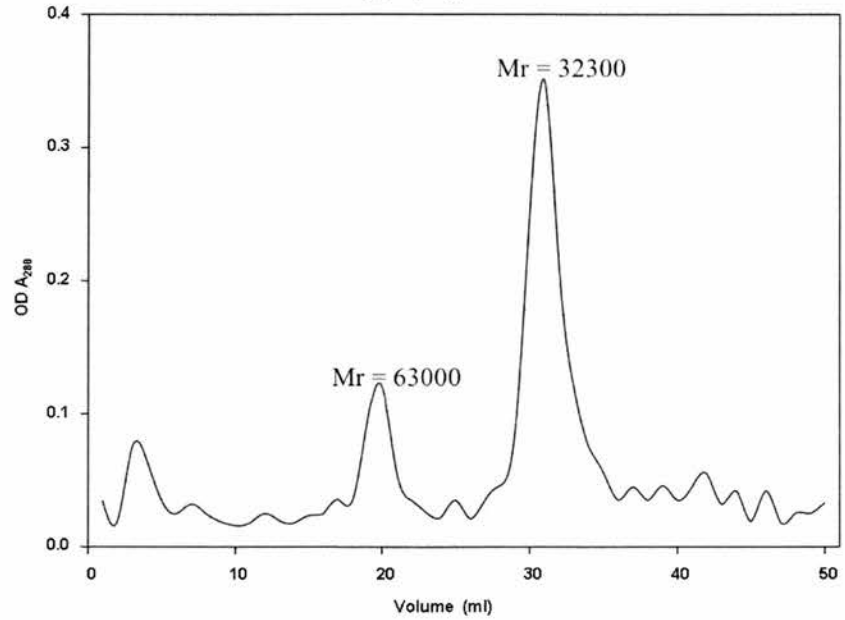

B). Size-exclusion chromatography of CLIC4

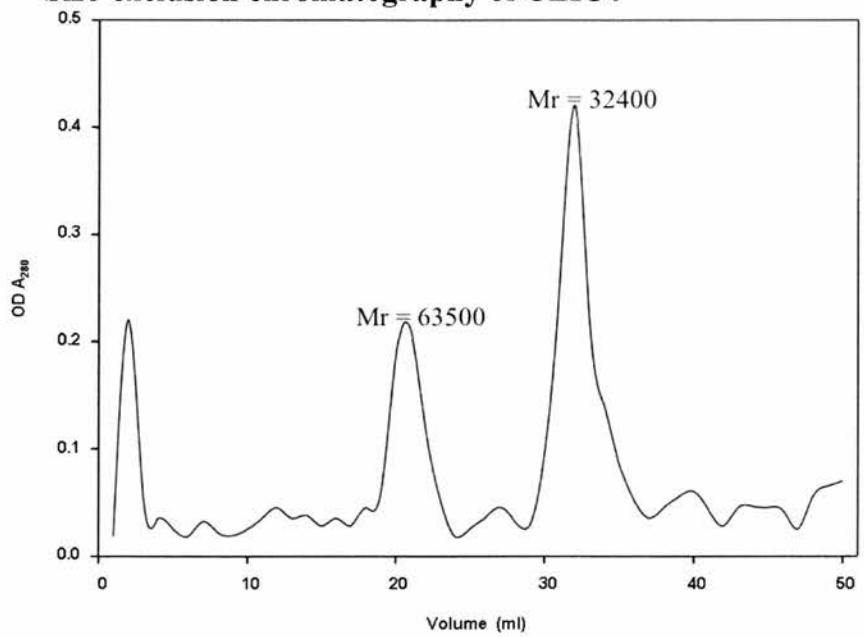

Fig 3.3. Size-exclusion chromatography of CLIC1 and CLIC4. The total amount of proteins injected into the column was 4 mg and 4.5 mg for CLIC1 and CLIC4, respectively. A). Size exclusion chromatography of CLIC1. Large peak corresponds to the molecular weight (Mr) of 32300 and second peak corresponds to Mr of 63000. B). Size exclusion chromatography of CLIC4. Large peak corresponds to the Mr of 32400 and a second peak corresponds to 63500.

A). Size-exclusion chromatography of CLIC5A

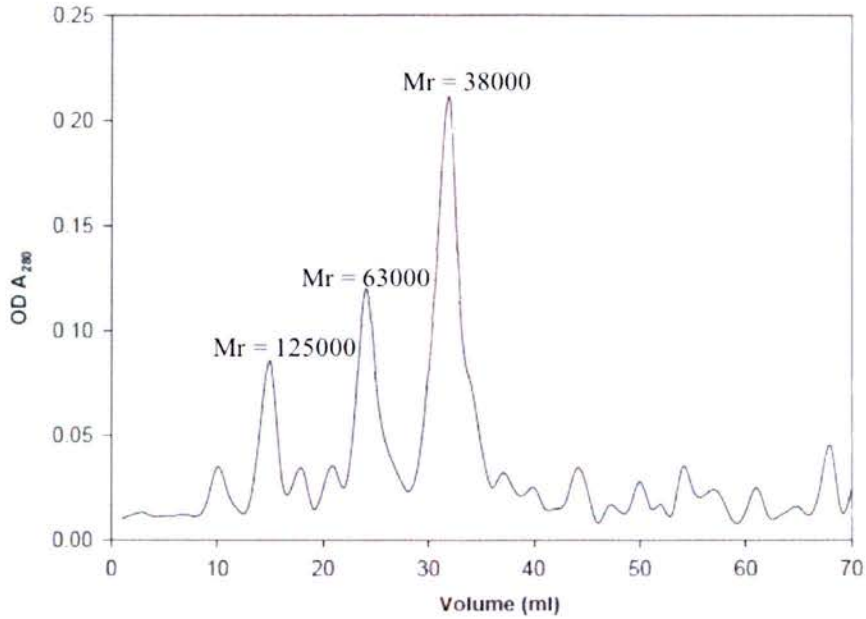

B). Purified CLIC proteins

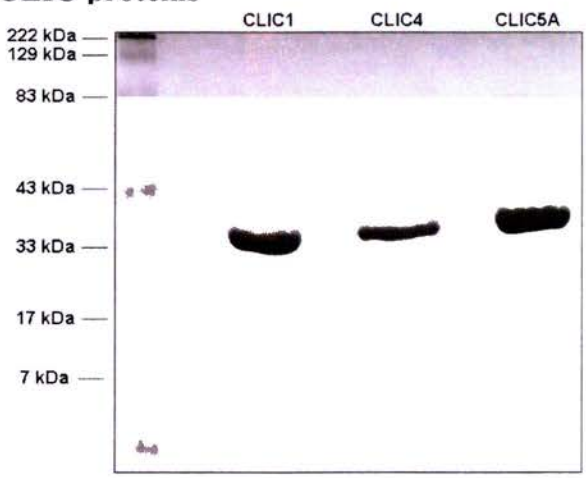

Fig 3.4. Size-exclusion chromatography of CLIC5A. (A). Large peak corresponds to the Mr of 38000 and two small peaks correspond to Mr of 63000 and 125000, respectively. The total amount of protein injected into the column was 4 mg. (B). Coomassie-blue stained gel of purified CLIC proteins. CLIC1, CLIC4 and CLIC5A monomers were run on SDS-PAGE after size exclusion chromatography. 5 µl of each sample were loaded on 10% (w/v) SDS-PAGE.

ribonuclease A (Mr 13700), ovalbumin (Mr 43000), albumin (Mr 67000) and pGEX vector (GST) (Mr 27897) (Fig 3.2). The molecular weight (Mr) of the proteins subjected to gel-exclusion FPLC was determined from a plot of log of (Mr) vs K_{av} (the corrected partition coefficient) (fig 3B):

$$K_{av} = (V_e - V_o)/(V_t - V_o) \qquad [1]$$

where V_e, V_o, and V_t represent the elution volume, the void volume, and the packed bed volume, respectively. V_o was measured with blue dextran and found to be 4.5 ml. V_t was measured by using Bromophenol blue, and was 70 ml for the column used.

5 ml fractions were combined from the broad peak and concentrated. The Mr of the collected fractions was obtained from a plot of log (Mr) *vs.* K_{av}, CLIC1 (32300) (Fig 3.3), CLIC4 (32400) (Fig 3.3), CLIC5A (38000) (Fig 3.4), short CLIC1 (12000) (Fig 3.5) and short CLIC4 (11000) (Fig 3.5). CLIC proteins readily oligomerise on oxidation. Even though FPLC was carried out under strong reducing conditions, higher molecular weight fractions were collected in all the experiments. The Mr of the CLIC1 oligomer corresponded to 63000 and CLIC4 was 63500. In CLIC5A, two distinct oligmers were obtained with corresponding Mr of 63000 and 125000. For short CLIC1, the Mr of oligomer was 23000 and for short CLIC4, it was 22000.

Monomers (Fig 3.4 and Fig 3.6) were separated from dimers and higher oligomers of CLICs and any other contaminating proteins. The protein aliquots were not exposed

A). Size-exclusion chromatography of truncated CLIC1

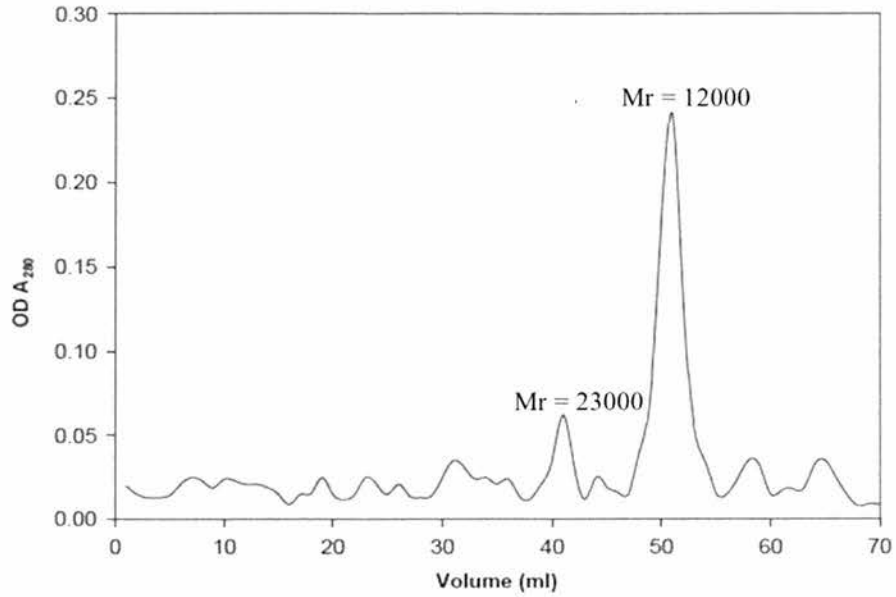

B). Size-exclusion chromatography of truncated CLIC4

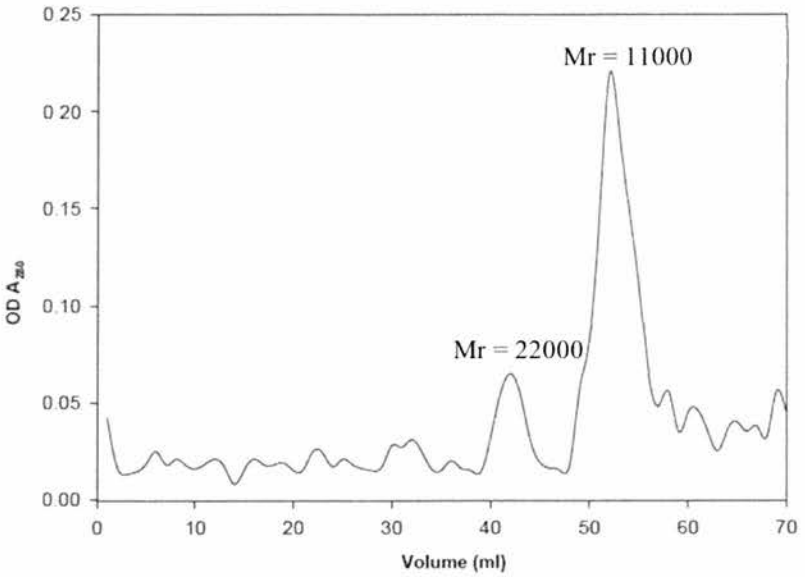

Fig. 3.5. Size-exclusion chromatography of truncated CLIC1 and truncated CLIC4. The total amount of proteins injected into the column was 2 mg and 2.5 mg for short CLIC1 and short CLIC4, respectively. (A). Size exclusion chromatography of short CLIC1 (1-58). Broad peak corresponds to Mr of 12000 and a second peak corresponds to Mr of 23000. (B). Size exclusion chromatography of short CLIC4 (1-62). Large peak corresponds to Mr of 11000 and a second peak corresponds to Mr of 22000.

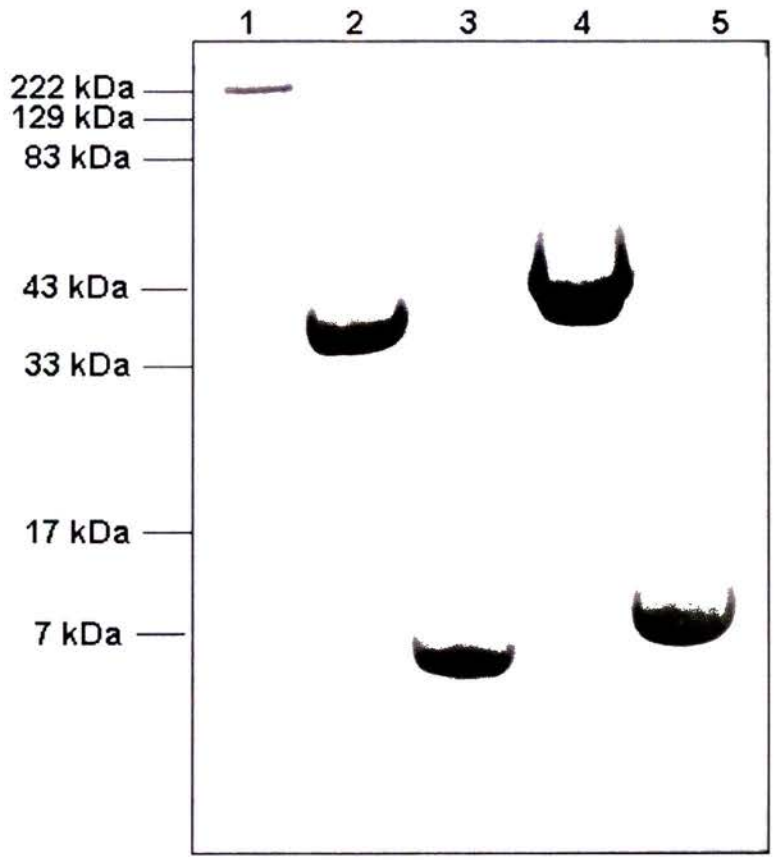

Fig. 3.6. Purified short CLIC proteins. Coomassie blue stained gel of short CLIC1 (1-58) and short CLIC4 (1-62). 5 µl of each sample (peak corresponding to monomers) of short CLIC1 and short CLIC4 was subjected to 10% (w/v) SDS-PAGE after size-exclusion chromatography. 1. Marker, 2. Full length CLIC4, 3. Short CLIC4 (1-62), 4. Full length CLIC1 and 5. short CLIC1 (1-58).

to detergents at any stage and were stored for up to 3 months at -70°C. A stoichiometric excess of DTT (5 mM) was maintained for CLIC1 and CLIC4 whereas β-mercaptoethanol (5 mM) was used for CLIC5A in all the buffers. The stronger reducing conditions were required for CLIC5A because it formed oligomers even in 5 mM DTT.

Purified CLIC1 and CLIC4 were also verified by whole-protein mass-spectrophotometry (MS), by comparing their calculated molecular weights with the MS peaks. This confirmation was carried out partly because CLIC1 and CLIC4 often run anomalously on SDS-PAGE.

3.7 Oligomerisation of CLICs proteins

CLICs have been predicted and have been shown to form oligomers (Harrop et al., 2001; Littler et al., 2004; Littler et al., 2005), and the crystal structure of CLIC1 showed a dimer (Littler et al., 2004). CLIC4 was recently shown to form trimers with a hydrogen-bond network and hydrophobic contacts (Li et al., 2006). CLIC1, CLIC4 and CLIC5A readily formed oligomers (Fig 3.7) when incubated with 5 mM H_2O_2 for 60 mins at 4°C (n=5). CLIC1, CLIC4 and CLIC5A can form intramolecular (Fig 3.7, marked as f) and intermolecular disulphide bonds (b-e). All bands corresponding to dimers, tetramers and higher oligomers were seen in all the proteins. CLIC4 showed an additional band corresponding to a trimeric position which fits with the published data (Li et al., 2006).

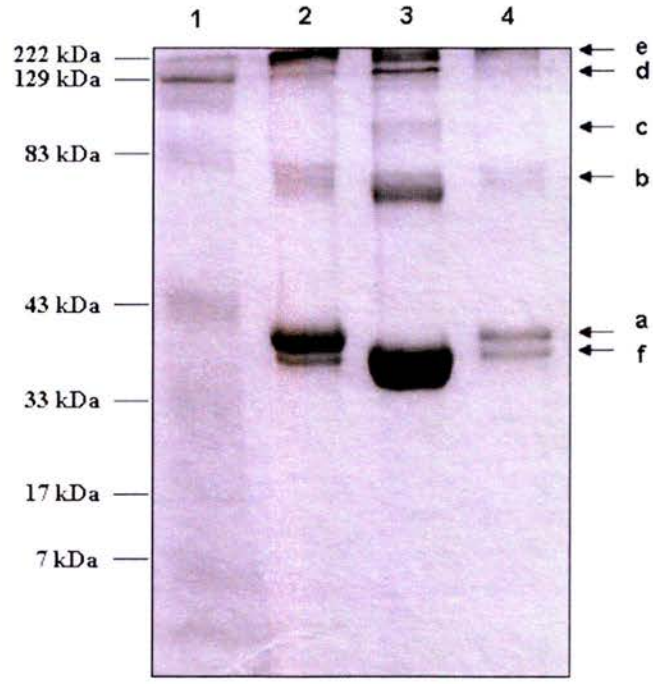

Fig 3.7. Oxidation of CLICs. Recombinant CLIC1 (lane 2), CLIC4 (lane 3) and CLIC5A (lane 4) were oxidised with 5 mM H_2O_2 for 60 mins at 4°C. Coomassie blue stained 10% (w/v) non-reducing SDS-PAGE of oxidised CLIC proteins shows probable intermolecular (b-e) and intramolecular (f) disulphide bonds.

3.8 Characterisation of anti-CLIC antibodies

Anti-CLIC1 (pAb1390) and Anti-CLIC4 (pAb1391) antibodies were generated for full-length recombinant CLIC1 and CLIC4 proteins, respectively (R.H. Ashley, unpublished data). Antibodies were affinity purified as explained in Chapter 2 (2.12). The specificity and cross-reactivity of the anti-CLIC antibodies were tested against previous anti-serum raised against the C-terminus of CLIC4 (referred to as pAb and pAb64H1). Affinity purified antibodies were more sensitive and did not cross react with other CLICs, as compared to the originating anti sera (pAb and pAb64H1). All the antibodies and anti sera were tested by dot blots (2.11.3) and Western blotting (2.11.2). Specificities and cross-reactivities of affinity-purified anti-CLICs are summarised in Table 3.1A for dot blots and Table 3.1B for Western blots. On dot blotting, anti-serum p64H1 and anti-serum 990 both detected 10 ng of CLIC1 and 100 ng of CLIC4 proteins, respectively, but were not specific. The anti-serum for p64H1 was sensitive to 1000ng of CLIC1 and CLIC4 but was not specific, whereas 990 anti-serum could detect 1500ng of both proteins. Affinity-purified anti-CLIC1 antibody was sensitive to 0.1 ng (dot blot) and 100 ng of CLIC1 (Western blot) and cross-reacted with 1000 ng CLIC4 in dot blots and with 1500 ng in western blots (Fig 3.10). Affinity-purified anti-CLIC4 was sensitive to 10 ng (dot blot) and 500 ng (Western blot) CLIC4, and did not cross-react with CLIC1 even when CLIC1 was present at 1000 ng (dot blot) or 1500 ng (Western blot) (fig 3.10).

A). Specificity and cross reactivity of antibodies on dot blots.

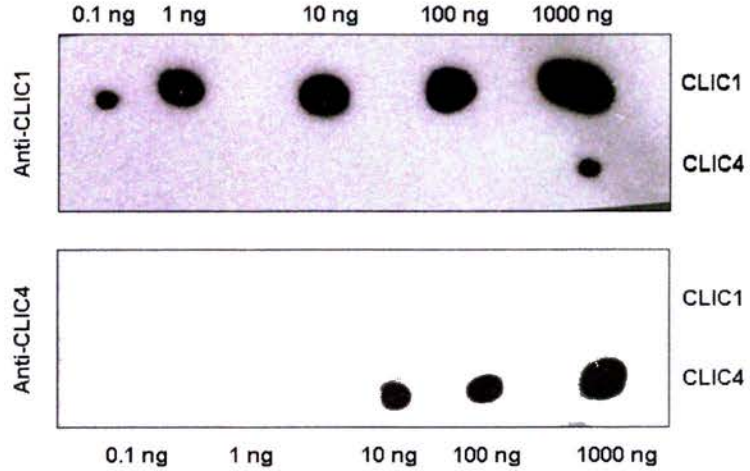

B). Specificity and cross reactivity of antibodies on western blots.

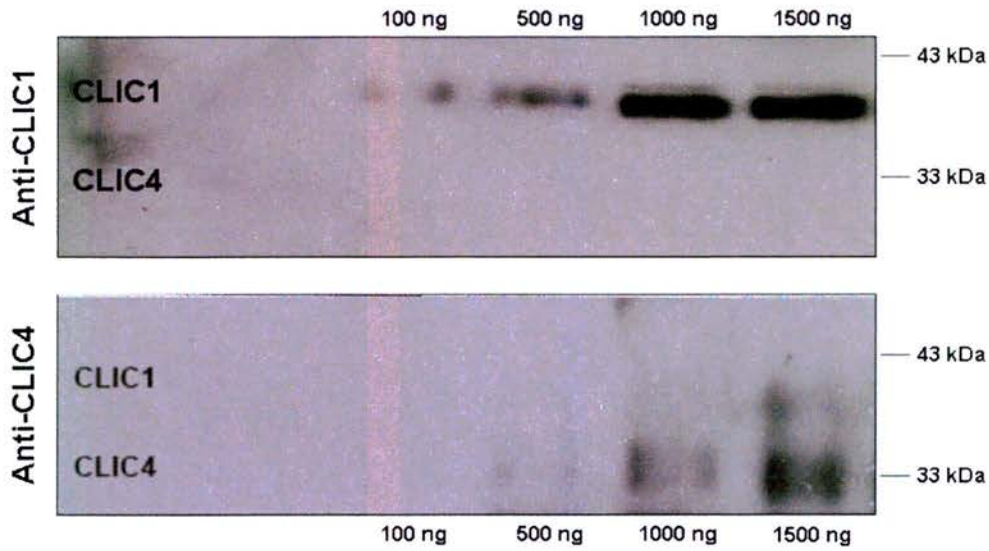

Fig 3.8. Characterisation of affinity-purified anti-CLIC1 and anti-CLIC4 antibodies. Antibodies against full-length recombinant CLIC1 and CLIC4 were affinity-purified, and characterised by dot blots and Western blots. The data are summarised in table 3.1. (A) Dot blots for CLIC1 and CLIC4 showing the specificity and cross-reactivities of anti-CLIC1 and anti-CLIC4 antibodies. (B) CLIC1 and CLIC4 were subjected to 10% (w/v) SDS-PAGE and Western blotting was performed with affinity-purified antibodies. Western blots were analysed for the specificity and cross-reactivity of respective antibodies.

A). Specificity and cross reactivity of antibodies on dot blots.

Antibodies	Proteins	0.01ng	0.1ng	1ng	10ng	100ng	1000ng
p64H1	CLIC 1	-	-	-	+	+	+
	CLIC4	-	-	-	-	+	+
990	CLIC 1	-	-	-	+	+	+
	CLIC 4	-	-	-	-	+	+
1390 Anti CLIC1	CLIC 1	-	+	+	+	+	+
	CLIC 4	-	-	-	-	-	+
1391 Anti CLIC4	CLIC 1	-	-	-	-	-	-
	CLIC 4	-	-	-	+	+	+

B). Specificity and cross reactivity of antibodies on Western blots.

Antibodies	Proteins	100ng	500ng	1000ng	1500ng
p64H1	CLIC 1	-	-	+	+
	CLIC4	-	-	+	+
990	CLIC 1	-	-	-	+
	CLIC 4	-	-	-	+
1390 Anti CLIC1	CLIC 1	+	+	+	+
	CLIC 4	-	-	-	-
1391 Anti CLIC4	CLIC 1	-	-	-	-
	CLIC 4	-	+	+	+

Table 3.1. Specificity and cross reactivity of antibodies. (A). Dot blots. Two antisera (p64H1 and 990) were tested on CLIC1 and CLIC4 along with affinity-purified anti-CLIC1 and anti-CLIC4 antibodies on dot blots. (B). Western blots. Two antisera (p64H1) and 990 were tested on CLIC1 and CLIC4 along with affinity purified anti-CLIC1 and anti-CLIC4 antibodies on dot blots.

3.9 Over-expression and purification of PRD constructs

Plasmids encoding the proline rich domain (PRD) of Dynamin I and its phospho-mimitic mutants (AA (S774 A, S778A) (S774E, S778E)) (Anggono et al., 2006) fused to GST in pGEX-4T-1 (Amersham) (Appendix I.2) vector were obtained from Dr. P Robinson, (Cell signalling unit, CMRI, Sydney Australia). They were overexpressed in *E.*coli BL21 (DE3) cells, and purified by affinity chromatography. The immobilized GST fusion proteins were either eluted using glutathione Sepharose 4B beads, or used as immobilised proteins to study the *in vitro* interaction with CLIC1 and CLIC4 (Chapter 7). Proteins were over-expressed and purified using glutathione Sepharose beads (see Methods, Chapter 2).

3.10 Discussion

Several different CLIC constructs were made by cloning and site-directed mutagenesis. DNA polymerase *Pfu* was used throughout for two specific reasons. Firstly, *Pfu* produces a blunt ended DNA for QuikChange site-directed mutagenesis so that extra nucleotides are not introduced by each cycle of PCR. Secondly, it has a low error rate (1.3×10^{-6} errors/nucleotide/cycle) compared to standard *Taq* DNA polymerase (8.0×10^{-6} errors/nucleotide/cycle) (Cline et al., 1996). This reduced the probability of introducing unwanted mutations into the DNA during amplification. All the constructs were sequenced and confirmed as error free. Additional precautions were taken by subcloning the mutagenised inserts into fresh pHis8 vector to ensure against mutations that may have been introduced into other critical parts of

A). Induction of PRD of DynaminI and its phosphomimitic mutants (AA and EE).

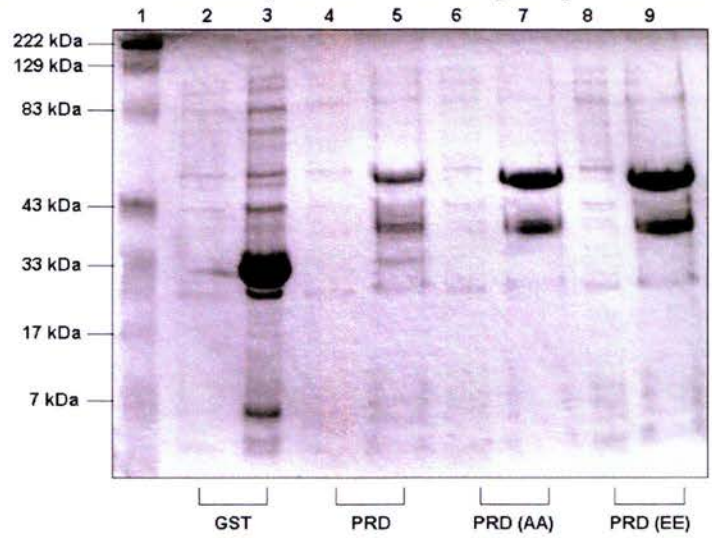

B). Purified PRD of DynaminI and its phosphomimitic mutants (AA and EE)

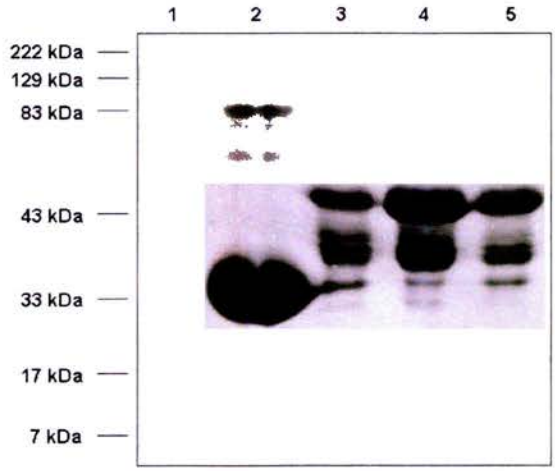

Fig 3.9. Overexpression and purification of PRD of dynamin I and its phospho mimetic mutants (AA and EE). (A). Overexpression of PRD of dynamin I and its mutants. PRD fused with GST was overexpressed and purified. 10 µl of each sample was boiled and subjected to 10% (w/v) SDS-PAGE. Uninduced (lane 2) and induced GST (lane 3) were loaded with uninduced (lane 4) and induced PRD (lane 5), uninduced (lane 6) and induced AA mutants of PRD (lane 7), and, uninduced (lane 8) and induced EE mutants of PRD (lane 9). (B). Purification of PRD of Dynamin I and its mutants. 10 µl of eluted protein samples were subjected to 10% (w/v) SDS-PAGE. Lane 1 contain GST without any fusion protein, lane 2, 3 and 4 contain PRD (wt), PRD (AA) and PRD (EE), respectively.

the plasmid. Primer design was also important, particularly for site-directed mutagensis. Long primers are likely to have internal secondary structure that can result in hairpin loops or dimers that can make annealing and therefore amplification difficult. Primers approximately 20 nucleotides in length were used.

The pHis8 vector has advantages over unmodified pET vectors. It is a modified pET-28a(+), with an *Nco* I site introduced after the thrombin cleavage site, and the N terminal hexahistidyl-coding sequence is extended to eight histidines (Jez et al., 2000), which increases the efficiency of Ni^{2+}-affinity chromatography. CLIC constructs were expressed in pHis8 and purified by Ni^{2+}-affinity chromatography. Specific conditions were optimized for overexpression and purification of proteins (e.g. temperature and incubation time for inductions, and the concentration of IPTG). All the CLIC proteins have conserved cysteines (CLIC1 has 6, CLIC4 has 4 and CLIC5A has 4 residues) hence they were always prepared and stored under reducing conditions. These precautions were necessary because oxidised CLIC1 was shown to form a dimer (Littler et al., 2003) and CLIC4 was shown to exist as a trimer (Lie et al., 2006) *in vitro*. CLIC1, CLIC4 and their constructs were purified and stored in buffers containing 5 mM DTT, whereas, CLIC5A required the strong reducing agent 2 mM β-mercaptoethanol as CLIC5A oligomerised in the presence of DTT.

The oligomerisation of CLIC1 was resultant of intramolecular disulphide bond between C24 and C59 (Littler et al., 2004). C59 is absent in other CLIC proteins, hence this mechanism of dimerisation is specific for CLIC1 only. Trimerisation of CLIC4 was attributed to the intermolecular hydrogen-bond formations and hydrophobic contacts between the three monomers. There was no intramolecular

disulphide bond formation in the case of CLIC4 (Li et al., 2006). CLIC1, CLIC4, and CLIC5A were incubated with a strong oxidising agent (H_2O_2) and were subjected to non-reducing SDS-PAGE. Intramolecular and intermolecular disulphide bond formation was observed in CLIC1, CLIC4 and CLIC5A proteins. CLIC4, in addition, also forms a trimer. The mammalian CLICs have three conserved cysteines throughout, and at least one cysteine is present before the putative TMD. CLIC1, CLIC4, and CLIC5A have 6, 4 and 4 cysteines respectively, in the whole sequence. These conserved cysteines could play an important functional role in CLICs which should be studied further.

CLIC4 was shown to interact directly with dynamin I (Suginta et al., 2001). The binding site of CLICs with dynamin I was not mapped. The PRD of dynamin I is involved in interaction with many of the proteins involved in endocytosis (Smillie and Cousin, 2005). Dynamin 1 is dephosphorylated at S774 and S778 in the PRD region during synaptic vesicle endocytosis in the nerve terminals (Anggono et al., 2006). The double mutants (AA and EE) of PRD of dynamin I were overexpressed and purified to investigate their role in interaction with CLIC proteins (Chapter 7).

CHAPTER 4

SINGLE-CHANNEL PROPERTIES OF CLIC PROTEINS

4.1 Introduction

Ion channels are located in the heterogeneous lipid matrix of the plasma membrane and the membranes of intracellular organelles. Lipid species partition asymmetrically within and across biological membrane leaflets. These non-random lipid associations produce domains that differ in composition and physicochemical properties from the bulk membrane. The lipid environment of membrane proteins that defines the local distribution of polarity, dielectric constant, and steric geometry has a central role in the determination of protein structure and function. It is known that lipids impose various constraints on ion channels such as: 1). the hydrophobic thickness matching of protein and lipid bilayers affects the structure and function, 2). affect the opening and closing of the channels, 3). the spontaneous curvature of lipids linked to the lateral pressure of the bilayer can modulate ion channel activity, and 4) channels require anionic lipids for their function (Sobko et al., 2006).

Lipid molecules self-assemble to form dynamic membrane bilayers. Artificial planar lipid bilayers are used for electrophysiological studies of ion channel proteins at the single-molecular level. In all ion channel reconstitution experiments, the bilayer is formed across a hole in the wall separating two fluid-filled chambers and this technique was introduced by Mueller and colleagues in 1960s (Mueller et al., 1962; Mueller and Rudin, 1969). CLIC channels were reconstituted in the past, but revealed a large variation between single-channel conductances. The variation in single-channel conductances was studied in this chapter. CLICs are putative pore-forming omega glutathione S-transferase (GSTs) homologs, synthesised without a

Protein	Method and conditions	Conductance
CLIC1	Single channel conductance transfected CH0-K1 cells[5,8]	8 pS, 16 pS
	Patch clamp (nuclei) transfected CHO- K1 cells[8]	33 pS
	Planar bilayers (PC and cholesterol)[7,9]	31 pS
	Planar bilayers (asolectin or PE/PS)[6]	60 and 120 pS
	Planar bilayers (PC)[11]	28 pS
CLIC4	Patch clamp transfected HEK-293 cells[10]	1 pS
	Planar bilayers (PE/PS)[3]	10 pS
	Planar bilayers (PC)[12]	30 pS, 58 pS and 86 pS
CLIC5B (p64)	Planar bilayers (asolectin)[1,4]	26, 100 and 400 pS
	Patch clamp (proteoliposomes of soybean phospholipid)[2]	100-150 pS

Table 4.1 Conductance of CLIC channels in specific conditions. The conductance of reconstituted CLICs differs between studies from different groups. The specific lipids used and the corresponding conductances of CLICs are shown in the table. (Landry[1] et al., 1989; Weber-Schurholz[2] et al., 1993; Duncan[3] et al., 1997; Edwards[4] et al., 1998; Tonini[5] et al., 2000; Tulk[6] et al., 2000; Tulk[7] et al., 2002; Valenzuela[8] et al., 2002; Warton[9] et al., 2002; Proutski[10] et al., 2002; Littler[11] et al., 2004; Littler[12] et al., 2005). Note that some of these differences may be explained by different ionic conditions.

leader sequence and thought to insert into cell membranes directly from the cytosol. Though they belong to the GST superfamily (Harrop et al., 2001), they do not have similar functional properties to GSTs and GSTs do not share the unusual "autoinserting" ability of CLIC proteins (Cromer et al., 2002).

After insertion into the membrane from the cytosol, CLIC1 and CLIC4 (p64H1) monomers span the membrane completely with an external (luminal) N-terminus and an odd number of transmembrane domain(s) (Duncan et al., 1997; Tonini et al., 2000; Proutski et al., 2002). The membrane forms of recombinant CLIC1 and CLIC4 are associated with novel ion channel-like activity (Valenzuela et al., 2000; Proutski et al., 2002). The cellular proteins exist almost entirely in a soluble cytosolic form (Suginta et al., 2001).

CLIC1 has been shown to be a pore-forming protein *in vitro* and shows variability in single-channel conductance (Table 4.1). Recombinant CLIC1 channels reconstituted by "tip-dipping" (Warton et al. 2002) proved to be similar to those recorded from the cells, but channels reconstituted in planar bilayers (Tulk et al. 2000; Tulk et al., 2002) had large single-channel conductance under similar ionic conditions. It was speculated (Warton et al., 2002) that CLIC1 could form channel "aggregates", with larger overall conductances, under specific conditions. Table 4.1 summarises the conductance of CLIC proteins reconstituted under specific conditions.

In contrast to CLIC1, relatively limited information is available on CLIC4-associated ion channels. Incorporation of microsomal membrane vesicles containing

Lipids	CLIC1	CLIC4	CLIC5
Diphytanolyphosphtaidylcholine (DPPC)	No	No	No
Palmitoyl- oleoyl (PO) phosphatidylcholine (PC)	No	No	NT
PO-phosphatidylethanolamine (PE)	No	No	NT
Soybean lecithin	No	No	No
POPC:POPE (1:1)	No	No	NT
POPC:POPE (2:1)	No	No	NT
POPC:POPE:Cholesterol (4:1:1)	Yes	Yes	Yes

Table 4.2. Reconstitution of CLIC proteins in specific lipids. Recombinant CLIC proteins were reconstituted in a specific lipid or lipid mixtures in specific proportions (mol:mol). Successful reconstitution with consistent channels is indicated by "Yes" otherwise it is indicated as "No". "NT" indicates lipid mixtures not tested. No channel-like activity was seen without the addition of CLIC proteins for 45 mins.

recombinant CLIC4 into planar lipid bilayers gave rise to a novel anion channel activity of 10-50 pS (Duncan et al., 1997). CLIC4 showed channel-like activity in "tip-dip" bilayers, but the data were very limited, and a range of conductances were observed (30 pS, 58 pS and 86 pS, Littler et al., 2005). CLIC4 was unable to autoinsert and form channels in the presence of DTT in planar lipid bilayers containing PC. The selectivity and regulation mechanism of CLIC4 channels were not investigated (Littler et al., 2005). Novel ion channels specifically shown to contain CLIC4 (FLAG-tagged) have also been recorded by patch-clamping the plasma membrane of cells over-expressing CLIC4. The overexpression of flag-tagged CLIC4 drives them to the plasma membrane of HEK-293 cells. In the presence of large cations, the conductance of individual CLIC4 channels was very low, of the order of 1pS (Proutski et al., 2002).

CLIC5A, has a splice variant CLIC5B (p64) which was shown to form ion channels in bilayers containing asolectin (Landry et al., 1989; Edwards et al. 1998). Table 4.1 summarises the variation between the conductances noted for CLIC5B. CLIC1 (Valenzuela et al., 1997), CLIC4 (Proutski et al., 2002) and CLIC5A (Berryman and Bretscher, 2000), have C-termini similar to CLIC5B (p64) and can localise to the plasma membrane. In contrast to CLIC1, CLIC4 and CLIC5B, channel formation by CLIC5A is yet to be investigated. In a chloride-efflux assay, using asolectin vesicles, CLIC5A was reported to form ion channels (Berryman et al., 2004). The chloride-efflux mediated by CLIC5A was not however comparable to the efflux rate expected for an ion channel.

In this chapter, the lipid-dependent reconstitution of CLIC proteins is described, and the single-channel conductance and selectivity of recombinant CLIC1, CLIC4 and CLIC5A are investigated.

4.2 Channel formation by CLIC proteins is lipid-dependent

CLIC1 and CLIC4 have been studied extensively by several groups, with large variation in channel conductance (Table 4.1) and selectivities. In previous work involving the single-channel reconstitution of CLIC proteins in bilayers, the membrane always contained phosphatidylcholine (PC) or phosphatidylethanolamine (PE), and sometimes both (including PE in partially-purified soybean lecithin). CLIC1 and CLIC4 proteins readily inserted into hemi-bilayers or monolayers containing POPC or equimolar POPS and POPE, even with an intact His-tag (R.H. Ashley, unpublished data). However, recombinant CLIC1 and CLIC4 failed to form well-defined ion channels in 20/20 and 7/7 experiments respectively, using planar bilayers containing specific lipids or lipid mixtures as summarised in the table 4.2, with or without 1 mM DTT or 10-100 μM H_2O_2 in one or both the chambers. These channels were not consistent, and had a detergent-like appearance (Fig 4.1a). This suggested that the proteins require specific lipids to insert, refold, and/or form oligomers, after insertion into the membranes. After extensive preliminary experiments testing a variety of lipid mixtures and conditions, highly reproducible ion channel activity was obtained with recombinant CLIC1 (110/115 independent experiments), CLIC4 (80/83 independent experiments) and CLIC5A (45/52 independent experiments), in bilayers containing POPE, POPS, and cholesterol in a

A).

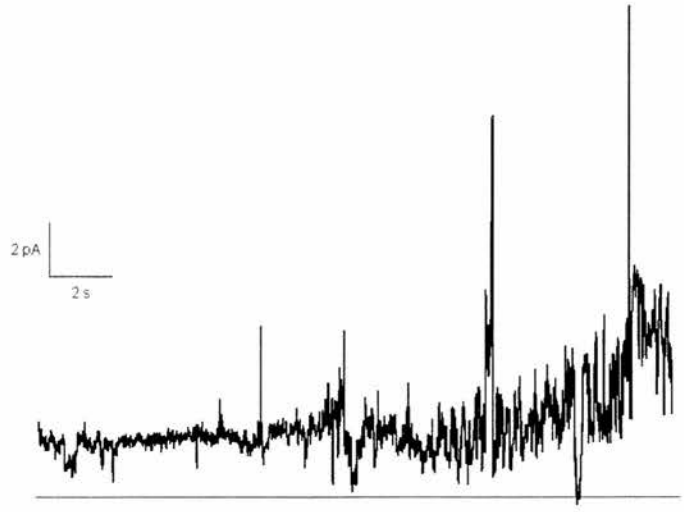

B).

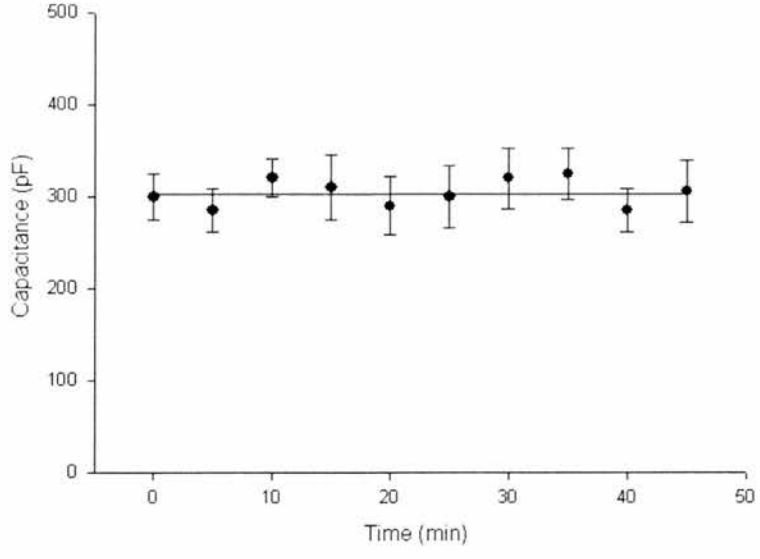

Fig 4.1. Detergent-like appearances and capacitance of the bilayer. (A) CLIC1 incorporated into the bilayers containing PC at +100 mV. The solid line indicates the closed level. Channels were not consistent and have a detergent-like appearance. (B) Capacitance (pF) was measured for 45 mins to test the thickness of the bilayer. The error bars are standard deviations for 20 independent experiments. The line was fitted by linear regression.

molar ratio of 4:1:1, respectively, in the presence of 1mM DTT.

Channels were also obtained in a glutathione buffer system (GSH: GSSG :: 10:1), and in the presence of H_2O_2 from oxidised soluble CLIC1, CLIC4 and CLIC5A proteins exposed to 100 μM H_2O_2 before insertion. There was no "detergent-like" bilayer instability (Fig 4.1a) as observed in other lipid mixtures, including soybean lecithin, which produced unstable anionic or cationic currents of varying amplitude in the bilayers. Subsequent experiments were carried out using planar bilayers containing POPE/POPS/cholesterol, in a molar ratio of 4:1:1. All the channels appeared to be identical and consistent, with or without an intact N-terminal His-tag.

There was no channel-like activity in bilayers in the absence of CLIC proteins. The bilayers were thinned to an appropriate capacitance (> 250 pF), and the capacitance was monitored for over 30 mins. During the experiments, the capacitance of the bilayer remained constant, as shown in fig 4.1.

4.3 Single-channel properties of CLIC1

After the addition of CLIC1, consistent channels appeared within 10 mins. The current/voltage (I/V) relationship of CLIC1 in asymmetrical 500:50 mM *cis versus trans* KCl is shown in Fig 4.2. Detailed inspection of CLIC1 unit currents

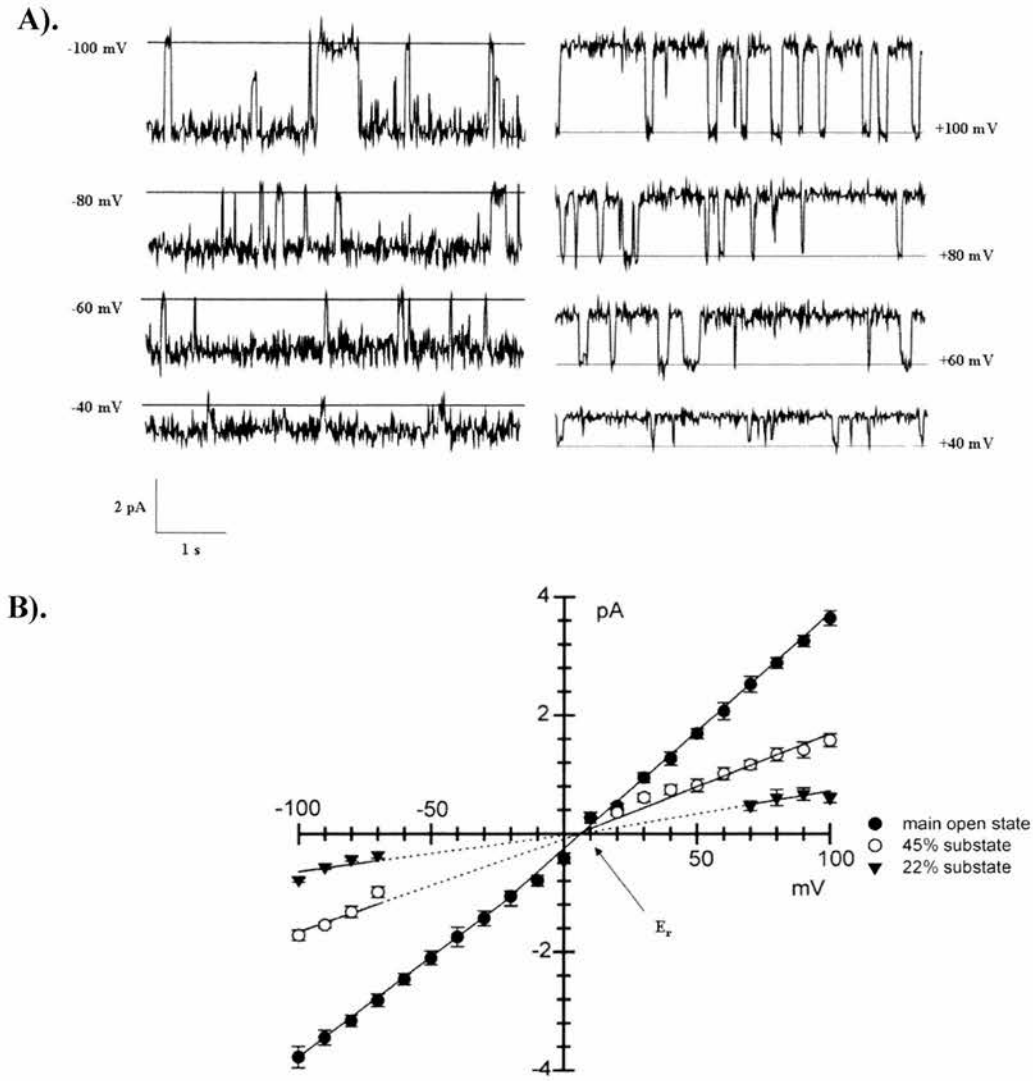

Fig 4.2. CLIC1 channels in asymmetric KCl. Single-channel recordings in 500:50 mM, *cis vs. trans* KCl containing 1 mM DTT in the planar lipid bilayer. The solid lines indicate the closed current levels. (A) Representative traces of single-channel currents for a range of holding potentials. (B) Corresponding current/voltage (I/V) relationships for the main open level and the two infrequent substates (shown as mean ± SD, n = 10–23). The dotted lines are extrapolations (e.g., where substate amplitudes became too small to measure) and hence, it was difficult to resolve the conductances at lower holding potentials. Reversal potential is indicated by an arrow.

showed two infrequent substates (Fig 4.3), at 45% and 22% of the main open level. The maximum slope conductance of the main open state in a 500 mM *cis vs.* 50 mM *trans* KCl is 38 ± 3pS (mean ± SD, n=23) in 1 mM DTT. The reversal potential (E_r) obtained from the current/voltage (I/V) plot for the main open state was + 6 ± 1.1 mV (mean ± SD, n=23 independent recordings), corresponding to a mean anion/cation permeability ratio (Pa/Pc) of 1.4 (corrected for ionic activities) calculated from the modified Goldman-Hodgkin-Katz (GHK) voltage-equation. The reversal potential and ionic selectivity of the main and sub-conductance levels were similar.

Previously, it was shown that pre-oxidised CLIC1 and CLIC4 can autoinsert to form ion channels (Littler et al., 2004; Littler et al., 2005). This was tested with the specific lipid mixtures in which consistent channels were obtained in the strong reducing conditions (1mM DTT). In the presence of 100 μM H_2O_2, the conductance of CLIC1 channels from pre-oxidised soluble proteins was reduced to 24 ± 1.5 pS (mean ± SD, n=10) (Fig 4.3c).

Channels were also obtained in the presence of 5 mM GSH instead of 1 mM DTT in both chambers (fig 4.3 d), with similar substates at 45% and 22% of the main open level. However, the single-channel conductance was substantially reduced ($P < 0.005$) compared to DTT, to 25 ± 1.5 pS (mean ± SD, n=13). CLIC1 channels remained open for 1-10s and hence, it was not experimentally feasible to collect enough data for gating analysis.

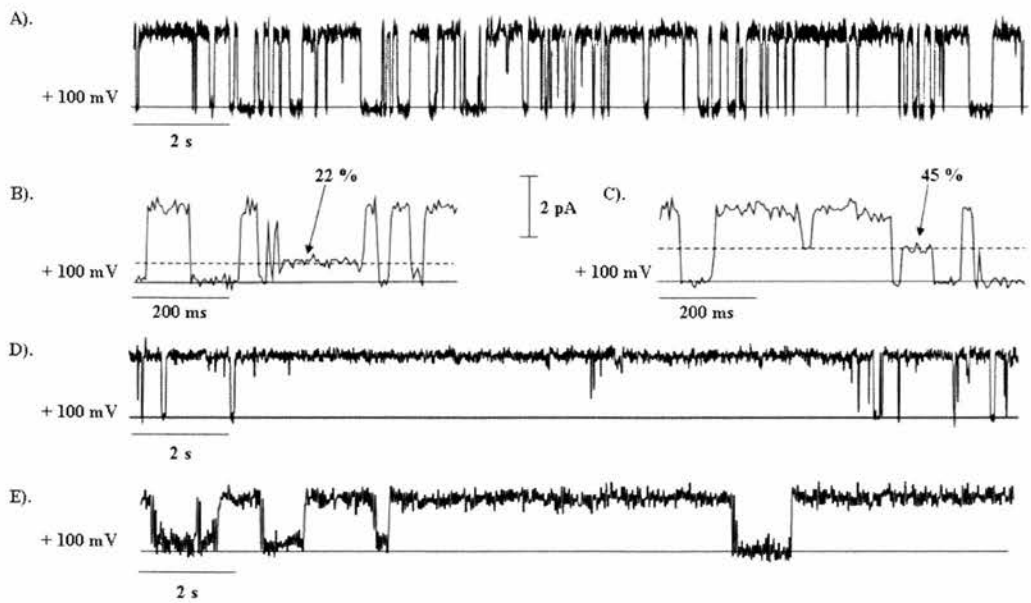

Fig 4.3. Single-channel recordings of CLIC1. Single channel recordings of CLIC1 in asymmetric 500 mM *vs.* 50 mM, *cis vs. trans* KCl. (A) Contiguous 20s recording of CLIC1 in 1 mM DTT. (B) and (C) Selected traces on an expanded timescale showing 45% and 22% substates, HP +100 mV. (D) Single-channel currents at +100 mV in 100 μM H_2O_2. (D) Single-channel currents at +100 mV in 5 mM GSH:GSSG buffer (molar ratio 10:1).

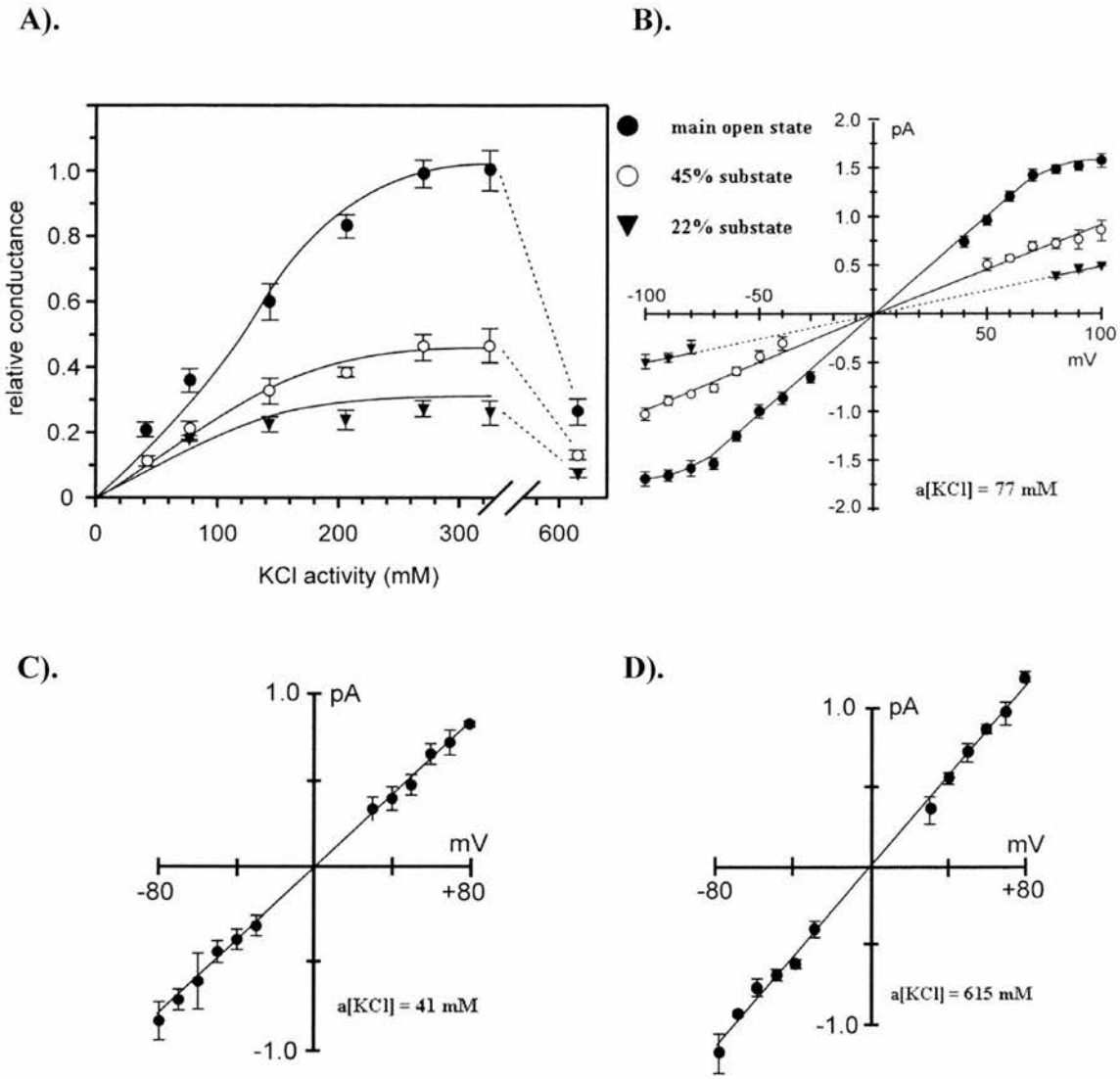

Fig 4.4. CLIC1 in symmetric KCl. (A) Relative single-channel conductance-activity relationships for each conductance level in symmetric KCl solutions (points are shown as mean ± SD, n = 3–7). The conductance in symmetric 500 mM KCl (a [KCl] = 325 mM) is set to 1.0. (Note the break in the x axis between 300 and 600 mM). (B) I/V relationships for each conductance level in 100 mM symmetric KCl (a [KCl] = 77 mM) (points are shown as mean ± SD, n = 5–7). The main open state is fitted to a straight line between +70 and –70 mV by linear regression ($r^2 > 0.99$). (C and D) Examples of I/V relationships in low and high KCl activities, showing the main open state only (points are shown as mean ± SD, n = 3).

Maximum slope conductance of CLIC1 was investigated in a range of symmetrical [KCl]. The current/voltage (I/V) relationship of CLIC1 in symmetric 100 mM KCl (corresponding to an activity of 77 mM) containing 1 mM DTT is shown in fig 4.4. The slope conductance of the main level was constant between + 70 mV and -70 mV, with a mean value of 20.5 $\pm$ 3 pS (mean $\pm$ SD, n=7), but the channel currents appeared to saturate at higher holding potentials. 45% and 22% sublevels were also observed in symmetric 100 mM KCl. The conductances of the fully-open state and the two substates had a non-hyperbolic dependence on KCl activity. Data could not be obtained at very low salt concentrations because the amplitudes (especially substate currents) were too small to resolve. The maximum slope conductance of the fully-open state was 57 $\pm$ 3.5 pS (mean $\pm$ SD, n=7) in symmetric 500 mM KCl (corresponding to an activity of 325 mM). There was a marked decline at higher salt activities (above 350 mM). The current/voltage (I/V) plots at specific salt activities are given in fig 4.4.

Single-channel currents were also recorded in Tris-Cl to replace a smaller cation with a larger cation ($Tris^+$) to analyse the selectivity of CLIC1. Channels were obtained in 500 mM *cis* Tris-HCl *vs.* 50 mM *trans* Tris-HCl (pH 7.4). The conductance of the channel was maintained at negative holding potentials, but reduced at positive holding potentials (Fig 4.5). The reversal potential of CLIC1 in Tris-HCl was + 45 mV $\pm$ 3.5 mV (mean $\pm$ SD, n=8), indicating a significant increase in anion *vs.* cation permeability to 13 $\pm$ 1.0 (mean $\pm$ SD, n=8, not corrected for activities).

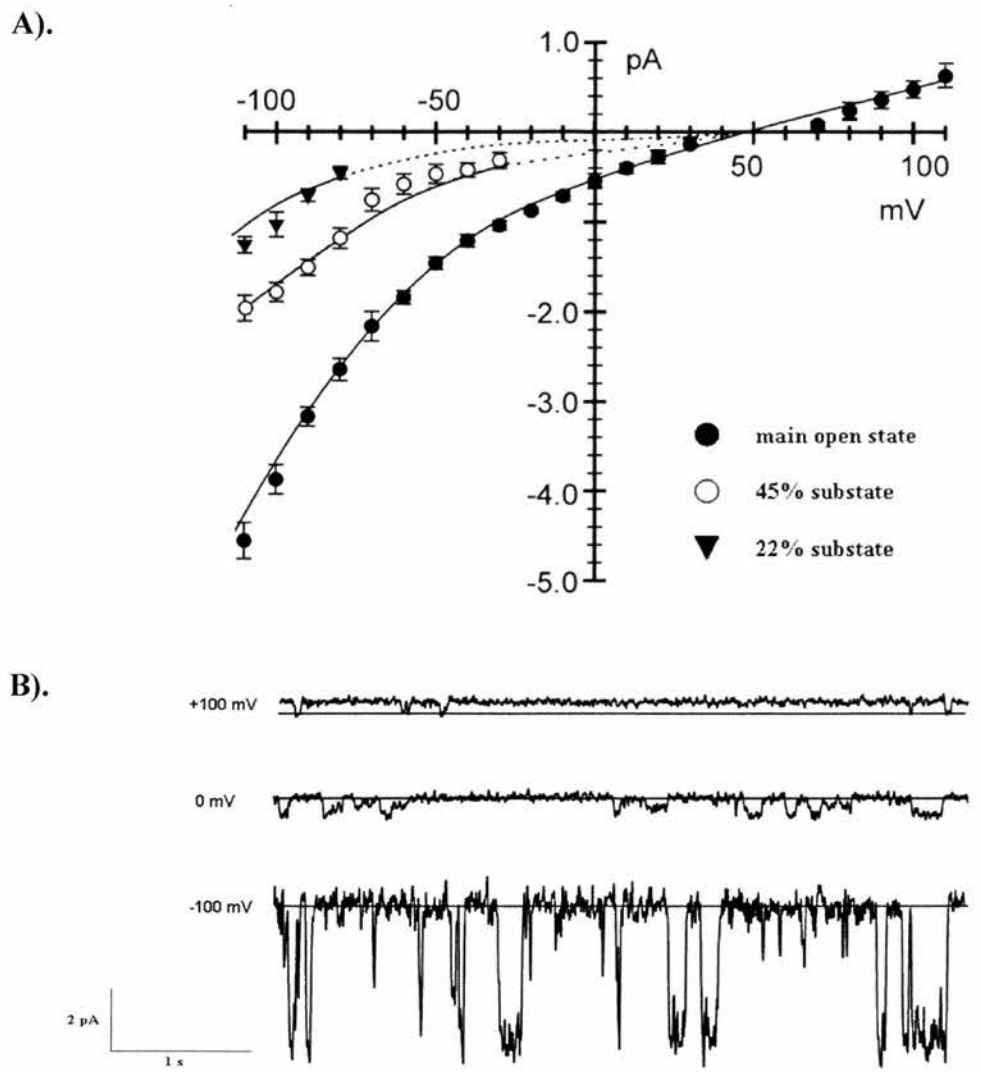

Fig 4.5 CLIC1 channels in Tris Cl. Channels were recorded in 1 mM DTT. (A) I/V relationships for each conductance level (points are shown as mean ± SD, n = 5-8). The mean reversal potential is +45 mV. (B) Examples of single-channel currents in asymmetric Tris-Cl (500:50 mM, *cis* versus *trans*). The solid lines indicate the closed current levels. Substate behaviour was observed in most traces.

The relative permeability of different anions was measured under equilibrium conditions by perfusing the *cis* chamber with either 50 mM or 110 mM KCl (corrected for activities), followed by perfusing different potassium salts with exactly the same activity into the *trans* chamber. At symmetrical salt activities of 50 mM KCl, the anion permeability sequence, calculated from the equilibrium potential was I^- (1.9 ± 0.1) > SCN^- (1.2 ± 0.2) ≥ Cl^- (set to 1.0) ≥ $NO^2{}_3{}^-$ (0.9 ± 0.1) ≥ Br^- (0.8 ± 0.1) ≥ F^- (0.7 ± 0.1). At 110 mM, the sequence became I^- (1.8 ± 0.1) > F^- (1.3 ± 0.15) = SCN^- (1.2 ± 0.3) > Cl^- (set to 1.0) = $NO^{2-}{}_3$ (1.0 ± 1.0) = Br^- (1 ± 1.6) (all mean ± SD, n=3 independent experiments).

4.4 Singe-channel properties of CLIC4

Previously, it has been shown that CLIC4 can autoinsert into PC bilayers and has channel-like activity (Littler et al., 2005). In Cl^- efflux assay, the time taken for Cl^- efflux was relatively high and not fully consistent with anion channel activity as only 30% of the ions could pass in 240 s when 27 μg/ml of CLIC4 was added (Littler et al., 2005). In cells, CLIC4 was shown to form small-conductance channels (1pS) (Proutski et al., 2002). CLIC4 recordings were inconsistent, much like CLIC1 channels, in experiments using POPC or equimolar POPE and POPS. Channel formation was highly-consistent for CLIC4 in 80/83 independent experiments containing POPE, POPS and cholesterol (molar ratio of 4:1:1, respectively), in the presence of 1 mM DTT, 5 mM GSH or with proteins preexposed to 100 μM H_2O_2 before reconstitution.

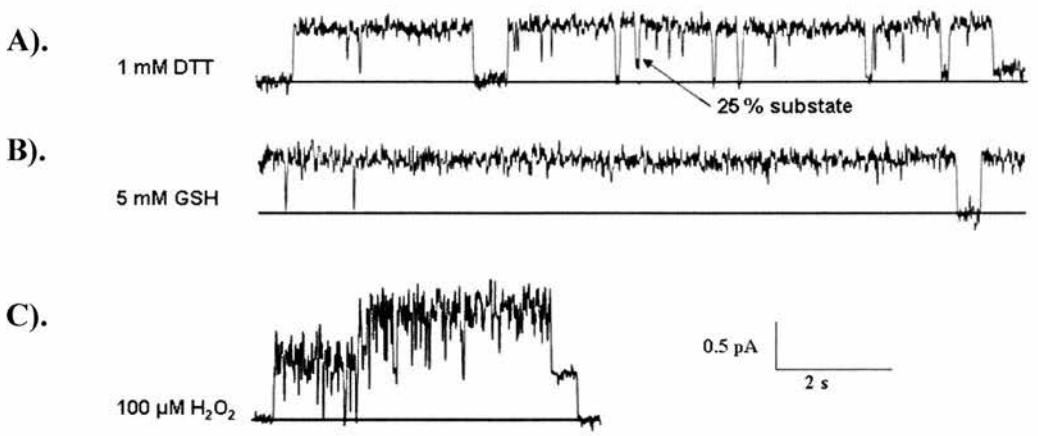

Fig 4.6. Single-channel recordings of CLIC4. Single channel recordings of CLIC4 in asymmetric 500 mM : 50 mM, *cis vs. trans* KCl. Prominent 25% substate level is indicated by an arrow. (A) Single-channel recording at a holding potential (HP) of +100 mV in 1 mM DTT. (B) Contiguous 20 s recording at HP of +100 mV in 5 mM GSH:GSSG (molar ratio 10:1). (C) Contiguous 20s recording at HP of +100 mV in 100 µM H_2O_2.

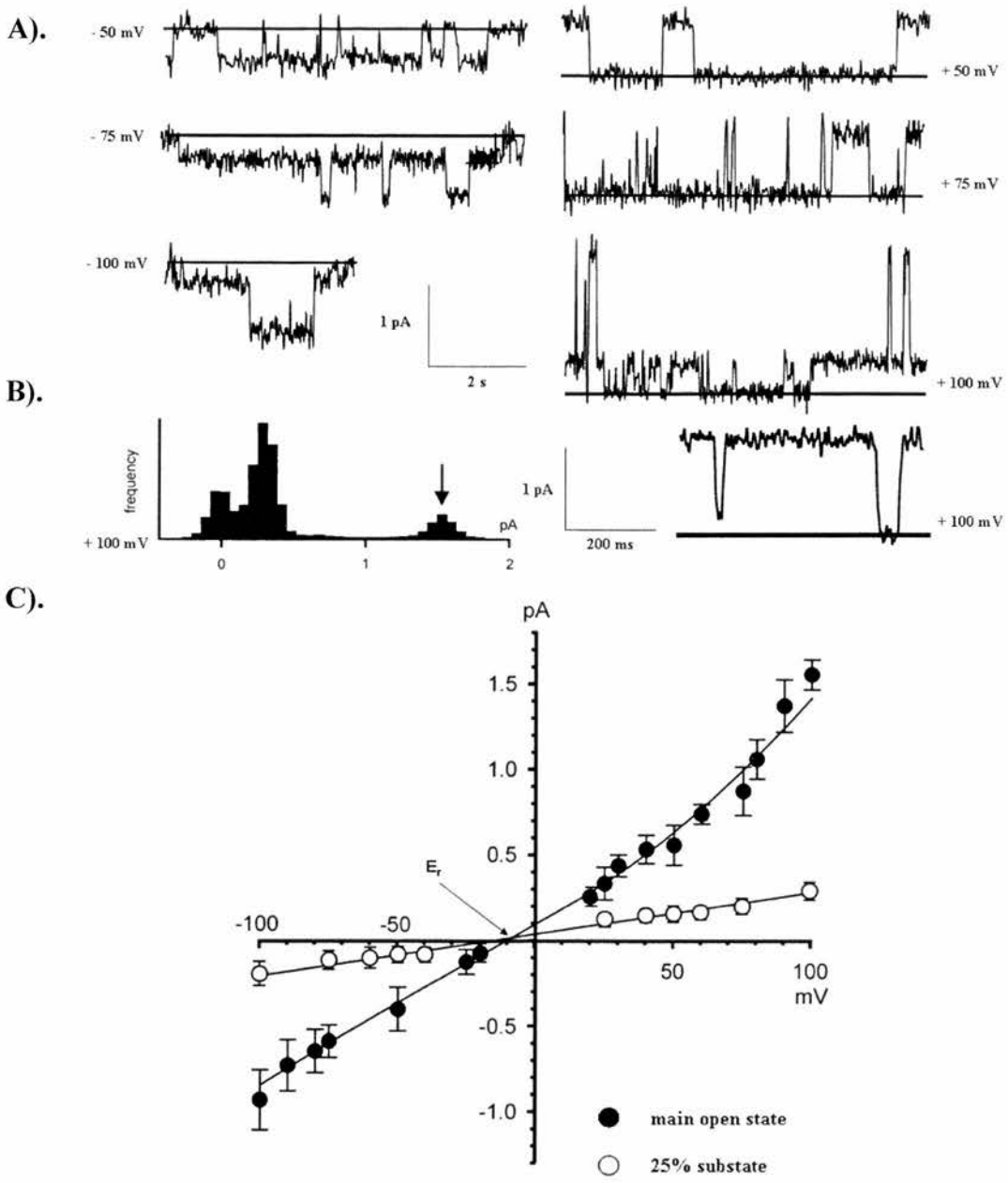

Fig 4.7. Single-channel recordings of CLIC4 in asymmetric KCl. Single-channel recordings in 500:50 mM *cis versus trans* KCl containing 1 mM DTT. The solid lines indicate the closed current levels. (A) Single-channel currents at a range of holding potentials, and an example of an all-points histogram from 30s of the +100 mV recording. The arrow indicates the maximum open level of CLIC4. (B) Shows examples of direct transitions between the ~25% substate and the main open level to the closed level, on an expanded time scale. (C) Corresponding current/voltage (I/V) relationships for the main open level and the prominent 25% sublevel (shown as mean ± SD, $n = 15$).

A).

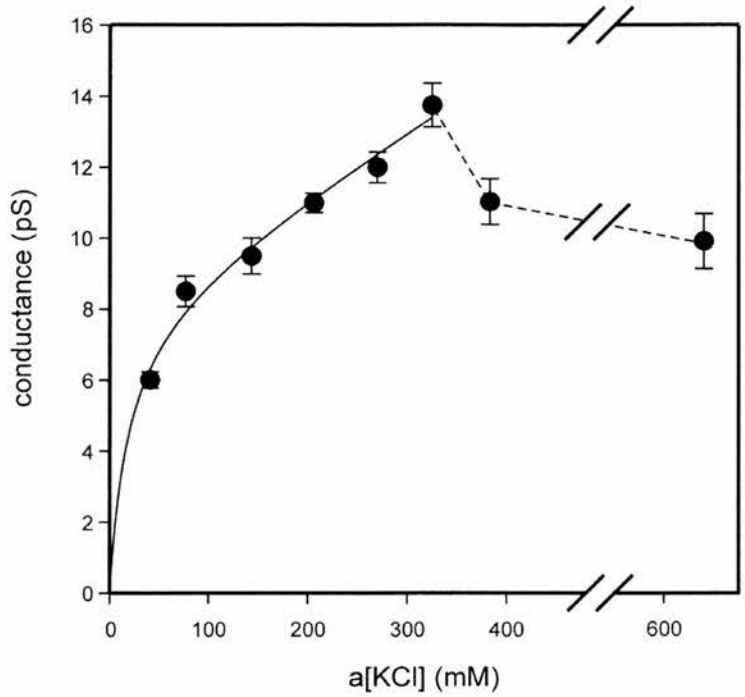

B).

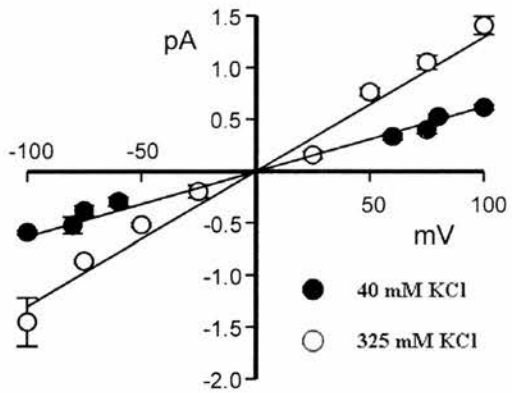

Fig 4.8. Conductance/activity relationship of CLIC4. (A) Relative single-channel conductance-activity relationship for each conductance level in symmetric KCl solutions (points are shown as mean ± SD, n = 5). The data in the main panel was fitted (by least squares) to the sum of a hyperbolic component with a g_{max} of 8.2 pS and a "Km" of 19.1 mM plus a non-saturating linear component of 0.017 pS per mM KCl. (B). The I/V relationships provide examples of the I/V data used to calculate the conductance at low (40 mM, closed circles) and high (325 mM, open circles) activities (points are means + SD, n = 5, lines fitted by linear regression).

Recordings obtained in 1 mM DTT, representing "fully-reducing" conditions, are shown in fig 4.7. The slope conductance of the main open state in a *cis vs. trans* gradient of 500-50 mM KCl in the presence of 1 mM DTT in both chambers was 10.3 ± 1.0 pS (mean ± SD, n=15), calculated by linear regression from the linear region of the I/V plot (-100 mV to +70 mV) in fig 4.7. CLIC4 showed several infrequent substates, including prominent ~25 % to the main open level (Fig 4.7). The reversal potential (E_r) of the main open state was calculated from the individual I/V plots for each experiment and it was -12.2 ± 3.3 mV (mean ± SD, n=15), corresponding to a mean Cl^-/K^+ selectivity of 0.54 ± 0.09. CLIC4 forms poorly-selective or even mildly cation-selective channels. The reversal potential for the prominent ~25% substate was similar to the main conductance level, and direct transitions to and from both states were observed in recordings.

The maximum slope conductance of CLIC4 in symmetrical 500 mM KCl was 13.8 ± 0.60 pS (mean ± SD, n=5). The main open state conductance was ohmic in symmetrical KCl solutions, but showed a complicated dependence on KCl activity (fig 4.8). The slope conductance increased up to ~350 mM KCl (activity) and declined at higher KCl activities, consistent with self-block as seen for CLIC1 earlier. Channels were obtained in 500 mM: 50 mM *cis vs. trans* Tris-Cl (pH 7.4), in the presence of 1 mM DTT. The conductance of CLIC4 in Tris-Cl was reduced to 2.6 ± 0.43 pS (mean ± SD, n=7), but the reversal potential was +11 ± 6.1 mV (mean ± Sd, n=7), giving a mean $Cl^-/Tris^+$ selectivity of 1.8 ± 0.51 (not corrected for activities). CLIC4 was mildly anion-selective in the presence of Tris-Cl when compared to KCl (Fig 4.9). The difference in relative *anion vs. cation* selectivity

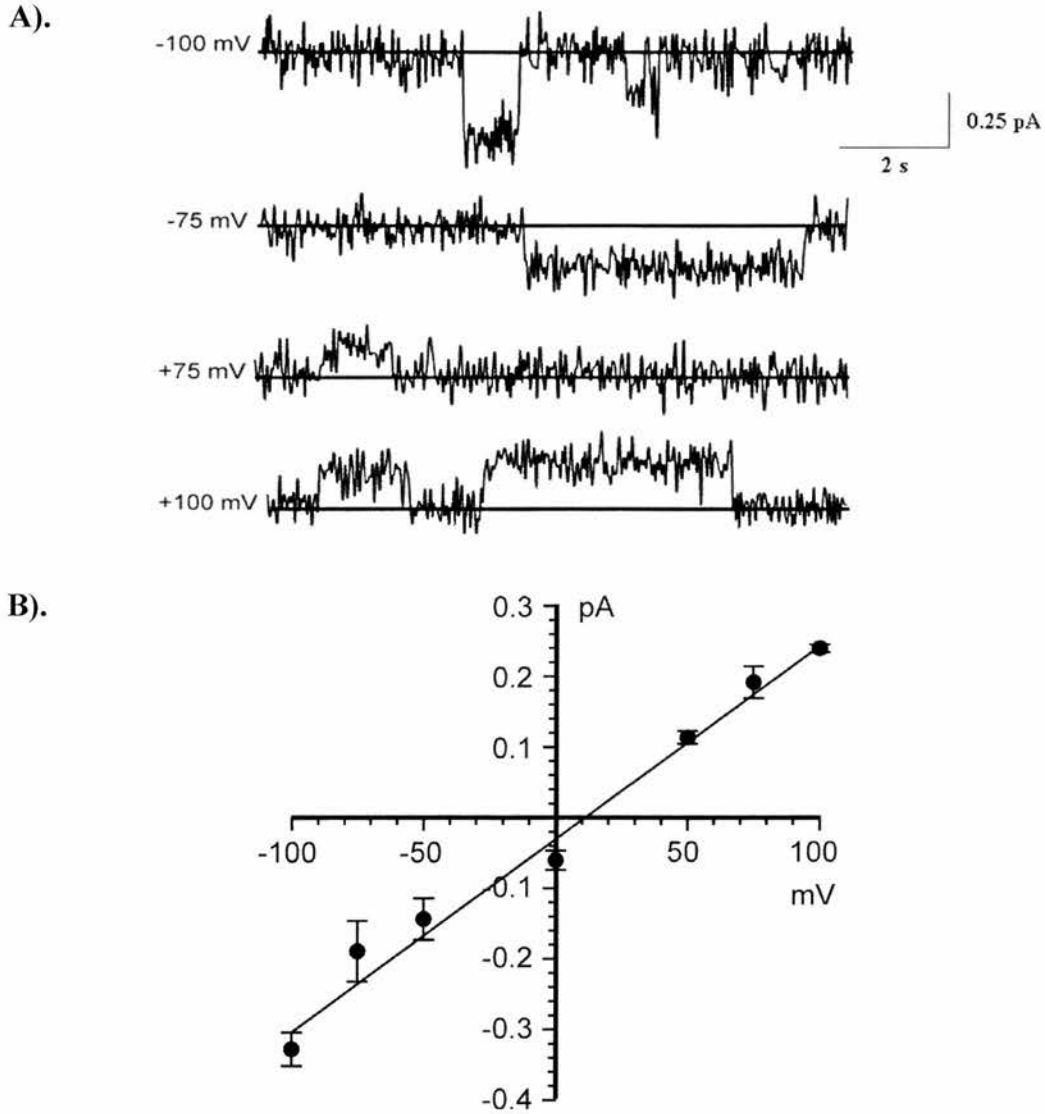

Fig 4.9. CLIC4 single-channel currents in Tris-HCl (pH 7.4). (A) Examples of single-channel currents in asymmetric Tris Cl (500:50 mM, *cis* versus *trans*). (B) I/V relationships for each conducting level (means ± SD, n = 7). The selectivity of channels increased significantly in the presence of large cation, as evident from the rightwards shift in the E_r.

compared to KCl is highly significant ($P < 0.001$). Unlike CLIC1, the conductance of CLIC4 was not decreased at positive holding potentials.

Relative anion permeabilities under equilibrium correlations were measured in the presence of 1 mM DTT by perfusing 50 mM KCl (corrected for activity) into the *cis* chamber, and different potassium salts with the same activity into the *trans* chamber. Relative anion permeabilities measured in symmetrical conditions were same for 5 test anions compared to Cl^- (set to 1.0) = SCN^-(0.97 $\pm$ 0.11) = $NO3^-$ (1.1 $\pm$ 0.50) = I^- (1.1 $\pm$ 0.96) = Br^- (1.3 $\pm$ 0.50) = F^- (1.4 $\pm$ 0.95) (mean $\pm$ SD, n=4), they are not significantly different ($P > 0.5$).

4.5 Single-channel properties of CLIC5A

CLIC5A was recently shown to have anion channel-like activity *in vitro*, by a chloride efflux assay in phospholipid vesicles made of asolectin (Berryman M. et. al., 2004). The maximum chloride efflux achieved was 2.5 % per second for 200 µg / ml of CLIC5A. These results are not consistent with normal ion channel activity, as the rate of efflux is very slow suggesting that more of the ion channels (if present) were closed.

Recombinant CLIC5A was reconstituted into planar bilayers containing 4:1:1 (molar ratio) POPE, POPS and cholesterol in the presence of either 1 mM DTT, 1 mM β-mercaptoethanol, 100 µM H_2O_2 or a glutathione buffer system. There was no significant difference between single-channel appearances under any of these conditions, but the single-channel conductance of CLIC5A showed more variability

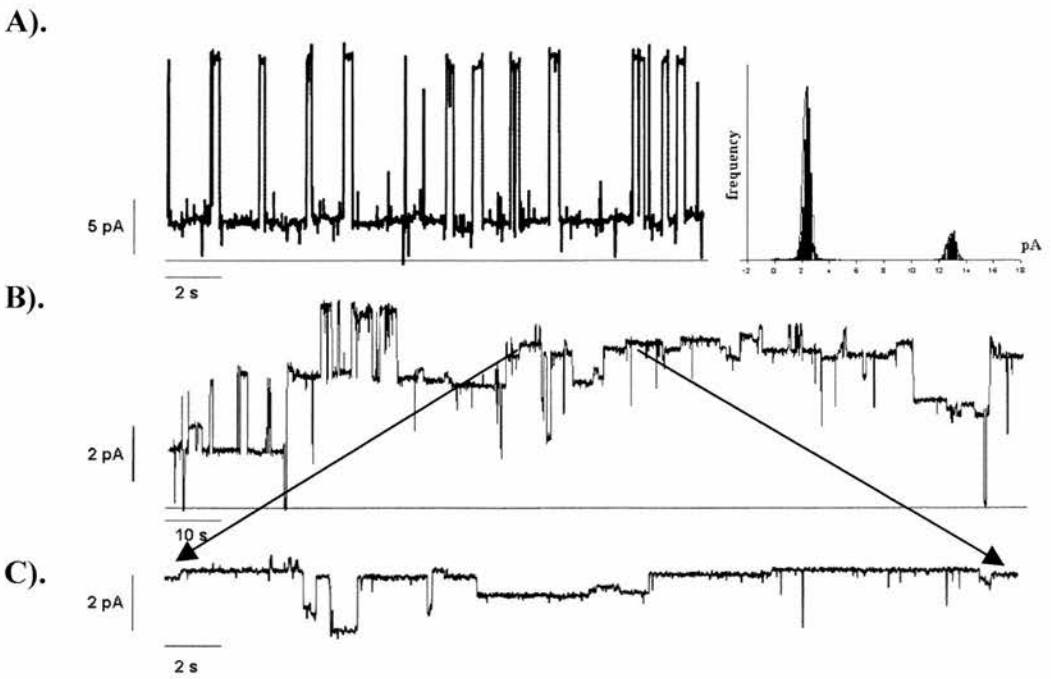

Fig 4.10. Single-channel recordings of CLIC5A in asymmetrical KCl. (A) Long recording of CLIC5A in 1 mM DTT showing large conductance channels. An all-points amplitude histogram was plotted which showed a single-channel current of 13 pA at +100 mV. Small-conductance channels (~ 2pA) were also noticed, but the resolution of small-conductance channels was poor. (B) Long recording of CLIC5A showing small and medium-conductance channels. The enlarged recording of the CLIC5A trace shows the current levels in more detail. All recordings at +100 mV, 500 mM *cis* KCl *vs.* 50 mM *trans* KCl.

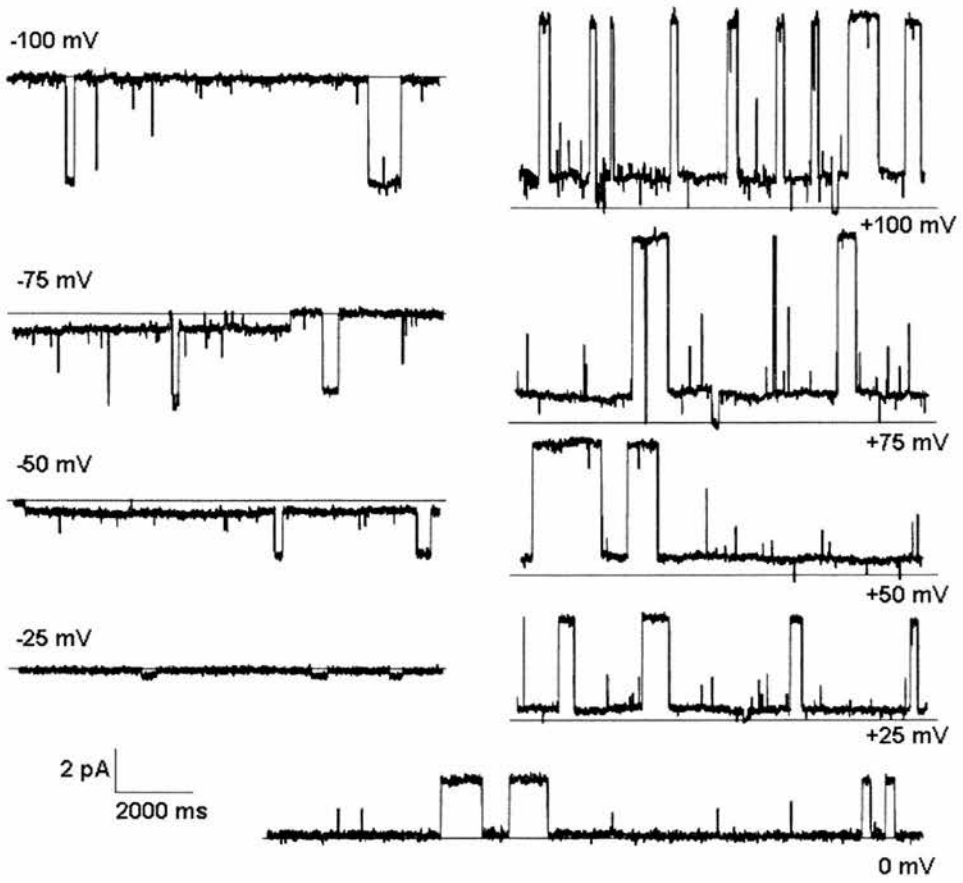

Fig 4.11. Singe-channel recordings of CLIC5A in 1 mM DTT. Single-channels were recorded in asymmetric 500 mM:50 mM (*cis vs. trans*) KCl. The solid line indicates the closed levels. (A) Single-channel traces of CLIC5A at various holding potentials. Sublevels are prominent in most of the traces.

A).

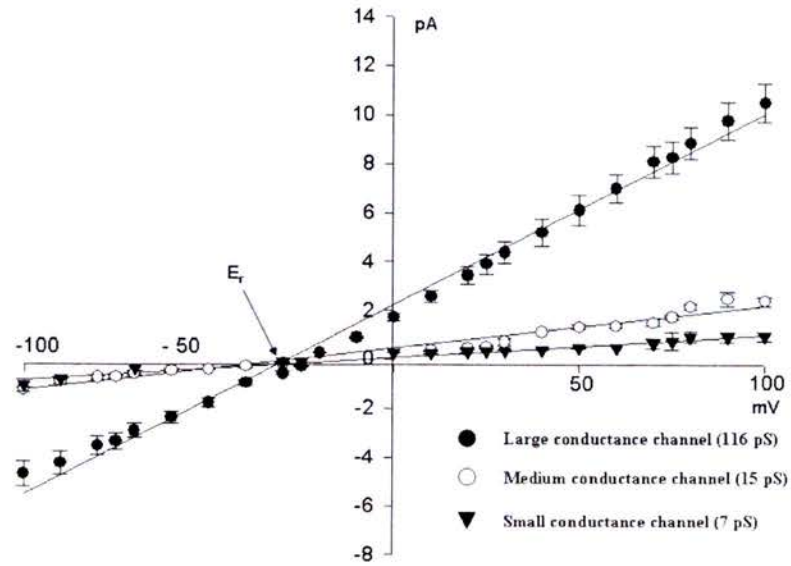

B).

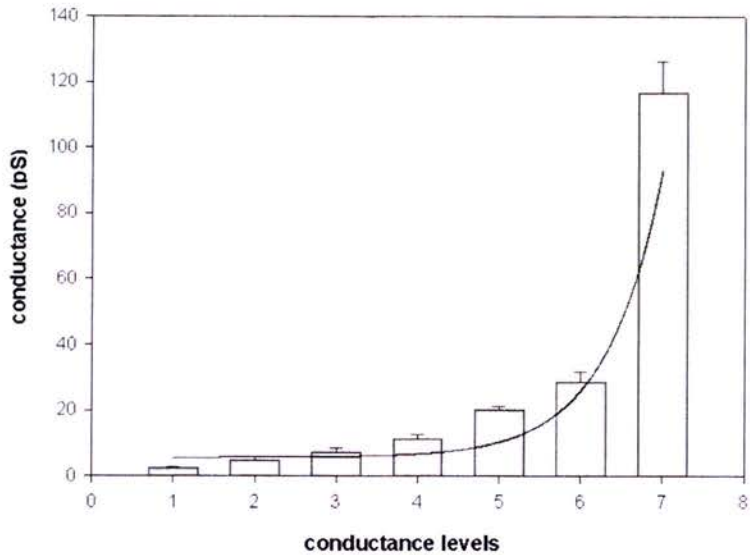

Fig 4.12. CLIC5A channels in 1 mM DTT. (A) Current/voltage (I/V) relationship of CLIC5A showing large and small-conductance levels. Channels were recorded in asymmetrical 500 mM *cis:* 50 mM *trans.* Lines were fitted by linear regression and all channels have an identical reversal potential and selectivity (points are mean $\pm$ SD, n= 3 to 7). (B) Histograms showing several independence conductance levels of CLIC5A. The fit parameters using a simple exponential, 3 parameter, fit (conductance = baseline conductance (fitted to 5.7 pS) plus $\underline{a}$ * ($\underline{b}^x$) where a = 0.0033, b = 4.3 and x = the conductance level from 1 to 7). R^2 was 0.99.

A).

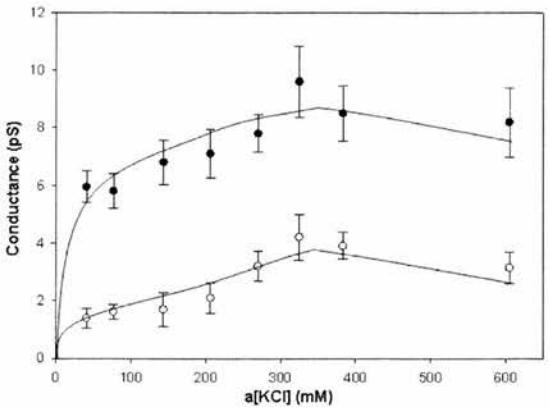

B).

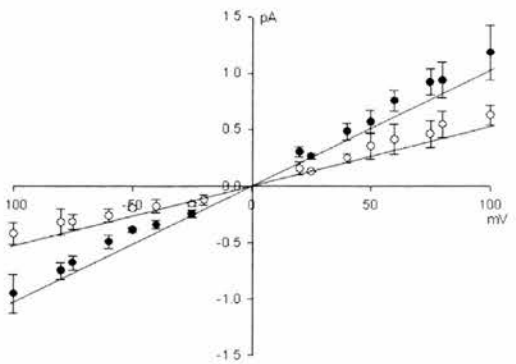

C).

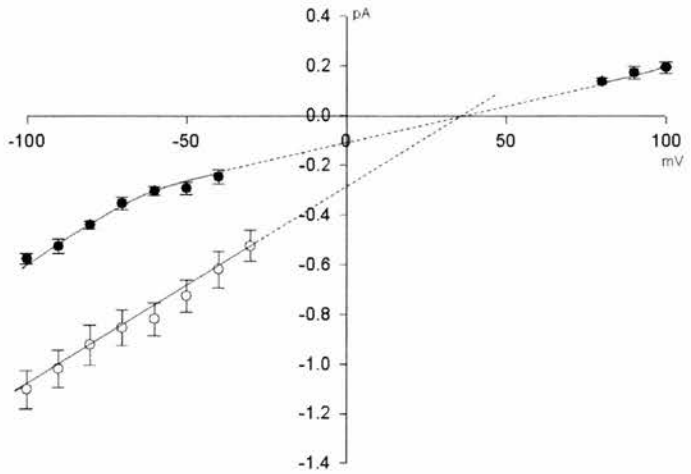

Fig 4.13. Conductance/activity relationship of CLIC5A. (A) Relative single-channel conductance-activity relationships for each conductance level in symmetric KCl solutions (mean ± SD, n = 6). The data for its minimum conductance levels in the main panel were fitted (by least squares) to the sum of a hyperbolic component with a g_{max} of 9.2 pS and a "Km" of 17.5 mM. (B). Current/voltage (I/V) relationships provide examples of the I/V data used to calculate the conductance at 500 mM KCl (points are means ± SD, n = 5, lines fitted by linear regression). (C). Current/voltage (I/V) relationship in asymmetrical 500 vs. 50 *cis vs. trans* Tris-HCl (the points are means ± SD, n = 4, lines fitted by linear regression and extrapolated manually).

than CLIC1 and CLIC4. It could form channels with maximum slope conductance ranging from 2.6 pS to 116 pS (Fig 4.10). These slope conductances, when closely analysed, could be categorised into 2.6 ± 0.7 pS (mean ± SD, n=6), 4.8 ± 1.2 pS (mean ± SD, n=5), 7.4 ± 1.1 pS (mean ± SD, n=7), 11.5 ± 1.3 pS (mean ± SD, n=7), 20.1 ± 1.4 pS (mean ± SD, n=8), 28.8 ± 3.2 pS (mean ± SD, n=5), 116.9 ± 9.4 pS (mean ± SD, n=5) and fit to simple exponential as shown in fig 4.12. Examples of large and small-conductance channels are shown in figs 4.10. All the conductance levels can be derived from these single-channel currents. Since the channels obtained in any of the reduced or oxidised conditions were significantly similar, 5 mM GSH/GSSG (10:1) was used for all subsequent experiments. Fig 4.12 summarises the current/voltage (I/V) plot of large and small-conductance channels. Examples of large-conductance channels at various holding potentials are shown in fig 4.11.

The current/voltage (I/V) relationship of CLIC5A in symmetric 100 mM KCl (corresponding to an activity of 77 mM) in 1 mM DTT is shown in fig 4.13. The maximum slope conductances of the two levels were 1.82 ± 0.35 pS (mean ± SD, n=5) and 5.8 ± 0.55 pS (mean ± SD, n=5). The conductance of the open state appeared to exhibit a non-hyperbolic dependence on KCl activity (Fig 4.13). The maximum slope conductance of the fully-open state was 9.6 ± 1.2 pS (mean ± SD, n=5) in symmetric 500 mM KCl (corresponding activity of 325 mM).

The conductance at higher concentrations of KCl (1000mM) was 8.2 ± 1.2 pS (mean ± SD, n=5), not significantly different from maximum slope conductance at 500 mM KCl. CLIC5A channels were obtained in a *cis vs. trans* gradient of 500:50 mM Tris-HCl (pH7.4). The channels were too small to resolve at positive holding potentials

and lower negative potentials. The current/voltage (I/V) relationship was plotted from the limited data (fig 4.13). The conductance of the channel decreased significantly to 1.3 ± 0.25 pS (mean ± SD, n=4). The reversal potential was + 35 ± 11 mV (mean ± SD, n=4), which shows a significant increase in anion/cation permeability to 7.7 ± 5.2 (mean ± SD, n=4). In KCl, the channels were non-selective or were cation-selective.

4.6 Discussion

It has been shown that CLIC proteins can autoinsert into monolayers, and bilayers containing different lipids. However, during the work for this Thesis it was found that they could only assemble or refold into specific ion channels in well-defined planar bilayers containing phosphatidylethanolamine, phosphatdiylserine, and cholesterol, in the molar ratio of 4:1:1, respectively. Cholesterol and the inverted cone shaped phospholipid PE are associated with "curvature stress" in planar membranes and may promote channel assembly by a physical role similar to the activation of the membrane associated protein kinase C (Ho et al., 2001). CLIC proteins may thus require the presence of cholesterol to form functional ion channels. CLICs may insert into other lipids and lipid mixtures, but failed to give consistent channels in any other lipid mixture tested so far. This suggests that CLICs can insert into most lipid mixtures, but native CLICs form functional ion channels only in membranes containing specific lipid components. In many channel-forming toxins, membrane cholesterol is known to regulate pore formation (Palmer, 2004), and it also promotes oligomerisation (*Vibrio cholerae* cytolysin) (Olson and Gouaux, 2005).

Protein	Conductance	Selectivity
CLIC1	38 pS ± 3 pS (DTT) 24 pS ± 1.4 pS (H_2O_2) 25 pS ± 1.5 pS (GSH/GSSG)	Non-selective
CLIC4	10.3 pS ± 1.0 pS (DTT) 8.9 pS ± 1.1 pS (H_2O_2) 14.8 pS ± 1.6 pS (GSH/GSSG)	Non-selective
CLIC5A	116.9 ± 9.4 pS 28.8 ± 3.2 pS 20.1 ± 1.4 pS 11.5 ± 1.3 pS 7.4 ± 1.1 pS 4.8 ± 1.2 pS 2.6 ± 0.7 pS	Cation-selective

Table 4.3 Single-channel and substate conductances of CLIC channels. Single-channel conductance of CLIC1 and CLIC4 in 1 mM DTT, 100 μM H_2O_2 and 5 mM GSH/GSSG. Single-channel conductance of CLIC5A was similar in 1 mM DTT, 100 μM H_2O_2 and 5 mM GSH/GSSG. CLIC1 and CLIC4 are non-selective and CLIC5A is a cation-selective channel.

In tip-dip experiments two substates of CLIC1 were reported (Warton et al., 2002), which were also observed in our experiments. They were at 22% and 45% of the main sublevel. Previously, similar substates were shown in anion channels reconstituted from rat brain microsomes (Clark et al., 1997) and sheep heart inner mitochondrial membrane vesicles (Hayman et al., 1993a; Hayman and Ashley, 1993b). This was interpreted in terms of a model with a minimum of four conducting "protomers" displaying different gating mechanisms, depending on the number of protomers open at any given instant. If a similar model is to be predicted for CLIC1 and CLIC4, a minimum of 16 subunits are required per channel (four per "protomer", since each subunit contain a single TMD). Similarly CLIC5A will have multiple "protomers" functioning together to give rise to 116 pS channels. This can explain some of the large conductances previously recorded for putative CLIC channels, which may reflect the association of groups of highly-cooperative subunits into even larger structures.

CLICs have conserved cysteine residues (CLIC1 has 6, CLIC4 has 5 and CLIC5A has 4), and the channels were reconstituted under a wide range of oxidising and reducing conditions, including DTT, H_2O_2 and GSH/GSSG. CLIC1 formed consistent channels under all the redox conditions tested but with much variation in single-channel conductance. The single-channel conductance of CLIC1 decreased in H_2O_2 and in a GSH/GSSG buffer system, and the channel had very long open and closed states. CLIC4 displayed more substates, and was nosier in DTT and H_2O_2 compared to GSH/GSSG. This suggests that the proteins optimally fold only under physiological redox conditions. CLIC5A was extremely sensitive to oxidation, and slight oxidation was enough to oligomerise the channel. This rapid oligomerisation

may have resulted in the wide range of single-channel conductance levels, as evident from the exponential growth of conductances in Fig 4.12.

The relative anion selectivities, non-hyperbolic relationships between conductance and activity, and the reduction in currents at very high activities, show that CLIC1 and CLIC4 channels are multi-ion channels (Lummis et al., 2005). Conductances obtained with CLIC1 and (trans-oxidised) CLIC4 were consistent with the values calculated for CLIC1 (Valenzuela et al., 2000) and CLIC4 in cell membranes (Proutski et al., 2002).

CLIC1 was slightly more anion-selective than CLIC4. CLIC1 anionic selectivity was similar to rat brain microsomal channels in 50mM KCl (Clark et al. 1997). CLIC4 was unable to discriminate between different anions, which shows that the pore region is poorly-selective. CLIC5A formed a cation-selective ion channel. The selectivity improved remarkably as the size of permeant cation (from K^+ to $Tris^+$) was increased for CLIC1, CLIC4 and CLIC5A, as observed before for rat brain microsomal anion channels (Clark et al., 1997). These results suggest that CLIC proteins are poorly-selective between anions and cations, in contrast to the widely-adopted "CLIC" nomenclature (Heiss and Poustka, 1997; Edwards, 1999).

CHAPTER 5

REDOX-REGULATION OF CLIC CHANNELS

5.1 Introduction

Cytosolic CLICs and GSTs share weak structural homology but have different functional roles (Cromer et al., 2002). The crystal structure of soluble CLIC4 (Littler et al., 2005) closely resembles the soluble form of CLIC1 (Harrop et al., 2001). They have two domains, an N-terminus domain (around 100 residues consisting of 4 β-sheets and 3 α-helices) with a thioredoxin fold, closely resembling glutaredoxin, and an all α-helical C-terminus domain. The putative pore-forming region is predicted to be in the N-terminus region. A cysteine residue in the N-terminus region is well-conserved in all mammalian CLICs. It is located near the putative pore-forming region of the channel.

Glutathione occupies a redox-active site in the CLIC1 and glutathione complex (Harrop et al., 2001), and hence it was predicted that CLIC1 and other CLICs are likely to be GSH-dependent redox-regulated proteins. Mammalian CLICs (CLIC2 and CLIC3) and one of the invertebratal CLICs (*dm*CLIC) also have a second cysteine residue near the N-terminus region. The N-terminus of helix h1 has a conserved Cys-Pro (CP)-motif in all the mammalian CLICs and in Ω-GST. In invertebrates, this CP-motif is absent, but other cysteine residues are present in the N-terminus region. The cysteine residue has been predicted to be located near to the entry point of the pore region. The atomic structure of the membrane form of CLIC proteins is not yet elucidated, but in order to auto-insert into the membrane it is likely that a major structural rearrangement is required, possibly in the N-terminus region.

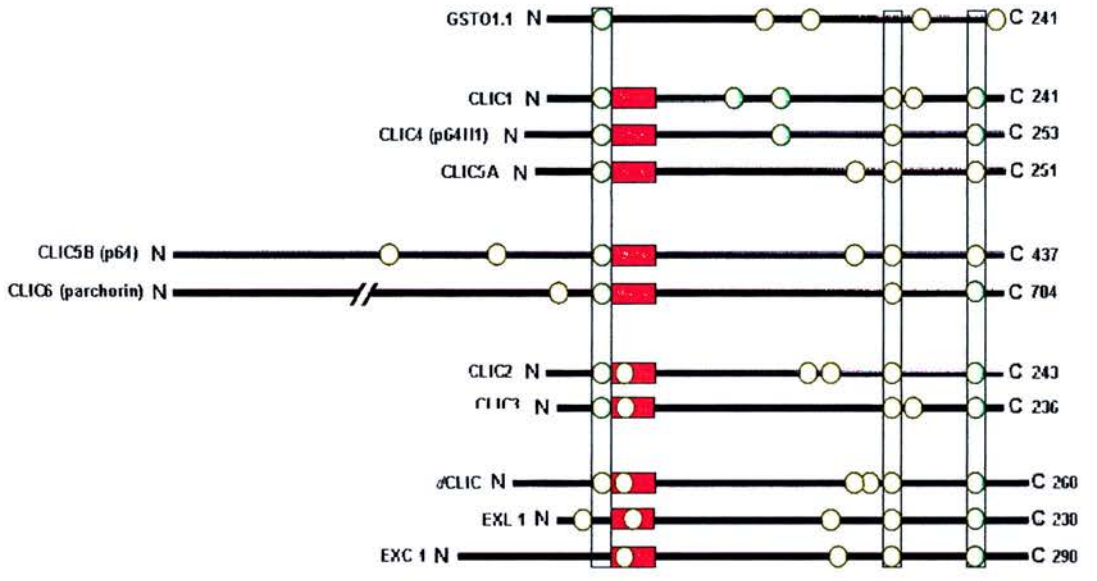

Fig 5.1. Schematic representation of the primary structures of GSTO1-1 and CLIC proteins. GSTO1-1, vertebrate (human) and invertebrate CLIC proteins were aligned by clustal analysis (Fig 1.7). Note several conserved cysteine residues (represented as yellow circles) in CLIC proteins. The conserved cysteine-proline (CP) motifs are represented by yellow-green circles. The putative transmembrane domain (red rectangles) is present in all the vertebrate and invertebrate CLICs, but absent in the GST. Conserved cysteine residues are boxed, and one of the conserved cysteine residues is located on 'top' of the transmembrane domain, towards the N-terminus. The total number of amino acid residues present in each protein is indicated at the C-terminus.

CLICs have a single predicted putative TMD, and to form a functional channel a minimum of four subunits are required to oligomerise. Studies with FLAG-tagged CLIC1 showed that on insertion into the plasma membrane the N-terminus is on the luminal side whereas the C-terminus is on the cytoplasmic side (Tonini et al., 2000).

In this chapter, membrane topology was predicted on the basis of sequence alignment and previous work carried out in several labs. The predicted topology of CLIC proteins is illustrated in fig 5.1 and is better established in subsequent chapters. Studying the effects of inhibitors and blockers, including their interaction with His-tag added to the membrane proteins, helped in determining their orientation. It has provided support for a specific structural model incorporating a novel functional role for a specific conserved N-terminus cysteine residue.

5.2. Inhibition of CLIC1 channels by IAA-94

p64 was originally isolated by affinity chromatography using indanyloxyacetic acid (IAA-94, a Cl^- channel inhibitor) (Landry et al., 1989). IAA-94 is structurally similar to ethacrynic acid, which is a known GST-binding molecule (Landry et al., 1989). In fact, the affinity purification experiments that first isolated p64 coincided with the isolation of a GST (Redhead et al., 1992). Ethacrynic acid is known to bind GSTs in the (hydrophobic) electrophilic substrate site ("H-site"), which is near the GSH binding site (Armstrong, 1997). The H-site in GSTs is formed by the loop connecting the β-strand s1 to the helices h1 and h4 along with the carboxy terminus and helix h9 (Harrop et al., 2001; Cromer et al., 2002). Due to the structural homology of IAA-94

with ethacrynic acid, CLIC proteins can also bind IAA-94. The proximity of the homologous fold of the H-site, to the GSH binding site in CLICs (Harrop et al., 2001) shows that the mechanisms of GSH and IAA-94 may be related to each other.

Previously, several groups have shown that CLIC1-associated channels could be inhibited by IAA-94 (Tulk et al., 2000; Tonini et al., 2000; Valenzuela et al., 2000; Harrop et al., 2001; Warton et al., 2002). The whole-cell currents associated with CLIC4 were reduced by 50% on application of 100 μM IAA-94 (Proutski et al., 2002). However, the single-channel conductance and IAA-sensitivity of CLIC-associated channels differ remarkably, depending on the reconstitution and recording conditions.

The effect of IAA-94 on recombinant CLICs was studied in bilayers. CLIC1 channels and their sublevels were inhibited by 1AA-94, when added to the *cis* chamber at high concentrations (≥ 10 μM) but not from the *trans* side. This effect was reversible when IAA-94 was perfused out from the *cis* chamber (Fig 5.2). However, CLIC4 and CLIC5A channels were not significantly affected by the application of very high concentrations (100 μM) of IAA-94 from either the *cis* or *trans* side of the channels. Previously, IAA-94 has been shown to block CLIC-like channels (Valenzuela et al., 2000; Proutski et al., 2002) and was shown to function as a neuroprotective agent in neuronal-microglial co-cultures (Novarino et al., 2005). However, the very high concentrations are likely to be non-specific, IAA-94 cannot therefore be used as a specific-blocker.

A).

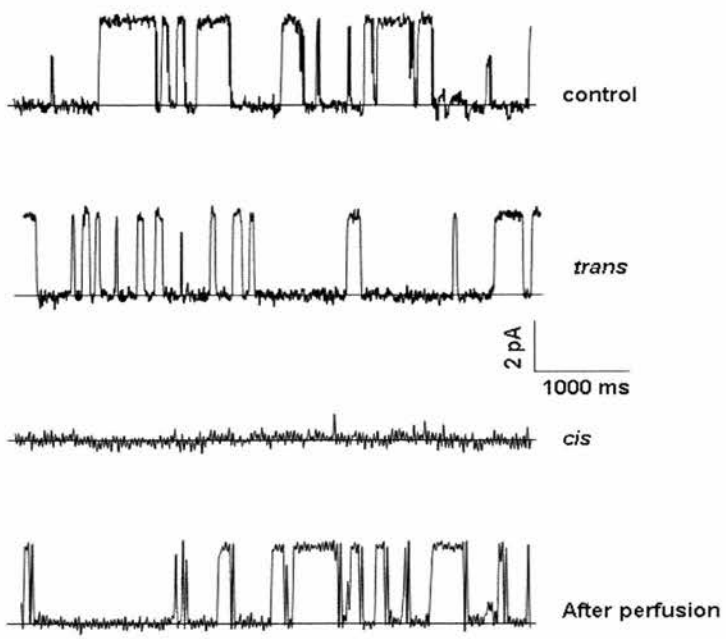

B).

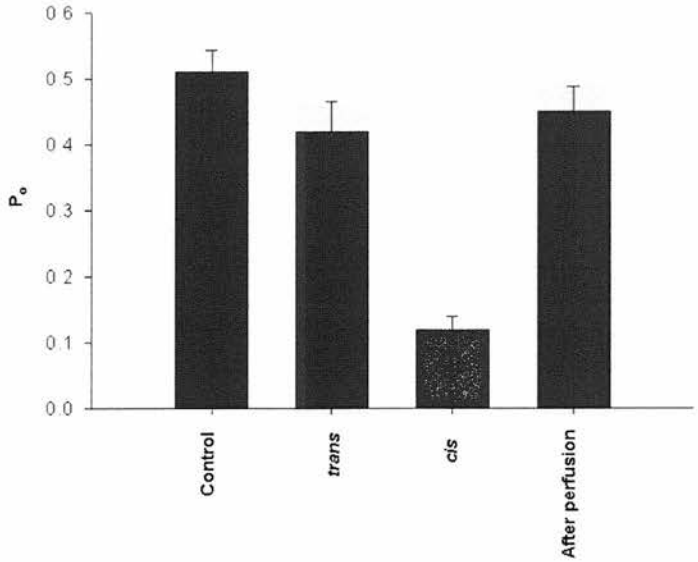

Fig 5.2. The effect of IAA-94 on CLIC1 channels. Single-channel currents were recorded in asymmetric KCl (500 *vs.* 50, *cis vs. trans*) in 1 mM DTT. All traces are obtained at a holding potential of +100 mV. The solid lines indicate the closed levels. (A) Single-channel recordings of CLIC1, showing reversible effect of 50 μM IAA-94 from the *cis* but not from the *trans* side. (B) Histograms showing the open probability of single-channel recordings. The open probability was measured from 60 s long traces (mean ± SD, n=5). Very high concentrations (≥ 10 μM) of IAA-94 was required to inhibit CLIC1 channels.

5.3. Orientation of reconstituted channels

Based on previous studies, it was predicted that the N-terminus of membrane CLIC proteins should be towards the luminal side of the membrane. To test this simple model in more detail, the topology of membrane CLIC proteins was investigated with an intact N-terminal octa His-tag. As stated in chapter 4, the tag did not affect the conductance and selectivity of reconstituted CLIC1 or CLIC4 channels.

CLIC1 channels with the N-terminal His-tag, reconstituted into planar bilayer were unaffected by 50 μM *cis* $NiCl_2$. When 50 μM $NiCl_2$ was added and stirred into the *trans* chamber, the channels were completely inactivated in 15/15 independent experiments (Fig 5.3). Non-tagged CLIC1 channels were unaffected in 15/15 experiments. This suggested that the N-terminus of CLIC1 was on the *trans* side of the bilayer. Similar experiments were carried out for CLIC4 and CLIC5A, but 50 μM $NiCl_2$ failed to block in 8/11 and 5/5 independent experiments for CLIC4 and CLIC5A, respectively, *trans* or *cis* side. CLIC4 could be partially blocked in 3/11 experiments by *trans* 50 μM $NiCl_2$. This failure of complete inhibition of CLIC4 and CLIC5A channels may be attributed to the longer N-terminus region.

As shown in fig 5.1, mammalian CLICs have a conserved cysteine residue in the CP-motif near the putative TMD. In CLIC1 this cysteine residue is located at position 24 and in CLIC4 it is located at position 35, and is therefore predicted to be on the *trans* side of the bilayer, close to the putative pore-forming region of oligomeric CLIC channels. The other cysteine residues (5 in case of CLIC1 and 4 in CLIC4) are

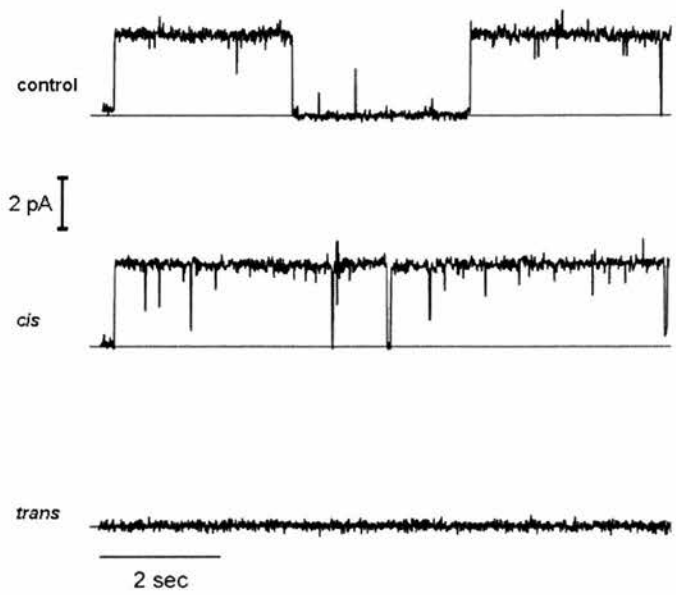

Fig 5.3. Effect of Ni^{2+} on CLIC1 channels. Single-channel recordings in 500 mM *vs.* 50 mM, *cis vs. trans* KCl in 1 mM DTT at a holding potential of +100 mV, using CLIC1 containing an intact N-terminal His-tag. The channels remain unaffected by addition of 50 μM *cis* Ni^{2+} but were completely blocked from the *trans* side (Solid lines indicate the closed levels). These CLIC1 channels show a "gearshift" in their gating kinetics with much large open and closed times. This "gearshift" was seen in about 10 % of all the channels acquired. Reperfusion of Ni^{2+} was ineffective on Ni^{2+} -blocked CLIC1 channels.

located on the cytosolic side the predicted transmembrane domain, much further into the primary sequence (Fig 5.1).

To test the hypothesis that C24 and C35 of CLIC1 and CLIC4, respectively, are located in the N-terminus region, cysteine-reactive compounds were applied to the respective channels. When 20 μM of thiol-reactive reagent N-ethylmaleimide (NEM) was added to the *trans* side of channels reconstituted from CLIC1 proteins, they were completely inactivated in all 9/9 experiments (Fig 5.4). These effects were quantified by measuring the probability of a given channel being open (Po) over successive periods for each condition. The mean Po for CLIC1 was 0.52 $\pm$ 0.25 before the addition of NEM, and was 0.49 $\pm$ 0.22 after the addition of *cis* NEM. The mean Po decreased significantly to 0.09 $\pm$ 0.05, with *trans* NEM (mean $\pm$ SD, n = 7). There was no effect from *cis* NEM, suggesting that there were no accessible cysteines present in the pore region towards the *cis* side. However, NEM failed to show any effect on CLIC4 channels from either side. There was no effect on the single-channel conductance of CLIC1 from the *cis* side suggesting that C59 (shown to be involved in intramolecular disulphide bond formation in soluble form) and the other 4 conserved cysteines are not located near to the pore region.

The relatively-bulky thiol-reactive reagent 5,5'-dithiobis-(2-nitrobenzoic acid) (DTNB) was then applied to CLIC4 channels, as NEM failed to block these channels. DTNB (200 μM) blocked CLIC4 channels from the *trans* but not the *cis* side (Fig 5.5). The Po decreased significantly to 0.05 $\pm$ 0.03 after the addition of *trans* DTNB (mean $\pm$ SD, n=6). There was a significant difference between the mean

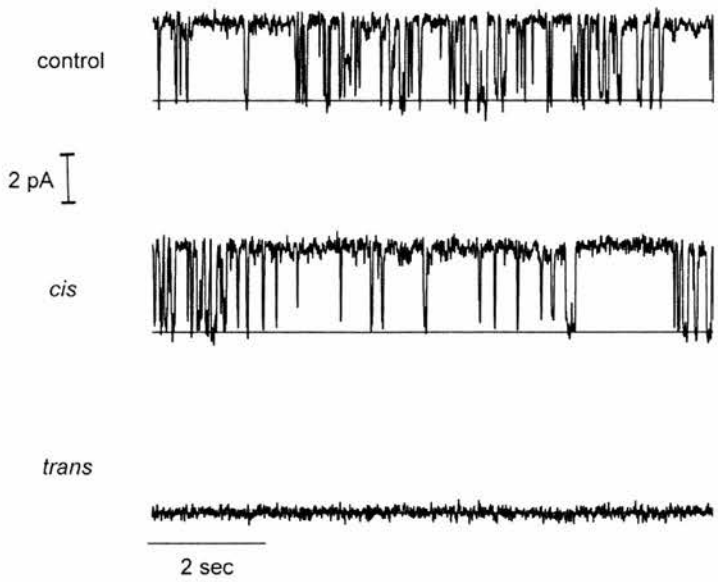

Fig 5.4. Effect of NEM on CLIC1 channels. Channels were recorded in asymmetrical KCl (500 *vs.* 50 KCl) at a holding potential of +100 mV. The DTT was removed by perfusion before addition of 20 μM NEM to the *cis* and *trans* chambers. NEM blocked the channel from the *trans* but not the *cis* side.

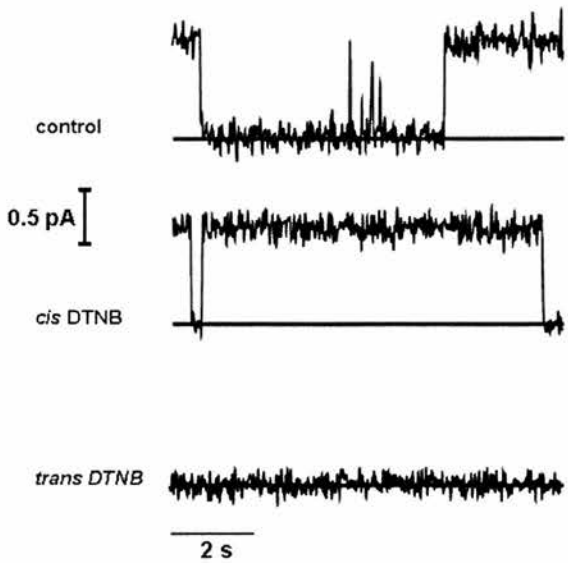

Fig 5.5. Effect of DTNB on CLIC4 channels. Channels were recorded in asymmetrical KCl (500 *vs.* 50 KCl) at +100 mV. DTT was removed by perfusion before adding DTNB. Addition of 200 μM DTNB to the *cis* and the *trans* side of CLIC4 reconstituted in the bilayer inhibited channels from the *trans* but not the *cis* side.

Po values for control and *trans* NEM/DTNB. The differences in Po between control and *cis* NEM/DTNB, and control and *trans* NEM/DTNB, were analysed channel by channel using paired t-tests (as the mean Po varied for each experiment). The mean Po for CLIC4 was 0.63 ± 0.21 before adding DTNB and 0.65 ± 0.26 after adding *cis* DTNB. There was no significant difference between control and *cis* NEM/DTNB for both CLIC1 and CLIC4 ($p > 0.5$ for both channels). The control and *trans* NEM/DTNB for both CLIC1 and CLIC4, showed significant difference ($p < 0.05$ and $p < 0.02$, respectively).

5.4. Redox-regulation of CLICs

Many cellular processes are regulated by the "redox state" of the cell (Schafer and Buettner, 2001). The redox state is a term which is used to describe the ratio between the oxidised and reduced state of a specific redox couple. The redox environment of a linked set of redox couples as found in biological fluids, organelles, cells or tissues is the sum of the reduction potential and reducing capacity of all the linked redox couples present in the system. Glutathione is the major thiol-disulphide redox buffer of the cell and its concentration is approximately 1-11 mM in the cytosol (Schafer and Buettner, 2001). The half-cell reaction is:

$$GSSG + 2H^+ + 2e^- \longrightarrow 2GSH \qquad [1]$$

The Nernst equation (Chapter 1, section 1.5) for the reduction potential of the GSSG/2GSH half-cell can be written as:

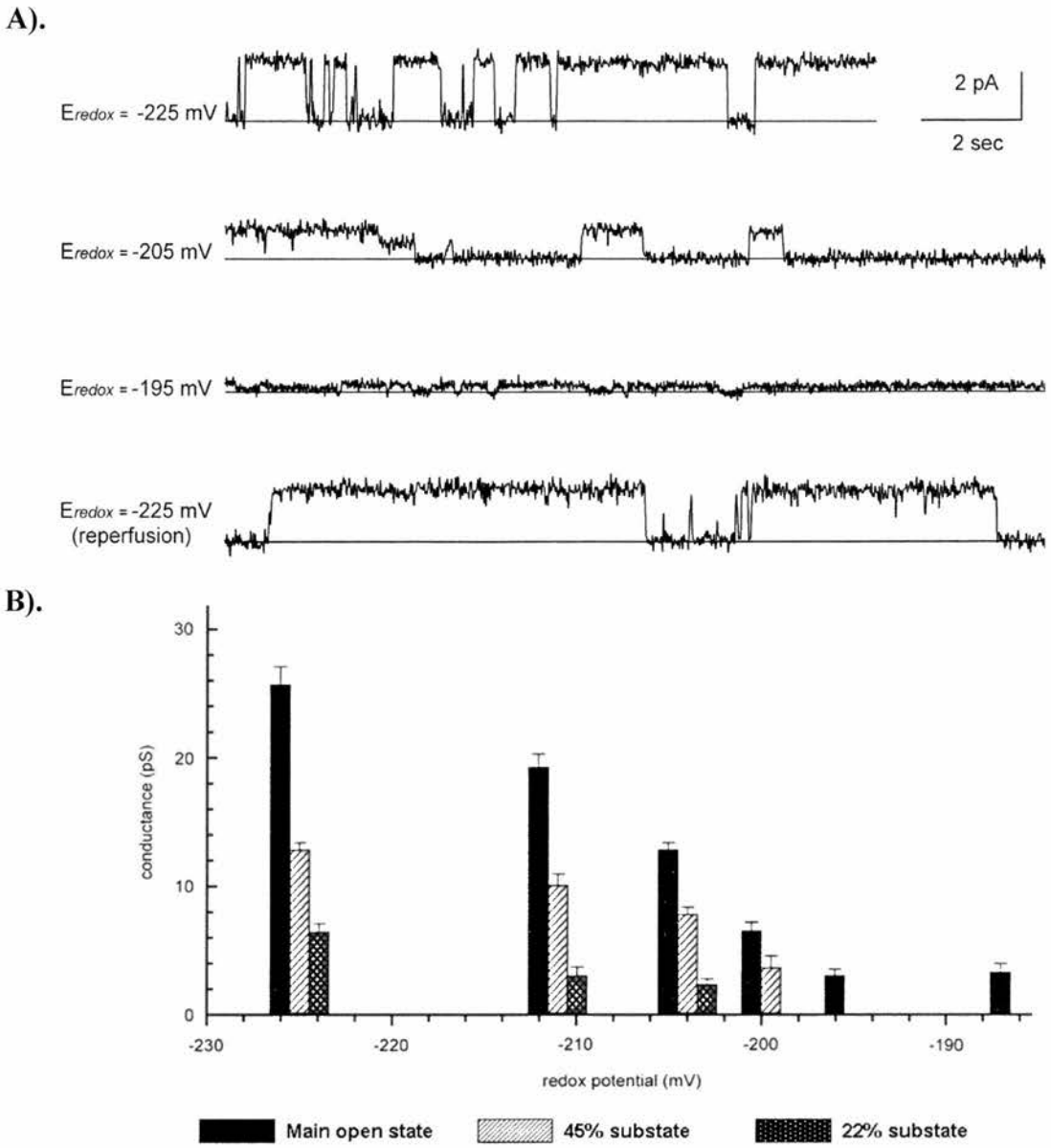

Fig 5.6. Effect of redox potential on single-channel conductance of CLIC1. (A) Examples of single-channel recordings in 500 *vs.* 50 mM KCl at a holding potential of +100 mV. The closed current levels are indicated by the solid lines. The single-channel conductance decreased as the redox-potential in the *trans* chamber was varied from -225 mV to -195 mV with GSSG/2GSH buffer system. This effect is reversible. (B) The slope conductance (mean ± SD, n=5) of CLIC1 is summarised for GSSG/2GSH buffers. The main open state conductance decreased ~ 10-fold with *trans* oxidation.

$$E_{hc} = -240 - (59.1/2) \log ([GSH]^2/[GSSG]) \text{ mV at } 25°C, \text{ pH } 7.0 \quad [2]$$

This indicates that the reduction potential is dependent on the GSH/GSSG ratio and the absolute concentration of GSH. The experimental pH was 7.4, hence a pH-dependent correction of (7.4-7.0) X 2.3(RT/F) = -24 mV was included in all calculations.

Channels were reconstituted in 5 mM GSH instead of 1 mM DTT to investigate the effects of redox potential in detail using a glutathione redox buffer system, corresponding to "physiological" redox conditions. The conductance of CLIC1 was lower in GSH but the substate pattern was similar to substates obtained in DTT. The channels remained open or closed for a longer duration (1-10s). However, the conductance of CLIC4 remained unaffected in GSH compared to DTT.

Oxidised glutathione (GSSG) was added in the *cis* and *trans* chambers sequentially. This addition of GSSG to the *cis* chamber showed no significant effect on the single-channel conductance, but when added to the *trans* chamber, the single-channel conductance of CLIC1 decreased from 26 ± 1.3 pS to a minimum of 2.9 ± 0.6 pS (mean $\pm$ SD, n=5) (Fig 5.6). The redox potential with 5 mM GSH and 0.5 mM GSSG was -225 mV, and it was reduced sequentially to -195 mV. The effect could be reversed by reverting to a redox potential of -225 mV in the *trans* chamber as shown in fig 5.6. Similar behaviour was shown by the substates of CLIC1, but they eventually became immeasurably small ($< \sim 0.1$ pA).

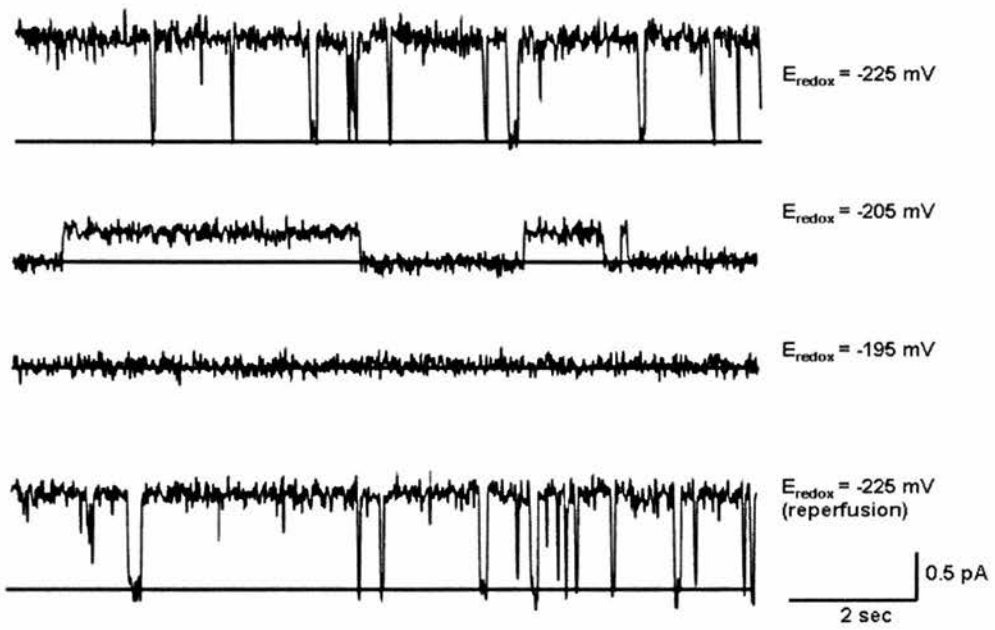

Fig 5.7. Effect of redox-regulation on CLIC4. Single-channel recordings in 5 mM GSH (*cis* and *trans*), with GSSG added sequentially to the *trans* chamber to obtain the indicated redox potentials. The data were obtained in 500 mM *cis* KCl *vs*. 50 mM *trans* KCl, at +100 mV. The solid line indicates the closed levels. The single-channel conductance of CLIC4 decreases as the redox potential in the *trans* chamber is varied from -225 mV to -195 mV with GSSG/2GSH buffer system and the effect is reversible.

The redox-regulation of CLIC4 channels was also studied in bilayers. When GSSG was added sequentially to the *cis* chamber, there was no effect on the single-channel conductance of CLIC4. However, the single-channel currents decreased markedly when GSSG was added to *trans* side of the CLIC4 channels (Fig 5.7) as the redox potential was increased from -225 mV to -195 mV with sequential addition of *trans* GSSG. This inhibition could be reversed when the redox potential was returned to -225 mV in the *trans* chamber, as shown in fig 5.7.

CLIC1 and CLIC4 channels were less noisy in the glutathione buffer system as compared to the channels obtained in DTT or H_2O_2, mainly because CLIC4 had fewer substates in the GSH buffer than under fully-reducing (DTT) or fully-oxidising conditions (H_2O_2). The channels occasionally "gearshifted" to a gating mode similar to that seen in strong reducing conditions (DTT) (Fig 5.3 and Fig 5.6). The excess noisy behaviour of the channels observed in the absence of the glutathione buffer could be attributed to short-lived, poorly-resolved substates. This may be due to the inability of CLIC1 or CLIC4 to fold optimally and form a single stable conformation in strongly-oxidising or fully-reducing conditions.

5.5 Membrane topology model for CLIC proteins

A simple structural model was designed to explain the *trans* redox-regulation of CLIC proteins. In the model, the reconstituted channels are formed by 4 (or more) CLIC1 oligomers (Fig 5.9), each contributing a single transmembrane domain. In this model, cysteine residue C24 located on the *trans* side of the bilayer was

predicted to be responsible for the redox-regulation of the channels. Changes in conductance were measured in 5 mM GSH and 2.5 mM GSH to test this idea, as summarised in fig 5.8, which reflects reduction (opening of the channels) and disulphide bond formation (closure of the open channels) for CLIC1. The reaction involved between neighbouring monomers of the channel subunits and the 2GSH/GSSG buffer system can be described by an equilibrium:

$$P(SH)_2 + GSSG \leftrightarrow P(SS) + 2GSH \qquad [3]$$

where "P(SS)" and "$P(SH)_2$" represent channel protomers or subunits with or without intersubunit disulphide bonds, respectively. The kinetics of the above equation are represented as "intra" subunit bondings because CLIC1 protomers must be closely associated with each other in the membrane bilayer by non-covalent interactions to form a functional channel. This implies that the subunits do not need to pre-associate by diffusing together before the reaction can occur, greatly simplifying the kinetics.

The step-like reduction (rather than a graded response) in conductance of CLIC1 and CLIC4 could be attributed to "switch-like" formation of disulphide bonds between the C24 residues in neighbouring subunits. The formation and breaking of disulphide bonds is so rapid that individual "blocking" events are not observed and under experimental resolution the ion channel current will show a smooth reduction in amplitude. This is an example of the "smooth" ion channel block frequently observed with (blocker) dissociation rates > 10^5 per sec (fig 5.10). This mechanism was qualitatively supported by the apparent increase in mean open time as the channels

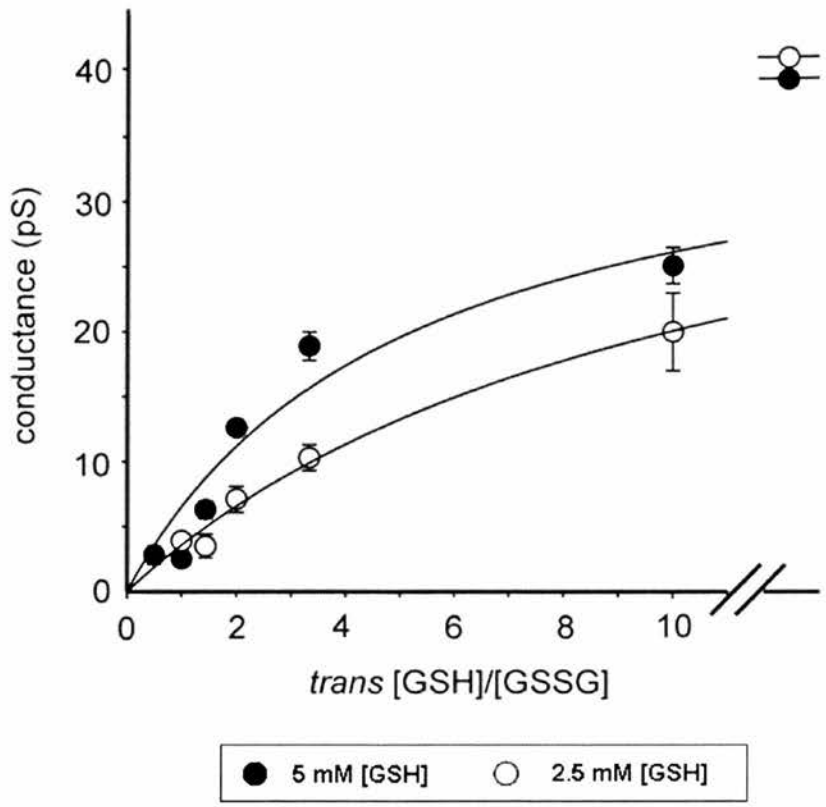

Fig 5.8. Effect of redox potential on CLIC1 channels in different GSH buffers. Conductance data for the fully-open state in 5 mM GSH (mean ± SD, n=5), together with conductance data for the fully open state in 2.5 mM GSH (mean ± SD, n=3), plotted against the [GSH]/[GSSG] ratio. The data were fitted (by least squares) to rectangular hyperbolae. The maximum conductances obtained from fits for 5 mM GSH and 2.5 mM GSH are 39 pS and 41 pS, respectively. The corresponding K_{ox} values are 25 mM and 26.5 mM. Note the break in the x-axis, and corresponding conductances at asymptotes (top right corner).

A).

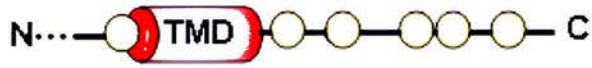

B).

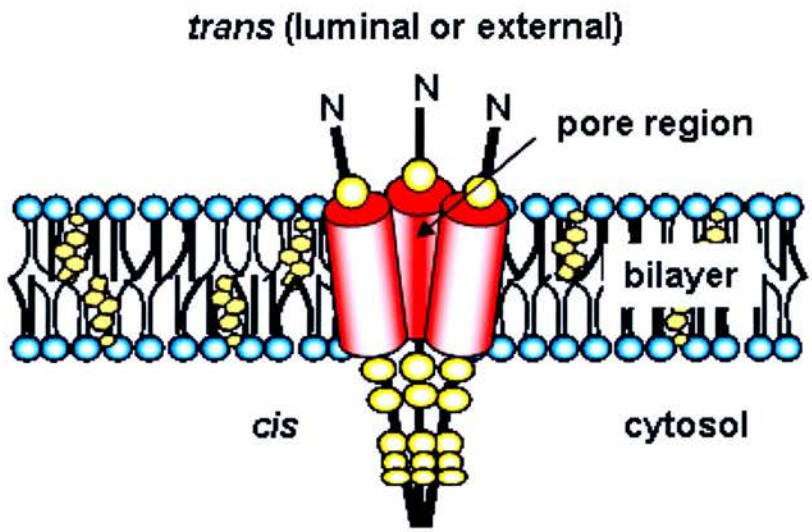

Fig 5.9. Topology model for CLIC1 channel assembly and redox-regulation. (A) Cartoon of the CLIC1 channel. Only C24 is present towards the N-terminus region before the single predicted putative TMD (not to scale). (B). Model of membrane CLIC1 as a tetrameric ion channel. The front subunit is removed from this model. The channel could also be formed with more than four subunits.

were *trans* oxidised. There were however even fewer openings than the channels generally observed under reducing conditions, hence detailed numerical lifetime analysis to confirm this mechanism was not possible.

In order to provide a more detailed, quantitative analysis based on these ideas, the kinetics of disulphide bond formation between CLIC subunits in a 2GSH/GSSG buffer system (in molar excess) were considered. In this model, the formation of disulphide bonds between neighbouring subunits resembles the formation of intrachain rather than an interchain bonds as already mentioned. In Fig 5.8, according to this model, the fitted curve approaches very closely the conductance of the fully-reduced channel (in DTT).

The disulphide and dithiol distributions were described in terms of an equilibrium constant (K_{ox}, molar units) and the ratio $[GSH]^2/GSSG$, by employing standard mass-action treatment:

$$K_{ox} = \{[P(SS)]\}/[P(SH)_2]\} \times \{[GSH]^2/[GSSG]\} \quad [4]$$

The total channel protein (P_t) is the "time-averaged" sum of the reduced $[P(SH)^2]$ and oxidised protein [P(SS)]. Hence, the proportion of reduced protein $[P(SH)^2]$ can be given as:

$$P_t = [P(SH)^2] + [P(SS)] \quad [5]$$

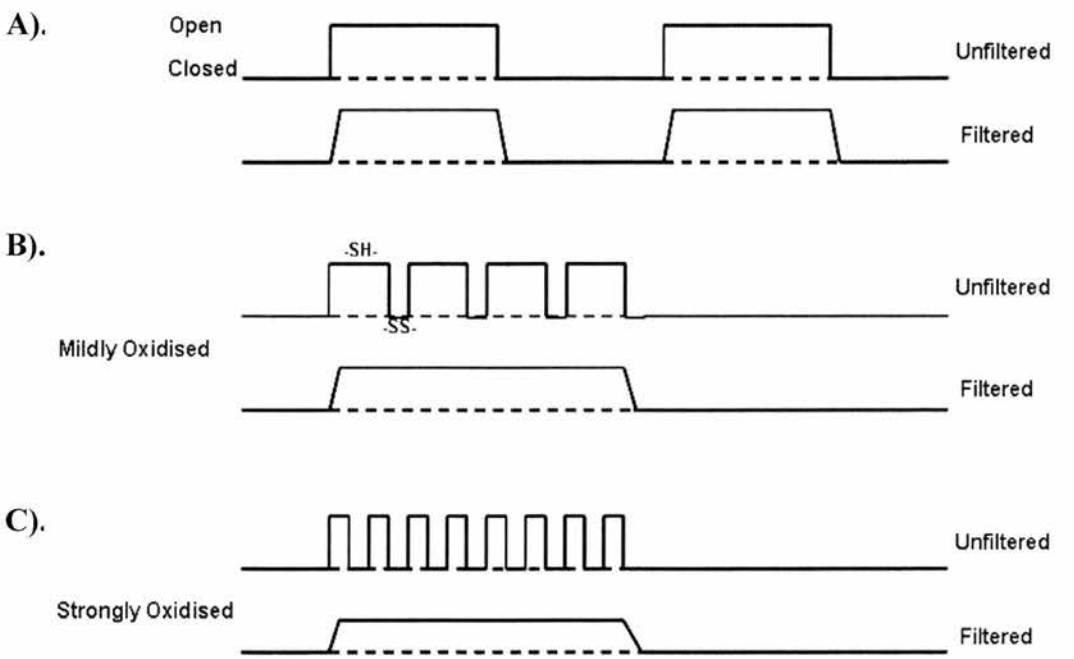

Fig 5.10. Smooth reduction (block) of single-channel conductance. The apparent small conductance is composed of filtered fluctuations between two different conductance states (Yellen, 1984) and in our experiments the data were heavily filtered at 50 Hz which gave poor resolution between short individual open and closed levels. (A) Representation of fully-reduced channels showing non-filtered and filtered traces. (B) Traces showing the effect of mild-oxidation on single-channel currents. The open level corresponds to the fully-reduced channel and closed levels indicate the formation of intermolecular disulphide bonds (-S-S-). Note the apparent reduction in amplitude as a result. (C) On strong oxidation, channel closure occurred more frequently, corresponding to the even more frequent formation of transient disulphide bonds.

So that:

$$[P(SH)_2]/\{[P(SS)] + [P(SH)_2]\} = \{[GSH]^2/[GSSG]\}/\{K_{ox} + [GSH]^2/[GSSG]\} \quad [6]$$

However, $[GSH]^2/[GSSG]$ can be written as R x [GSH], where R is defined as [GSH]/[GSSG], so that:

$$[P(SH)_2]/[Pt] = R \times [GSH]/\{K_{ox} + R \times [GSH]\} \quad [7]$$

The data summarized in fig 5.8 were therefore fitted to a rectangular hyperbola, as predicted from equation 7. Additional data obtained in 2.5 mM GSH buffer were also plotted and these could also be fitted to a rectangular hyperbola. The maximum conductance of CLIC1 was found to be 40 pS, similar to fully-reducing conditions (DTT). It is not possible (in our conditions) to obtain fully-reduced conditions with GSH as a small amount of GSSG is always present in the buffer (from auto-oxidation). The values of R required for half-reduction (half of the maximum conductance of the channel) correspond to $K_{ox}/[GSH]$, giving ~25 mM for K_{ox}, which is independent of the GSH concentration, as predicted.

Analysis by mass action normally requires a system containing very large number of molecules, but this can be related to the analysis of 'gating' events in single ion channels provided the events are stochastic, and many thousands of individual events are collected (as occurs for example when measuring 'reduced' single-channel currents). In other words, compared to a mass action "snapshot" from millions (or

billions) of interacting molecules, the analysis provided here uses a small number of interacting molecules, but they are effectively observed over many thousands of independent reactions to produce an equivalent "average" picture of events.

5.6 Role of C24 in redox-regulation

The crystal structure of oxidised CLIC1 showed a non-covalently linked dimer stabilised by intramolecular disulphide bonds between C24 and C59 (Littler et al., 2003). In each subunit C24 (and its equivalents) is conserved in all mammalian CLICs but C59 is unique to CLIC1. In the topology model in fig 5.9, C24 is predicted to be located in the luminal side of the membrane. CLIC1 was *trans* redox regulated, which suggested C24 might be playing an important role in this regulation. Cysteine residues present on the cytosolic side were not involved in this redox-regulation. The cysteine-reactive compound NEM could inactivate the channel only from the *trans* but not from the *cis* side. To further investigate the role of C24, this residue was mutated to alanine (C24A).

CLIC1 C24A was reconstituted in planar bilayer in 5 mM GSH to obtain channels. Unlike the C24S mutant of CLIC1 (Littler et al., 2003), CLIC1 C24A could autoinsert and form channels (but the single-channel conductance was reduced to 14.2 $\pm$ 1.1 pS (mean $\pm$ SD, n=9)). The reversal potential in asymmetrical (500 mM *cis vs.* 50 mM *trans*) KCl of CLIC1 C24A channels was similar (+ 5.7 $\pm$ 1.5 mV, mean $\pm$ SD, n=9) to non-mutagenised CLIC1 channels (Chapter 4). Hence the selectivity of CLIC1 C24A channels was similar to CLIC1 channels. The mutated (C24A) channels were reconstituted with an intact N-terminus His-tag, and similar

channels were obtained in planar bilayers. Much like CLIC1, CLIC1 C24A could be blocked by *trans* Ni^{2+}, confirming the orientation of the channels (the N- terminal tag faced the *trans* chamber, fig 5.11). These mutated channels were however insensitive to a *trans* thiol-reactive reagent (NEM). When these channels were exposed to sequential *trans* oxidation, they were not blocked like unmodified CLIC1 (Fig 5.11).

5.7 Discussion

p64 was affinity purified by IAA-94 (Landry et al., 1989), and since then IAA-94 has been shown to inhibit CLIC associated channels or chloride-efflux by various groups (Tulk et al., 2000; Tonini et al., 2000; Valenzuela et al., 2000; Harrop et al., 2001; Proutski et al., 2002; Warton et al., 2002; Berryman et al., 2004). IAA-94 was also shown to abolish the release of TNF-α and nitrite production, as well as the consequent neurotoxicity and neuronal apoptosis in neurons cultured with Aβ-treated microglia (Novarino et al., 2004). In our experiments, very high concentrations of (>10 μM) IAA-94 could inhibit CLIC1 channels but not CLIC4. This shows that IAA-94 is not a very specific blocker of CLIC proteins.

The topology of the channels as predicted in fig 5.9 was tested in this chapter by using Ni^{2+} and the cysteine-reactive compounds NEM and DTNB. CLIC1 and CLIC4 inserted into planar bilayers with a well-defined orientation, with their N-terminus facing the extracellular or luminal side of the membrane. CLIC1 channels incorporated with an intact N-terminal His-tag appeared to insert and form channels similar to the cleaved CLIC1 and could be inhibited with Ni^{2+} from the luminal but

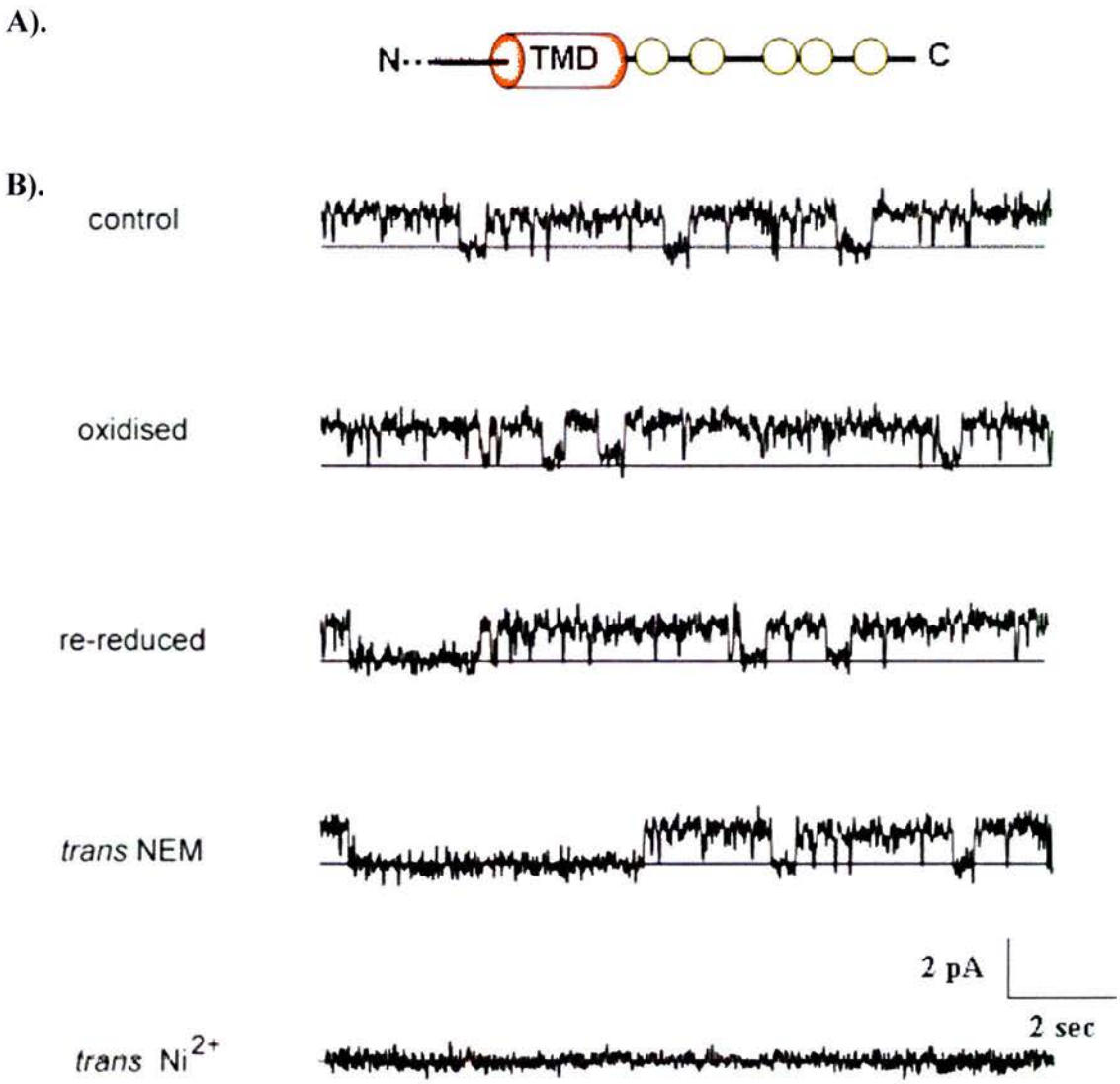

Fig 5.11. Single-channel currents recorded from CLIC1 C24A. (A) The cartoon displays the cysteines remaining in CLIC1 C24A. Note that C24 was mutated to alanine. (B) CLIC1 C24A single-channel currents in 5 mM GSH are the control traces at +100 mV. When CLIC1 C24A was *trans* oxidised (from -225 mV to -195 mV), it showed no block in the channel activity. Similarly there was no effect of *trans* NEM on mutated channels. 50 μM *trans* Ni^{2+} inactivated the channel like the wild type CLIC1. The solid lines indicate the closed current levels.

not the cytosolic side. However, CLIC4 failed to show the same effect when Ni^{2+} was applied from either the *cis* or *trans* sides. This may be due to the longer N-terminus of CLIC4 compared to CLIC1. CLIC1 C24A (with an intact N-terminus His-tag) was also blocked by *trans* (luminal) Ni^{2+}, showing the same orientation. This may also involve least consumption of energy to unfold and refold in order to insert into bilayers. Thiol-reactive compounds such as NEM and DTNB could inhibit CLIC1 and CLIC4 respectively, from the *trans* side. The predicted orientation places the N-terminus on the *trans* side of the channel, exposing C24 of CLIC1 and C35 of CLIC4 immediately before the predicted TMD to the changes in redox-potential on the luminal side of the channel.

The maximum slope conductance of CLIC1 and CLIC4 could be reversibly reduced by increasing the *trans* redox-potential in a glutathione buffer, and this could be attributed to reversible disulphide bond formation involving pairs of subunits in the presence of GSH and GSSG. The "smooth" reduction in single-channel currents was consistent with the rapid reduction and oxidation of thiol groups in the presence of a glutathione buffer system, with rapid channel gating making it impossible to resolve single-channel opening events (under the current filtering conditions).

The sensitivity of the channels to luminal redox conditions could partly explain the discrepancy in data obtained earlier for CLICs *in vitro* and *in vivo* (Table 4.1). The single-channel conductance ranges from 7 to 120 pS for CLIC1, 1 to 86 pS for CLIC4 and 26 to 400 pS for CLIC5B. Similarly, channels were reported with varying selectivity, which could in part depend on the size of the permeant ions.

In cells, major signalling pathways involve two protein modifications, phosphorylation of proteins and changes in the thiol status of proteins due to changes in the redox environment. The oxidative and reductive stress can trigger redox cascades that bring changes in the thiol status of the cells. Changes in redox potential from -240 mV to -170 mV could result in cell proliferation (-240 mV), cell differentiation (-200 mV) and apoptosis (-170 mV) (Schafer and Buettner, 2001). CLIC1-associated currents were shown to be increased during the G2/M phase during the cell-cycle (Valenzuela et al., 2000), and CLIC4 has been implicated in apoptosis (reviewed by Suh and Yuspa, 2005). These results suggest that CLICs are involved in cellular processes that are regulated by the redox potential of the cellular environment.

CHAPTER 6

IDENTIFICATION OF A POSSIBLE PORE-FORMING REGION IN CLIC PROTEINS

6.1 Introduction

Ion channels are pore-forming transmembrane proteins that allow ions to permeate otherwise impermeant biological membranes. The pore structure and amino acid composition play a crucial role in determining ion permeation and selectivity of particular channels. The conductance depends on the structural characteristics of these pores, which includes hydrophobicity, the diameter of the conduction pathway and cycles involving transitions between microstates of the selectivity filter (Zhou and Mackinnon, 2004).

Ionic diffusion across the membrane and gating of channels is regulated in response to a variety of stimuli, such as variation in the lateral pressure (Treptow and Tarek, 2006), variation in pH, change in the membrane potential (voltage-gated), or binding of transmitters or hormones which tune the channel (ligand-gated) (Hille, 1992). In the past few decades, several studies have been carried out to identify key elements of the pore regions of different classes of ion channel. The selectivity of ion channel pores has generally been considered to be constant and specific, but under specific conditions pores can allow normally impermeant ions or they may be non-selective. The diffusion of ions through the channel requires a hydrophilic pathway for perfect ion coordination. This hydrophilic pathway or environment may be provided by coordinating groups of proteins or by transient hydration of the ionic conduction pathway (Jiang et al., 2002). The diffusion of ions is energetically-restrained by closure of the channel or narrowing of the activation gate that exclude water molecules from the

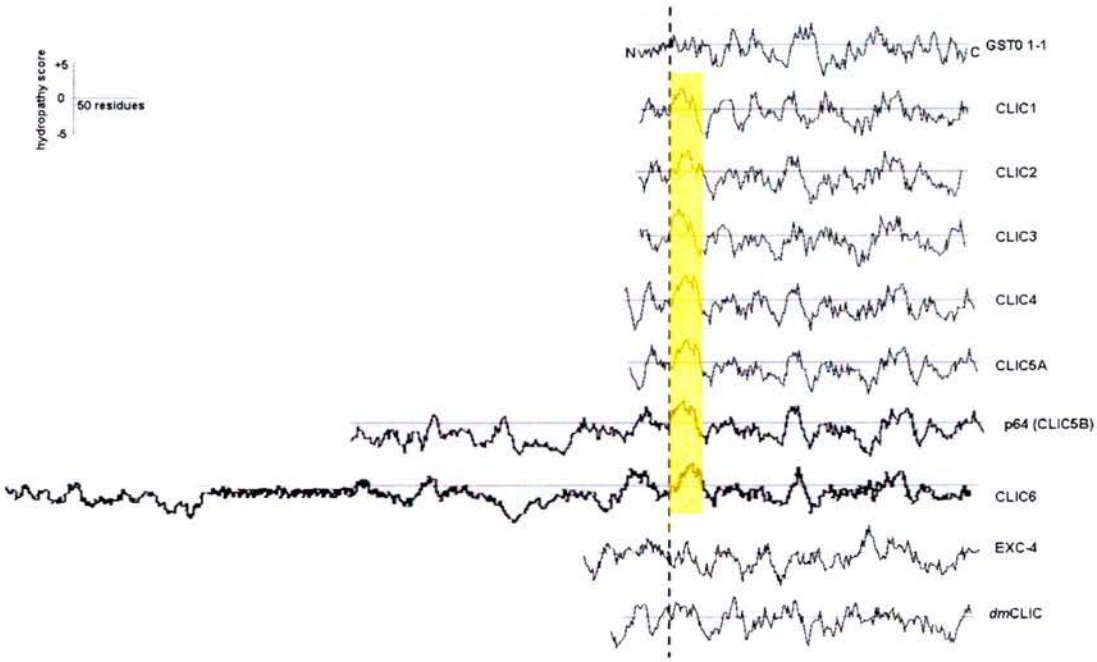

Fig 6.1. Hydropathy plots of vertebrate and invertebrate CLICs and GSTO 1-1. Kyte-Doolittle hydropathy plots (window size 9 residues) of human and invertebral (EXC-4 and *dm*CLIC) CLICs, and GSTO 1-1, aligned against the well-conserved N-terminal cysteine (vertical dotted line compared to C24 of human CLIC1). The predicted TMD is highlighted by a yellow box. (extended and redrawn from Ashley, 2003)

permeation pathway (Spronk et al., 2006).

Sequence alignments and hydrophobic plots strongly predict the single TMD near the N –terminus region, following the first cysteine residue in all mammalian CLICs. The predicted TMD is absent in Ω-GSTs, which are unable to insert into membranes. A TMD near N-terminus would involve much less disruption of the soluble protein structure compared to the large scale rearrangements required for the membrane insertion of a TMD further into the primary sequence, or multiple TMDs. With a single TMD, if CLICs can form a channel, they need a minimum of four monomeric proteins to form a channel pore or a functional 'protomer' in the membrane. Like other ion channels, CLICs should have a central cavity lined by hydrophilic amino acids or a selectivity filter. They should also have a gating mechanism to control their open and closing.

6.2 Reconstitution of truncated channels

A putative pore-forming region was identified on the basis of sequence alignments (Fig 1.7), hydropathy plots (Fig 6.1) (Ashley, 2003), protease digestion studies (Duncan et al., 1997), the sidedness of the N- and C-termini (Tonini et al., 2000), and EXC-4 truncation studies (Berry et al., 2003; Berry and Hobert, 2006). In the predicted model, the luminal (or external) side of each subunit contains a single cysteine residue located just before the putative pore entrance. The pore-forming region consists of a putative TMD. To test this

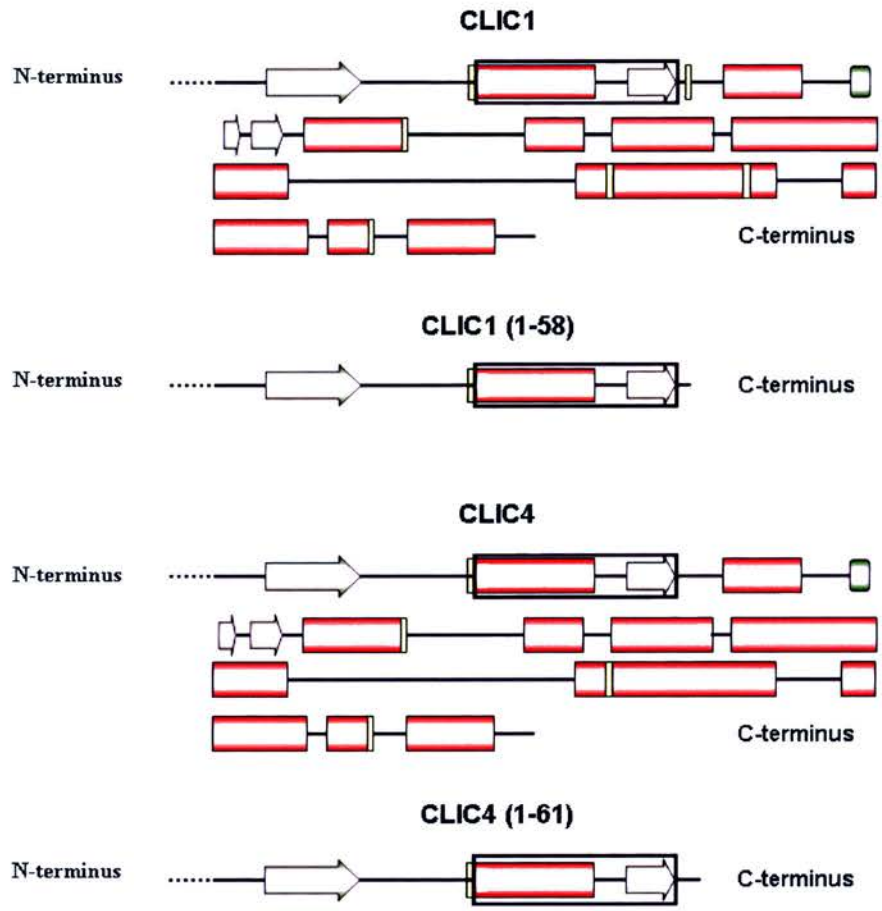

Fig 6.2. Schematic representation of full-length and truncated CLIC1 and CLIC4 proteins. β-strands are indicated by green arrows and α-helices are represented by red cylinders. Cysteine residues are marked by yellow bars and the his-tag at the N-terminus is indicated by dotted lines. Putative transmembrane domains (TMD) are highlighted with boxes. Truncated CLIC1 (1-58) and CLIC4 (1-61) had intact N-termini and an intact putative TMD, with C24 and C35 (respectively) present just in front of the TMD. The His-tag was removed by thrombin digestion leaving behind 8 residues (GGLVPRGS) in front of the N-terminus of CLIC1 and CLIC4.

hypothesis, Truncated recombinant human CLIC1 and rat brain CLIC4 (p64H1) with 58 and 61 amino acids, respectively, containing the N-terminus and putative TMD were overexpressed and purified by FPLC (Chapter 3). The truncated proteins were reconstituted into planar bilayers containing POPE, POPS and cholesterol 4:1:1 mol/mol, respectively. They autoinserted into the bilayers to form redox–sensitive ion channels, and showed a similar orientation to the full-length proteins.

Both the truncated proteins have conserved cysteines at position 24 in CLIC1 and its equivalent 35 in CLIC4. The truncated CLICs formed channels less readily, often taking upto 40 min compared to less than 10 min for full length CLIC1 and CLIC4 proteins. However, once channels appeared in the bilayers, channel recordings were highly consistent between experiments, typically showing infrequent low-amplitude currents of ~0.5 pA at a holding potential of +100 mV (with 500 mM *cis* KCl *vs.* 50 mM *trans* KCl).

In some experiments large amplitude currents of +1.5 pA at the same holding potential were observed (Fig 6.4). Large conductances were infrequent but more-persistent in the presence of H_2O_2. The conductance of truncated CLIC1 and CLIC4 channels were not significantly different ($P > 0.05$). The maximum slope conductance of CLIC1 (1-58) in 500 mM *cis* KCl *vs.* 50 mM *trans* KCl in the presence of 1 mM DTT was 5.1 $\pm$ 0.65 (mean $\pm$ SD, n=7) (Fig 6.3) and for CLIC4 (1-61) it was 5.5 $\pm$ 0.58 pS (mean $\pm$ SD, n=5) under similar conditions (Fig 6.4). The reversal potentials were 0.0 $\pm$ 2 mV (mean $\pm$ SD, n=7) and 0 $\pm$ 2.2 mV (mean

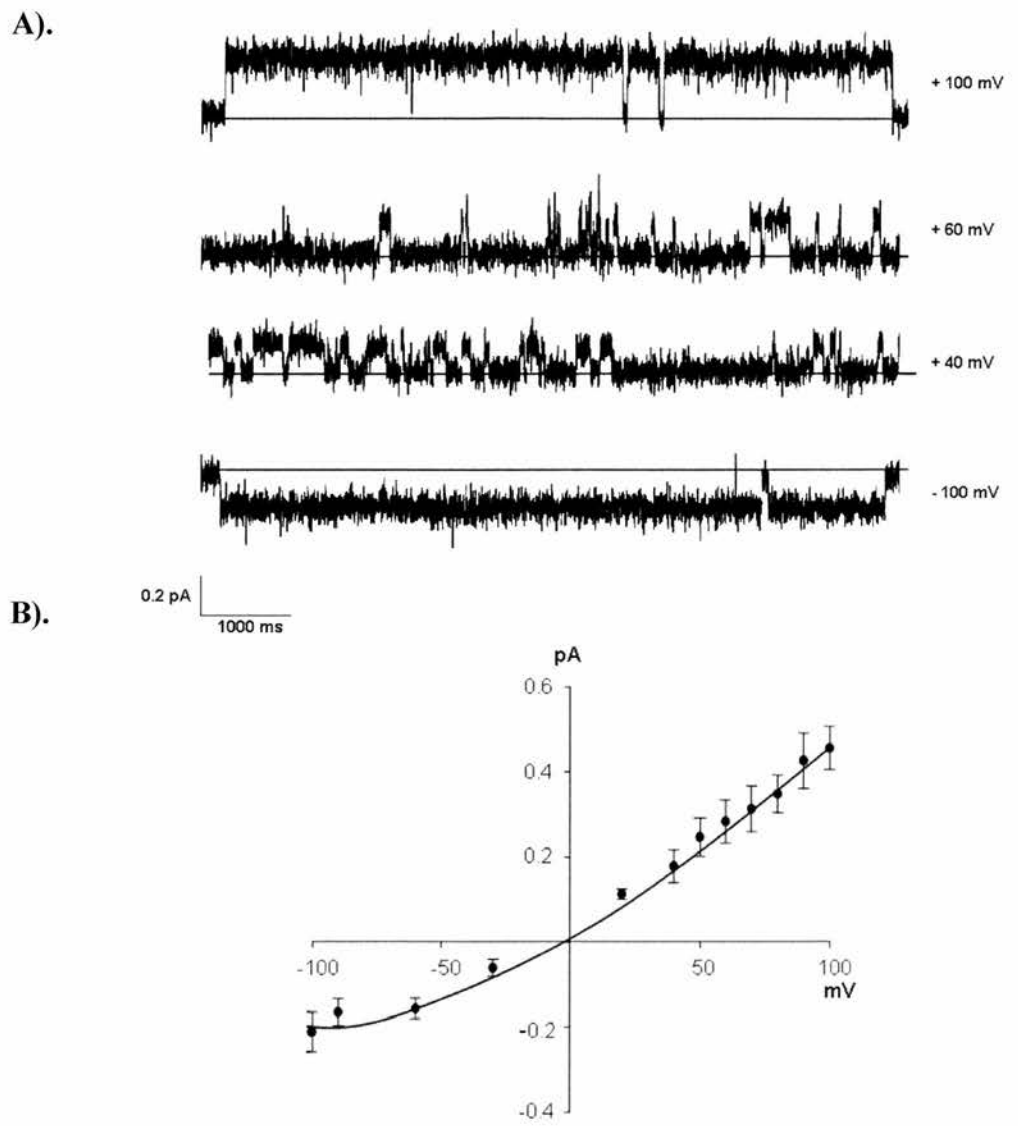

Fig 6.3. Reconstitution of truncated CLIC1 (1-58). Single-channel currents from truncated CLIC1 (1-58) were recorded in asymmetrical (500 mM *versus* 50 mM) KCl in the presence of 1 mM DTT. The solid lines indicate the closed levels. (A) Examples of single-channel traces at different holding potentials. The channels appeared smaller in conductance at negative holding potentials as compared to positive holding potentials. (B) Current-voltage (I/V) relationship for CLIC1 (1-58). The maximum slope conductance was calculated between 0 and +100 mV (mean $\pm$ SD, n=7). The truncated CLIC1 channels are non-selective (E_r = ~ 0 mV).

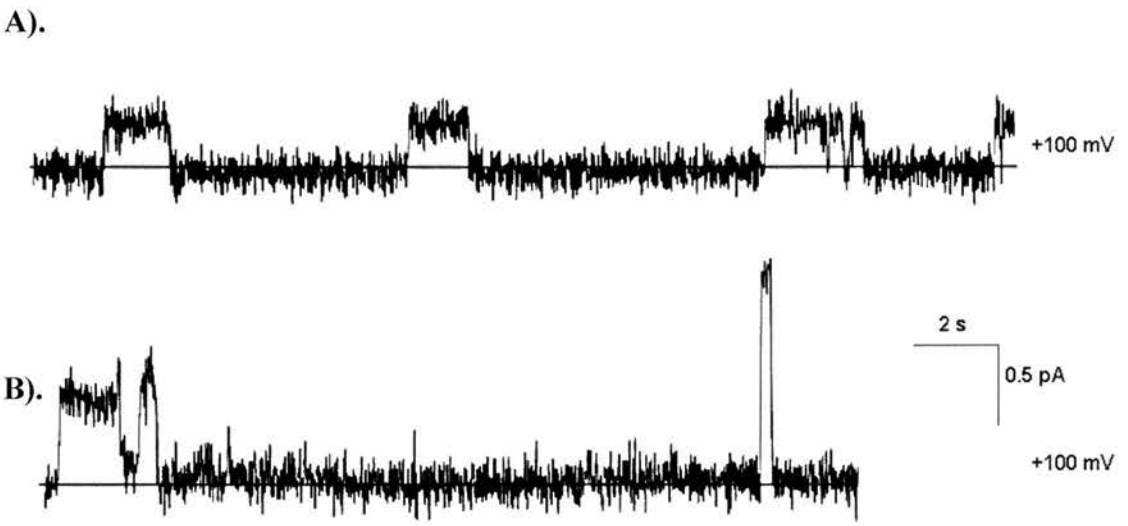

Fig 6.4 Bilayer reconstitution of truncated CLIC4 (1-61). Single-channel currents were recorded with 500 mM *cis* KCl *versus* 50 mM *trans* KCl. (A) Channels reconstituted in the presence of a 5 mM GSH buffer system. (B) Channels reconstituted in the presence of 100 μM H_2O_2 showing infrequent large-amplitude openings in addition to frequent small openings (mean ± SD for 5 independent experiments in each case). The solid lines indicate the closed levels.

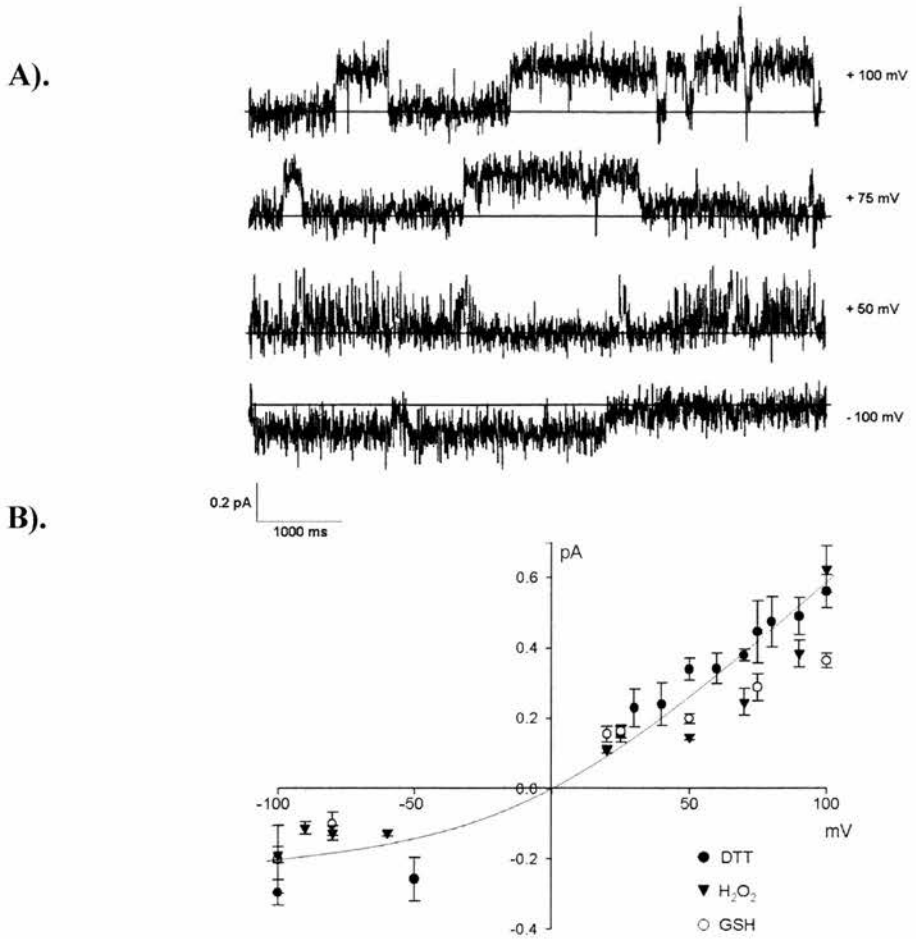

Fig 6.5. Single-channel recordings of CLIC4 (1-61). Single-channel recordings of truncated CLIC4 (1-61) in asymmetrical (500 mM *versus* 50 mM) KCl in the presence 1 mM DTT. The solid lines indicate the closed levels. (A) Examples of single-channel currents at different holding potentials. Channel currents decrease at negative holding potentials compared to positive holding potentials. Occasional large opening can be seen at +100 mV. (B) Current-voltage (I/V) relationship of CLIC4 (1-61) in the presence of either 1 mM DTT, 100 μM H_2O_2 or a glutathione buffer system (mean ± SD for 5-7 independent experiments in each case). The maximum-slope conductance was calculated between 0 mV and +100 mV. The truncated CLIC4 channels were non- selective. The conductance of the small channel was 3.8 ± 0.53 pS (mean ± SD, n=5) measured over the same interval (+25 mV to +100 mV). The relative anion *versus* cation selectivity was 1.2 ± 0.98 (mean ± SD, n=5). These values are not significantly different from the truncated protein in the presence of either DTT or 5 mM GSH (P>0.5).

± SD, n=5) for CLIC1 (1-58) and CLIC4 (1-61), respectively. The relative anion *versus* cation permeability was 1.1 ± 0.23 (means ± SD, n=5) for truncated CLIC1.

All subsequent experiments were carried out with truncated CLIC4 (1-61). On comparing (Fig 6.4 and Fig 6.5) the appearance of channels formed by the truncated CLIC4 proteins in the presence of 1 mM DTT, 5mM GSH buffer system and 100μM H_2O_2 were similar. The overall conductances and anion *versus* cation selectivities of the truncated protein were very similar in the presence of 1mM DTT, or 5 mM GSH buffers. From an analysis of several independent experiments, the single-channel slope conductances, calculated by linear regression between +25 mV and + 100 mV, were 5.5 ± 0.58 pS and 4.8 ± 0.61 pS (both means ± SD, n=5), respectively for the DTT and GSH buffers. The values were not significantly different ($P > 0.5$). The relative anion *vs.* cation selectivities of the truncated CLIC4 proteins, determined from equilibrium potentials measured under the same conditions, were 1.1 ± 0.27 and 1.0 ± 0.45, respectively (both means ± SD, n=5). Again, these values were indistinguishable ($P > 0.5$) and could be fitted to a single line for both conditions (Fig 6.4).

Truncated CLIC4 (1-61) proteins reconstituted in the presence of 100μM H_2O_2 formed infrequent channels of both low and high conductance (Fig 6.4). The slope conductance of small channel was 3.8 ± 0.53 pS (mean ± SD, n=5) measured over the same interval (+25 mV to +100 mV). The relative anion *vs.* cation selectivity was 1.2 ± 0.98 (mean ± SD, n=5). These values are not significantly different from the truncated protein in the presence of DTT or glutathione buffer system (P

> 0.5), but the experimental points do not appear to align well with the corresponding data obtained with DTT or a glutathione buffer.

6.3 Orientation of truncated membrane CLIC4 (1-61)

In previous studies with CLIC1 and CLIC4, investigations were carried out to explore the orientation of channels with Ni^{2+} (added to His-tagged proteins) a cysteine-reactive compounds (NEM and DTNB). As in previous experiments, truncated CLIC4 with an intact N-terminal His-tag was reconstituted and 50 μM histidine-reactive Ni^{2+} was added from the *cis* and the *trans* sides, sequentially. As observed earlier for full-length CLIC4, truncated CLIC4 was not blocked by either *cis* or *trans* Ni^{2+} possibly, because of the long and more flexible N-terminus of truncated CLIC4.

As an alternative, cysteine-specific reagents, as previously for full-length CLIC4, were added to truncated CLIC4. Truncated CLIC4 was successfully inhibited by *trans* DTNB but not by *cis* DTNB. The mean open probability (Po) of truncated CLIC4 exposed to 5 mM GSH was 0.52 ± 0.35 (mean ± SD, n=6), calculated from recordings lasting 60 s. GSH was removed by perfusion from the *cis* and *trans* side before 0.2 mM DTNB was added. Po after the addition of 0.2 mM *cis* DTNB was 0.53 ± 0.34 (mean ± SD, n=6), which was reduced to 0.04 ± 0.03 (mean ± SD, n=6) after the addition of 0.2 mM *trans* DTNB. Fig 6.5 shows example traces of truncated CLIC4, and inhibition of currents by *trans* but not *cis* DTNB. Mean Po between control, *cis* and *trans* DTNB was also analysed channel

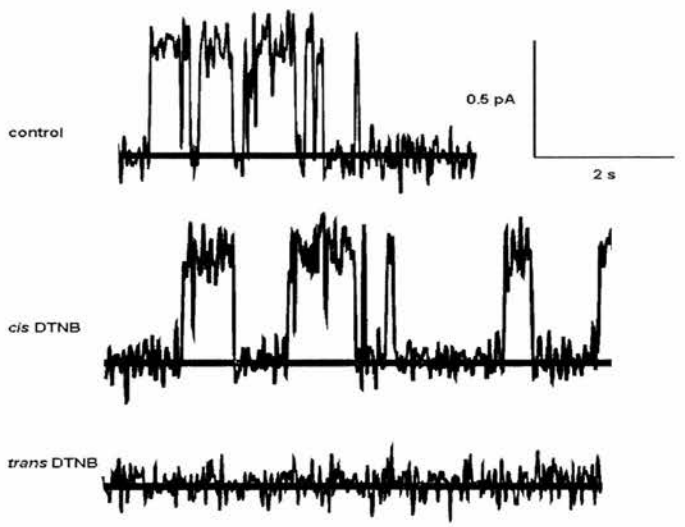

Fig 6.6 Inhibition of truncated CLIC4 by DTNB. Single-channel recordings of truncated CLIC4 in 5 mM GSH at a holding potential of +100 mV. The recordings were made in 500 mM KCl *cis versus* 50 mM KCl *trans*. GSH was perfused with GSH-free solutions before adding DTNB. 0.2 mM *cis* DTNB had no effect on the single-channel currents but *trans* DTNB inhibited the channels. This is a representative section from 60 s long recordings (used for Po analysis). Note that recordings in the presence of GSH buffers were much less noisy than recordings in DTT.

by channel by paired *t*-tests, because of the large variation in control Po from channel to channel. The mean Po differed significantly ($P < 0.002$) for control and the *trans* DTNB, but there was no significant difference between control and the *cis* DTNB ($P > 0.05$).

6.4 Redox-regulation of truncated CLIC4

In chapter 5, CLIC1 and CLIC4 were shown to be *trans* redox-sensitive. The cysteine residue just before the predicted TMD was shown to be involved in this redox-regulation. Both CLIC1 and CLIC4 have cysteine residues, immediately in front of the predicted TMD. In truncated CLIC1 and CLIC4, only these cysteine residues alone were present. The C24A mutant of CLIC1 was insensitive to *trans* redox-regulation (Chapter 5), which supported the idea that C24 was present towards the luminal side of the membrane. To further test this model on CLIC4, truncated CLIC4 containing only C35 was reconstituted in a 5 mM GSH buffer system.

Sequential increases of the *trans* redox-potential (by addition of GSSG) from -225 mV to -195 mV inhibited the truncated CLIC4 channels, and this effect could be reversed by decreasing the redox potential to -225 mV. There was no effect on single-channel currents from changes in *cis* redox potential. Example traces are shown in fig 6.6, with corresponding redox potentials.

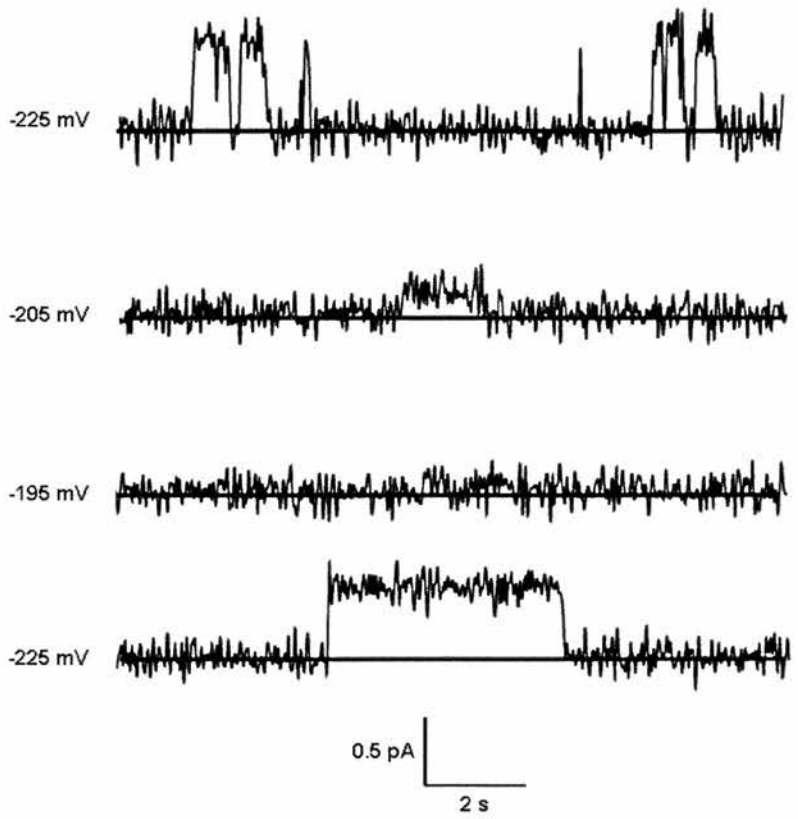

Fig 6.7 Redox-regulation of truncated CLIC4. Single-channel currents were recorded in assymetic 500 mM *cis* KCl *vs.* 50 mM *trans* KCl at +100 mV in 2GSH/GSSG buffer system. The sequential increase of GSH: GSSG ratio from 10 to 1 on the *trans* but not the *cis* side of truncated CLIC4 inhibited the channel. This effect was reversible by reperfusion of GSH: GSSG:: 10:1. The same results were obtained in 6/6 experiments.

6.5 Discussion

Previously it was predicted that CLICs have a single (Ashley, 2003) or an odd number of TMDs (Proutski et al., 2002). Sequence alignments and hydrophobicity plots localised it to the N-terminus region. This predicted TMD (which is absent in Ω-GSTs, Ashley, 2003), was preceded by the first cysteine residue in both CLIC1 and CLIC4. All mammalian CLICs (except CLIC3) have a tryptophan residue in the TMD and this could promote auto-insertion of the proteins into membranes. The presence of a single TMD is supported by protease digestion studies, where it was incompletely removed on digestion (Duncan et al., 1997) and by studies showing the position of N- and C- termini of CLIC1 in CHO cells (Tonini et al., 2000). Studies on the worm CLIC, EXC-4, involving truncation, mutagenesis and localisation further supported the single TMD prediction (Ashley, 2003; Berry et al., 2003; Berry and Hobert, 2006). This suggests that CLIC1 and CLIC4 channels must exist as oligomers containing a minimum of four subunits (Fig 6.8), because in order to form a functional pore, a minimum of four subunits are required for a protein containing only a single TMD.

The possibility that the putative TMD could form ion channels was explored by incorporating truncated CLIC1 and CLIC4, containing putative TMD including a single remaining conserved cysteine residue just before the putative TMD, into planar bilayers. These truncated proteins formed channels less rapidly but with consistent appearances in several different experiments.

A).

```
M...CPFSQRLFMVLWLKGVTFNVTTVDTKRRTETVQKLCP.....CLIC1
M...CPFCQRLFMILWLKGVKFNVTTVDMTRKPEELKDLAP.....CLIC2
M...CPSCQRLFMVLLLKGVPFTLTTVDTRRSPDVLKDFAP.....CLIC3
M...CPFSQRLFMILWLKGVVFSVTTVDLKRKPADLQNLAP.....CLIC4
M...CPFSQRLFMILWLKGVVFNVTTVDLKRKPADLHNLAP.....CLIC5A
M...CPFSQRLFMILWLKGVVFNVTTVDLKRKPADLHNLAP.....CLIC5B
M...CPFSQRLFMILWLKGVIFNVTTVDLKRKPADLQNLAP.....CLIC6
```

B).

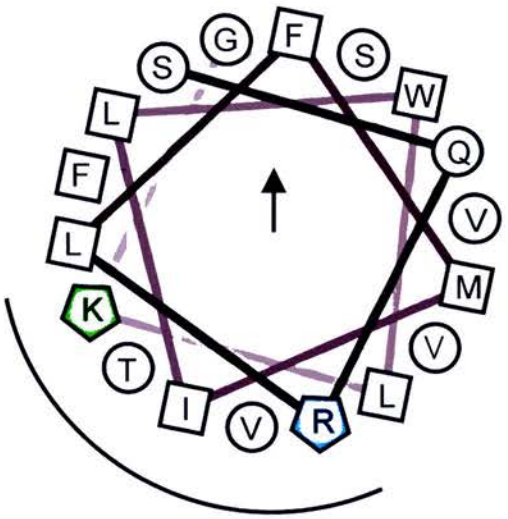

C).

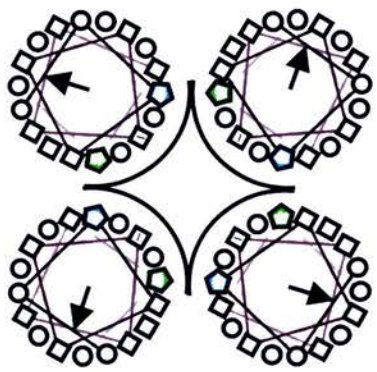

Fig 6.8. Putative transmembrane domain of CLIC proteins. (A) N-termini region of mammalian CLIC proteins. The first cysteine residue and the conserved CP motif are highlighted. The putative TMD (yellow background), differences within residues (blue), and the tryptophan residue (red) are also highlighted. The truncated CLIC1 and CLIC4 proteins contained intact N-termini with putative TMD (shown as boxed residues). (B) Helical wheel projection of TMD of CLIC4 looking down the helix from the N to the C-terminus (Armstrong and Zidovetzki, http://rzlab.ucr.edu/scripts.wheel/wheel.cgi). Squares, circles and polygons indicate relatively hydrophobic, hydrophilic and positively-charged residues respectively. Arrows indicate the direction of the hydrophobic moment and an arc indicates the suggested pore-lining. (C) Proteins with a single predicted TMD require minimum of 4 subunits to form an ion channel. The predicted "tetrameric" cartoon shown indicates the hydrophilic pore. Conserved arginine and lysine residues predicted to form the charged rings in the pore region are highlighted in sequence alignments and helical wheel projections.

The maximum slope conductance of the channels was reduced significantly when compared to full-length proteins. Truncated CLIC1 and CLIC4 formed similar channels in terms of their slope conductance, unlike full-length proteins. The TMD residues are well conserved in all mammalian CLICs (Fig 6.8), and the formation of similar channels by truncated CLIC1 and CLIC4 channels suggests that differences in reduction in conductance and regulation are attributable to the missing parts of the proteins. The all α-helix C-terminus of the CLIC proteins may contribute to the pore forming region. This is consistent with the idea that the missing parts of the proteins form charged channel vestibules that gather permeant ions near the pore region, as shown in BK channels which have a ring of eight negatively charged glutamate residues at the entrance to the intracellular vestibule (Brelidze et al., 2003).

The channels obtained from truncated CLIC1 and CLIC4 were non-selective, irrespective of redox conditions. This suggests that the missing portion of the protein is necessary for the selectivity and conductance of the channel, rather than specific ion-binding sites in the pore. This suggest that regardless of redox conditions and an absence of much of the protein, the truncated subunits continue to oligomerise (by non-covalent interactions) to form a functional pore. Under strongly oxidising conditions, truncated CLIC4 also formed less-frequent functional pores. These channels had two conductance levels, one similar to the conductance observed in the presence of strong or mildly reducing conditions, and the other with a large-conductance. The oxidised proteins may insert into the

bilayers as preformed disulphide-linked dimers and then oligomerise with other similar dimers within the membrane to form functional channels.

CLIC1 and CLIC4 were shown to insert into planar bilayers in a well-defined orientation and the same orientation was predicted for truncated CLIC4 channels. In this model the N-terminus containing C35 was predicted to be on the luminal side. The cysteine-reactive compound DTNB inhibited the channels by forming mixed disulphides from the *trans* side but not the *cis* side, which shows that the pore-associated cysteine (in this case the only cysteine left in the protein) is exposed to the *trans* side. This confirmed that the predicted orientation of the truncated CLIC4 is similar to full length CLIC1 and CLIC4 proteins.

Much like full-length CLIC1 and CLIC4, the truncated CLIC4 showed *trans* redox regulation which was again predicted since the residue responsible for this sensitivity was left intact on the *trans* side of the membrane.

CHAPTER 7

INTERACTION OF CLIC PROTEINS WITH ACTIN AND DYNAMIN I

7.1 Introduction

CLIC proteins are widely-expressed in specific tissues and exist in soluble and integral membrane forms. The functional roles of CLICs are not well-established. Over expression of the proteins was linked to apoptosis (Suh et al., 2005), and also gave rise to specific ion channels (Table 4.1). Consensus phosphorylation sites for PKA, PKC, CKII and tyrosine kinases on CLIC proteins indicate that post-translational modifications may also affect the physiological roles of these proteins.

CLIC proteins have a distinct localisation and distribution in cells and tissues with some overlap (Table 7.1) among each other. This may result in functional overlaps as well, as evident from the viable mouse knock-out model for CLIC1 (Qiu, 2003). The other possibility is that some CLIC proteins form functional ion channels under specific conditions and the soluble forms interact with cytosolic proteins to play an important role in cellular functions. Previously, it has been shown that CLIC4 interacts directly with brain dynamin I and 14-3-3 but does not co-sediment with F-actin alone (Suginta et al., 2001). CLIC5A was identified as a component of cytoskeletal complex containing α-actinin, actin, ezrin, gelsolin and IQGAP1 from placental microvilli (Berryman, and Bretscher, 2000). Several CLIC proteins, including CLIC1, CLIC4, CLIC5A, CLIC5B and CLIC6 (Parchorin), can bind directly to the scaffolding protein AKAP350 that sequesters several signalling enzymes in the Golgi-centrosome region of a variety of cell types (Shanks et al., 2002). CLIC5A was shown to colocalise with ezrin in JEG-3 cells (Berryman et al., 2004) and with actin in bundles of inner and outer hair cells (Gagnon et al., 2006).

Protein	Tissue distribution	Subcellular localisation
p64 (CLIC5B)	Heart[1], kidney cortex[1] and skeletal muscle[1]	Cytoplasm[3], plasma membrane[3], intracellular membranes[3] and secretory vesicles[3].
CLIC1	Most tissues, but low expression in skeletal muscle and brain[4,6,7,9]	Cytoplasm. nucleoplasm, plasma membrane and intracellular membranes[4,6,7,9]
CLIC2	Adult muscle[5] and foetal liver[5]	Not known
CLIC3	Placenta[8,17], lung[8], heart[8] and low amounts in skeletal muscles[8], kidney[8] and pancreas[8]	Nucleus[8, 17] and plasma membranes[17]
CLIC4	High expression in brain[2, 10, 11], liver[2, 11], testis[2], kidney[2, 11], lungs[2, 11] and skeletal muscles[2]	Cytoplasm[11,12,14,15], nucleus[12,14,15], intracellular organelles[2,12,14] (mitochondria[12], endoplasmic reticulum[2], golgi complex[12] etc.), LDCV[10], plasma membrane[11,12,14] and intracellular membranes[11,12,114]
CLIC5	High in heart and skeletal muscles [12]. Moderate levels in kidney [12], lung and placenta [12]	Cytoplasm [12]
CLIC6	High levels in choroid plexus and gastric mucosa [13]. Low levels in kidney but absent in brain, heart or lung [13]	Cytoplasm and plasma membrane [13]
EXC-4	Excretory canal[16]	Cytoplasm and luminal membrane[16]

Table 7.1. Distribution and localisation of CLIC proteins. All CLIC proteins may have an intracellular localisation but it varies between the family members. They exhibit distinct localisation, although there are certain overlaps (Landry et al., 1993[1], Duncan et al., 1997[2]; Redhead et al., 1997[3]; Valenzuela et al., 1997[4]; Heiss and Poustka, 1997[5]; Schlesinger, 1997[6]; Tulk and Edwards, 1998[7]; Qian et al., 1999[8]; Edwards, 1999[9]; Chuang et al., 1999[10]; Fernandez-Salas et al., 1999[11]; Berryman and Bretscher, 2000[12]; Nishizawa et al., 2000[13]; Suginta et al., 2001[14]; Suh et al., 2005[15]; Berry et al., 2003[16], Money et al., 2006[17]).

The principal aim of this chapter is to investigate the interaction of CLICs and various cytoskeletal proteins including dynamin I and actin in cells, and to study the consequences of these interactions on the functions of membrane CLIC proteins.

7.2 CLICs in nerve terminals

CLIC4 (p64H1) was originally isolated from rat brain (Duncan et al., 1997), and localised to the hippocampal region, the septum, the amygdala, and the hypothalamus, certain areas of the cortex and the cerebellum (Chuang et al., 1999). Subcellular localisation showed that CLIC4 is present in large dense core vesicles (LDCV) (Chuang et al., 1999). CLIC4 interacts directly with rat brain dynamin I and 14-3-3 (Suginta et al., 2001), which supports the idea that these interactions have physiological relevance. CLIC1 was shown to be involved in microglia-mediated β-amyloid induced neurtoxicity (Novarino et al., 2004). To test the possible functional role of CLICs, they were studied in synaptic vesicles.

Synaptosomes from rat brain were purified by Percoll gradient fractionation and lysed with lysis buffer (Chapter 2, 2.13). Synaptosomes were stimulated with KCl for 2 mins at 37°C before lysis. The cytosolic and membrane fractions of stimulated and non-stimulated synaptosomes were probed with affinity-purified anti-CLIC1 and anti-CLIC4 antibodies. CLIC1 and CLIC4 were present in both stimulated and non-stimulated cytosolic and membrane fractions of synaptosomes (Fig 7.1). No remarkable differences were noticed between stimulated or non-stimulated synaptosomes. On Western blots (Fig 7.1), native CLIC1 and CLIC4 migrated at

relatively higher molecular weights as compared to recombinant CLIC1 and CLIC4, respectively. This may be attributed to post-translational modifications such as phosphorylation (Duncan et al., 1997) of the CLIC proteins.

7.3 CLICs in the complex of proteins interacting with Dynamin I

The dephosphins (dynamin I, amphiphysin I, amphiphysin II, AP180, epsin, eps15, PIPKIγ and synaptojanin I) are essential for the formation and scission of synaptic vesicles in endocytosis (Cousin and Robinson 2001). Dynamin I is the neuron-specific isoform of dynamin (Obar et al., 1990). It is a large GTPase enzyme, required for vesicle fission in synaptic vesicle endocytosis (SVE) (Schmid et al., 1998). The schematic representation of dynamin I is shown in fig 7.3.

The proline-rich domain (PRD) at the C-terminus region of dynamin I contains several binding motifs for src-3 homology (SH3) domains, through which it interacts with proteins such as amphiphysin I (Grabbs et al., 1997), endophilin I (Ringstad et al., 1997) and syndapin I (Qualmann et al., 1999). The PRD of the dynamin I is also a site for the phosphorylation of endogenous dynamin I at the synapse (Robinson, 1993). Serines 774 and 778 in the PRD of dynamin I were shown to be phosphorylated by Cdk5 (Tan et al., 2003). The functional role of phosphorylation of dynamin I in the synaptic vesicle recycling was recently established, and it was shown that synadpin I is a central component of the endocytic protein complex for SVE via stimulus-dependent recruitment of dynamin I (Anggono et al., 2006).

A). CLIC1 in synaptosomes

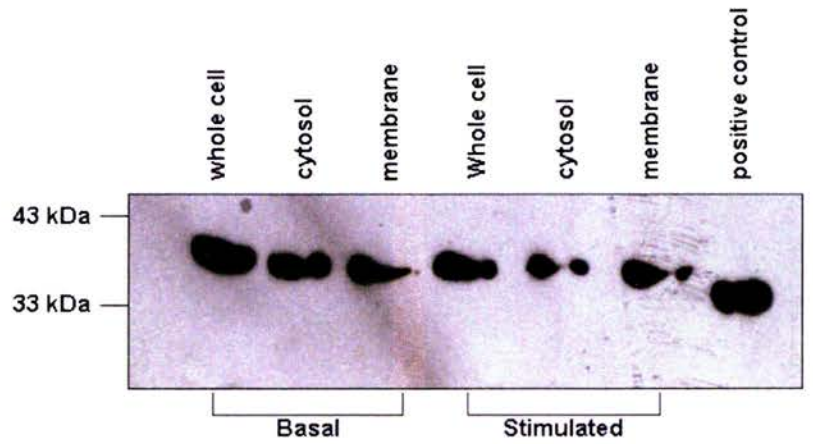

B). CLIC4 in synaptosomes

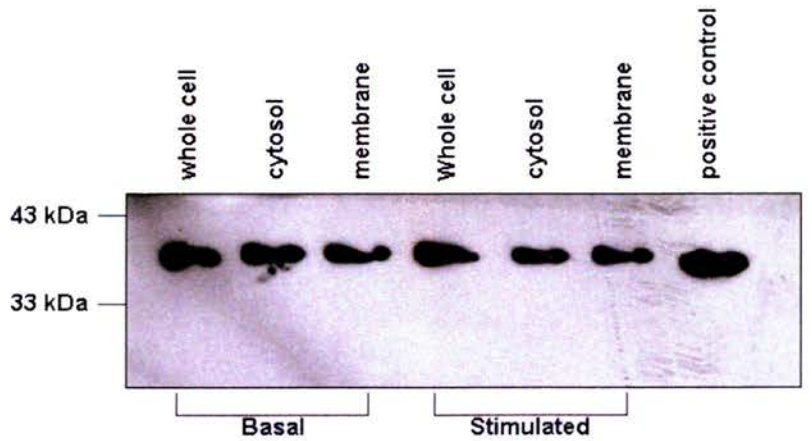

Fig 7.1 Western blots showing CLIC1 and CLIC4 in synaptosomes. Stimulated and non-stimulated Percoll purified synaptosomes (1 mg) were lysed and suspended in 50 µl of 3X sample buffer and boiled for min. 5 µl of samples were immunoblotted for CLIC proteins. The recombinant proteins were used as positive controls. (A) Western blot for CLIC1, showing the presence of CLIC1 in synaptosomes. (B) Western blot for CLIC4, showing the presence of CLIC4 in synaptosomes. There was no difference between stimulated and non-stimulated synaptosomes (n = 5).

CLIC4 was shown to be directly associated with brain dynamin I and overexpression of dynamin I in HEK-293 cells drives endogenous CLIC4 to membranes. CLIC4 has a potential motif recognized by SH3-domain proteins (Suginta et al., 2001). This interaction was probed and verified in synaptosomes by performing immunoprecipitation (IP). IPs with anti-dynamin I was carried on the Percoll-purified synaptosomal lysates (2 mg/ml). When probed with respective antibodies both CLIC1 and CLIC4 were present in the complex of proteins pulled down with dynamin I (using 0.4 μg of anti-dynamin I). Reverse-IPs were carried out with affinity-purified anti-CLIC1 (2 μg) and anti-CLIC4 (2 μg), and membranes were probed for dynamin I. Dynamin I was present in the protein complex immunoprecipitated with anti-CLIC antibodies (Fig 7.2). This showed the direct or indirect interaction between CLIC proteins (both CLIC1 and CLIC4) and dynamin I in a protein complex in synaptosomes.

PRD of dynamin I was expressed as GST tagged proteins. Serines at position 774 and 778 were mutated to alanine or glutamic acid (shown in Fig 7.3), to generate phosphorylated (EE) and dephosphorylated (AA) mimics of PRDs (Anggono et al., 2006). Pull down experiments from rat brain synaptosomes for CLIC1 and CLIC4 were performed with the PRD of dynamin I. Both CLIC1 and CLIC4 were pulled down with the GST-PRD of dynamin I. There was no difference in the binding of CLIC1 or CLIC4 to the PRD or its phosphomimetic mutants (Fig 7.3). Hence, phosphorylation of the PRD of dynamin I do not appear to affect its binding to either CLIC1 or CLIC4.

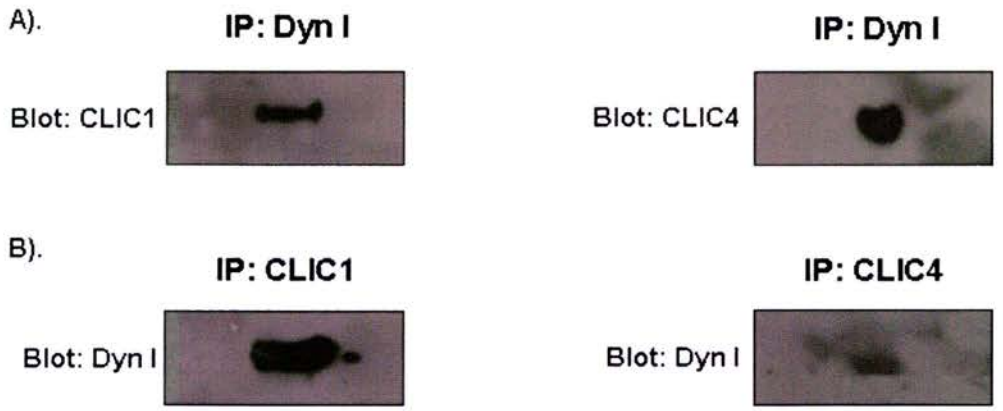

Fig 7.2 CLIC proteins and dynamin I complex in syanptosomes. (A) Synaptosomes were lysed and co-immunoprecipitated (Co-IP) with anti-dynamin I (0.4 μg), and then probed with anti-CLIC1 and CLIC4 as indicated. (B) Co-IPs were performed on the synaptosome lysates using anti-CLIC1 (2 μg) and anti-CLIC4 (2 μg) antibodies (n=4). The immunoprecipitated proteins were probed with anti-dynamin I. CLIC proteins and dynamin I were present in a protein complex in the synaptosomes. There was no binding of CLICs or dynamin I with glutathione beads alone. Representative of 4 independent experiments.

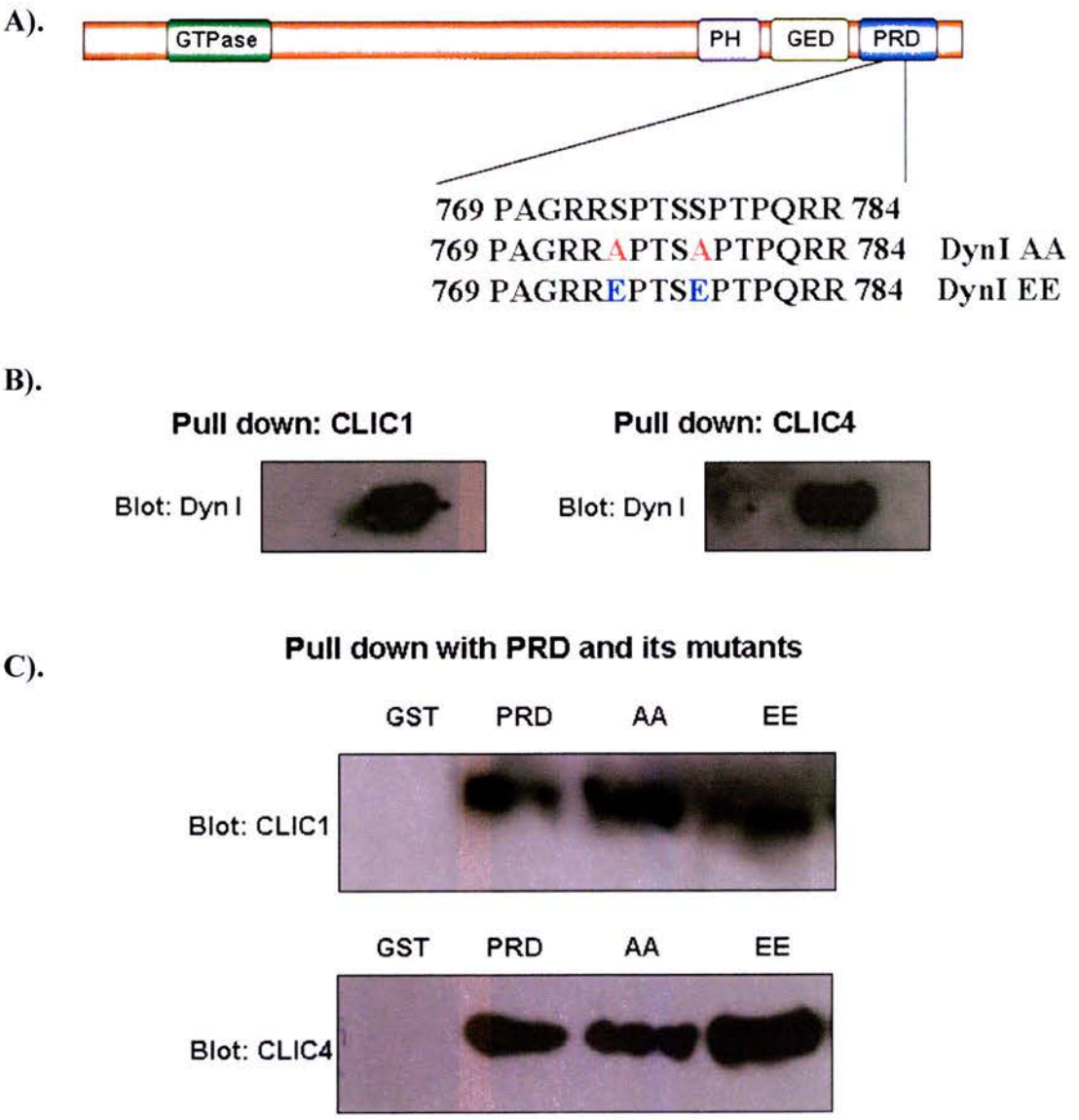

Fig 7.3 PRD of dynamin I directly interact with CLICs. (A) Schematic of the domain structure of dynamin I. The GTPase domain, pleckstrin homology (PH) domain, GTPase effector domain (GED) and the proline-rich domain (PRD) are shown. Serines at position 774 and 778 were substituted for either alanine (AA) or glutamic acid (EE). (B) Nickel-bound recombinant His-CLIC1 and His-CLIC4 interacts directly with recombinant GST-PRD. (C) GST-PRD and the mutant GST-PRDs showed no difference in binding with CLIC1 or CLIC4. There was no binding of CLICs or PRD of dynamin I to glutathione beads. Representative of 5 independent experiments.

7.4 Cellular distribution of CLIC1 and CLIC4

Bovine p64 (CLIC5B), a splice variant of CLIC5A, has been localised in intracellular membranes and intracellular vesicles in various cell types including PancI (Redhead et al., 1992, Landry et al., 1993, Redhead et al., 1997). It did not appear to enter the plasma membrane of cells as noted in *Xenopus* oocytes (Landry et al. 1993). CLIC1 was localised to the nucleus and nuclear membrane in transfected CHO-K1 cells. Very small amounts were noted in the cytoplasm and on the cell membrane (Valenzuela et al., 1997). However, a highly specific anti-CLIC1 antibody failed to detect CLIC1 in the nucleus of placental trophoblast cells, but did show CLIC1 in the cytoplasm of the cells (Berryman and Bretscher, 2000). Recently, CLIC1 localisation to membranes was shown to be accelerated by activating microglial cells (Novarino et al., 2005). CLIC3 was also noted in the nucleus and cytoplasm in transfected CV-1 cells (Qian et al., 1999).

Rat brain CLIC4 has been localised to the endoplasmic reticulum in transfected cells (Duncan et al., 1997) and later it was also localised to the membranes of large dense core vesicles (Chuang et al., 1999) and the plasma membrane (Suginta et al., 2002). Mouse CLIC4 was shown to reside in the cytoplasm and compartments of mitochondria in keratinocytes and is enriched in mitochondrial fractions of rat liver homogenates (Fernandez-Salas et al., 1999). CLIC4 and CLIC5A were localised to the apical membranes and cytoplasm in trophoblast cells (Berryman and Bretscher, 2000). In JEG-3 cells, CLIC5A was shown in the cytoplasm and in the apical membranes with distinct puncta in the plasma membrane (Berryman et al., 2004)

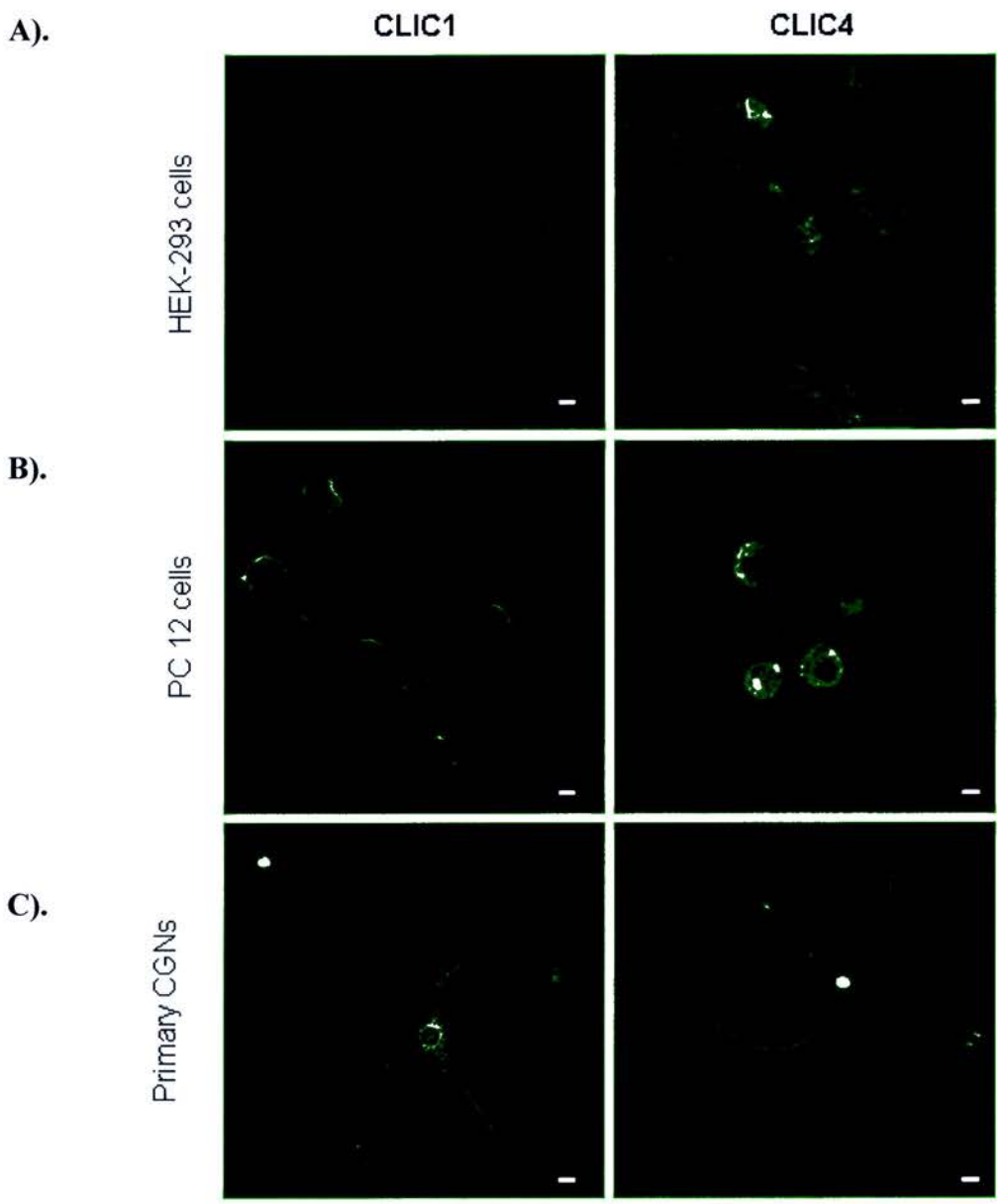

Fig. 7.4 Localisation of CLICs. Cells were stained with affinity purified anti-CLIC antibodies (1:500) and FITC labelled secondary antibody (1:10000). Scale bar indicates 10 μm. (A) Localisation of CLIC1 and CLIC4 in stably-transfected HEK-293 cells. The expression of CLIC1 and CLIC4 is very low (n=150 cells for both CLIC1 and CLIC4). (B) Native CLIC1 and CLIC4 in PC12 cells (n=25 cells). (C) Native CLIC1 and CLIC4 in primary cerebellar granular neurons (n=45 cells). In all cell types CLIC1 is localised to the cytoplasm and perinuclear spaces. Nuclear localisation was seen in some cells. The secondary antibody showed no labelling in control cells.

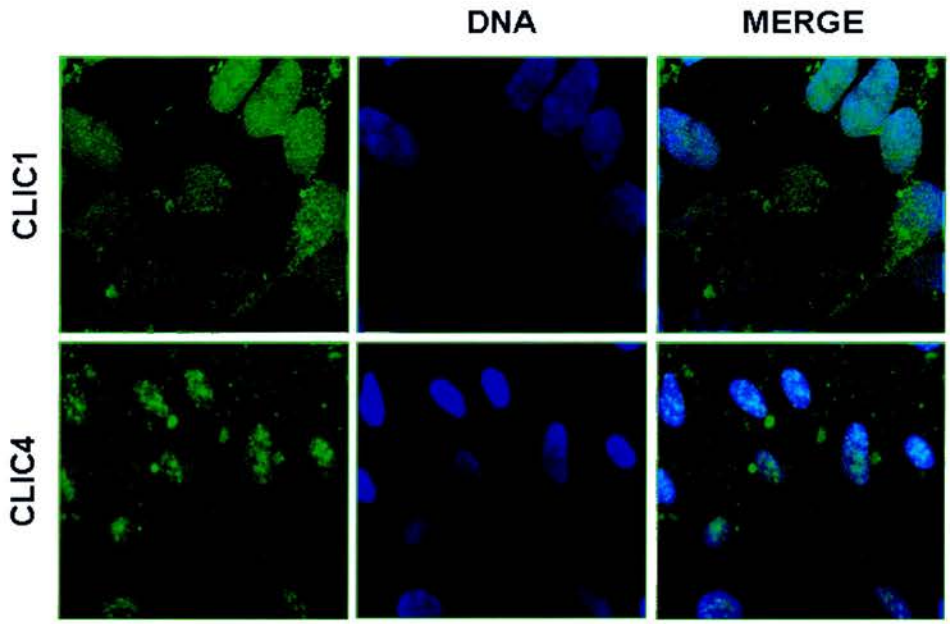

Fig 7.5 Localisation of CLIC1 and CLIC4 in HEK-293 cells. Fluorescence microscopy of stably-transfected HEK-293 cells showed the localisation of CLIC1 and CLIC4. Co-staining with DAPI showed that CLIC1 is localised to the nucleus in addition to the cytoplasm. CLIC4 was less abundant in the cytoplasm but showed a marked localisation inside the nucleus (n=30 cells for both CLIC1 and CLIC4).

and, recently, it was localised to the apical membranes in the interdental cells and columnar cells of kolliker's organ (Gagnon et al., 2006). CLIC6 was localised to the cytoplasm and perinuclear structures in transfected Cos-7 and MDCK cells (Friedli et al., 2003).

With this background information, the localisation of CLIC1 and CLIC4 was studied in stably-transfected HEK-293 and native CLICs were studied in PC-12 cells and primary cerebral granular neurons (CGNs). Even though HEK-293 cells were stably-transfected with CLIC1 and CLIC4, the expression of CLIC1 and CLIC4 was very low (Fig 7.4). It is possible that overexpressing cells were lost by apoptosis, it may be the case that only mildly-overexpressing cells survive. PC-12 cells and primary CGNs on the other hand have high concentrations of CLIC1 and CLIC4 in the cytoplasm and nucleus. Nuclear localisation was confined to some cells, and may be attributed to changes in the physiological state of these cells, such as apoptosis and cell cycling. CLIC1 and CLIC4 were present on the plasma membrane, and other intracellular membranes in all the cell types (Fig 7.4). In stably-transfected HEK-293 cells, CLIC1 was localised to the cytoplasm and nucleoplasm, but CLIC4 was localised to specific sites inside the nucleus. Expression of CLIC4 in the cytoplasm was lower than comparable expression of CLIC1 in HEK-293 cells (Fig 7.5).

7.5 Co-localisation of CLICs with other proteins

To investigate the co-localisation of native CLICs, rat brain CGNs were fixed and

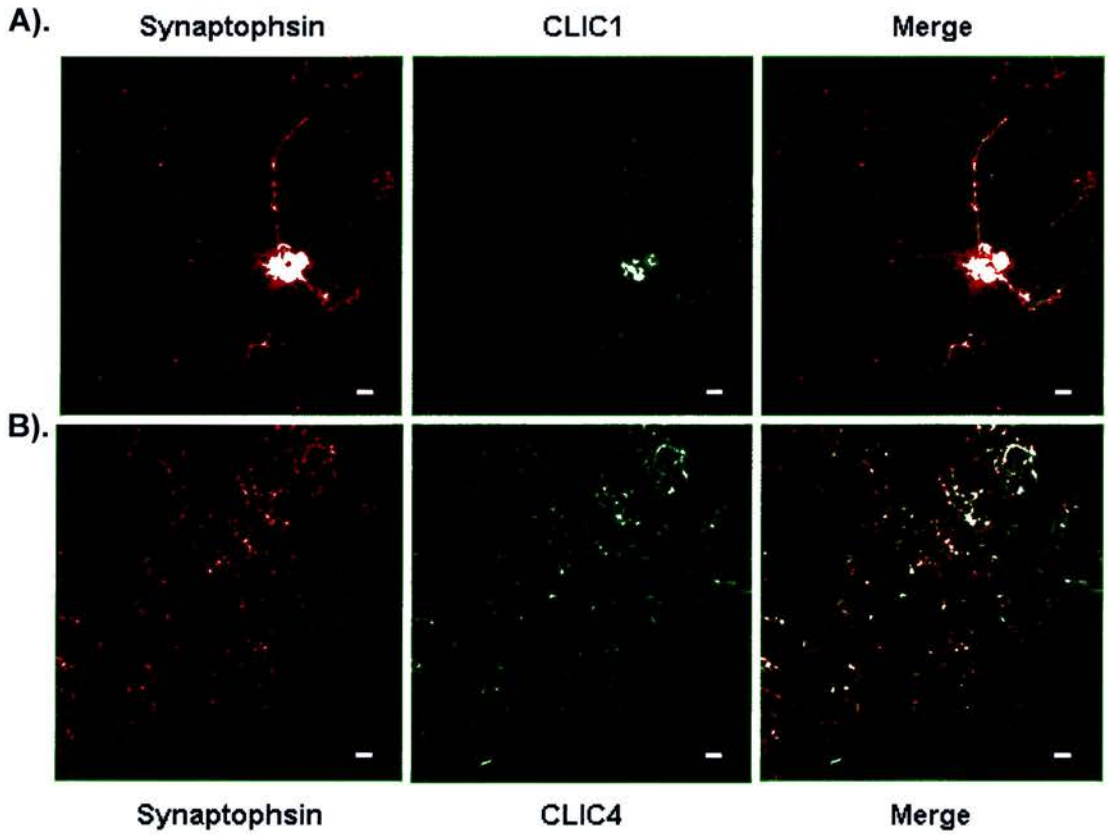

Fig 7.6 Co-localisation of CLIC1 and CLIC4 in nerve terminals in primary CGNs. CLIC1 and CLIC4 (green) were co-stained with a nerve terminal marker synaptophysin I (red). CLIC proteins were co-localised in nerve terminals with synaptophysin I (yellow). Scale bar indicates 10 μm. (A) Co-localisation of CLIC1 with synaptophysin I (n=130 cells). (B) Co-localisation of CLIC4 with synaptophysin I (n=150 cells).

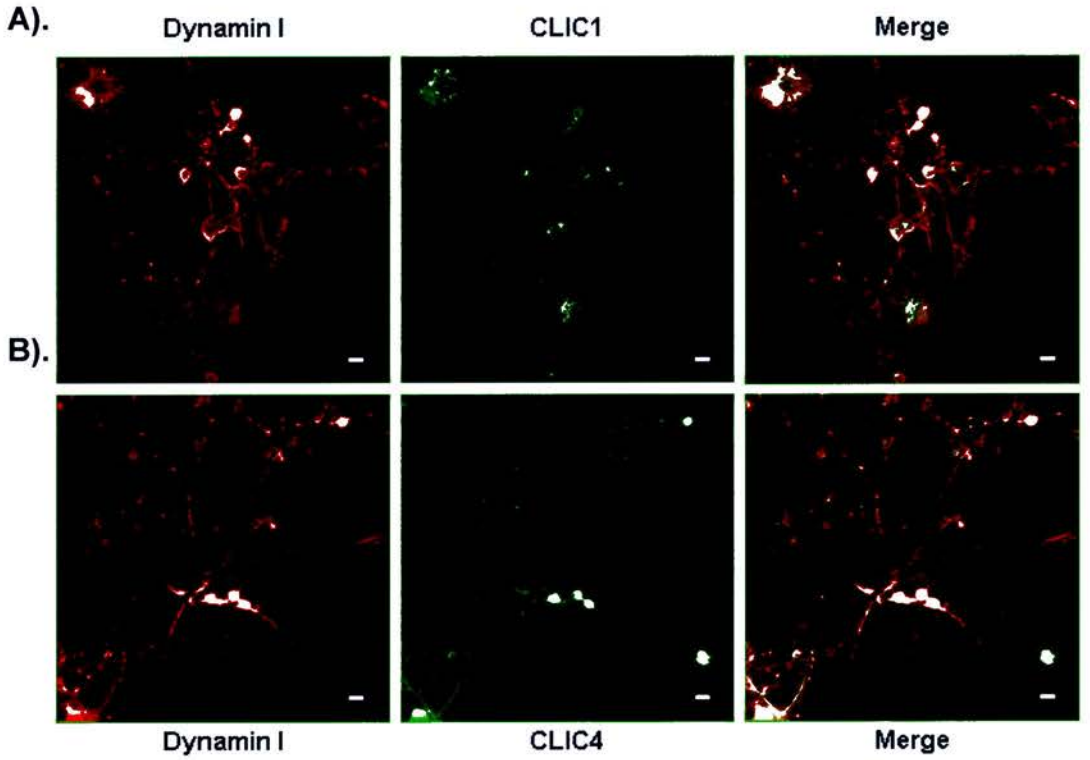

Fig 7.7 Co-localisation of CLIC1 and CLIC4 with dynamin I in cultured primary CGNs. CLIC1 and CLIC4 (green) were co-stained with dynamin I (red) to study their localisation in primary CGNs. Scale bar indicates 10 μm. (A) CLIC1 co-localises with dynamin I in the cytoplasm (n=120 cells) (yellow). (B) CLIC4 co-localises with dynamin I in the cytoplasm (n=130 cells).

co-stained with anti-CLIC1 and anti-CLIC4 antibodies with a nerve terminal marker (anti-synaptophysin I). Synaptophysin I present in synaptic vesicles provides a molecular marker for the synapse (Wiedenmann and Franke, 1985). CLIC1 and CLIC4 were colocalised with synaptophysin I in the nerve terminals and were also found in the cell body of the CGNs (Fig 7.6). Localisation of CLICs in the nerve terminal may play a significant role in synaptic vesicle recycling which needs to be elucidated. CLIC1 and CLIC4 were shown to interact directly with dynamin I both *in vivo* and *in vitro* by biochemical analysis (Chapter 7 section 7.2/3). The GTPase dynamin I has been implicated in the clathrin-mediated endocytosis of synaptic vesicle membranes at the presynaptic nerve terminal. CLIC1 and CLIC4 are also present in nerve terminals (Fig 7.6). To further establish the co-localisation of CLIC1 and CLIC4 with dynamin I, they were co-stained with dynamin I in CGNs. Both proteins showed remarkable co-localisation with dynamin I in the cytoplasm of rat brain CGNs (Fig 7.7).

CLIC4 was localised in mitochondria and was shown to be involved in apoptosis (Suh et al., 2005; Suh and Yuspa, 2005). To test the localisation of CLIC1 and CLIC4 in mitochondria, they were co-stained with a mitochondrial marker (anti-DOC2α). "Anti-DOC2α" was demonstrated to be immuno-reactive for mitochondrial complex III core protein 2 (Duncan et al., 2000). In rat brain primary CGNs, CLIC1 showed complete localisation whereas CLIC4 showed very little localisation to the mitochondria (Fig 7.8). This shows that other CLICs are also present in the mitochondria and may play a role in apoptosis as seen with CLIC4 (Suh et al., 2005).

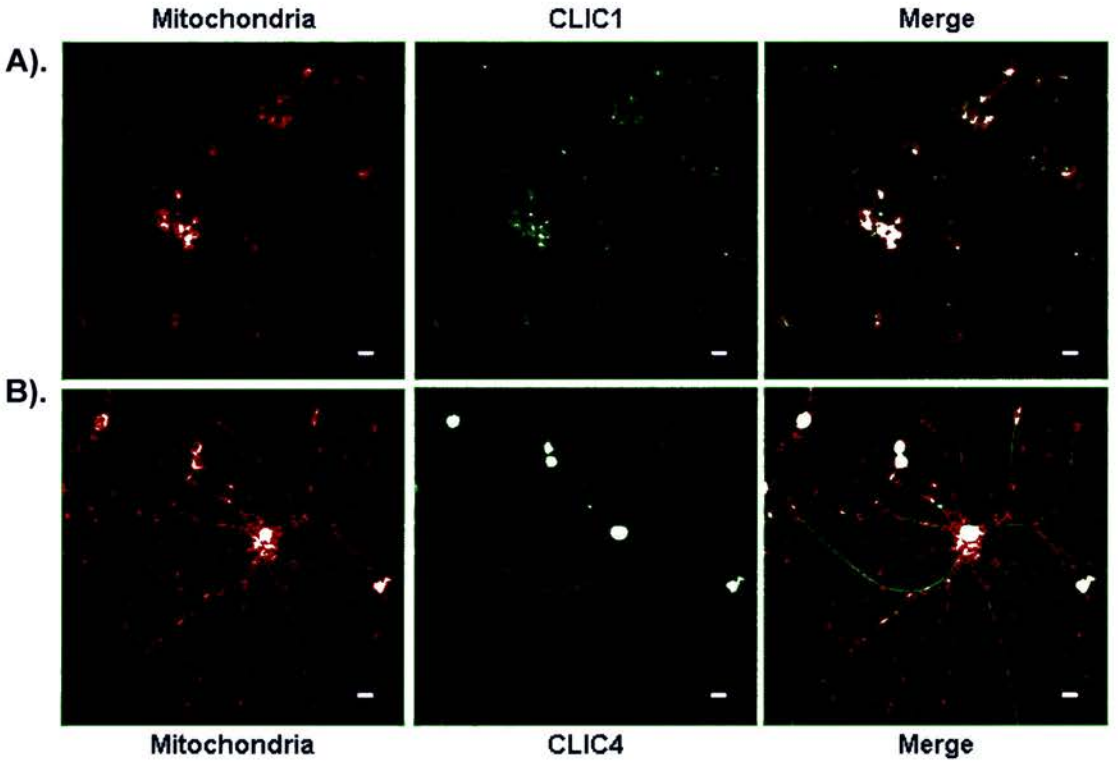

Fig 7.8 Localisation of CLIC1 and CLIC4 in the mitochondria of cultured primary CGNs. Rat brain primary CGNs were fixed and probed for CLIC1 and CLIC4 (green) in mitochondria. Anti-Doc2α was used to mark mitochondria in CGNs (red). Scale bar indicates 10 μM. (A) CLIC1 shows localisation to the mitochondria (n=125 cells) (yellow). (B) CLIC4 is localised in nucleus and cytoplasm and shows very little localisation in the mitochondria (n=140 cells) (yellow).

7.6 GFP-CLICs

In order to study the functional role of CLICs in synaptic vesicle recycling, tagged CLIC constructs were made. CLIC1 and CLIC4 were cloned in pEGFP as well as pEYFP vectors. GFP and YFP CLICs were transfected into rat brain CGNs. Unfortunately, over-expression of CLICs caused cell death (presumably apoptosis) in less than 16 hours, and hence no functional studies could be performed.

7.7 CLIC channels are inhibited by actin-polymerisation

The cytoskeleton has been shown to play a significant role in cell volume regulation. Dynamic changes in the cytoskeleton rearrangement are fundamental to most of the biological processes including embryogenesis, morphogenesis, cell movement, wound healing and cancer metastasis (Stossel, 1993). Volume regulation is linked to the selective activation of volume-sensitive K^+ and Cl^- channels, and other types of transporters (Okada, 1997).

Ion transport mechanisms in various tissues are regulated by the cortical actin cytoskeleton. Cytoskeleton elements were shown to be responsible for the localisation and clustering of channels in plasma membrane (Smith et al., 1995). Cytoskeleton rearrangement can change the specific functional characteristics of single channels (Janmey, 1998). Actin-depolymerisation or disruption by cytochalasin has been shown to activate amiloride-sensitive sodium channels (Cantiello et al., 1991), volume-regulated Cl^- channels (Schwiebert et al., 1994) and

ATP-sensitive K^+ channel activity (Terzic and Kurachi, 1996), whereas, K^+ channels in the rat cortical collecting duct are inhibited by actin depolymerisation (Wang et al., 1996). The non-voltage-gated sodium channels of leukaemia cells were activated by cytochalasin D and gelsolin, which interact with actin, and inactivated by actin-polymerising agents (Negulyaev et al., 2000; Shumilina et al., 2003).

Increasing lines of evidence indicate that cytoskeletal filaments have a significant role in regulating CLIC proteins (Berryman et al., 2004). These interactions may be direct (CLIC4 with dynamin I) (Suginta et al., 2001) or indirect (CLIC5A and actin) (Berryman et al., 2004) with no specific functions attributed to these interactions. To test the effect of actin polymerisation on CLIC channels, CLIC1, CLIC4 and CLIC5A were reconstituted in 5 mM GSH. G-actin (2 μg or 22 μM) was polymerised in the *cis* and *trans* chambers with KCl (100 mM), $MgCl_2$ (5 mM) and ATP (0.5 mM). G-actin polymerises when its concentration exceeds the critical concentration (CC), which is 0.03 mg/ml in the presence of Mg^{2+} (2 mM) and KCl (50 mM) and 3 mg/ml in absence of these ions. Bovine serum albumin (100 μg/ml) was added before the addition of G-actin to block non-specific protein binding sites in the plastic chambers. There was no effect from BSA or actin polymerising agents on CLIC1, CLIC4 and CLIC5A channels in the absence of G-actin. The data were plotted as the mean current from 60 s long traces. It was found that the addition of G-actin to the *cis* or *trans* chambers in the absence of actin polymerising agents did not affect CLIC1, CLIC4 and CLIC5A channels. In contrast, when G-actin was polymerised on the *cis* but not the *trans* side, CLIC1 and CLIC5A channel currents were abolished ($P < 0.0001$). There was no effect on the conductance or open

A).

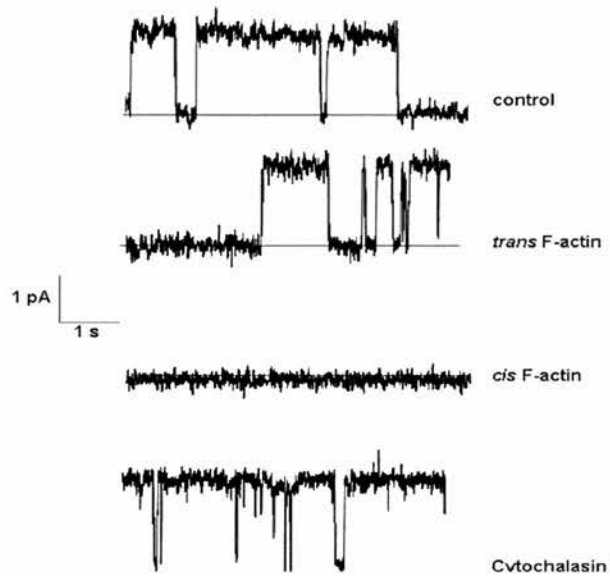

B).

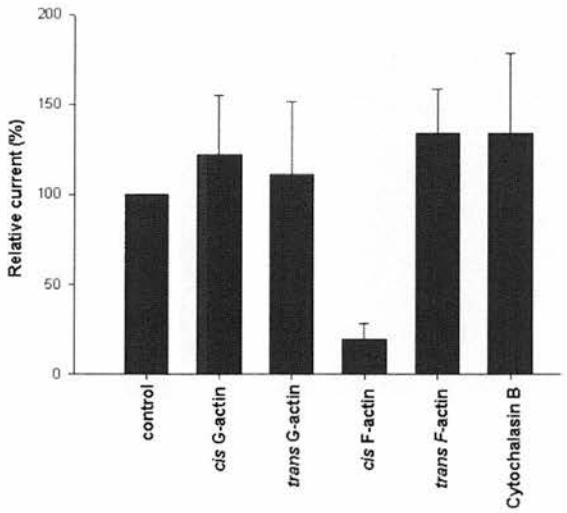

Fig 7.9. CLIC1 channels blocked or inhibited by *cis* actin polymerisation. (A) Single-channel currents showing the effect of actin polymerisation (n=7). After the addition of 10 μM cytochalasin B to the F-actin inhibited-CLIC1 channels (n=7), channel activity is similar to the original control traces (n=5). The solid lines indicate the closed levels (B) Histogram summarising the effect of *cis* actin polymerisation on CLIC1 channels. Mean current from 60 s long traces were analysed as described in the text. There was no effect on CLIC1 channels of *cis* G-actin, *trans* G-actin, or *trans* F-actin (mean ± SD, n = 5 to 7).

A).

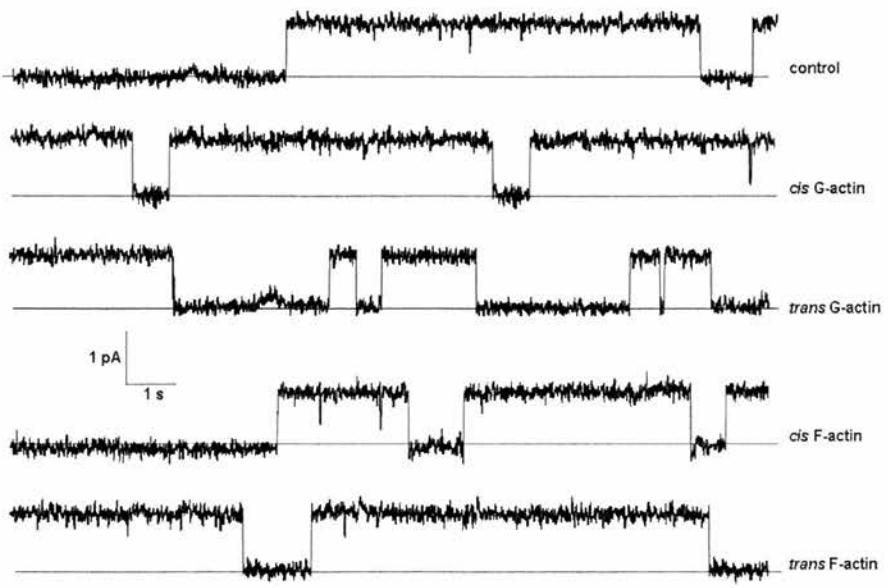

B).

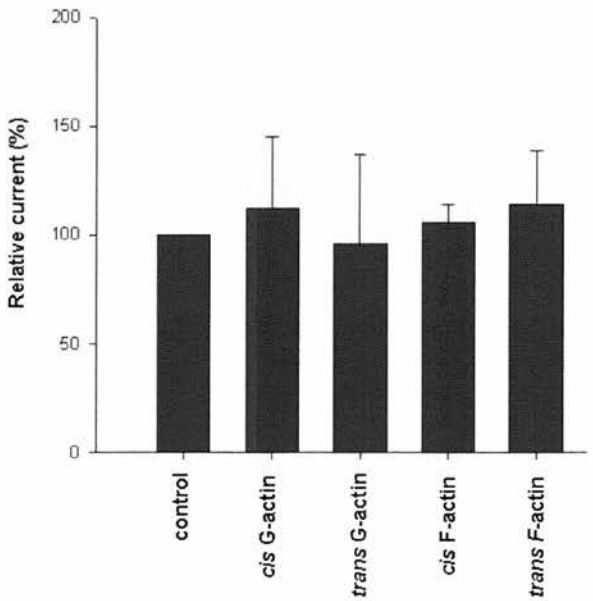

Fig 7.10 CLIC4 channels are not blocked or inactivated by *cis* actin polymerisation. (A) Single-channel currents showing CLIC4 channels. The solid lines indicate the closed levels (B) Histogram summarising CLIC4 mean currents from 60 s long traces. There was no effect on CLIC4 channels of *cis* G-actin, *trans* G-actin, *cis* F-actin or *trans* F-actin (mean ± SD, n=4 to 6).

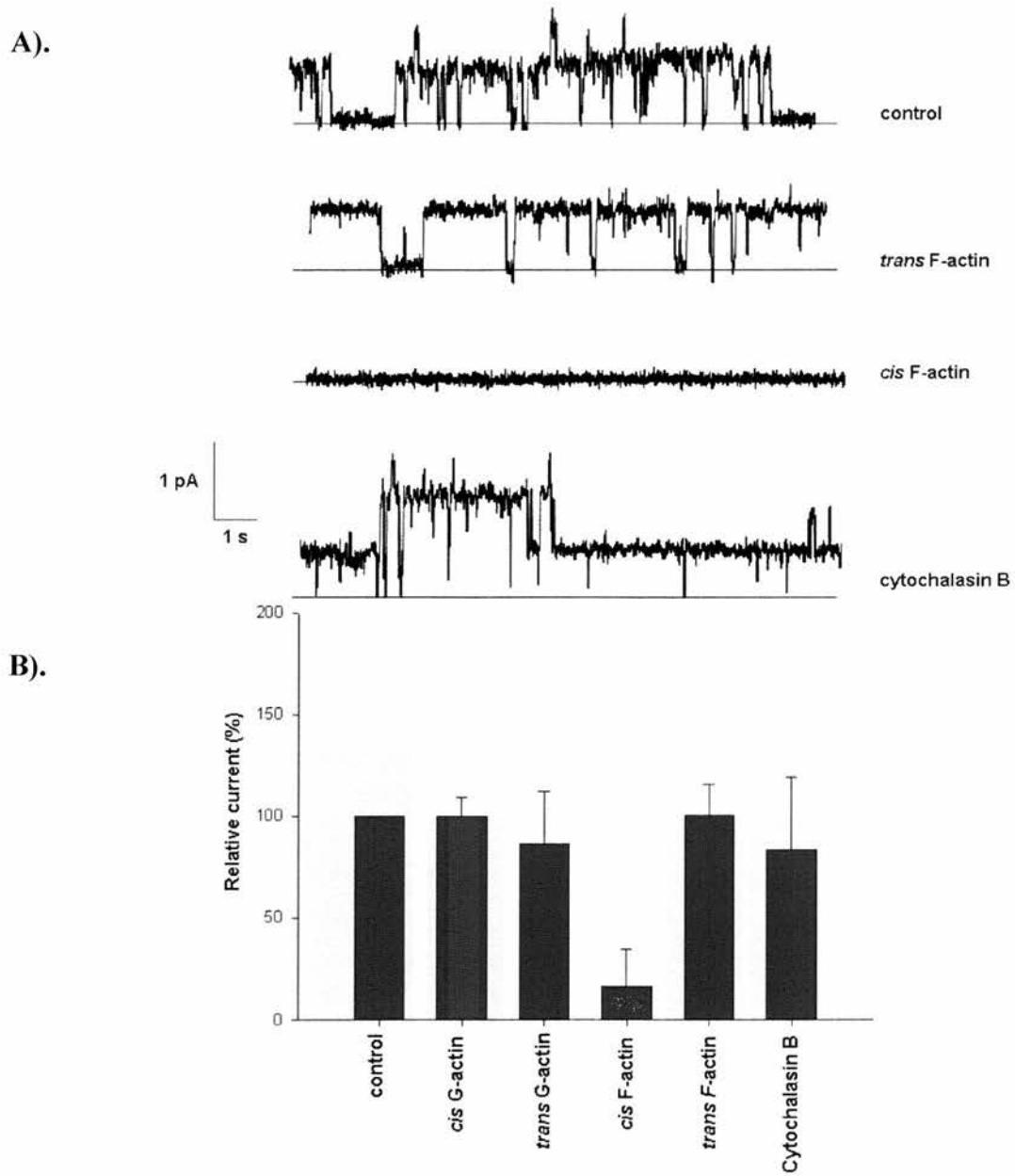

Fig 7.11 CLIC5A channels are blocked by *cis* actin polymerisation. (A) Single-channel currents showing the effect of actin polymerisation. After the addition of 10 μM cytochalasin B to the CLIC5A channels inhibited by F-actin, the channel activity is similar to the original control traces. The solid lines indicate the closed levels (B) Histogram summarising the effect of *cis* actin polymerisation on CLIC5A channels. There was no effect on CLIC5A channels of *cis* G-actin, *trans* G-actin, and *trans* F-actin (mean ± SD, n= 7 to 9 experiments).

probability of CLIC4 channels. Figs 7.9, 7.10 and 7.11 summarise the inhibition or block of CLIC1 and CLIC5A channels by *cis* not *trans* actin polymerisation but CLIC4 channels remained unaffected.

To disrupt F-actin, 10 μM cytochalasin B was added to the *cis* chamber. There was no effect of cytochalasin B alone on CLIC1 (Fig 7.9), CLIC4 (Fig 7.10) or CLIC5A (Fig 7.11) channels in the absence of F-actin. On addition of cytochalasin B to CLIC1 (Fig 7.9) and CLIC5A (Fig 7.11), channels were blocked or inhibited by F-actin, the effect of actin polymerisation was reversed and there was no significant difference between the mean conductance of CLIC1 and CLIC5A channels ($P < 0.001$) compared to mean control currents. This suggests that actin polymerisation on the cytosolic side of the cell may be a factor regulating the activity of the CLIC1 and CLIC5A channels but not CLIC4 channels (Fig 7.10), and it appears that the interaction of F-actin with CLIC1 and CLIC5A is direct, without any adaptor molecule(s).

7.8 Regulation of CLIC1 and CLIC4 by actin-polymerisation in HEK-293 cells

Actin polymerisation contributes significantly to the regulation of CLIC1 and CLIC5A, but not CLIC4 channels, from the luminal side *in vitro*. CLIC5A was shown to interact with F-actin in an ezrin-bound complex (Berryman et al., 2004), but CLIC4 was not pulled down in a pelleting assay (Suginta et al., 2001). CLIC1 on the other hand interacted directly with F-actin *in vitro* in bilayers. These interactions

were further tested and verified *in vivo* in preliminary experiments using HEK-293 cells.

CLIC1 and CLIC4 stably-transfected HEK-293 cells were studied in order to test the regulation of CLICs by actin polymerisation. Whole-cell currents from stably-transfected HEK-293 cells were recorded and analysed. Stably-transfected HEK-293 cells were incubated in bath solution for 30 mins and currents were recorded in 5 mM GSH. Channels were subjected to an increase in the redox potential from the luminal side by increasing the concentration of GSSG in the bath solution. As reported in chapter 5, increase in the luminal redox-potential decreased the apparent conductance of CLIC1 and CLIC4 as shown in Fig 7.13. This effect was fully-reversible on reperfusion with 5 mM GSH buffer. On addition of cytochalasin B to the bath solution, the CLIC1 channel currents increased significantly by 10 fold in CLIC1-transfected HEK-293 cells. In non-transfected HEK-293 cells and CLIC4-transfected HEK-293 cells this increase was 5 fold. This increase may be attributed to the low expression of native CLIC1 in non-transfected HEK-293 as well as CLIC4-transfected HEK-293 cells. These preliminary data were very limited (maximum of 5 experiments), hence no statistical analyses were carried out. Interestingly, in some experiments, changes in redox potential appeared to induce different patterns of rectification. Again, this was not investigated in detail in these preliminary experiments.

7.9 Discussion

CLIC4 was shown to be present in LDCV by immunoelectron microscopic analysis

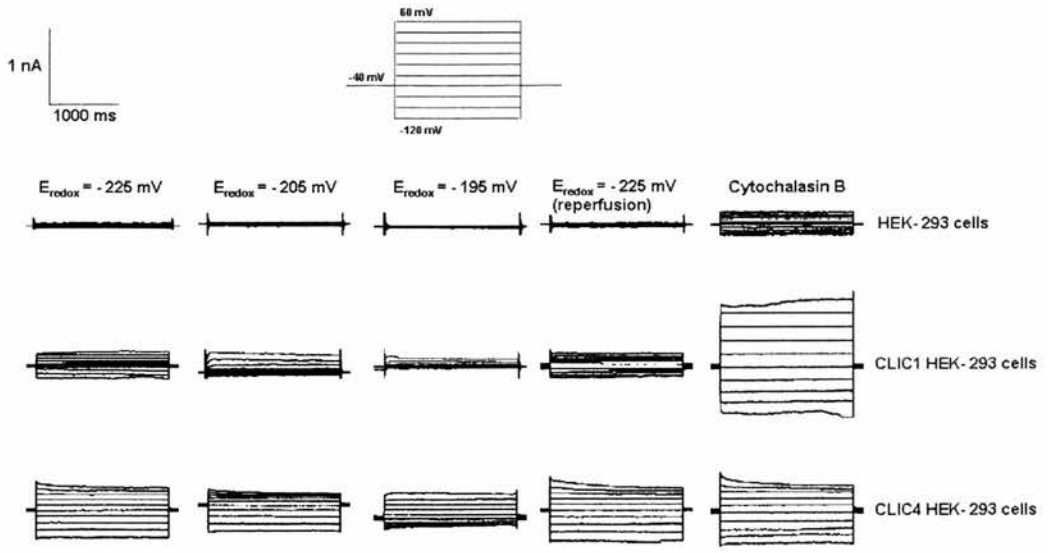

Fig 7.12 CLIC whole-cell currents in HEK-293 cells. In preliminary experiments, whole cell currents in CLIC1-transfected HEK-293 cells appeared to increase when 5 μM cytochalaisn B was added to the bath solution (n=3). There was no increase in the whole cell currents in HEK-293 cells transfected with CLIC4 (n=3). Whole cell currents in CLIC1- and CLIC4-transfected HEK-293 cells decreased when the redox potential was increased from -225 mV to -195 mV on the luminal side (bath) of the channels (n=3). This effect was reversed when the redox potential was decreased to -225 mV by reperfusion of 5 mM GSH/GSSG (10:1) buffers (n=3). In the case of HEK-293 cells stably transfected with CLIC4, there was also a change in rectification on luminal oxidation.

and immunoblotting (Chaung et al., 1999). This result suggested that CLIC4 may be involved in the acidification of LCDVs. Acidification is an active process in which H^+ is pumped into the endosomal lumen. The charge should be balanced by either outward movement of cations such as K^+ and/or inward movement of anions such as Cl^-. Ion substitution, inhibitor, and endosomal pH/Cl^- measurements indicate that Cl^- is a principal ion responsible for balancing the positive potential produced by active H^+ entry. It has been proposed earlier (without any evidence) that intracellular chloride channels are responsible for some or all endosomal Cl^- conductance in many cell types. Localisation of CLIC1 and CLIC4 to synaptosomes in this chapter can be linked to the acidification of synaptic vesicles.

The association of CLIC1 and CLIC4 with the PRD of dynamin I suggests that they may be playing a significant role in SV trafficking. The exact mechanism of SV trafficking to the active zone has not been resolved yet. Dynamin I has been shown to participate in the fission of synaptic vesicle during endocytosis. GTPase activity (Urrutia et al., 1997) and conformational changes induced by GTP hydrolysis are essential for the fission (Marks et al., 2001). The C-terminus of CLIC1 and CLIC4 channels has a potential motif recognised by SH3-domain proteins (Ashley, 2003). SH3 domains are commonly found in proteins associated with endocytosis. Hence, CLIC1 and CLIC4 (and other CLIC proteins) could be playing a significant role in SV vesicle recycling either with or without the mediation of dynamin I. Fluorescent microscopy showed that CLIC1 and CLIC4 are expressed and localised in the nerve terminals of primary CGNs. They were also shown to be co-localised with dynamin

I. These biochemical and colocalisation studies further provide the evidence that CLIC1 and CLIC4 are playing an important role in nerve terminals.

Several studies have revealed localisation of CLICs in the cytosol and membranes. CLIC4 was earlier shown to be present in mitochondria where it plays an important role in apoptosis (Fernandez-Salas et al., 2002; Suh et al., 2004). In this chapter, CLIC1 was shown to be localised to mitochondria as well. The localisation to the nucleus depends on the physiological state of the cell, as localisation to the nucleus was confined to only in 10% of the cells. A critical amount of CLIC proteins is required to maintain the physiological state of the cell. Overexpression or knocking down CLIC4 caused apoptosis. Therefore, the level of protein expression and localisation to specific organelles must be tightly regulated.

The actin cytoskeleton has been implicated in ion transport, cell volume regulation and in several stages during the endocytosis process including deformation of the membrane, force generation of the fission reaction, SV detachment from the plasma membrane and trafficking of the newly formed SVs to the recycling pool (Levina et al., 1994; Smith et al., 1995; Lamaze et al., 1997; Qualmann et al., 2000; Gundelfinger et al., 2003). CLIC5A was earlier shown to indirectly associate with actin in apical trophoblast (Berryman and Bretscher, 2000). The regulation of CLIC1 and CLIC5A but not CLIC4 channels by actin polymerisation demonstrates a novel mechanism of channel modulation. Disruption of the actin cytoskeleton activates CLIC1 channels but not CLIC4 channels in stably-transfected HEK-293 cells. These results show that CLIC1 and CLIC5A can be regulated by volume

changes (involving disruption of the actin cytoskeleton). It implies that CLIC1 and CLIC5A channels are not completely active in normal physiological conditions and are activated when cells undergo physiological changes such as swelling, cell division or apoptosis. Redox-regulation of CLIC1 will be more significant when actin cytoskeleton is disrupted.

It can be speculated that CLIC1 and CLIC4 (and other CLIC proteins) might be associated with redox-sensitive ion channels in cells. They may be involved in redistribution of channel-containing vesicles during vesicle trafficking, including membrane redistribution and retrieval associated with actin-mediated changes in cell shape. Destabilisation of the actin cytoskeleton during the cell cycle and apoptosis or cell swelling could involve the activation of CLIC1 and CLIC5A channels.

CHAPTER 8

DISCUSSION

8.1 Introduction

In the late 1980s, when intracellular anion channels studies were gathering momentum after being sidelined for more than 50 years, p64 was isolated and purified with a molecular mass of 64 kDa (Landry et al., 1989; Landry et al., 1993). Its cDNA was cloned in 1993 (Redhead et al., 1992) and found to encode a protein of 437 residues. p64H1 was the first p64 (CLIC5B) homologue to be identified at the molecular level (Duncan et al., 1997). The first human homolog of p64 was called NCC27 (Nuclear Chloride Channel-27) due to its presence in the nucleus of a monocyte-derived cell line, and it was later renamed CLIC1. The CLIC nomenclature was suggested by Heiss and Poutska (1997) and Edwards (1999).

CLICs have approximately 240 residues and are distantly related to Ω-GSTs (Dulhunty et al., 2001). They are expressed in wide varieties of tissues in multi-cellular organisms and are shown to localise to the plasma membrane (Tonini et al., 2000; Money et al., 2006), Golgi membrane (Shanks et al., 2002), inner mitochondrial membrane (Fernandez-Salas et al., 1999), the nuclear membrane (Valenzuela et al., 1997; Tonini et al., 2000), dense core vesicles (Chuang et al., 1999), lysosomal membranes, cell-cell junctions (Berryman and Goldring, 2003) and the luminal membrane of the excretory canal (*Caenorhabditis elegans*) (Berry et al., 2003). CLICs were shown to be regulated in bone resorption (Schlesinger, et al., 1997), and involved in regulation of cell motility (Ronnov-Jessen et al., 2002), apoptosis (Fernandez-Salas et al., 1999; Fernandez-Salas et al., 2002; Suh

et al., 2004; Suh et al., 2005), β-amyloid induced neurotoxicity (Novarino et al., 2004) and tubologenesis (Berry et al., 2003; Berry and Hobert, 2006).

Several lines of evidence indicate that CLICs can span the membrane an odd number of times (Tonini et al., 2000; Proutski et al., 2002) and form functional ion channels in transfected cells and planar bilayers (reviewed by Ashley, 2003). The regulatory mechanisms and functions of CLIC proteins as ion channels *in vivo* are yet to be elucidated. Six mammalian CLICs have been identified so far, and they might have functional overlaps or distinct functions. The Invertebrate CLIC, EXC-4, was shown to be responsible for tubulogenesis (Berry et al., 2003), but it not clear whether mammalian CLICs have similar functions. The molecular functions of soluble CLIC proteins are not well understood at either its biochemical or physiological levels.

8.2 Channel formation is lipid-dependent

CLICs share structural homology with Ω-GSTs but have distinct functions. Ω-GSTs are soluble proteins that are not associated with ion channel activity (Dulhunty et al., 2001). CLIC1 and CLIC4 (and other CLICs) can insert into monolayers containing different lipids or lipid mixtures, but consistent channels were always obtained in well-defined planar bilayers containing POPE, POPS and cholesterol in the molar ratio 4:1:1. No consistent channels were obtained in any other lipid mixtures tested in this thesis (Table 4.2).

CLIC4 was previously localised to specific cholesterol-rich domains of membranes like caveolae (Suginta et al., 2001). Caveolae, cholesterol and sphingolipid-rich surface microdomains abundant in most cell types, are flask-shaped plasma membrane invaginations involved in the endocytosis of glycosphingolipids, glycosylphosphatidylinositol-anchored proteins, bacterial toxins, non-enveloped viruses and extracellular ligands (Pelkmans and Helenius, 2002; Nabi and Le, 2003). Membrane cholesterol regulates pore-formation of many channel toxins (Palmer, 2004) and facilitates oligomerisation (Olson and Gouaux, 2005). The free cholesterol content of the membrane caveolae controls signal transduction to the nucleus, regulates signal traffic in response to extracellular stimuli, and exerts an influence on cell growth, division, adhesion and hormonal response (Fielding and Fielding, 2000).

Channel formation in cholesterol-rich bilayers suggests that CLICs may only be functional in caveolae or specific cholesterol-rich microdomains in membranes. These domains may facilitate the insertion and proper refolding of the proteins to form functional channels, indicating a possible role in the refolding of CLIC proteins. Alternatively, the presence of cholesterol might be essential to maintain the correct lipid order of the membrane.

Membrane rafts are proposed to form platforms for receptor-mediated processes like signal transduction, and are an ideal docking site for protein kinases (Pichler and Riezman, 2004), with possible implications for CLICs localised to these cholesterol-rich domains.

8.3 Single-channel properties of CLICs

After the elucidation of the crystal structure of the KcsA K^+ channel (Doyle et al., 1998), ClCs are the only other selective ion-conducting protein with a known membrane structure (Dutzler et al., 2002). ClC channels have a broad range of physiological functions (Jenstch et al., 2002), but very limited information is available for CLIC proteins. Recent observations in cochlear and vestibular hair cells (Gagnon et al., 2006), human placenta (Money et al., 2006), and microglia (Novarino et al., 2004) strongly support the idea that CLICs have significant roles in the functions of the cells. CLIC1, CLIC4 and CLIC5B can autoinsert into bilayers and have channel-like activities (Table 4.1). CLIC1 was recently shown to form channels in microglia cells (Novarino et al., 2004), but the mechanism of channel formation and the membrane structure of CLICs is undetermined. Much like CLIC proteins, bacterial toxins and porins (Parker and Pattus, 1993), the eukaryotic proteins, Bcl-2 and Bax (Schendel et al., 1998), and a voltage-dependent anion channel (Colombini, 1989), are synthesised as soluble proteins and insert post-translationally into the membranes from a soluble pool.

In our experiments, CLIC1 and CLIC4 formed non-selective channels whereas CLIC5A formed cation-selective channels in planar bilayers. They all had substates which shared the same selectivity as the main open level; however CLIC5A channels had several complex conductance levels. This evidence that CLIC1, CLIC4 and CLIC5A can autoinsert and span the membrane to form well-defined consistent channels when proteins were added to only one side of the

membrane supports the prediction that CLIC proteins can form ion channels *in vivo* under specific conditions. The substate behaviour of CLIC proteins is similar to anion channels reconstituted from rat brain microsomes (Clark et al., 1997) and sheep heart inner mitochondrial membrane vesicles (Hayman et al., 1993; Hayman & Ashley, 1993). This is consistent with the presence of minimum of four conducting "protomers" displaying different gating cooperativities depending on the number of protomers open at a given instant (Fig 8.2). The large-conductance of CLIC5A suggests that cross-linked multiple protomer complexes of functional CLIC5A channels will have a relatively large mass (> 1,000,000 daltons) and cross-linked complexes of membrane forms of CLIC1 and CLIC4 may have a molecular mass of approximately 450,000 daltons. The previously-recorded large conductances of CLIC1 channels could be attributed to the association of groups of highly cooperative subunits into larger complexes.

CLICs form multi-ion channels (Hille, 1984), as demonstrated by the dependence of relative anion selectivities (by reversal potential) on ionic activity, the non-hyperbolic relationship between conductance and activity (for CLIC1 and CLIC4), and the reduction in currents at high ionic activities. CLIC1 and CLIC4 channels are non-selective, and CLIC5A forms cation-selective ion channels in bilayers. The selectivity for anions improves when the size of the cation is increased. CLIC channels are poorly-selective between anions and cations, and the widely accepted "CLIC" nomenclature may need to be re-evaluated. The poor-selectivity can be attributed to a wide pore lacking specific ion-binding sites, but the maximum conductances of CLIC1 (36 pS), CLIC4 (15 pS) and CLIC5A (78

pS) in KCl are inconsistent with a wide water-filled pore (like bacterial-porins). Similar behaviour was observed in the neuronal "background" Cl^- channels, where it was suggested that anions and cations crossed the membrane as counter ions (Franciolini and Nonner, 1994a; Franciolini and Nonner, 1994b). A model for the pore-region was described in chapter 6. The pore region consists of the putative TMD and requires minimum of four subunits as they have only single TMD. The C-terminus also plays a crucial role in maintaining the selectivity and conductance of the channel. Strong oxidation of soluble CLIC1 induces conformational changes due to intramolecular disulphide bond formation (Littler et al., 2004) but a similar mechanism in CLIC4 is not possible due to the absence of the cysteine residue equivalent to C59 of CLIC1 (Littler et al., 2005). Hence, the pore-lining region of CLIC4 and CLIC5A (and other CLICs) remain the same irrespective of oxidation and reduction.

8.4 Identification of pore-forming region

To understand how ion channels facilitate the passage of ions across the bilayer, protein architecture and shape, and how these shapes are related to the passageway across the bilayer need to be studied. It has been established that K^+ and Cl^- channels are multiion pores, which use the mutual repulsion between neighbouring ions to lower the barriers for ions diffusing through the channel (Zhou and Mackinon, 2003). The recent ClC study has suggested multiion pores, also true of CFTR, but this is not obvious in the ClC crystal structure of a Cl/H transporter where a crucial Asp residue acts as a "gate" in the pore. Eukaryotic

channels lack this gate, and act as true channels. The binding sites of K^+ channels are not fully occupied, but the ClC Cl^- selectivity filter is always fully occupied by 3 Cl^- ions (Lobet and Dutzler, 2006). K^+ channels and Cl^- channels have a different molecular framework for selective ion channel proteins.

The pore-forming region of CLIC proteins has not previously been identified. On the basis of Kyte-Doolittle hydropathy analysis and sequence alignments, a single hydrophobic region was identified in the N-terminus region of CLIC proteins. This hydrophobic region contains a predicted TMD following the first conserved cysteine residue in all of the mammalian CLIC proteins. A helical wheel alignment of four subunits reveals two distinct rings of positively charged residues at the neck and the bottom of the putative pore. The arginine and lysine residues lining the pore region could bind to anions and provide an opportunity for counter ions to cross the membrane without encountering repulsive forces. Larger cations will not be able to pass through the pore, and hence selectivity for anions in the presence of large cations will improve.

The possibility for N-terminus of CLICs giving rise to channels was explored in Chapter 5. Truncated CLIC1 and CLIC4 proteins, containing intact N-terminus, putative TMD and the only conserved cysteine residue provided evidence that the transmembrane domain can autoinsert and form functional channels in bilayers. The conductance of the truncated channel was reduced compared to the full-length protein. This reduction is consistent with the idea that the missing C-terminus forms a charged channel vestibule that concentrate permeant ions near

the entrance to the pore (*cf* Brelidze et al., 2003). The all α-helical, C-terminus half of CLIC proteins contains few residues of known function. A well-conserved aspartic acid after h6 is conserved in GST enzymes, and is thought to function as a buried residue playing an important role in protein folding (Wilce et al., 1997). This region could be involved in protein folding after the insertion of protein into the membrane. In EXC-4, the N-terminus region (comprising first 66 amino acids) was shown to be responsible for targeting the protein to the luminal membrane, and the putative TMD is a required component for functional specificity (Berry et al., 2003; Berry and Hobert, 2006).

8.5 Redox-regulation of CLIC channels

Direction of many cellular processes depends on the redox-state of the cell. Redox-state is linked to set of redox couples found in a biological fluid, organelle, cell, or tissue. The redox-state of the cell is measured as the total 2GSH/GSSG content which varies within the intracellular compartments. Mitochondria have 5-11 mM GSH whereas its concentration is much less than 1 mM in extracellular environment. In contrast to mitochondria or nucleus the GSH/GSSG ratio in ER is 1:1 (mol/mol) as compare to >30:1 (mol/mol) (upto 100:1) in the cytosol (Schaffer and Buettner, 2001). The redox-potential in normal cells is above -240 mV which changes with the physiological state of the cell (Fig 8.1).

Many proteins contain sulphydryl groups (PSH) due to their cysteine content. The concentration of PSH is much higher than the concentration of GSH in the

cytosol. Protein refolding studies have revealed that disulphide bond formation and rearrangement are reversible thiol-disulphide (SH-SS) exchange reactions affected by the redox state of the environment. Most of the naturally-occurring amino acids in proteins can be oxidised, however, only the oxidation of cysteine and methionine is readily reversible. Oxidised cysteine can be easily reduced back by reducing agents such as DTT, or GSH buffers. A small fraction of cysteines in proteins can be divided into two subgroups: free cysteine (Cys-SH) and disulphide-bonding half cysteine (Cys-SS). The intracellular environment is maintained in the reduced state which prevents the formation of disulphide bonds in intracellular proteins (Poulsen and Ziegler, 1977), and are extensively found in the extracelullar proteins. The oxidation of proteins has been linked to both aging and neurodegenerative diseases (Finkel and Holbrook, 2000; Vignols et al, 2003). However, the exact mechanism by which oxidation affects enzymatic activity and signal transduction processes is poorly understood.

CLIC proteins are homologs of Ω-GSTs, but Ω-GSTs remain soluble and have no ion channel activity. Ω-GSTs have weak GSH-dependent thioltransferase activities (Cromer et al., 2000). It has been speculated that this could involve transfer of thiol, between GSH bound at the G-site and S-thiolated substrates in an adjacent ligand-binding site (H-site). CLICs do not have enzymatic activity, but the putative TMD is preceded by a Ω-GST-like "G-site" cysteine residue, in a cysteine-proline motif. An increase in redox potential from the luminal side of CLIC1 and CLIC4 channels decreases the apparent channel conductance. The

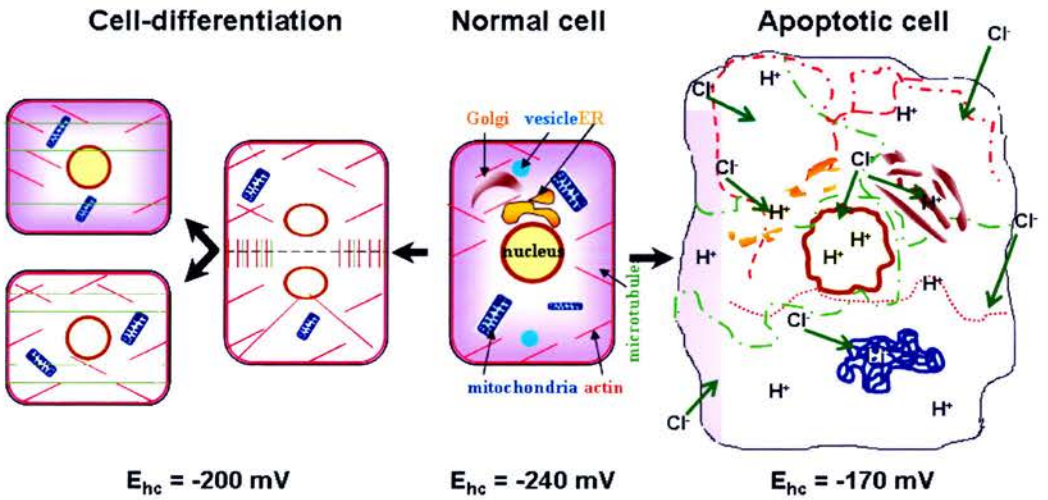

Fig 8.1 Physiological states of eukaryotic cells. Cells in their normal physiological state have a stable membrane and intracellular organelles. Ionic homeostasis in the cell and several cellular compartments are maintained. Redox-potential of a normal cell (cytoplasm) is between -240 mV and -260 mV, which changes depending on the physiological state of the cell. At -200 mV cells undergo differentiation and above -170 mV apoptosis. Mislocalisation and changes in expression of intracellular chloride channels can change the chloride contents and alter pH in cell and intracellular compartments. One consequence of high chloride ion flux into the cytosol or intracellular organelles is acidification of the cell environment, sequentially causing swelling, cell-blebbing, membrane breakdown, shrinkage, fragmentation of intracellular organelles and disintegration of cytoskeleton structures. Similarly, expression of Cl^- currents is cell-cycle dependent. In the cell-cycle, cytoskeleton structures undergo disintegration and reformation. Cell organelles are colour coded; nucleus (yellow), ER (gold), Golgi (brown), mitochondria (blue), vesicle/lysosome (light blue), microtubule (green) and actin (red).

redox potential was altered by changing the ratio of GSH/GSSG in the buffer. The GSH/GSSG ratio differs within the cell and it is around 30:1 in skeletal muscle cytoplasm (Hidalgo et al., 2004), where the activity of RyR1 channels is affected by redox potential (Oba et al., 2002b).

Trans redox-regulation of CLIC1 and CLIC4 suggested that at least one of its cysteine residue might be functionally important (Fig 8.2). This idea was further supported by *trans* NEM and *trans* DTNB block of CLIC1 and CLIC4 channels, respectively. The orientation of the channels was further supported by *trans* Ni^{2+} block of CLIC1 channels. On mutating C24 from CLIC1 *trans* redox regulation and *trans* NEM block were abolished, indicating that C24 plays a crucial role in redox-regulation of CLIC proteins from the luminal side. This residue is conserved in all the mammalian CLICs. The single-channel conductance of CLIC1 was reduced when C24 was mutated to alanine and was eliminated on mutation to serine (Littler et al., 2005). Full-length and truncated CLIC proteins retained this *trans* redox regulation mechanism suggesting that this novel mechanism plays a significant role in regulation of CLIC channels in cells. Preliminary experiments in stably-transfected HEK-293 cells further supported this novel *trans* redox regulation mechanism, suggesting it may be worthy of further study in future work at the cellular level.

8.6 Regulation of CLICs by F-actin

Cells undergo rapid remodelling of their actin cytoskeleton networks to regulate critical processes like endocytosis, cytokinesis, cell-polarity and cell-

morphogenesis. It is disrupted during apoptosis and during the cell-cycle (Fig 8.1). The cortical actin cytoskeleton controls ion transport mechanisms in several tissues and cells. It changes the distribution and localisation of ion channels, and results in changes in the functional characteristics of single channels. CLIC5A was shown to interact with F-actin in an ezrin-bound complex (Berryman and Bretscher, 2000). However, there was no evidence of direct interaction of CLIC5A and F-actin. CLIC4 on the other hand was shown to directly interact with dynamin I and tubulin, but could not be shown to interact directly with F-actin (Suginta et al., 2001). Work was carried out to investigate the consequence of this interaction of actin with CLIC proteins.

In planar bilayers, CLIC1 and CLIC5A but not CLIC4 were blocked or inactivated by *cis* actin polymerisation without any adapter molecule (Fig 8.2). This effect was fully reversible on addition of actin-destabilising compounds such as cytochalasin B. In stably-transfected HEK-293 cells, CLIC1-associated currents increased significantly when cytochalasin B was added but there was no significant change in the whole cell currents associated with stably-transfected CLIC4 HEK-293 cells. This is a novel mechanism of CLIC1 and CLIC5A regulation in cells and may further establish the link between functional roles of CLICs in the cell cycle and apoptosis.

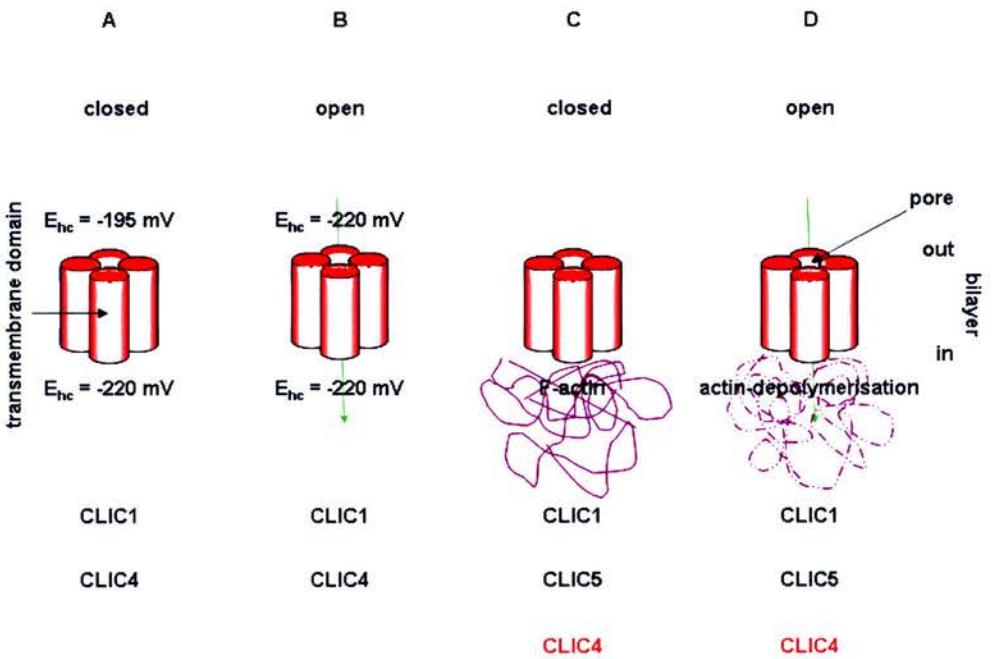

Fig 8.2 Modulation of CLIC channels. Summary of a novel mechanism of regulation of CLIC channels. CLIC proteins have a single transmembrane domain, hence a minimum of four subunits are required to form functional channels. A and B represents *trans* or luminal redox-regulation of CLIC1 and CLIC4 channels. C and D represent regulation of CLIC1 and CLIC5A (but not CLIC4) by *cis* or cytosolic actin-polymerisation.

CLIC1 and CLIC5A channels may be inactive under normal physiological conditions, but become active under specific physiological conditions such as cell division, apoptosis or in other conditions where cells undergo active volume regulation. The inactivation of CLIC channels on polymerisation of actin could be due to actin assembly at the cytoplasmic membrane surface, or to an interaction of the channels with preformed filaments in the cytosol. Unlike other ion channels (e.g. volume-regulated K^+ channels in melanoma cells and transport proteins (Na^+ transporter and K^+ transporter)) (Okada, 1997), CLICs are directly modulated by F-actin without any requirement for an adapter molecule.

VRChlC channels were shown to be activated by membrane stress (Levitan et al., 1995), much like mechanosensitive cation channels in yeast spheroplasts (Sackin, 1995). One way to control membrane tension is through the interaction of cytoskeletal proteins linked to integral membrane proteins. Disassembly of the cytoskeleton and its linkages to integral membrane proteins like VRCHlC allows an increase in membrane tension with a corresponding increase in VRChlC activation (Levitan et al., 1995). It may be speculated that CLICs in cells require membrane tension for activation.

8.7 CLICs interact with dynamin I

To further identify their interactions of recombinant CLIC proteins with dynamin I, the PRD domain and phosphomimitic (AA and EE) mutants of the PRD of dynamin I were overexpressed and purified. Serines at position 774 and 778 were

mutated to alanines or glutamic acids to generate AA and EE mutants. CLIC4 was localised to LDCV (Large dense core vesicles) (Chuang et al., 1999) and it was shown to interact directly with dynamin I (Suginta et al., 2001). In this study, it was shown that CLIC1 and CLIC4 can directly interact with dynamin I and this interaction was mapped to the PRD of dynamin I. CLIC1 and CLIC4 were further shown to be present in the membranes and the lysate of synaptosomes, and CLIC1 and CLIC4 were co-localised with dynamin I, to the nerve terminals of rat brain CGNs. Most dynamin I in the nerve terminal is in a dephosphorylated state, bound to the plasma membrane (Robinson et al., 1994). Dynamin I may affect the distribution of CLIC1 and CLIC4 (and other CLICs) directly or indirectly, or regulate the channel activity of CLIC proteins. This may play an important role in charge compensation and in turn in synaptic vesicle recycling.

To further investigate the functional role of this interaction, CLIC distributions could be monitored in a dynamin I KO-model. Over-expression and knocking down the expression of CLICs in nerve terminals with a specific endocytosis assay might help to reveal the functional significance of CLICs in nerve terminals. If CLICs play a role in endocytosis, electron microscopy could be performed on CGNs in order to determine at which stage of the endocytosis pathway they are required, and CLICs could be silenced by using siRNA. Previously, knocking-out CLIC1 was not shown to have marked effect, which may be attributed to the functional overlap between different CLICs. Hence, specific knock-out models may not reveal the functional role of these proteins. Controlled expression of specific CLIC proteins or knocking down multiple CLIC proteins might however

contribute to the determination of their possible functional significance in SV recycling.

8.8 Future work

The crystal structures of soluble CLIC1 and CLIC4 have been reported. However, the membrane structure of CLIC proteins will be necessary to fully understand the physiological role of CLIC proteins. It will however be extremely important to obtain membrane structures for CLICs that are relevant to functional channels, with predictable electrophysiological properties, and not the structures of proteins that simply insert into membranes without giving rise to consistent ion channels.

It is likely that CLIC proteins have important biological functions as they are very well-conserved among vertebrates and invertebrates, and they have been implicated in a variety of fundamental cellular processes (Ashley, 2003). The results presented in this thesis demonstrate that CLIC1 and CLIC4 (and other CLICs) can form *trans* redox-regulated ion channels *in vitro* and *in vivo*. Redox-regulation may provide an insight into the roles of CLICs *in vivo* in a variety of physiological processes. The cysteine residue in front of the putative TMD was shown to be responsible for this redox regulation mechanism. These experiments show that C24 is located near the pore region, and further work to support and extend this model could include recordings at much enhanced resolution, mutations of the remaining cysteines, and investigation of the potential role of the neighbouring proline residue (P25) in the CP motif.

The CP motif in 5-HT3 receptors were shown to be responsible for the gating of the channels. *Cis-trans* isomerisation of the proline residue, which links two transmembrane helices near the entrance of the pore region (Lummis et al., 2005), gated the channels. Proline 25 in the CP motif is well-conserved in all mammalian CLICs, and the disulphide bond might interfere with side-chain flipping. These predictions could be tested by overexpressing CLIC mutants (e.g. C24A) in cells. Elucidating the role of redox-regulation *in vivo* could also provide essential insights into role of CLICs in apoptosis.

CLIC1 and CLIC5A were regulated by actin polymerisation in addition to the *trans* redox potential. Further investigation of the regulation of CLICs *in vivo* and its functional consequences could be investigated in cells. The interaction of dynamin I and actin (and other proteins) with CLICs could provide evidence for a possible role for soluble or membrane CLICs in synaptic vesicle recycling. One main focus might be to identify more binding partners for CLIC proteins, and investigate the functional consequences of these interactions. The mouse knock-out model of CLIC1 was not sufficient to address the functional role of CLICs in mammals, as other CLICs might have functional overlaps in the cells. However, future KO models and specific assays could provide an insight into the functional roles of these proteins in mammalian cells.

The insertion mechanism of CLICs in the membranes also needs to be addressed. It is fascinating to note that the channel pore is formed by unfolding and refolding of a β-strand and an α-helix. The information obtained from the incorporation of

truncated proteins, and a helical wheel projection, has given us a preliminary and testable physical outline model of the channel pore. In future studies, site-directed fluorescence labelling and site-directed measurements of distances using FRET and FLIM techniques could provide a more complete picture of conformational changes in the pore region, and the role of the C-terminus in the selectivity of the channels. All these techniques, combined with the crystal structure of a membrane form of a CLIC protein, would provide a solid basis to develop an atomic level account of the structural changes underlying channel function.

REFERENCES

Adams, D.J., S.J. Smith, and S.H. Thompson. 1980. Ionic currents in molluscan soma. *Annu. Rev. Neurosci.* 3:141-167.

Anggono, V., K.J. Smillie, M.E. Graham, V.A. Valova, M.A. Cousin, and P.J. Robinson. 2006. Syndapin I is the phosphorylation-regulated dynamin I partner in synaptic vesicle endocytosis. *Nat. Neurosci.* 9:752-760.

Armstrong, R.N. 1997. Structure, catalytic mechanism, and evolution of the glutathione transferases. *Chem. Res. Toxicol.* 10:2-18.

Ashcroft, F.M. 2000. Ion Channels and Diseases. Academic Press, New York.

Ashley, R.H. 1989. Activation and conductance properties of ryanodine-sensitive calcium channels from brain microsomal membranes incorporated into planar lipid bilayers. *J. Membr. Biol.* 111:179-189.

Ashley, R.H. 1995. Intracellular calcium channels. *Essays Biochem.* 30:97-117.

Ashley, R.H. 2003. Challenging accepted ion channel biology: p64 and the CLIC family of putative intracellular anion channel proteins (Review). *Mol. Membr. Biol.* 20:1-11.

Bauer, C.K., K. Steinmeyer, J.R. Schwarz, and T.J. Jentsch. 1991. Completely functional double-barreled chloride channel expressed from a single Torpedo cDNA. *Proc. Natl. Acad. Sci. U S A.* 88:11052-6.

Benz, R., O. Frohlich, P. Lauger, and M. Montal. 1975. Electrical capacity of black lipid films and of lipid bilayers made from monolayers. *Biochim. Biophys. Acta.* 394:323-34.

Berry, K.L., H.E. Bulow, D.H. Hall, and O. Hobert. 2003. A C. elegans CLIC-like protein required for intracellular tube formation and maintenance. *Science.* 302:2134-2137.

Berry, K.L. and O. Hobert. 2006. Mapping functional domains of chloride intracellular channel (CLIC) proteins in vivo. *J. Mol. Biol.* 359:1316-1333.

Berryman, M., J. Bruno, J. Price, and J.C. Edwards. 2004. CLIC-5A functions as a chloride channel in vitro and associates with the cortical actin cytoskeleton in vitro and in vivo. *J. Biol. Chem.* 279:34794-34801.

Berryman, M. and A. Bretscher. 2000. Identification of a novel member of the chloride intracellular channel gene family (CLIC5) that associates with the actin cytoskeleton of placental microvilli. *Mol. Biol. Cell.* 11:1509-1521.

Berryman, M.A. and J.R. Goldenring. 2003. CLIC4 is enriched at cell-cell junctions and colocalizes with AKAP350 at the centrosome and midbody of cultured mammalian cells. *Cell Motil. Cytoskeleton.* 56:159-172.

Berryman, M., and S. Tanda. 2005. The *Drosophila* CLIC-like gene is critical for viability during development, adult lifespan and resistance to oxidative stress. *Drosophila* Research Conference; Genetics Society of America, San Diego, CA.

Betz, H. 1990. Ligand-gated ion channels in the brain: the amino acid receptor superfamily. *Neuron.* 5: 383-392.

Blachly-Dyson, E. and M. Forte. 2001. VDAC channels. *IUBMB Life*. 52:113-8.

Board, P.G., M. Coggan, S. Watson, P.W. Gage, and A.F. Dulhunty. 2004. CLIC-2 modulates cardiac ryanodine receptor Ca^{2+} release channels. *Int. J. Biochem. Cell Biol.* 36:1599-1612.

Bradford, M.M. 1976. A rapid and sensitive method for the quantitation of microgram quantities of protein utilizing the principle of protein-dye binding. *Anal. Biochem.* 72:248-54.

Brelidze, T.I., X. Niu, and K.L. Magleby. 2003. A ring of eight conserved negatively charged amino acids doubles the conductance of BK channels and prevents inward rectification. *Proc. Natl. Acad. Sci. U S A.* 100:9017-22.

Cantiello, H.F., J.L. Stow, A.G. Prat, and D.A. Ausiello. 1991. Actin filaments regulate epithelial Na^+ channel activity. *Am. J. Physiol.* 261:C882-8.

Chen, B. and A.E. Przybyla. 1994. An efficient site-directed mutagenesis method based on PCR. *Biotechniques.* 17:657-9.

Chen, C.Y., J.H. Jia, X.L. Pan, Y.S. Meng, and Z.H. Tu. 2003. Comparative proteomics research of apoptosis initiation induced by homoharringtonine in HL-60 cells. *Zhonghua Xue Ye Xue Za Zhi.* 24:624-628.

Chuang, J.Z., T.A. Milner, M. Zhu, and C.H. Sung. 1999. A 29 kDa intracellular chloride channel p64H1 is associated with large dense-core vesicles in rat hippocampal neurons. *J. Neurosci.* 19:2919-2928.

Clark, A.G., D. Murray, and R.H. Ashley. 1997. Single-channel properties of a rat brain endoplasmic reticulum anion channel. *Biophys. J.* 73:168–178.

Cline, J., J.C. Braman, and H.H. Hogrefe. 1996. PCR fidelity of pfu DNA polymerase and other thermostable DNA polymerases. *Nucleic Acids Res.* 24:3546-51.

Colombini, M. 1989. Voltage gating in the mitochondrial channel, VDAC. *J. Membr. Biol.* 111:103-11.

Cousin, M.A. and P.J. Robinson. 2001. The dephosphins: dephosphorylation by calcineurin triggers synaptic vesicle endocytosis. *Trends in Neurosci.* 24:659-665.

Cromer, B.A., C.J. Morton, P.G. Board, and M.W. Parker. 2002. From glutathione transferase to pore in a CLIC. *Eur. Biophys. J.* 31:356-364.

Doyle, D.A., C.J. Morais, R.A. Pfuetzner, A. Kuo, J.M. Gulbis, S.L. Cohen. B.T. Chait and R. MacKinnon. 1998. The structure of the potassium channel: molecular basis of K^+ conduction and selectivity. *Science.* 280:69-77.

Du, K., M. Sharma, and G.L. Lukacs. 2005. The Delta F508 cystic fibrosis mutation impairs domain-domain interactions and arrests post-translational folding of CFTR. *Nat. Struct. Mol. Biol.* 12:17–25.

Dulhunty, A.F., P. Pouliquin, M. Coggan, P.W. Gage, and P.G. Board. 2005. A recently identified member of the glutathione transferase structural family modifies cardiac RyR2 substate activity, coupled gating and activation by Ca^{2+} and ATP. *Biochem. J.* 390:333-343.

Dulhunty, A.F., P. Gage, S. Curtis, G. Chelvanayagam, and P. Board. 2001. The glutathione transferase structural family includes a nuclear chloride channel and a ryanodine receptor calcium release channel modulator. *J. Biol. Chem.* 276:3319-3323.

Duncan, R.R., Apps, D.K., Learmonth, M.P., Shipston, M.J, and R.H. Chow. 2000. Is double C2 protein (DOC2) expressed in bovine adrenal medulla? A commercial anti-DOC2 monoclonal antibody recognizes a major bovine mitochondrial antigen. *Biochem. J.* 351:33-7.

Duncan, R.R., P.K. Westwood, A. Boyd, and R.H. Ashley. 1997. Rat brain p64H1, expression of a new member of the p64 chloride channel protein family in endoplasmic reticulum. *J. Biol. Chem.* 272:23880-23886.

Dunkley, P.R., P.E. Jarvie, J.W. Heath, G.J. Kidd and J.A. Rostas. 1986. A rapid method for isolation of synaptosomes on Percoll gradients. *Brain Res.* 372:115-29.

Dutzler, R., E.B. Campbell, M. Cadene, B.T. Chait, and R. MacKinnon. 2002. X-ray structure of a ClC chloride channel at 3.0 A reveals the molecular basis of anion selectivity. *Nature*. 415:287-94.

Dutzler, R., E.B. Campbell, and R. MacKinnon. 2003. Gating the selectivity filter in ClC chloride channels. *Science*. 300:108-12.

Edwards, J.C., Tulk, B., and P.H. Schlesinger. 1998. Functional expression of p64, an intracellular chloride channel protein. *J. Membr. Biol*. 163:119-27.

Edwards, J.C. and S. Kapadia. 2000. Regulation of the bovine kidney microsomal chloride channel p64 by p59fyn, a Src family tyrosine kinase. *J. Biol. Chem.* 275:31826-32.

Edwards, J.C. 1999. A novel p64-related Cl- channel: subcellular distribution and nephron segment-specific expression. *Am. J. Physiol.* 276:F398-F408.

Elter. A., E. Fischer-Schliebs, U. Lüttge, and G. Thiel. 2004. AT-CLIC, a chlorid channel in plants? *13th International Workshop on Plant Membrane Biology*. P7-21.

Evans, M.G. and A. Marty. 1986. Calcium-dependent chloride currents in isolated cells from rat lacrimal glands. *J. Physiol. (Lond)*. 378: 437-460.

Fan, L., W. Yu, and X. Zhu. 2003. Interaction of Sedlin with chloride intracellular channel proteins. *FEBS Lett.* 540:77-80.

Fernandez-Salas, E., K.S. Suh, V.V. Speransky, W.L. Bowers, J.M. Levy, T. Adams, K.R. Pathak, L.E. Edwards, D.D. Hayes, C. Cheng, A.C. Steven, W.C. Weinberg, and S.H. Yuspa. 2002. mtCLIC/CLIC4, an organellular chloride channel protein, is

increased by DNA damage and participates in the apoptotic response to p53. *Mol. Cell Biol.* 22:3610-3620.

Fernandez-Salas, E., M. Sagar, C. Cheng, S.H. Yuspa, and W.C. Weinberg. 1999. p53 and tumor necrosis factor alpha regulate the expression of a mitochondrial chloride channel protein. *J. Biol. Chem.* 274:36488-36497.

Forte, M., H.R. Guy, and C.A. Manella. 1987. Molecular genetics of the VDAC ion channel: structural model and sequence analysis. *J. Bioenerg. Biomembr.* 19:341-50.

Franciolini, F. and W. Nonner. 1994. A multi-ion permeation mechanism in neuronal background chloride channels. *J. Gen. Physiol.* 104:725-46.

Friedli, M., M. Guipponi, S. Bertrand, D. Bertrand, M. Neerman-Arbez, H.S. Scott, S.E. Antonarakis, and A. Reymond. 2003. Identification of a novel member of the CLIC family, CLIC6, mapping to 21q22.12. *Gene.* 320:31-40.

Furukawa, T., T. Ogura, Y. Katayama, and M. Hiraoka. 1998. Characteristics of rabbit ClC-2 current expressed in Xenopus oocytes and its contribution to volume regulation. *Am. J. Physiol.* 274:C500-12.

Gagnon, L.H., C.M. Longo-Guess, M. Berryman, J.B. Shin, K.W. Saylor, H. Yu, P.G. Gillespie, and K.R. Johnson. 2006. The chloride intracellular channel protein CLIC5 is expressed at high levels in hair cell stereocilia and is essential for normal inner ear function. *J. Neurosci.* 26:10188-10198.

Goldman, D.E. 1943. Potentail, impedance, rectification in membranes. *J. Gen. Physiol.* 27: 37-60.

Grabs, D., V.I. Slepnev, S.Y. Zhou, C. David, M. Lynch, L.C. Cantley, and P. DeCamilli. 1997. The SH3 domain of amphiphysin binds the proline-rich domain of

dynamin at a single site that defines a new SH3 binding consensus sequence. *J. Biol. Chem.* 272:13419-13425.

Griffon, N., F. Jeanneteau, F. Prieur, J. Diaz, and P. Sokoloff. 2003. CLIC6, a member of the intracellular chloride channel family, interacts with dopamine D(2)-like receptors. *Brain Res. Mol. Brain Res.* 117:47-57.

Guggino, W.B. 1993. Outwardly rectifying chloride channels and CF: a divorce and remarriage. *J. Bioenerg. Biomembr.* 1993 25:27-35.

Gundelfinger, E.D., M.M. Kessels, and B. Qualmann. 2003. Temporal and spatial coordination of exocytosis and endocytosis. *Nat. Rev. Mol. Cell Biol.* 4:127-39.

Gunther, W., A. Luchow, F. Cluzeaud, A. Vandewalle, and T.J. Jentsch. 1998. ClC-5, the chloride channel mutated in Dent's disease, colocalizes with the proton pump in endocytotically active kidney cells. *Proc. Natl. Acad. Sci. U S A.* 95:8075-80.

Hamill, O.P., A. Marty, E. Neher, B. Sakmann, and F.J. Sigworth. 1981. Improved patch-clamp techniques for high-resolution current recording from cells and cell-free membrane patches. *Pflugers Arch.* 391:85-100.

Harrop, S.J., M.Z. DeMaere, W.D. Fairlie, T. Reztsova, S.M. Valenzuela, M. Mazzanti, R. Tonini, M.R. Qiu, L. Jankova, K. Warton, A.R. Bauskin, W.M. Wu, S. Pankhurst, T.J. Campbell, S.N. Breit, and P.M. Curmi. 2001. Crystal structure of a soluble form of the intracellular chloride ion channel CLIC1 (NCC27) at 1.4-A resolution. *J. Biol. Chem.* 276:44993-45000.

Harte, R. and C.A. Ouzounis. 2002. Genome-wide detection and family clustering of ion channels. *FEBS Lett.* 514:129-34.

Hartzell, C., Z. Qu, I. Putzier, L. Artinian, L.T. Chien, and Y. Cui. 2005. Looking chloride channels straight in the eye: bestrophins, lipofuscinosis, and retinal degeneration. *Physiology (Bethesda).* 20:292-302.

Hattori, M., A. Fujiyama, and Y. Sakaki. 2001. The DNA sequence of human chromosome 21.*Tanpakushitsu Kakusan Koso*. 46:2254-61.

Hayman, K.A., T.S. Spurway, and R.H. Ashley. 1993. Single anion channels reconstituted from cardiac mitoplasts. *J. Membr. Biol.* 136:181–190.

Heiss, N.S. and A. Poustka. 1997. Genomic structure of a novel chloride channel gene, CLIC2, in Xq28. *Genomics.* 45:224-228.

Hidalgo, C., R. Bull, M.I. Behrens, and P. Donoso. 2004. Redox regulation of RyR-mediated Ca^{2+} release in muscle and neurons. *Biol. Res.* 37:539-52.

Hille, B. 1984. Ionic Channels of Excitable Membranes. 2nd edn. Sunderland, Massachusetts, Sinauer Associates Inc.

Hille, B. 1992. Ionic Channels of Excitable Membranes. 3rd edn. Sunderland, Massachusetts, Sinauer Associates Inc.

Ho C., S.J. Slater, B. Stagliano, C.D. Stubbs. 2001. The C1 domain of protein kinase C as a lipid bilayer surface sensing module. *Biochemistry*. 40:10334-41.

Hodgkin, A.L. and B. Katz. 1949. The effect of sodium ions on the electrical activity of the giant axon of the squid. *J. Physiol*. 108:37-77.

Hodgkin, A.L. and A.F. Huxley. 1952. The components of membrane conductance in the giant axon of Loligo. *J. Physiol*. 116:473-496.

Howell, S., R.R. Duncan, and R.H. Ashley. 1996. Identification and characterisation of a homologue of p64 in rat tissues. *FEBS Lett.* 390:207-210.

Huang, J.S., C.C. Chao, T.L. Su, S.H. Yeh, D.S. Chen, C.T. Chen, P.J. Chen, and Y.S. Jou. 2004. Diverse cellular transformation capability of overexpressed genes in human hepatocellular carcinoma. *Biochem. Biophys. Res. Commun.* 315:950-958.

Janmey, P.A. 1998. The cytoskeleton and cell signaling: component localization and mechanical coupling. *Physiol. Rev.* 78:763-81.

Jentsch, T.J., K. Steinmeyer, and G. Schwarz. 1990. Primary structure of Torpedo marmorata chloride channel isolated by expression cloning in Xenopus oocytes. *Nature.* 348:510-4.

Jentsch, T.J. 1996. Chloride channels: a molecular perspective. *Curr. Opin. Neurobiol.* 6:303-10.

Jentsch, T.J., T. Friedrich, A. Schriever, and H. Yamada. 1999. The CLC chloride channel family. *Eur. J. Physiol.* 437:783–795.

Jentsch, T.J., V. Stein, F. Weinreich, and A.A. Zdebik. 2002. Molecular structure and physiological function of chloride channels. *Physiol. Rev.* 82:503-68.

Jentsch, T.J., I. Neagoe, and O. Scheel. 2005. CLC chloride channels and transporters. *Curr. Opin. Neurobiol.* 15:319-25.

Jez, J.M., Ferrer, J.L., Bowman, M.E., Dixon, R.A., and J.P. Noel. 2000. Dissection of malonyl-coenzyme A decarboxylation from polyketide formation in the reaction mechanism of a plant polyketide synthase. *Biochemistry.* 39:890–902.

Jiang, Y., A. Lee, J. Chen, M. Cadene, B.T. Chait, and R. MacKinnon. 2002. Crystal structure and mechanism of a calcium-gated potassium channel. *Nature.* 417:515-22.

Kitamura, A., M. Nishizuka, K. Tominaga, T. Tsuchiya, T. Nishihara, and M. Imagawa. 2001. Expression of p68 RNA helicase is closely related to the early stage of adipocyte differentiation of mouse 3T3-L1 cells. *Biochem. Biophys. Res. Commun.* 287:435-9.

Kornak, U., D. Kasper, M.R. Bosl, E. Kaiser, M. Schweizer, A. Schulz, W. Friedrich, G. Delling and T.J. Jentsch. 2001. Loss of the ClC-7 chloride channel leads to osteopetrosis in mice and man. *Cell.* 104:205-15.

Kunzelmann, K., G.L. Kiser, R. Schreiber, and J.R. Riordan. 1997. Inhibition of epithelial Na+ currents by intracellular domains of the cystic fibrosis transmembrane conductance regulator. *FEBS Lett.* 400:341-4.

Lamaze, C., L.M. Fujimoto, H.L. Yin, and S.L. Schmid. 1997. The actin cytoskeleton is required for receptor-mediated endocytosis in mammalian cells. *J. Biol. Chem.* 272:20332-5.

Landry, D.W., S. Sullivan, M. Nicolaides, C. Redhead, A. Edelman, M. Field, Q. Alawqati, and J. Edwards. 1993. Molecular-cloning and characterization of p64, a chloride channel protein from kidney microsomes. *J. Biol. Chem.* 268:14948-14955.

Landry, D.W., M.H. Akabas, C. Redhead, A. Edelman, E.J. Cragoe, Jr., and Q. Al Awqati. 1989. Purification and reconstitution of chloride channels from kidney and trachea. *Science.* 244:1469-1472.

Landry, D.W., M. Reitman, E.J.Jr. Cragoe, and Q. Al-Awqati. 1987. Epithelial chloride channel. Development of inhibitory ligands. *J. Gen. Physiol.* 90:779-98.

Levina, N.N., R.R. Lew, and I.B. Heath. 1994. Cytoskeletal regulation of ion channel distribution in the tip-growing organism Saprolegnia ferax. *J. Cell Sci.* 107:127-34.

Levitan, I., C. Almonte, P. Mollard and S.S. Garber. 1995. Modulation of a volume-regulated chloride current by F-actin. *J. Membr. Biol.* 147:283-94.

Li, M., J.D. McCann, C.M. Liedtke, A.C. Nairn, P. Greengard, and M.J. Welsh. 1988. Cyclic AMP-dependent protein kinase opens chloride channels in normal but not cystic fibrosis airway epithelium. *Nature.* 331:358-60.

Li, X. and S.A. Weinman. 2002. Chloride channels and hepatocellular function: prospects for molecular identification. *Annu. Rev. Physiol.* 64:609-33.

Li, Y., D. Li, Z. Zeng, and D. Wang. 2006. Trimeric structure of the wild soluble chloride intracellular ion channel CLIC4 observed in crystals. *Biochem. Biophys. Res. Commun.* 343:1272-1278.

Lindstrom, J., R. Anand, X. Peng, V. Gerzanich, F. Wang, and Y. Li. 1995. Neuronal nicotinic receptor subtypes. *Ann. NY. Acad. Sci* 757: 100-116.

Littler, D.R., N.N. Assaad, S.J. Harrop, L.J. Brown, G.J. Pankhurst, P. Luciani, M.I. Aguilar, M. Mazzanti, M.A. Berryman, S.N. Breit, and P.M. Curmi. 2005. Crystal structure of the soluble form of the redox-regulated chloride ion channel protein CLIC4. *FEBS J.* 272:4996-5007.

Littler, D.R., S.J. Harrop, W.D. Fairlie, L.J. Brown, G.J. Pankhurst, S. Pankhurst, M.Z. DeMaere, T.J. Campbell, A.R. Bauskin, R. Tonini, M. Mazzanti, S.N. Breit, and P.M. Curmi. 2004. The intracellular chloride ion channel protein CLIC1 undergoes a redox-controlled structural transition. *J. Biol. Chem.* 279:9298-9305.

Lobet, S. and R. Dutzler. 2006. Ion-binding properties of the ClC chloride selectivity filter. *EMBO J.* 25:24-33.

Lummis, S.C.R., D.L. Breene, L.W. Lee, H.A. Lester, R.W. Broadhurst, and D.A. Dougherty. 2005. *Cis-trans* isomerization at a proline opens the pore of a neurotransmitter-gated ion channel. *Nature.* 438:248–252.

Maduke, M., C. Miller, and J.A. Mindell. 2000. A decade of CLC chloride channels: structure, mechanism, and many unsettled questions. *Annu. Rev. Biophys. Biomol. Struct.* 29:411-38.

Maricq, A.V., A.S. Peterson, A.J. Brake, R.M. Myers, and D. Julius. 1991. Primary structure and functional expression of the $5HT_3$ receptor, a serotonin-gated ion channel. *Science.* 254: 432-437.

Marks, B., M.H. Stowell, Y. Vallis, I.G. Mills, A. Gibson, C.R. Hopkins, and H.T. McMahon. 2001. GTPase activity of dynamin and resulting conformation change are essential for endocytosis. *Nature*. 410:231-5.

Marmorstein, L.Y., P.J. McLaughlin, J.B. Stanton, L. Yan, J.W. Crabb, and A.D. Marmorstein. 2002. Bestrophin interacts physically and functionally with protein phosphatase 2A. *J. Biol. Chem.* 277:30591-7.

Martin, C. and R.H. Ashley. 1993. Reconstitution of a voltage-activated calcium conducting cation channel from brain microsomes. *Cell Calcium.* 14:427-438.

McAllister, R.E, D. Noble, and R.W. Tsien. 1975. Reconstruction of the construction of the electrical activity of cardiac Purkinje fibres. *J. Physiol*. 251:1-59.

Miller, C. 1982. Open-state substructure of single chloride channels from Torpedo electroplax. *Philos. Trans. R. Soc. Lond. B. Biol. Sci*. 299:401-11.

Mizukawa, Y., T. Nishizawa, T. Nagao, K. Kitamura, and T. Urushidani. 2002. Cellular distribution of parchorin, a chloride intracellular channel-related protein, in various tissues. *Am. J. Physiol. Cell Physiol.* 282:C786-C795.

Money, T.T., R.G. King, M.H. Wong, J.L. Stevenson, B. Kalionis, J.J. Erwich, M.A. Huisman, A. Timmer, U. Hiden, G. Desoye, and N.M. Gude. 2006. Expression and Cellular Localisation of Chloride Intracellular Channel 3 in Human Placenta and Fetal Membranes. *Placenta*. (in press).

Montal, M. and P. Mueller. 1972. Formation of bimolecular membranes from lipid monolayers and a study of their electrical properties. *Proc. Natl. Acad. Sci. USA.* 69:3561-6.

Mueller, P., D. Rudin, H.T. Tien and W.C. Wescott. 1962. Reconstitution of cell membrane structure in vitro and its transformation into an excitable system *Nature*. 194:979-80.

Mueller, P. and D.O. Rudin. 1968. Action potentials induced in biomolecular lipid membranes. *Nature*. 1968. 217:713-9.

Mullis, K., F. Faloona, S. Scharf, R. Saiki, G. Horn, and H. Erlich. Specific enzymatic amplification of DNA in vitro: the polymerase chain reaction. *Cold Spring Harb. Symp. Quant. Biol.* 1986. 51:263-73.

Myers, K., P.R. Somanath, M. Berryman, and S. Vijayaraghavan. 2004. Identification of chloride intracellular channel proteins in spermatozoa. *FEBS Lett.* 566:136-140.

Nabi, I.R. and P.U. Le. 2003. Caveolae/raft-dependent endocytosis. *J. Cell Biol.* 161:673-7.

Nagasawa, M., M. Kanzaki, Y. Iino, Y. Morishita, and I. Kojima. 2001. Identification of a novel chloride channel expressed in the endoplasmic reticulum, golgi apparatus, and nucleus. *J. Biol. Chem*. 276:20413-8.

Negulyaev, Y.A., S.Y. Khaitlina, H. Hinssen, E.V. Shumilina, and E.A. Vedernikova. 2000. Sodium channel activity in leukemia cells is directly controlled by actin polymerization. *J. Biol. Chem.* 275:40933-7.

Neher, E. and B. Sakmann. 1976. Single-channel currents recorded from membrane of denervated frog muscle fibres. *Nature*. 260:799-802.

Nicholls, D.G. 1993. The glutamatergic nerve terminal. *Eur. J. Biochem.* 212:613-31.

Nilius, B. and G. Droogmans. 2003. Amazing chloride channels: an overview. *Acta. Physiol. Scand.* 177:119–147.

Nishizawa, T., T. Nagao, T. Iwatsubo, J.G. Forte, and T. Urushidani. 2000. Molecular cloning and characterization of a novel chloride intracellular channel-related protein, parchorin, expressed in water-secreting cells. *J. Biol. Chem.* 275:11164-11173.

Novarino, G., C. Fabrizi, R. Tonini, M.A. Denti, F. Malchiodi-Albedi, G.M. Lauro, B. Sacchetti, S. Paradisi, A. Ferroni, P.M. Curmi, S.N. Breit, and M. Mazzanti. 2004. Involvement of the intracellular ion channel CLIC1 in microglia-mediated beta-amyloid-induced neurotoxicity. *J. Neurosci.* 24:5322-5330.

Oba, T., T. Murayama, and Y. Ogawa. 2002. Redox states of type 1 ryanodine receptor alter Ca^{2+} release channel response to modulators. *Am. J. Physiol. Cell Physiol.* 282:C684-92.

Obar, R.A., C.A. Collins, J.A. Hammarback, H.S. Shpetner, and R.B. Vallee. 1990. Molecular-cloning of the microtubule-associated mechanochemical enzyme dynamin reveals homology with a new family of GTP-binding proteins. *Nature.* 347:256-261.

Okada, Y. 1997. Volume expansion-sensing outward-rectifier Cl^- channel: fresh start to the molecular identity and volume sensor. *Am. J. Physiol.* 273:C755-89.

Olsen, R.W., T.M. Delorey, M. Gordey, and M.H. Kang. 1999. GABA receptor function and epilepsy. *Adv. Neurol.* 79: 499-510.

Olson, R. and E. Gouaux. 2005. Crystal structure of the *Vibrio cholerae* cytolysin (VCC) pro-toxin and its assembly into a heptameric transmembrane pore. *J. Mol. Biol.* 29:997–1016.

Palmer, M. 2004. Cholesterol and the activity of bacterial toxins. *FEMS Microbiol. Lett.* 238:281–289.

Parker, M.W. and F. Pattus. 1993. Rendering a membrane protein soluble in water: a common packing motif in bacterial protein toxins. *Trends Biochem. Sci.* 18:391-5.

Pelkmans, L. and A. Helenius. 2002. Endocytosis via caveolae. *Traffic.* 3:311-20.

Peterson, G.L. 1977. A simplification of the protein assay method of Lowry et al. which is more generally applicable. *Anal. Biochem.* 83:346-56.

Pichler, H. and H. Riezman. 2004. Where sterols are required for endocytosis. *Biochim. Biophys. Acta.* 1666:51-61.

Poulsen, L.L. and D.M. Ziegler. 1977. Microsomal mixed-function oxidase-dependent renaturation of reduced ribonuclease. *Arch. Biochem. Biophys.*183:563-70.

Proutski, I., N. Karoulias, and R.H. Ashley. 2002. Overexpressed chloride intracellular channel protein CLIC4 (p64H1) is an essential component of novel plasma membrane anion channels. *Biochem. Biophys. Res. Commun.* 297:317-322.

Qian, Z., D. Okuhara, M.K. Abe, and M.R. Rosner. 1999. Molecular cloning and characterization of a mitogen-activated protein kinase-associated intracellular chloride channel. *J. Biol. Chem.* 274:1621-1627.

Qiu, M.R. 2003. Functional and Molecular Aspects of Ion Channels in Macrophages. [PhD Thesis]. University of New South Wales, Sydney, Australia. 294pp.

Qualmann, B., J. Roos, P.J. DiGregorio, and R.B. Kelly. 1999. Syndapin I, a synaptic dynamin binding protein that associates with the neural Wiskott-Aldrich syndrome protein. *Mol. Biol. Cell.* 10:501-513.

Qualmann, B., M.M. Kessels, and R.B. Kelly. 2000. Molecular links between endocytosis and the actin cytoskeleton. *J. Cell. Biol.* 150:F111-6.

Redhead, C., S.K. Sullivan, C. Koseki, K. Fujiwara, and J.C. Edwards. 1997. Subcellular distribution and targeting of the intracellular chloride channel p64. *Mol. Biol. Cell.* 8:691-704.

Redhead, C.R., A.E. Edelman, D. Brown, D.W. Landry, and Q. Alawqati. 1992. A ubiquitous 64-kda protein is a component of a chloride channel of plasma and intracellular membranes. *Proc. Natl. Acad. Sci. USA.* 89:3716-3720.

Reeves, H.L., M.J.P. Arthur, G. Narla, A. Katz, E. Hod, and S.L. Friedman. 2003. Novel growth suppressor targets of the KLF6 tumour suppressor gene identified by microarray analysis. *BASL Meeting.*

Reymond, A., V. Marigo, M.B. Yaylaoglu, A. Leoni, C. Ucla, N. Scamuffa, C. Caccioppoli, E.T. Dermitzakis, R. Lyle, S. Banfi, G. Eichele, S.E. Antonarakis, and A. Ballabio. 2002. Human chromosome 21 gene expression atlas in the mouse. *Nature.* 420:582-6.

Ringstad, N., Y. Nemoto, and P. DeCamilli. 1997. The SH3p4/Sh3p8/SH3p13 protein family: Binding partners for synaptojanin and dynamin via a Grb2-like Src homology 3 domain. *Proc. Natl. Acad. Sci. USA.* 94:8569-8574.

Riordan, J.R., J.M. Rommens, B. Kerem, N. Alon, R. Rozmahel, Z. Grzelczak, J. Zielenski, S. Lok, N. Plavsic, and J.L. Chou. 1989. Identification of the cystic fibrosis gene: cloning and characterization of complementary DNA. *Science.* 245:1066-73.

Robinson, P.J., J.M. Sontag, J.P. Liu, E.M. Fykse, C. Slaughter, H. Mcmahon, and T.C. Sudhof. 1993. Dynamin GTPase regulated by protein-kinase-C phosphorylation in nerve-terminals. *Nature.* 365:163-166.

Rogner, U.C., N.S. Heiss, P. Kioschis, S.Wiemann, B. Korn, and A. Postka. 1996. Transcriptional analysis of the candidate region for incontinentia pigment (IP2) in Xq28. *Genome Res.* 6: 922-934.

Ronnov-Jessen, L., R. Villadsen, J.C. Edwards, and O.W. Petersen. 2002. Differential expression of a chloride intracellular channel gene, CLIC4, in transforming growth factor-beta1-mediated conversion of fibroblasts to myofibroblasts. *Am. J. Pathol.* 161:471-480.

Sackin, H. 1995. Mechanosensitive channels. *Annu. Rev. Physiol.* 57:333-53.

Saeki, K., E. Yasugi, E. Okuma, S.N. Breit, M. Nakamura, T. Toda, Y. Kaburagi, and A. Yuo. 2005. Proteomic analysis on insulin signaling in human hematopoietic cells: identification of CLIC1 and SRp20 as novel downstream effectors of insulin. *Am. J. Physiol. Endocrinol. Metab.* 289:E419-E428.

Sambrook, J., E.F. Fritsch and T. Maniatis. 1989. *Molecular cloning a laboratory manual (second edition).* Cold Spring Harbor Press. Cold Spring Harbor.

Schafer, F.Q. and G.R. Buettner. 2001. Redox environment of the cell as viewed through the redox state of the glutathione disulfide/glutathione couple. *Free Radic. Biol. Med.* 30:1191-212.

Schaller, S., K. Henriksen, M.G. Sorensen, and M.A. Karsdal. 2005. The role of chloride channels in osteoclasts: ClC-7 as a target for osteoporosis treatment. *Drug News Perspect.* 18:489-495.

Schendel, S.L., M. Montal, and J.C. Reed. 1998. Bcl-2 family proteins as ion-channels. *Cell Death Differ.* 5:372-80.

Schlesinger, P.H., Blair, H.C., Teitelbaum, S.L., and J.C. Edwards. 1997. Characterization of the osteoclast ruffled border chloride channel and its role in bone resorption. *J. Biol. Chem.* 272:18636-43.

Schmid, S.L., M.A. McNiven, and P.De Camilli. 1998. Dynamin and its partners: a progress report. *Curr. Opin. Cell Biol.* 10:504-512.

Schwiebert, E.M., J.W. Mills, and B.A. Stanton. 1994. Actin-based cytoskeleton regulates a chloride channel and cell volume in a renal cortical collecting duct cell line. *J. Biol. Chem.* 269:7081-9.

Shanks, R.A., M.C. Larocca, M. Berryman, J.C. Edwards, T. Urushidani, J. Navarre, and J.R. Goldenring. 2002. AKAP350 at the Golgi apparatus. II. Association of AKAP350 with a novel chloride intracellular channel (CLIC) family member. *J. Biol. Chem.* 277:40973-40980.

Sheppard, D.N. and M.J. Welsh MJ. 1999. Structure and function of the CFTR chloride channel. *Physiol. Rev.* 79:S23-45.

Shiang, R., S.G. Ryan, Y.Z. Zhu, A.F. Hahn, P.O' Connell, and J.J. Wasmuth. 1993. Mutations in the alpha 1 subunit of the inhibitory glycine receptor cause the dominant neurologic disorder, hyperekplexia. *Nat. Genet.* 5: 351-358.

Shorning, B.Y., D.B. Wilson, R.R. Meehan, and R.H. Ashley. 2003. Molecular cloning and developmental expression of two Chloride Intracellular Channel (CLIC) genes in Xenopus laevis. *Dev. Genes Evol.* 213:514-518.

Shumilina, E.V., Y.A. Negulyaev, E.A. Morachevskaya, H. Hinssen, and S.Y. Khaitlina. 2003. Regulation of sodium channel activity by capping of actin filaments. *Mol. Biol. Cell.* 4:1709-16.

Singer, S.J. and G.L. Nicolson. 1972. The fluid mosaic model of the structure of cell membranes. *Science*. 175:720-31.

Smillie, K.J. and M.A. Cousin. 2005. Dynamin I phosphorylation and the control of synaptic vesicle endocytosis. *Biochem. Soc. Symp.* 72:87-97.

Smith, P.R., L.C. Stoner, S.C. Viggiano, K.J. Angelides, and D.J. Benos. 1995. Effects of vasopressin and aldosterone on the lateral mobility of epithelial Na^+ channels in A6 renal epithelial cells. *J. Membr. Biol.* 147:195-205.

Sobko, A.A., E.A. Kotova, Y.N. Antonenko, S.D. Zakharov, and W.A. Cramer. 2006. Lipid dependence of the channel properties of a colicin E1-lipid toroidal pore. *J. Biol. Chem.* 281:14408-14416.

Spronk, S.A., D.E. Elmore, and D.A. Dougherty. 2006. Voltage-dependent hydration and conduction properties of the hydrophobic pore of the mechanosensitive channel of small conductance. *Biophys. J.* 90:3555-69.

Stobrawa, S.M., T. Breiderhoff, S. Takamori, D. Engel, M. Schweizer, A.A. Zdebik, M.R. Bosl, K. Ruether, H. Jahn, A. Draguhn, R. Jahn, and T.J. Jentsch. 2001.

Disruption of ClC-3, a chloride channel expressed on synaptic vesicles, leads to a loss of the hippocampus. *Neuron*. 29:185-96.

Stoscheck, C.M. 1990. Quantitation of protein. *Methods Enzymol*. 182:50-68.

Stossel, T.P. 1993. On the crawling of animal cells. *Science*. 260:1086-94.

Strippoli, P., P. D'Addabbo, L. Lenzi, S. Giannone, S. Canaider, R. Casadei, L. Vitale, P. Carinci, and M. Zannotti. 2002. Segmental paralogy in the human genome: a large-scale triplication on 1p, 6p, and 21q. *Mamm. Genome.* 13:456-462.

Suginta, W., N. Karoulias, A. Aitken, and R.H. Ashley. 2001. Chloride intracellular channel protein CLIC4 (p64H1) binds directly to brain dynamin I in a complex containing actin, tubulin and 14-3-3 isoforms. *Biochem. J.* 359:55-64.

Suh, K.S., M. Mutoh, K. Nagashima, E. Fernandez-Salas, L.E. Edwards, D.D. Hayes, J.M. Crutchley, K.G. Marin, R.A. Dumont, J.M. Levy, C. Cheng, S. Garfield, and S.H. Yuspa. 2004. The organellular chloride channel protein CLIC4/mtCLIC translocates to the nucleus in response to cellular stress and accelerates apoptosis. *J. Biol. Chem.* 279:4632-4641.

Suh, K.S., M. Mutoh, M. Gerdes, J.M. Crutchley, T. Mutoh, L.E. Edwards, R.A. Dumont, P. Sodha, C. Cheng, A. Glick, and S.H. Yuspa. 2005. Antisense suppression of the chloride intracellular channel family induces apoptosis, enhances tumor necrosis factor α-induced apoptosis, and inhibits tumor growth. *Cancer Res.* 65:562-571.

Suh, K.S. and S.H. Yuspa. 2005. Intracellular chloride channels: critical mediators of cell viability and potential targets for cancer therapy. *Curr. Pharm. Des.* 11:2753-2764.

Suh, K.S., M. Mutoh, M. Gerdes, and S.H. Yuspa. 2005. CLIC4, an intracellular chloride channel protein, is a novel molecular target for cancer therapy. *J. Investig. Dermatol. Symp. Proc.* 10:105-109.

Sun, H., T. Tsunenari, K.W. Yau, and J. Nathans. 2002. The vitelliform macular dystrophy protein defines a new family of chloride channels. *Proc. Natl. Acad. Sci. USA.* 99: 4008–4013.

Suzuki. T., R. Morita, Y. Sugimoto, T. Sugawara, D.S. Bai, M.E. Alonso, M.T. Medina, J.N. Bailey, A. Rasmussen, J. Ramos-Peek, S. Cordova, F. Rubio-Donnadieu, A. Ochoa, A. Jara-Prado, J. Inazawa, A.V. Delgado-Escueta, and K. Yamakawa. 2002. Identification and mutational analysis of candidate genes for juvenile myoclonic epilepsy on 6p11-p12: LRRC1, GCLC, KIAA0057 and CLIC5. *Epilepsy Res.* 50:265-75.

Tan, T.C., V.A. Valova, C.S. Malladi, M.E. Graham, L.A. Berven, O.J. Jupp, G. Hansra, S.J. McClure, B. Sarcevic, R.A. Boadle, M.R. Larsen, M.A. Cousin and P.J. Robinson. 2003. Cdk5 is essential for synaptic vesicle endocytosis. *Nat. Cell. Biol.* 5:701-10.

Terzic, A. and Y. Kurachi. 1996. Actin microfilament disrupters enhance K(ATP) channel opening in patches from guinea-pig cardiomyocytes. *J. Physiol.* 492:395-404.

Tonini, R., A. Ferroni, S.M. Valenzuela, K. Warton, T.J. Campbell, S.N. Breit, and M. Mazzanti. 2000. Functional characterization of the NCC27 nuclear protein in stable transfected CHO-K1 cells. *FASEB J.* 14:1171-1178.

Treptow, W. and M. Tarek M. 2006. Molecular restraints in the permeation pathway of ion channels. *Biophys. J.* 91:L26-8.

Tulk, B.M. and J.C. Edwards. 1998. NCC27, a homolog of intracellular Cl- channel p64, is expressed in brush border of renal proximal tubule. *Am. J. Physiol* 274:F1140-F1149.

Tulk, B.M., P.H. Schlesinger, S.A. Kapadia, and J.C. Edwards. 2000. CLIC-1 functions as a chloride channel when expressed and purified from bacteria. *J. Biol. Chem.* 275:26986-26993.

Tulk, B.M., S. Kapadia, and J.C. Edwards. 2002. CLIC1 inserts from the aqueous phase into phospholipid membranes, where it functions as an anion channel. *Am. J. Physiol. Cell Physiol.* 282:C1103-C1112.

Urrutia, R., J.R. Henley, T. Cook, and M.A. McNiven. 1997. The dynamins: redundant or distinct functions for an expanding family of related GTPases? *Proc. Natl. Acad. Sci. U S A.* 94:377-84.

Urushidani, T., D. Chow, and J.G. Forte. 1999. Redistribution of a 120 kDa phosphoprotein in the parietal cell associated with stimulation. *J. Membr. Biol.* 1999 168:209-20.

Valenzuela, S.M., D.K. Martin, S.B. Por, J.M. Robbins, K. Warton, M.R. Bootcov, P.R. Schofield, T.J. Campbell, and S.N. Breit. 1997. Molecular cloning and expression of a chloride ion channel of cell nuclei. *J. Biol. Chem.* 272:12575-12582.

Valenzuela, S.M., M. Mazzanti, R. Tonini, M.R. Qiu, K. Warton, E.A. Musgrove, T.J. Campbell, and S.N. Breit. 2000. The nuclear chloride ion channel NCC27 is involved in regulation of the cell cycle. *J. Physiol.* 529:541-552.

Vannier, C. and A. Triller. 1997. Biology of the postsynaptic glycine receptor. *Int. Rev. Cytol.* 176: 201-244.

Vignols, F., N. Mouaheb, D. Thomas, and Y. Meyer. 2003. Redox control of Hsp70-Co-chaperone interaction revealed by expression of a thioredoxin-like Arabidopsis protein. *J. Biol. Chem.* 278:4516-23.

Wang, W.H., A. Cassola, and G. Giebisch. 1994. Involvement of actin cytoskeleton in modulation of apical K channel activity in rat collecting duct. *Am. J. Physiol.* 267:F592-8.

Warton, K., R. Tonini, W.D. Fairlie, J.M. Matthews, S.M. Valenzuela, M.R. Qiu, W.M. Wu, S. Pankhurst, A.R. Bauskin, S.J. Harrop, T.J. Campbell, P.M. Curmi, S.N. Breit, and M. Mazzanti. 2002. Recombinant CLIC1 (NCC27) assembles in lipid bilayers via a pH-dependent two-state process to form chloride ion channels with identical characteristics to those observed in Chinese hamster ovary cells expressing CLIC1. *J. Biol. Chem.* 277:26003-26011.

Weber-Schurholz, S., E. Wischmeyer, M. Laurien, H. Jockusch, T. Schurholz, D.W. Landry, and Q. al-Awqati. 1993. Indanyloxyacetic acid-sensitive chloride channels from outer membranes of skeletal muscle. *J. Biol. Chem.* 268:547-51.

Wiedenmann, B. and W.W. Franke. 1985. Identification and localization of synaptophysin, an integral membrane glycoprotein of Mr 38,000 characteristic of presynaptic vesicles. *Cell.* 41:1017-28.

Wilce, M.C. and M.W. Parker. 1994. Structure and function of glutathione S-transferases. *Biochim. Biophys. Acta.* 1205:1–18.

Zhou, M. and R. MacKinnon. 2004. A mutant KcsA K^+ channel with altered conduction properties and selectivity filter ion distribution. *J. Mol. Biol.* 338:839-46.

Zhou, Y. and R. MacKinnon. 2003. The occupancy of ions in the K^+ selectivity filter: charge balance and coupling of ion binding to a protein conformational change underlie high conduction rates. *J. Mol. Biol.* 333:965-75.

APPENDICES

Appendix I : Vector maps

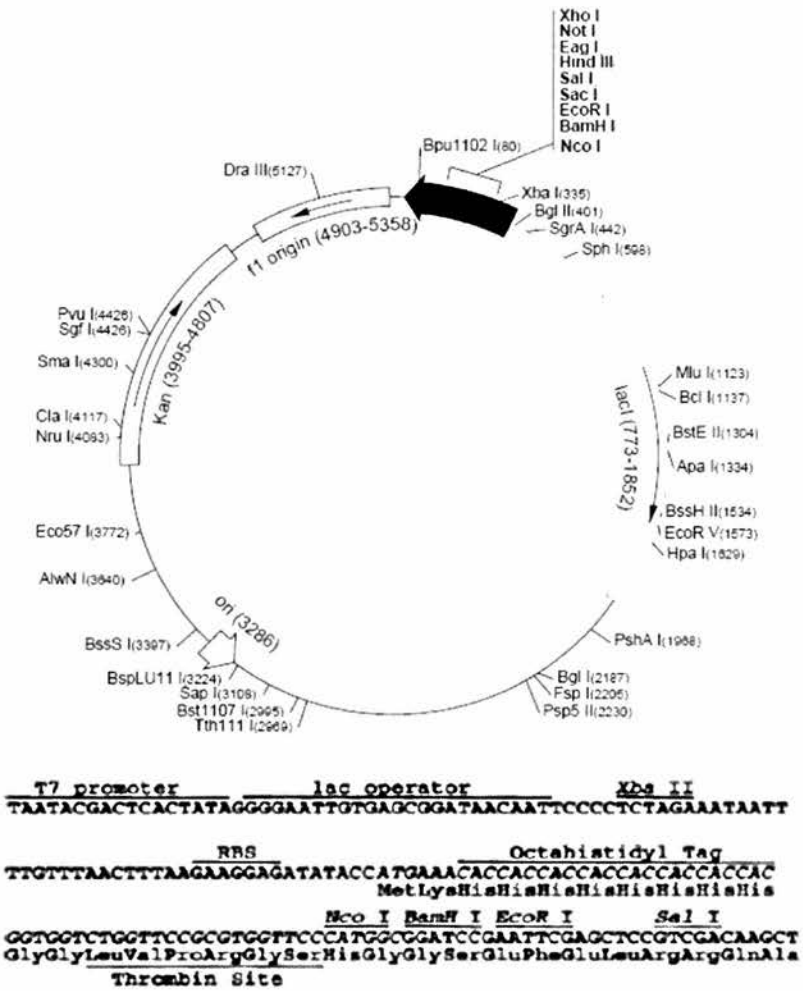

Fig 1. Vector map of pHis-8. pHis-8 vector is a modified pET 28a (+) encoding an N-terminal octa-His tag and a thrombin cleavage site (Jez et al., 2000). CLIC constructs in pHis-8 were used in single-channel analysis and in biochemical studies.

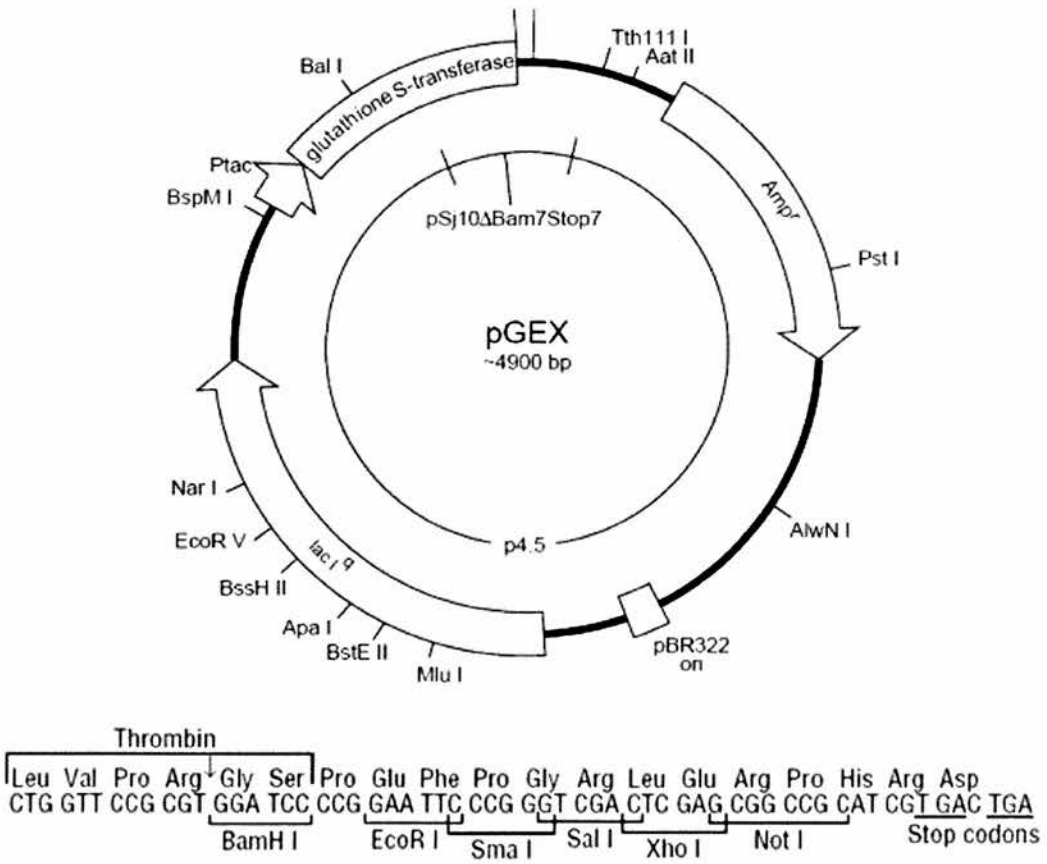

Fig 2. Vector map of pGEX-4T-1. The PRD of dynamin I was cloned into pGEX-4T-1. pGEX-4T-1 has a *tac* promoter, a *lac* gene, a thrombin-cleavage and PreScission protease sites (GE Healthcare).

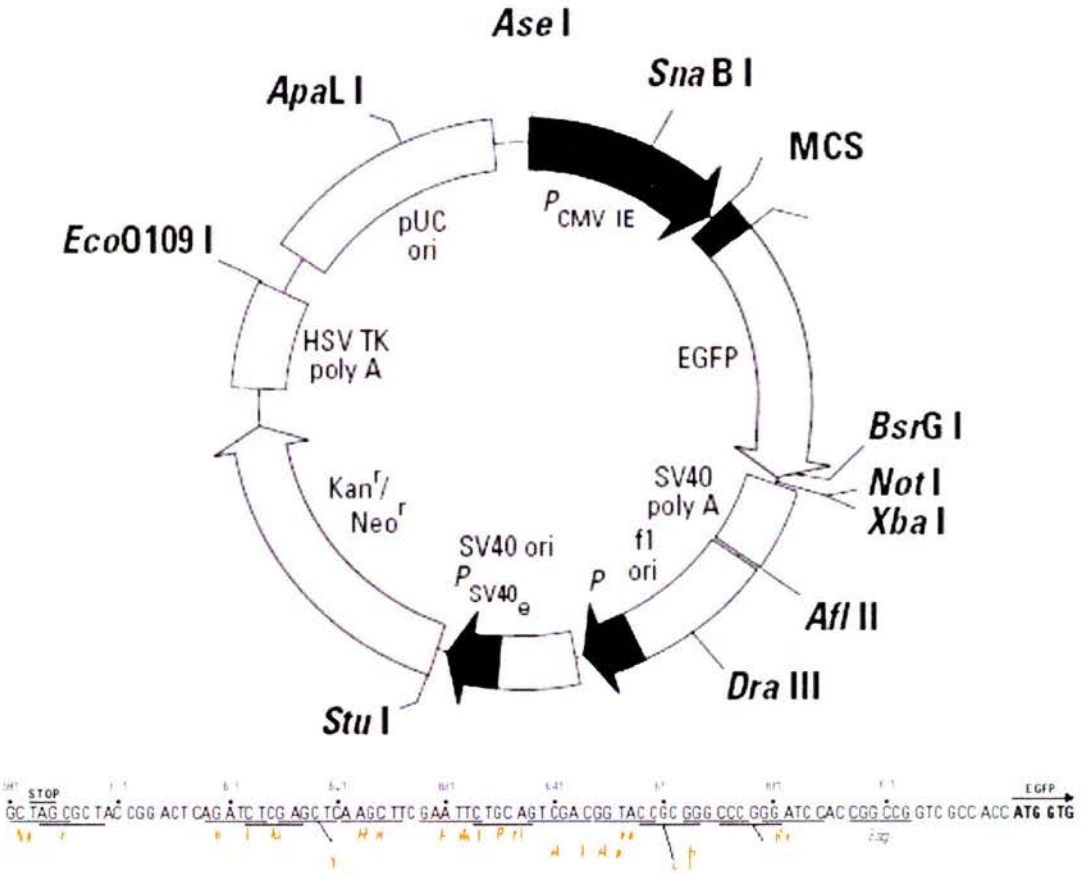

Fig 3. Vector map of pEGFP-N2. pEGFP-N2 encodes a red-shifted variant of wild-type GFP. The MCS in pEGFP-N2 lies between the immediate early promoter of CMV and the EGFP coding sequences (Clontech). CLIC1 and CLIC4 were cloned into pEGFP-N2 for transfection into CGNs.

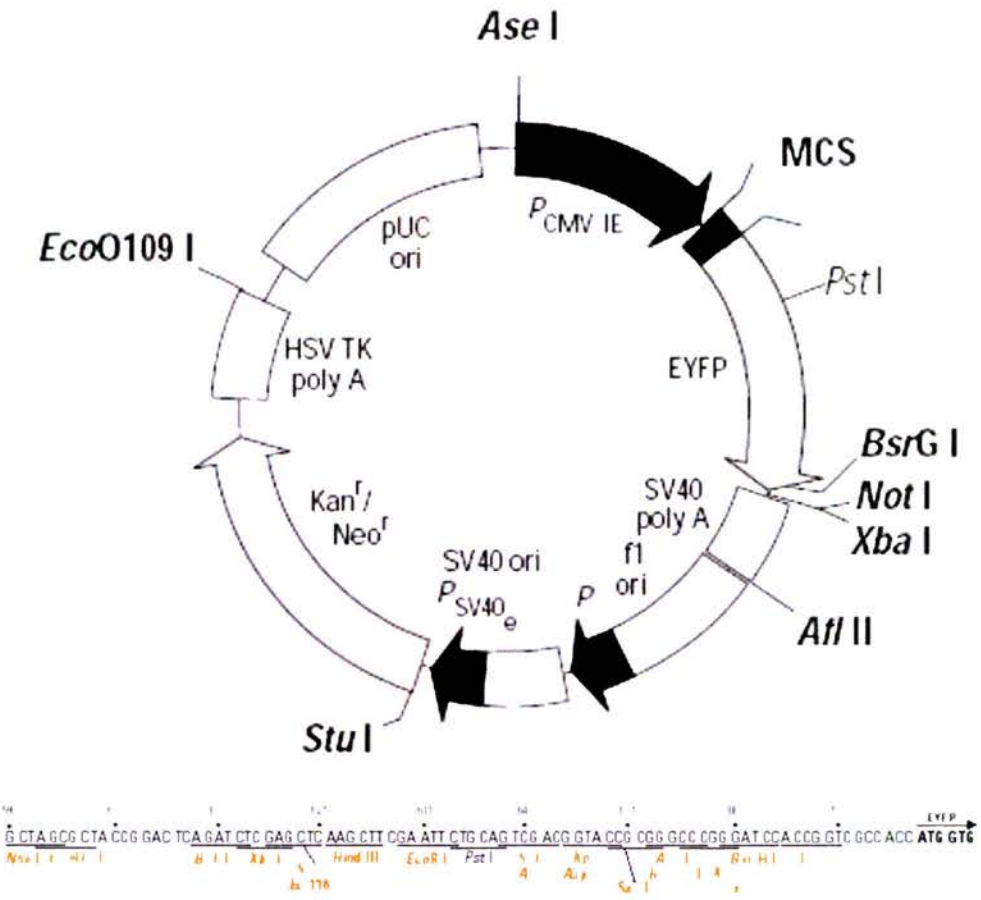

Fig 4. Vector map of pEYFP-N2. pEYFP-N1 encodes an enhanced yellow-green variant of the *Aequorea victoria* green fluorescent protein (GFP). The MCS in pEYFP-N1 lies between the immediate early promoter of CMV and the EYFP coding sequences. CLIC1 and CLIC4 were cloned into pEGFP-N2 for transfection into CGNs (Clontech).

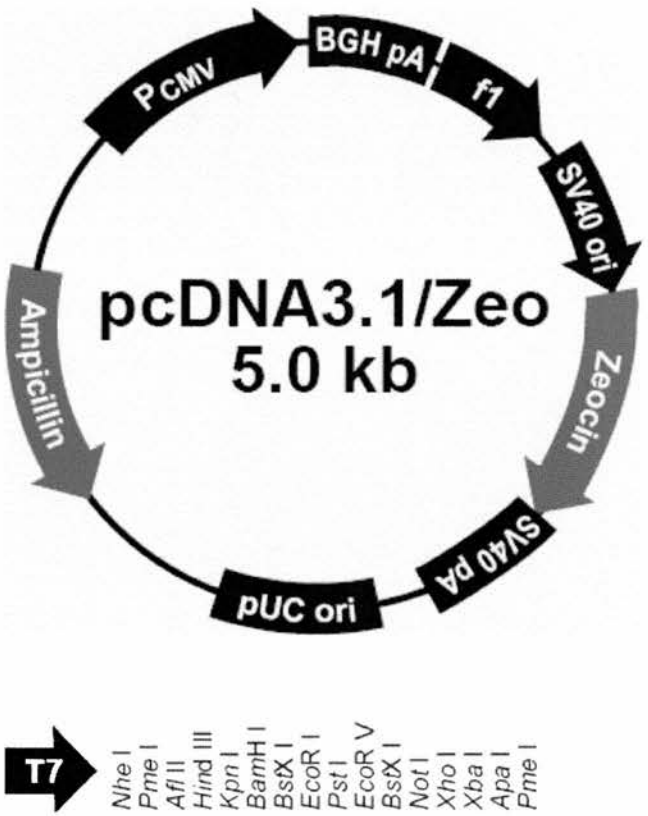

Fig 4. Vector map of pcDNA3.1/Zeo. pcDNA3.1/Zeo is an mammalian expression vector under control of the CMV promoter. The MCS lies immediately after the early CMV promoter. Stably-transfected HEK-293 cell lines expressing CLIC1 and CLIC4 cloned into pcDNA3.1/Zeo, were available in the laboratory.

Appendix II: Primers

CLIC1

Forward 5' ACG GAT CCA TGG CTG AAG AAC 3'

Reverse 5' ATC TCG AGT TAT TTG AGG GCC 3'

CLIC1 c24a

Forward 5' GAT TGG GAA CGC CCC ATT CTC CCA GAG ACT G 3'

Reverse 5' CAG ACT CAG GGA GAA TGG GGC GTT CCC AAT C 3'

CLIC1 1-58

Forward 5' GTG CAG AAG CTG TGA CCA GGG GGG 3'

Reverse 5' CAC GTC TTC GAC ACT GGT CCC CCC 3'

CLIC1 1-144

Forward 5' GACAATTACTTATGATCCCCCCTCCCAG 3'

Reverse 5' CTGGGAGGGGGGATCATAAGTAATTGTC 3'

CLIC1 (GFP/YFP)

Forward 5' GGC AAG CTT ATG GCT GAA GAA C 3'

Reverse 5' TAT GGA TCC CCT TTG AGG GCC TTT GC 3'

CLIC4 1-61

Forward 5' CTG AAA AGG TAG CCT GCA CAT CTG 3'

Reverse 5' GAC TTT TCC ATC GGA CGT GTA GAC 3'

CLIC4 (GFP/YFP)

Forward 5' GGT AAG CTT ATG GCG CTG TCG AT 3'

Reverse 5' TAT GGA TCC TTG GTG AGT CTT TTG GC 3'

CLIC5

Forward 5' TAG GAT CCA TGG CAG ACT AGG 3'

Reverse 5’ ATC TCG AGT CAG GAT CGG CTG 3’

Appendix III: PCR programs

CLIC1 full length

Component	µl
10X PCR Buffer	5
dNTP mixture (10 mM)	1
forward primer (10 µM)	1
Reverse primer (10 µM)	1
Template DNA (10 ng/µl)	1
Pfu Polymerase	0.5
DEPC treated water	40.5

Program

Temperature (°C)	time
94	5 min
94	30 s
50	30 s
72	2 min
Go to step 2 for 5 times	
94	30 s
53	30 s
72	2 min
Go to step 6 for 25 times	
72	7 min
4	Infinity

CLIC1 c24a

Component	µl
10X PCR Buffer	5

dNTP mixture (10 mM each)	1.5
forward primer (10 µM)	1.5
Reverse primer (10 µM)	1.5
Template DNA (10 ng/µl)	1.0
Pfu Polymerase	0.5
DEPC treated water	39

Program

Temperature (°C)	time
95	5 min
95	30 s
55	1 min
68	6 min 45 s
Go to step 2 for 25 times	
68	7 min
4	Infinity

CLIC1 N-terminus (1-58)

Component	µl
10X PCR Buffer	5
dNTP mixture (10 mM each)	1
forward primer (10 µM)	1
Reverse primer (10 µM)	1
Template DNA (10 ng/µl)	1
Pfu Polymerase	0.5
DEPC treated water	40.5

Program

Temperature (°C)	time
95	5 min

95	30 s
55	1 min
68	6 min 45 sec
Go to step 2 for 25 times	
68	7 min
4	infinity

CLIC1 N terminus (1-144)

Component	µl
10X PCR Buffer	5
dNTP mixture (10 mM)	1.5
forward primer (10 µM)	1.5
Reverse primer (10 µM)	1.5
Template DNA (10 ng/µl)	1.0
Pfu Polymerase	0.5
DEPC treated water	39

Program

Temperature (°C)	time
95	5 min
95	45 s
55	1 min
72	7 min sec
Go to step 2 for 25 times	
72	7 min
4	infinity

CLIC4 N terminus (1-61)

Component	µl
10X PCR Buffer	5
dNTP mixture (10 mM each)	1
forward primer (10 µM)	1.25
Reverse primer (10 µM)	1.25
Template DNA (10 ng/µl)	1
Pfu Polymerase	0.5
DEPC treated water	40

Program

Temperature (°C)	time
95	5 min
95	30 s
57	1 min
68	6 min 30 sec
Go to step 2 for 25 times	
68	7 min
4	infinity

CLIC5

Component	µl
10X PCR Buffer	5
dNTP mixture (10 mM)	1
forward primer (10 µM)	1
Reverse primer (10 µM)	1
Template DNA (10 ng/µl)	1
Pfu Polymerase	0.5
DEPC treated water	40.5

Program

Temperature (°C)	time
94	5 min
94	30 s
50	30 s
72	2 min
Go to step 2 for 5 times	
94	30 s
53	30 s
72	2 min
Go to step 6 for 25 times	
72	7 min
4	Infinity

APPENDIX IV

PUBLICATIONS

Redox Regulation of CLIC1 by Cysteine Residues Associated with the Putative Channel Pore

Harpreet Singh and Richard H. Ashley
Biomedical Sciences, University of Edinburgh Medical School, Edinburgh, United Kingdom

ABSTRACT Chloride intracellular channels (CLICs) are putative pore-forming glutathione-S-transferase homologs that are thought to insert into cell membranes directly from the cytosol. We incorporated soluble, recombinant human CLIC1 into planar lipid bilayers to investigate the associated ion channels, and noted that channel assembly (unlike membrane insertion) required a specific lipid mixture. The channels formed by reduced CLIC1 were similar to those previously recorded from cells and "tip-dip" bilayers, and specific anti-CLIC1 antibodies inhibited them. However, the amplitudes of the filtered single-channel currents were strictly regulated by the redox potential on the "extracellular" (or "luminal") side of the membrane, with minimal currents under strongly oxidizing conditions. We carried out covalent functional modification and site-directed mutagenesis of this controversial ion channel to test the idea that cysteine 24 is a critical redox-sensitive residue located on the extracellular (or luminal) side of membrane CLIC1 subunits, in a cysteine-proline motif close to the putative channel pore. Our findings support a simple structural hypothesis to explain how CLIC1 oligomers form pores in membranes, and suggest that native channels may be regulated by a novel mechanism involving the formation and reduction of intersubunit disulphide bonds.

INTRODUCTION

The pore-forming subunits of well-established eukaryotic ion channels are processed in the secretory pathway as conventional membrane proteins. In contrast, chloride intracellular channel (CLIC) proteins, including the putative anion channels CLIC1 (1) and CLIC4 (p64H1) (2), are synthesized without a leader sequence, and appear to insert into cell membranes directly, by a mechanism yet to be elucidated. Although CLIC proteins are members of the glutathione-S-transferase (GST) superfamily (3,4), other GST proteins, including omega GSTs (their closest structural relatives), do not share this unusual "autoinserting" ability (5). If CLICs prove to be biologically relevant ion channels, their remarkable properties will present a substantial challenge to our current understanding of membrane protein biogenesis and ion channel regulation (6).

Once inserted from the cytosol, CLIC1 and CLIC4 monomers span the cell (or organelle) membrane completely, with an external (or intraluminal) N-terminus and an odd number of transmembrane domains (TMDs), as demonstrated by protease digestion experiments and terminus-directed antibodies (2,7,8). Although the membrane forms of recombinant CLIC1 and CLIC4 are both associated with novel ion channel activity (8,9), these channels could be an artifact of artificial overexpression. The cellular proteins exist almost entirely in their soluble, cytosolic form (see, e.g., Suginta et al. (10)), and endogenous CLIC channels have been hard to detect. However, native CLICs appear to be more likely to form ion channels under specific conditions. For example, channel activity is promoted when nucleoplasmic CLIC1 is liberated during cell division (9), and the probability of recording CLIC1-like channels from microglia increases significantly after exposure to Alzheimer's Aβ peptide (11).

CLIC1 has been shown to be a pore-forming protein in vitro, but single-channel recordings have been inconsistent. Recombinant CLIC1 channels reconstituted by "tip-dipping" (12) proved to be similar to those recorded from cells, but CLIC1 channels reconstituted in planar bilayers (13,14) had much larger amplitudes under similar ionic conditions. It was speculated (12) that CLIC1 could form channel "aggregates", with larger overall conductances, under certain conditions. Reminiscent of this behavior, patch-clamped CLIC4 channels had a unit conductance of ~1 pS (8), compared to novel unit currents of 10–50 pS when brain microsomes containing the recombinant protein were reconstituted in bilayers (2). Although this might represent channel "aggregation" in microsomes, an alternative explanation is that CLIC4 can regulate other cellular channels, as demonstrated recently for CLIC2 (15). CLICs might also form channel complexes involving different CLIC isoforms, or other unidentified proteins.

Experiments involving Cl^- efflux through CLIC1 incorporated into small unilamellar liposomes (e.g., Tulk et al. (14) and Littler et al. (16)) have also been difficult to interpret. Most of the entrapped Cl^- was only released by detergents, suggesting that very few liposomes contained functional channels, and efflux was exceptionally prolonged, extending over tens of seconds or several minutes, even with an inside negative membrane potential. Under these conditions, small vesicles containing just a single active channel should empty within a few milliseconds (17). We speculated that some of these inconsistencies might be related to the bilayer lipid composition, and began our present study by surveying the

Submitted August 15, 2005, and accepted for publication November 16, 2005.

Address reprint requests to Richard H. Ashley, Biomedical Sciences, University of Edinburgh Medical School, Edinburgh EH8 9XD, UK. E-mail: richard.ashley@ed.ac.uk.

0006-3495/06/03/1628/11 $2.00

doi: 10.1529/biophysj.105.072678

effects of membrane lipids on protein insertion and channel formation. Finally, another notable feature of CLIC1, CLIC4, and other CLIC proteins is the presence of several cysteine residues (like other GST family members), making them potentially susceptible to intrachain or intersubunit disulphide bond formation, or both. Indeed, membrane CLIC1 has been reported to form channels after the protein is first oxidized by H_2O_2 to produce an intrasubunit disulphide bond (16).

In this article, we describe the lipid-dependent reconstitution of CLIC1, analyze its single-channel conductance and selectivity, and identify specific, functionally important, redox-sensitive cysteine residues close to the extracellular (or luminal) side of the channel pore. To our knowledge, this is the first structure/function study of this novel class of putative ion channel, and it leads to a readily testable hypothesis to explain how cellular CLIC1 channels may be regulated in vivo.

MATERIALS AND METHODS

Expression and purification of CLIC1

Human *CLIC1* (cDNA clone MGC:74817 IMAGE:5585323, MRC geneservice, Cambridge, UK) was inserted into pHis8, a modified pET vector encoding an N-terminal octa-His tag and a thrombin cleavage site (18). The codon for cysteine 24 was altered to alanine by the "QuikChange" polymerase chain reaction method. Rat *CLIC4* cDNA (2) was also cloned into the same vector, and all the inserts were verified by sequencing (MWG Biotech, Ebersberg, Germany). Soluble octa-His tagged fusion proteins were expressed in *Escherichia coli* BL21 (DE3) cells and purified from cell lysates by Ni^{2+}-NTA affinity chromatography. Nonspecifically bound proteins were removed by extensive washing in 20 mM imidazole, and the tagged CLIC proteins were eluted by 150 mM imidazole in 150 mM NaCl containing 20 mM Tris-HCl (pH 8.0). All the solutions contained a stoichiometric excess of dithiothreitol (DTT). Enzymatic cleavage of the His tag left eight linker residues (sequence: GGLVPRGS) before the initiating methionine. The thrombin was removed by adding benzamidine Sepharose beads during dialysis to eliminate the imidazole, and fresh Ni-NTA beads were added to remove the cleaved His tags and any uncleaved protein. Some protein samples were also subjected to size-exclusion chromatography, but this step was not essential for subsequent experiments. The yield of CLIC1 was 4.4 ± 0.75 mg/l culture medium (mean ± SD, $n = 7$), and protein aliquots were stored for up to 3 months at −70°C in buffer containing 5 mM DTT. Note that all the proteins were completely free of any detergent.

Preparation of affinity-purified anti-CLIC antibodies

Recombinant CLIC1 and CLIC4 were subjected to sodium dodecyl sulfate polyacrylamide gel electrophoresis and electrophoretically transferred to polyvinylidene difluoride membranes. Membrane strips containing the proteins were blocked with 5% (w/v) nonfat milk in phosphate-buffered saline (PBS), washed in PBS, and incubated overnight at 4°C with rabbit anti-CLIC antiserum raised to soluble, properly folded, full-length CLIC1 or full-length CLIC4. After extensive washing in PBS containing 0.05% (v/v) Tween-20, then PBS alone, specifically bound antibodies were eluted with 100 mM glycine-HCl (pH 2.5), immediately readjusted to a pH of 8.0 with a precalibrated amount of Tris base, and stored in small aliquots at −70°C. Western blotting with enhanced chemiluminescence detection was carried out as previously described (10). When assessed by immunoblotting against pure protein standards, the affinity-purified anti-CLIC1 and anti-CLIC4 pAbs could detect a minimum of 0.1 ng CLIC1 and 10 ng CLIC4, respectively, and only showed measurable cross-reactivity when the proteins were increased to at least 1 μg. Protein concentrations were determined by absorbance measurements using calculated extinction coefficients, or by the micro Bio-Rad procedure (Pierce, Perbio Science, Cramlington, UK), using appropriate standards.

Protein incorporation into lipid monolayers

Monolayers (Langmuir-Blodgett films) were spread in a Teflon trough, as previously described (19), after the surface of the aqueous subphase had been cleaned repeatedly until the initial surface (lateral) pressure was <1 mN/m. Pressure/area isotherms after monolayer formation showed typical changes in surface pressure as the surface area was reduced, with shearing at ~45 mN/m. The monolayers were compressed to 20 mN/m (the lateral pressure of a typical lipid bilayer), and the surface area was then monitored under constant pressure conditions after the addition of soluble proteins directly to the subphase.

Incorporation of channels into planar lipid bilayers

Planar bilayers were prepared at room temperature (~20°C) from several different lipids, including purified soybean lecithin (Type IV, Sigma, Poole, UK), diphytanoylphosphatidylcholine, palmitoyl-oleoyl (PO) phosphatidylcholine, PO-phosphatidylethanolamine, PO-phosphatidylserine, and cholesterol (Avanti, Alabaster, AL). The lipids were suspended in *n*-decane (25 μg total lipid/μl), and films were cast across a 0.3-mm hole in a polystyrene partition separating two solution-filled chambers, designated *cis* and *trans*. Using agar salt bridges, the *cis* chamber was voltage-clamped by an Axopatch 200-B amplifier, and the *trans* chamber was grounded, minimizing and offsetting liquid junction potentials, as described in detail previously (20). After thinning spontaneously to a capacitance of at least 250 pF, bilayers were bathed in 500 mM KCl *cis* vs. 50 mM KCl *trans* (all the solutions contained 10 mM Tris-HCl, pH 7.4 and 1 mM DTT, unless otherwise specified), and up to 25 ng/ml (~1 nM) CLIC1 was stirred into the *cis* chamber. Transmembrane currents normally appeared within 10 min., and were digitally recorded. Concentrated salt solutions were stirred into the relevant chamber as required, or the contents were changed by perfusion (at least 10 volumes). Unless otherwise specified, reagents were added to both chambers. Currents are labeled as positive or negative following the standard convention (i.e., positive currents represent net cation flux *cis* to *trans*).

Single channel analysis

Single-channel currents were filtered at 50 Hz (8-pole, low-pass Bessel-type response) and analyzed using pClamp8 software (Axon Instruments, Foster City, CA) and pStat (SPSS, Chicago, IL). Channel amplitudes were measured by fitting amplitude histograms to Gaussian distributions. Salt concentrations were corrected for activity using standard tables, and (relative) anion permeabilities (P) were calculated from the Nernst equation adapted for bi-ionic conditions:

$$P_{\text{anion}}/P_{\text{Cl}} = a[\text{Cl}]_{\text{cis}}/a[\text{anion}]_{\text{trans}} \times \exp(-zFEr/RT), \quad (1)$$

where a is the activity coefficient of the relevant salt, Er is the reversal or equilibrium potential, and z, F, R, and T have their usual significance. Relative anion versus cation permeabilities were calculated from the following form of the Goldman-Hodgkin-Katz voltage equation:

$$P_{\text{anion}}/P_{\text{cation}} = \{n \times \exp(Er/k) - 1\}/\{n - \exp(Er/k)\}, \quad (2)$$

where n is the *cis*/*trans* salt activity ratio and $k = RT/F$ (26 mV). The redox or half-cell (E_{redox} or E_{hc}) potential of the buffer pair 2GSH/GSSG (two reduced glutathione molecules equilibrated with oxidized glutathione in a

reaction involving the transfer of two protons and two electrons) was calculated from

$$E_{redox} = E^0 - RT/2F \times \ln([GSH]^2/[GSSG])\,mV, \quad (3)$$

where E^0 (−240 mV) is the standard redox potential. We took account of the experimental pH of 7.4 by including a pH-dependent correction of $(7.4 - 7.0) \times 2.3(RT/F) = -24$ mV.

RESULTS

Incorporation of CLIC1 into artificial membranes

In previous work involving the single-channel reconstitution of CLIC1 in bilayers, the membranes always contained phosphatidylcholine (PC) or phosphatidylethanolamine (PE), and sometimes both (including the PE in partially purified soybean lecithin (14)). Using these conditions as a starting point for our study, we compressed lipid monolayers to form "hemibilayers" (21) (Fig. 1 *A*), and confirmed, by observing membrane expansion under constant lateral pressure conditions (e.g., Fig. 1 *B*), that recombinant CLIC1 autoinserted readily into membranes containing POPC or equimolar POPS and POPE, even with an intact His tag.

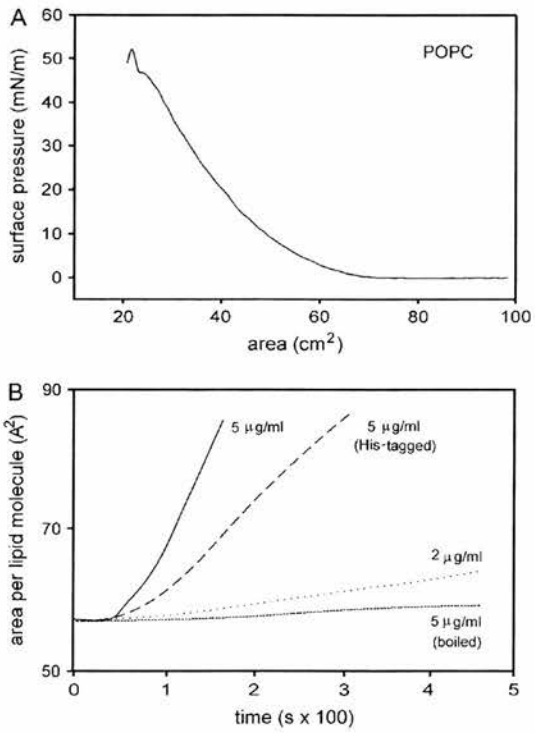

FIGURE 1 Insertion of CLIC1 into lipid monolayers. (*A*) Example of a pressure/area isotherm for a POPC monolayer at room temperature. The lipid was dispersed in chloroform and added carefully to the surface 20 min earlier. (*B*) Insertion of CLIC1 into monolayers maintained at a "bilayer-like" surface pressure of 20 mN/m. The initial area per lipid molecule (calculated from the known amount of lipid applied to the surface) was 55–60 Å^2, and because the amount of lipid is fixed, membrane expansion arises mainly or exclusively from protein insertion.

Surprisingly, CLIC1 failed to form well-defined ion channels in more than 20 experiments using planar bilayers containing the same lipids, with or without 1 mM DTT or 10–100 μM H_2O_2 in both chambers. This suggested that CLIC1 might require specific lipids to refold or form oligomers after membrane insertion. After extensive preliminary experiments testing a variety of lipid mixtures, we obtained highly reproducible ion channel activity in 110 of 115 experiments using POPE, POPS, and cholesterol in a molar ratio of 4:1:1 in 1 mM DTT (e.g., Fig. 2 *A*). We also obtained channels in the same lipid mixture in the presence of H_2O_2 from oxidized soluble CLIC1 exposed to 100 μM H_2O_2 before insertion (Fig. 2 *B*). This contrasted with "detergent-like" bilayer instability in other lipid mixtures, including soybean lecithin, which characteristically produced unstable anionic or cationic currents of varying amplitude. All the following data were obtained using bilayers containing POPE/POPS/cholesterol, 4:1:1 (molar), and the channels appeared to be identical with or without an intact N-terminal His tag.

Careful inspection of CLIC1 unit currents (Fig. 2 *C*) revealed two infrequent substates, at 45% and 22% of the main open level. As illustrated in Fig. 2, *D* and *E*, the maximum slope conductance of the main open state in a *cis*:*trans* gradient of 500 vs. 50 mM KCl containing 1 mM DTT in both chambers was 38 ± 3 pS (mean ± SD, $n = 23$), and the reversal potential (*Er*) of the main open state was +6 ± 1.1 mV (mean ± SD, $n = 23$ independent recordings), corresponding to a mean anion/cation permeability ratio of 1.4 (corrected for ionic activities). We noted that the conductance of channels formed from H_2O_2-oxidized CLIC1 was 24 ± 1.5 pS (mean ± SD, $n = 10$). Channels were also obtained in the presence of 5 mM GSH in both chambers, with similar substates at 45% and 22% of the main open level. However, the apparent single-channel conductance was substantially reduced compared to DTT, to 25 ± 1.5 pS (mean ± SD, $n = 13$).

CLIC1 channels were inhibited by IAA-94 (indanyloxyacetic acid, Sigma, Gillingham, UK), added to the *cis* chamber, but this required very high concentrations (≥10 μM, data not shown), as previously observed (12,13). We therefore used affinity-purified anti-CLIC antibodies as potentially more specific functional inhibitors. Unlike our previous anti-CLIC4 antibodies (see, e.g., Proutski et al. (8)), the originating anti-CLIC1 and anti-CLIC4 antisera were generated to soluble, full-length proteins rather than N-terminally truncated proteins (see Methods). The activity of CLIC1 was completely inhibited from the *trans* side of incorporated channels by 10 μg/ml anti-CLIC1 (but not anti-CLIC4) within 30–60 s in six of six experiments, whereas prior addition of nonspecific IgG for up to 10 min had no effect (Fig. 3).

CLIC1 forms a poorly selective multi-ion pore

Fig. 4 *A* illustrates the current/voltage (I/V) relationship of CLIC1 in symmetric 100 mM KCl containing 1 mM DTT.

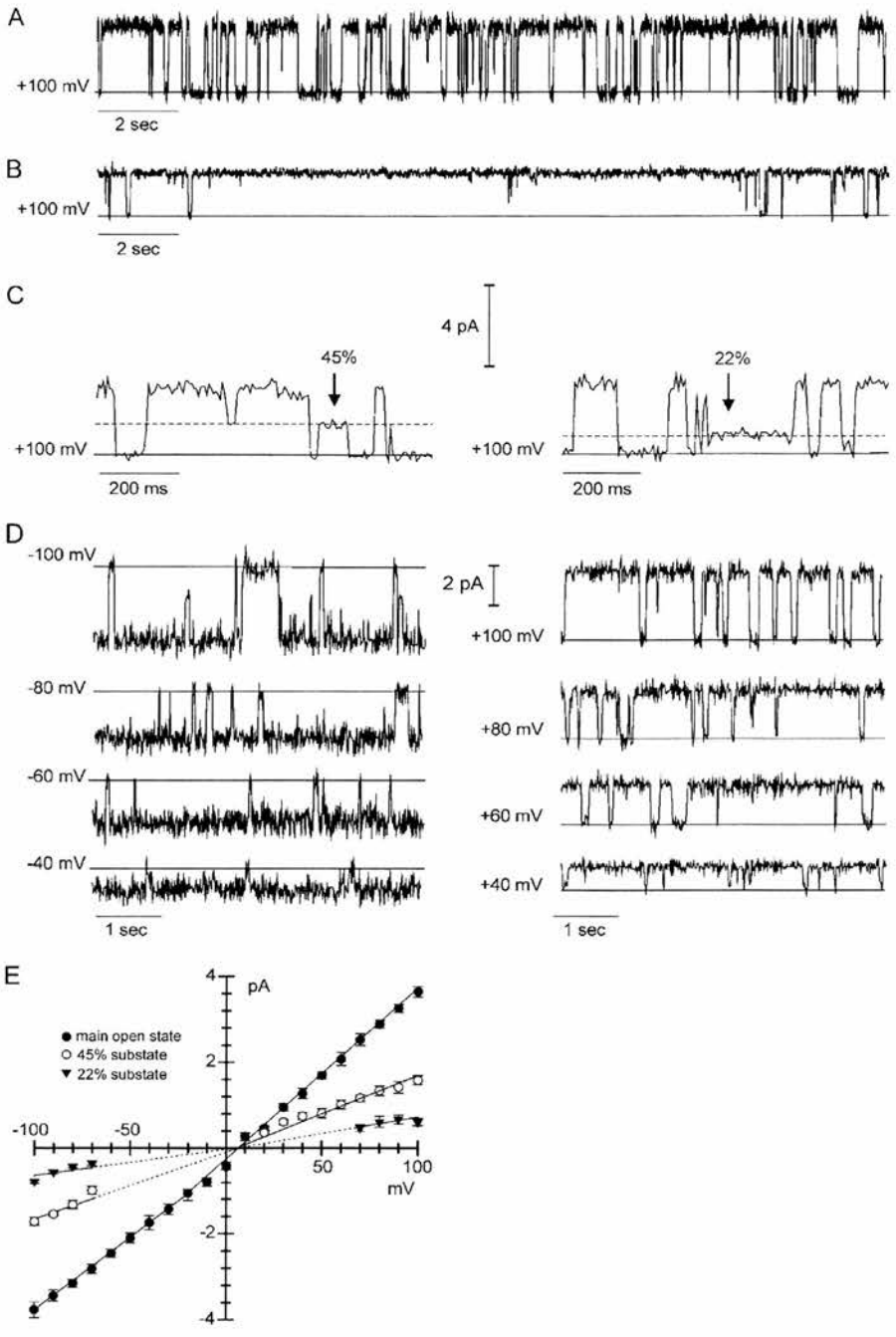

FIGURE 2 CLIC1 channels in asymmetric KCl. Single-channel recordings in 500:50 mM *cis* versus *trans* KCl containing 1 mM DTT, except where indicated. The solid lines indicate the closed current levels. (*A*) Contiguous 20-s recording at a holding potential (HP) of +100 mV. (*B*) Contiguous 20-s recording at +100 mV after exposure of CLIC1 to 100 μM H_2O_2 before and during the recording (without DTT). (*C*) Selected traces on an expanded timescale showing 45% and 22% substates, HP +100 mV. (*D*) Single-channel currents at a range of holding potentials. (*E*) Corresponding current/voltage (I/V) relationships for the main open level and the two substates (shown as mean ± SD, $n = 10$–23). The dotted lines are extrapolations (e.g., where substate amplitudes became too small to measure).

The channel currents appeared to saturate at elevated holding potentials, but the slope conductance of the main open state was constant between +70 mV and −70 mV, with a mean value of 20.5 ± 3 pS (mean ± SD, $n = 7$). Examples of I/V plots for full openings at relatively high and low values for [KCl] are summarized in Fig. 4 *B*. The conductances of the fully open state and the two substates appeared to show a nonhyperbolic dependence on KCl activity (Fig. 4 *C*), although we could not obtain measurements at very low salt concentrations to confirm this behavior, and the maximum conductance of the fully open state was 57 ± 3.5 pS (mean ± SD, $n = 7$) in symmetric 500 mM KCl (corresponding to an activity of 325 mM). However, there was a marked decline in conductance at higher salt activities (also illustrated in Fig. 4 *B*). The conductance of the channel was maintained at negative holding potentials, but reduced at positive potentials, in a *cis* versus

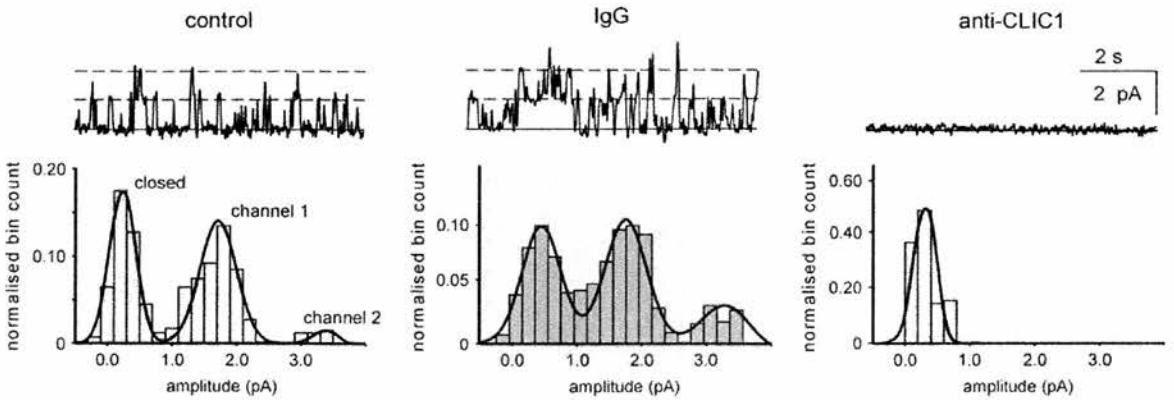

FIGURE 3 Effect of antibodies on CLIC1. Up to three recombinant CLIC1 channels in symmetrical 100 mM KCl containing 1 mM DTT. The zero-current levels are indicated by solid lines, and open channels are indicated by dashed lines. Nonspecific IgG and specific anti-CLIC1 antibodies were added where shown to a final concentration of 10 μg/ml. The amplitude histograms were constructed from long contiguous recordings lasting 60 s.

trans gradient of 500:50 mM Tris-HCl (pH 7.4) (Fig. 5 *A*), with a reversal potential of +45 ± 3.2 mV (mean ± SD, $n = 8$) (Fig. 5 *B*), reflecting a substantial increase in anion/cation permeability to 13 ± 1.0 (mean ± SD, $n = 8$, not corrected for activities).

The relative permeability of a series of anions was measured under equilibrium conditions (see Methods) by perfusing the *cis* chamber with either 50 mM or 110 mM KCl (corrected for activities), followed by perfusing different potassium salts with exactly the same activity into the *trans* chamber. With (symmetrical) salt activities of 50 mM, the anion permeability sequence, calculated from the equilibrium potential as described under Methods, was I^- (1.9 ± 0.1) > SCN^- (1.2 ± 0.2) ≥ Cl^- (set to 1.0) ≥ NO_3^{2-} (0.9 ± 0.1) ≥ Br^- (0.8 ± 0.1) ≥ F^- (0.7 ± 0.1). At 110 mM, the sequence became I^- (1.8 ± 0.1) > F^- (1.3 ± 0.15) = SCN^- (1.2 ± 0.3) > Cl^- (set to 1.0) = NO_3^{2-} (1.0 ± 1.0) = Br^- (1 ± 1.6) (all mean ± SD, $n = 3$ independent experiments).

CLIC1 is sensitive to redox potential

CLIC1 was reconstituted in the presence of 5 mM GSH instead of 1 mM DTT to investigate the effects of redox potential in detail, using a glutathione redox buffer system. As noted earlier, the conductance of the channels was lower in GSH (this appeared to be due to *trans* rather than *cis* GSH), although they retained the same substate pattern. They also remained open or closed for longer, often 1–10 s at our resolution (see, e.g., Fig. 6 *A*), too long to collect enough events for detailed gating analysis. Channels occasionally "gearshifted" into a similar gating mode in DTT, and an example of this behavior is shown later. Additions of GSSG to the *cis* chamber did not affect the single-channel conductance, but sequential additions of GSSG to the *trans* chamber decreased it from 26 ± 1.3 pS to a minimum of 2.9 ± 0.6 pS (mean ± SD, $n = 5$) at a redox potential of −195 mV. The effect could be reversed by reverting to a redox potential of −225 mV (5 mM GSH with 0.5 mM GSSG) in the *trans* chamber (Fig. 6 *A*). The substate amplitudes were also reduced, eventually becoming immeasurably small (<~0.1 pA).

Based on a simple model for channel formation consistent with the previously proposed topology for membrane CLICs (6) (Fig. 7 *A*), we tested the idea that the conductance changes summarized in Fig. 6 *B* reflect disulphide bond formation (leading to the "closure" of an open channel) and reduction (channel opening). In that case, reactions between neighboring pairs of channel subunits can be described by the equilibrium

$$P(SH)_2 + GSSG \rightleftharpoons P(SS) + 2GSH, \quad (4)$$

where "P(SS)" and "$P(SH)_2$" represent channel subunits with and without disulphide bonds, respectively. The kinetics are represented as intersubunit bonding because CLIC1 subunits must already be closely associated with each other in the membrane (by noncovalent interactions) to form a functional channel. The channels could undergo "graded" changes in amplitude, without resolving individual "step-like" changes between conducting (free thiol) and nonconducting (disulphide-bonded) conformations, if the disulphides are reduced relatively rapidly. This recalls the "smooth" ion channel block normally seen with (blocker) dissociation rates $>10^5$/s, but the analogous rate in the model could of course be much slower, given the relatively heavy filtering used (22).

Employing standard mass-action treatment for the equilibrium, the disulphide and dithiol distributions can be described in terms of an equilibrium constant (K_{ox}, molar units) and the ratio $[GSH]^2/[GSSG]$:

$$K_{ox} = \{[P(SS)]/[P(SH)_2]\} \times \{[GSH]^2/[GSSG]\}. \quad (5)$$

The total channel protein (P_t) is the "time-averaged" sum of the reduced and oxidized protein ($[P(SH)_2] + [P(SS)]$), giving the proportion of reduced protein (corresponding to the relative conductance of the channel) as

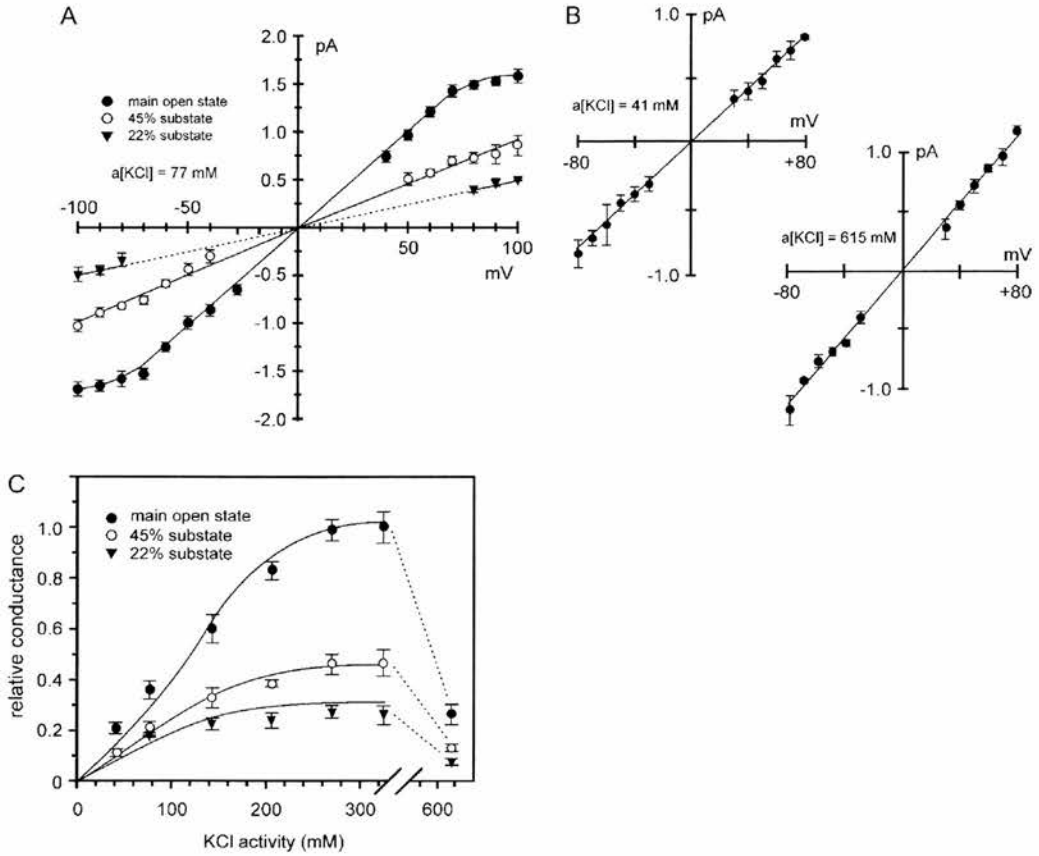

FIGURE 4 CLIC1 channels in symmetric KCl. (*A*) I/V relationships for each conductance level in 100 mM symmetric KCl (a[KCl] = 77 mM) containing 1 mM DTT (points are shown as mean ± SD, $n = 5$–7). The main open state is fitted to a straight line between +70 and −70 mV by linear regression ($r^2 > 0.99$). Other points are fitted by eye, with dotted lines to indicate extrapolations. (*B*) Examples of I/V relationships in low and high KCl activities, showing the main open state only (points are shown as mean ± SD, $n = 3$). (*C*) Relative single-channel conductance-activity relationships for each conductance level in symmetric KCl solutions (points are shown as mean ± SD, $n = 3$–7), fitted by eye. The conductance in symmetric 500 mM KCl (a[KCl] = 325 mM) is set to 1.0. Note the break in the x axis between 300 and 600 mM.

$$[P(SH)_2]/\{[P(SS)] + [P(SH)_2]\} = \{[GSH]^2/[GSSG]\}/\{K_{ox} + [GSH]^2/[GSSG]\}. \quad (6)$$

Abbreviating $[GSH]^2/[GSSG]$ to $R \times [GSH]$ (where R is defined as [GSH]/[GSSG]),

$$[P(SH)_2]/[P_t] = R \times [GSH]/\{K_{ox} + R \times [GSH]\}. \quad (7)$$

As predicted, a plot of the (main open state) channel conductance versus the [GSH]/[GSSG] ratio R, using the data summarized in Fig. 6 *B*, can be fitted to a rectangular hyperbola (Fig. 7 *B*). Additional data obtained at a GSH concentration of 2.5 mM are also plotted and fitted in the same way. The maximum conductances (at the asymptotes) coincide at ~40 pS, similar to the conductance in fully reducing conditions (DTT). The channels cannot be fully reduced in GSH containing even minor amounts of contaminating GSSG (e.g., from autooxidation). The values of R required for half-reduction (i.e., half the maximum channel conductance) correspond to K_{ox}/[GSH], yielding ~25 mM for K_{ox}, irrespective of the GSH concentration.

Membrane topology of CLIC1

To test our simple model in more detail, we investigated the topology of membrane CLIC1 after preserving the N-terminal His tag. As described earlier, the tag did not affect the conductance or selectivity of the reconstituted channels. Whereas the channels remained unaffected by 50 μM *cis* $NiCl_2$, channel activity disappeared in 15 of 15 experiments after stirring 50 μM $NiCl_2$ into the *trans* chamber (e.g., Fig. 8 *A*, which also provides an example of a "gearshifted" channel, as described earlier). Nontagged channels were unaffected (15 experiments). This suggested that the N-terminus of CLIC1 was on the *trans* side of the bilayer. The first cysteine residue (C24) is

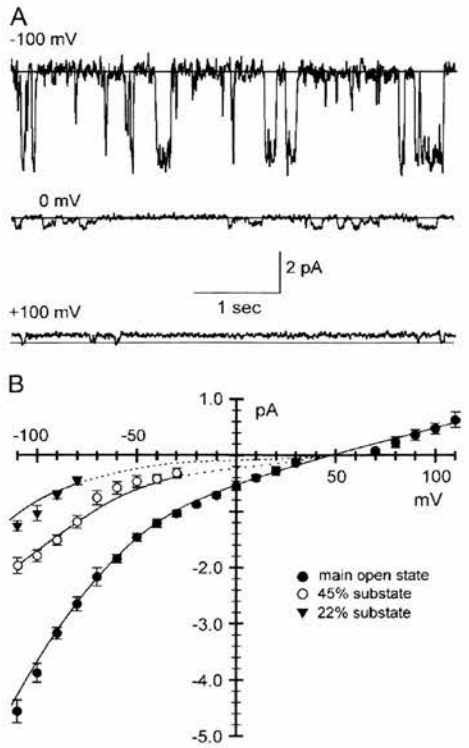

FIGURE 5 CLIC1 channels in Tris Cl. (*A*) Examples of single-channel currents in asymmetric Tris Cl (500:50 mM, *cis* versus *trans*) containing 1 mM DTT. The solid lines indicate the closed current levels. (*B*) I/V relationships for each conducting level (points are shown as mean ± SD, $n = 5$–8), fitted by eye. The mean reversal potential is +45 mV.

located just before the start of the putative TMD (6), and is therefore also predicted to be on the *trans* side of the bilayer, close to the putative pore-forming region of (oligomeric) CLIC1 channels (Fig. 7 *A*). Consistent with this location, 20 μM of the relatively bulky thiol-reactive reagent *N*-ethylmaleimide (NEM) blocked CLIC1 channels from the *trans* side in nine of nine experiments (e.g., Fig. 8 *B*). NEM had no effect from the *cis* side, suggesting that any cysteine residues located on this side of the bilayer are inaccessible to NEM, or they are located well away from the pore.

To further investigate the role of C24 as a potential redox- and NEM-sensitive residue on the *trans* side of the channel, it was changed to alanine. CLIC1 C24A formed channels with a reduced conductance of 14.2 ± 1.1 pS (mean ± SD, $n = 9$) in 5 mM GSH, although the reversal potential (in 500 mM vs. 50 mM KCl) was unaltered (+5.7 ± 1.5 mV, mean ± SD, $n = 9$). Addition of Ni^{2+} to His-tagged proteins confirmed the channels remained orientated with the N-terminal tag facing the *trans* chamber. However, in nine successive experiments, the mutagenized channels, in contrast to unmodified CLIC1, were insensitive to both *trans* oxidation and *trans* NEM (e.g., Fig. 9).

DISCUSSION

Channel formation by CLIC1 is lipid-dependent

Although CLIC1 inserted readily into monolayers containing different lipids, it only assembled into specific ion channels in well-defined planar bilayers containing phosphatidylethanolamine, phosphatidylserine, and cholesterol, 4:1:1 (mol/mol). Highly specific anti-CLIC1 antibodies inhibited CLIC1 activity from the opposite side of the bilayer after adding soluble CLIC1, confirming that the protein was an essential molecular component of the channels, and that it extended through the membrane. Other lipid mixtures may prove to be equally effective, but we did not obtain consistent channel activity in any of the other lipids we tested. This suggests that although CLIC1 monomers may be able to insert into a variety of lipid membranes, native membrane CLIC1 may only assemble into functional ion channels in organelles or membrane domains containing specific lipid components. Membrane cholesterol is known to regulate pore formation by many channel-forming toxins (23), and it may be particularly relevant that in some cases (e.g., *Vibrio cholerae* cytolysin), it may help to promote oligomerization (24).

Recent observations in microglia strongly support the idea that CLIC1 channels have an important role in cells (11), and other CLIC family members may also form ion channels by a broadly similar mechanism, although the membrane structures remain undetermined. CLIC4 (originally called p64H1), the first CLIC protein to be described, was cloned (25) in an attempt to identify the gene family encoding an intracellular IAA-94-sensitive anion channel (26) colocalized with rat brain ryanodine-sensitive Ca^{2+}-release channels (27). Rat CLIC4 is 98% identical to human CLIC4 and 67% identical to human CLIC1, and CLIC1 and CLIC4 are expressed together even in relatively primitive nervous systems (28), raising the possibility of an extended ion channel family. One reassuring characteristic of "authentic" ion channels is the accompanying evolution of regulatory mechanisms at several different levels. In this respect, many CLICs (including p64, or CLIC5B (29)) are targeted to specific organelles, where they may be localized and possibly regulated by specific protein/protein interactions (10,30). The function of membrane CLIC1 also appears to be controlled by a novel mechanism involving cysteine oxidation, and this new finding is discussed in more detail later.

Ion permeation through CLIC1

CLIC1, with six cysteine thiols, was always prepared and stored under reducing conditions, normally a stoichiometric excess of DTT. These precautions are necessary because oxidized, soluble CLIC1 forms a noncovalently linked dimer containing an intramolecular disulphide bond (16). Although the oxidized protein inserted into tip-dip bilayers to form channels of ~30 pS (16), compared to our finding of 24 pS for "preoxidized" CLIC1 channels, soluble CLIC1 is unlikely to exist in an oxidized form in the cytosol, which is

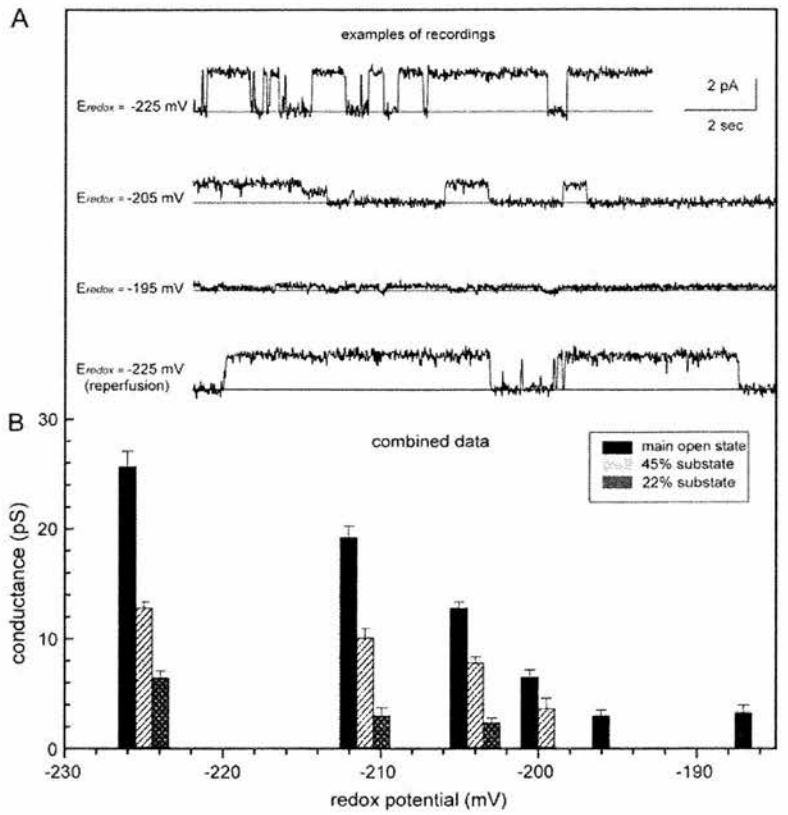

FIGURE 6 Effect of redox potential on CLIC1. (*A*) Selected traces in 500 vs. 50 mM KCl, HP +100 mV. The solid lines indicate the closed current levels. CLIC1 currents decrease as the redox potential in the *trans* chamber is varied from −225 mV to −195 mV using a 5 mM 2GSH/GSSG buffer system, and the effect is reversible. (*B*) Summary of single-channel slope conductances (shown as mean ± SD, $n = 5$) in 2GSH/GSSG buffers providing the indicated redox potentials in the *trans* chamber. Overall, the main open state conductance decreases ~10-fold with oxidation (see text).

relatively reducing and contains up to 10 mM GSH. We therefore maintained CLIC1 (or at least "cytosolic" CLIC1) in reducing conditions, and took care not to oxidize the protein before reconstituting it.

CLIC1's substates, at 22% and 45% of the main open level, resemble two of the substates reported earlier in tip-dip bilayers (12). Similar substates in anion channels reconstituted from rat brain microsomes (26) and sheep heart inner mitochondrial membrane vesicles (20,31) were shown to be consistent with the presence of four conducting "protomers" displaying different gating cooperativities or correlations, depending on the number of protomers open at a given instant. A similar model for CLIC1 channels requires a minimum of 16 subunits per channel (four per "protomer", if each subunit contains just a single TMD), suggesting that cross-linked membrane complexes of functional CLIC1 channels will have a relatively large mass of at least 450,000 daltons. Some of the large conductances previously recorded for putative CLIC channels may reflect the association of groups of highly cooperative subunits into even larger structures.

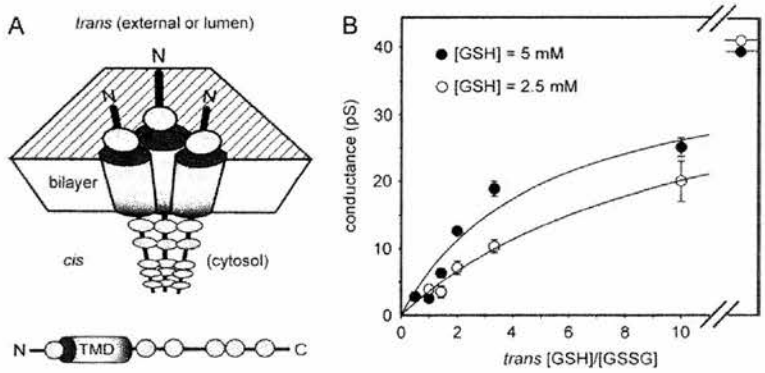

FIGURE 7 A model for CLIC1 channel assembly and regulation. (*A*) Cartoon view (from above and to the side) of membrane CLIC1 subunits modeled as a tetrameric ion channel, with the front subunit removed. "TMD" is a single putative transmembrane domain, and the six cysteine residues in each subunit are indicated (not to scale). Note that each membrane subunit has a single *trans* cysteine, close to the "external" pore entrance. The channels could also be modeled with more than four subunits. (*B*) Conductance data for the fully open state from Fig. 6 *B* (●, mean ± SD, $n = 5$), together with similar data from additional experiments in the presence of 2.5 mM GSH (○, mean ± SD, $n = 3$), plotted against the [GSH]/[GSSG] ratio and fitted (by least squares) to rectangular hyperbolae. The fits give maximum conductances of 39 pS and 41 pS, respectively (indicated on the asymptotes, *upper right*). The corresponding K_{ox} values (described in the text) are 25 mM and 26.5 mM, respectively.

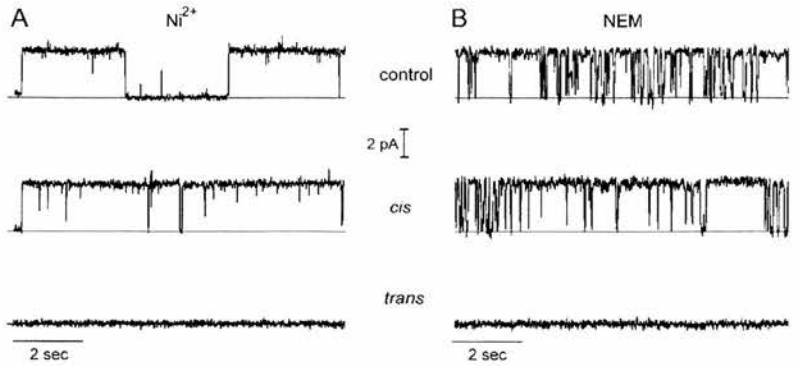

FIGURE 8 Effects of Ni^{2+} and NEM on CLIC1. (*A*) Addition of 50 μM Ni^{2+} to the *cis* and *trans* chambers of His-tagged channels reconstituted in 500 mM vs. 50 mM KCl in the presence of 1 mM DTT, HP +100 mV. Note the "alternative" gating mode shown in this example (see text). (*B*) Addition of 20 μM NEM to the *cis* and *trans* chambers of CLIC1 channels reconstituted in 500 vs. 50 mM KCl in the presence of 1 mM DTT, HP +100 mV. The DTT was removed by perfusion before making any additions. In each recording, the solid lines indicate the closed current levels.

CLIC1 is clearly a multi-ion channel (32), as demonstrated by the dependence of relative anion selectivities (as defined by reversal potentials) on ionic activity, the apparently nonhyperbolic relationship between conductance and activity, and the dramatic reduction in currents at very high activities. Although the conductances reported here are consistent with values calculated for CLIC1 in cell membranes (9), very little information is available on the selectivity of cellular CLIC1, and its relative anion versus cation selectivity has not been determined in cells. The reconstituted channels are poorly selective for anions versus cations, although their selectivity for anions improves markedly as the size of the permeant cation is increased, similar to the behavior of rat brain microsomal anion channels (26), which also showed a similar anion permeability sequence at equivalent (50 mM) activities. Overall, our results suggest that CLIC1 is a nonselective pore rather than a specific anion channel, and this obviously has significant functional implications for CLICs in cells (as well as for their nomenclature).

Redox regulation and cysteine 24

The striking *trans* redox sensitivity of CLIC1 suggested that at least one of its cysteine residues might be functionally important. Supporting this idea, *trans* NEM blocked CLIC1 (after removing free thiols from solution), but *cis* NEM had no effect. Together with a subtle but consistent voltage dependence (slightly noisier openings at negative holding potentials), this suggested the channels were inserted in a specific direction in the membrane. Because NEM actually blocked the channels, the reactive *trans* cysteine(s) were probably located in or near the pore. To help orientate CLIC1, we reconstituted the protein with an intact N-terminal His tag, knowing that membrane insertion continued under these circumstances. The tagged channels appeared to assemble normally, and their properties were indistinguishable from nontagged proteins, except that $NiCl_2$ interfered with channel activity from the *trans*, but not the *cis*, chamber. Thus, both the N-terminus, and the relevant cysteine residue(s), were

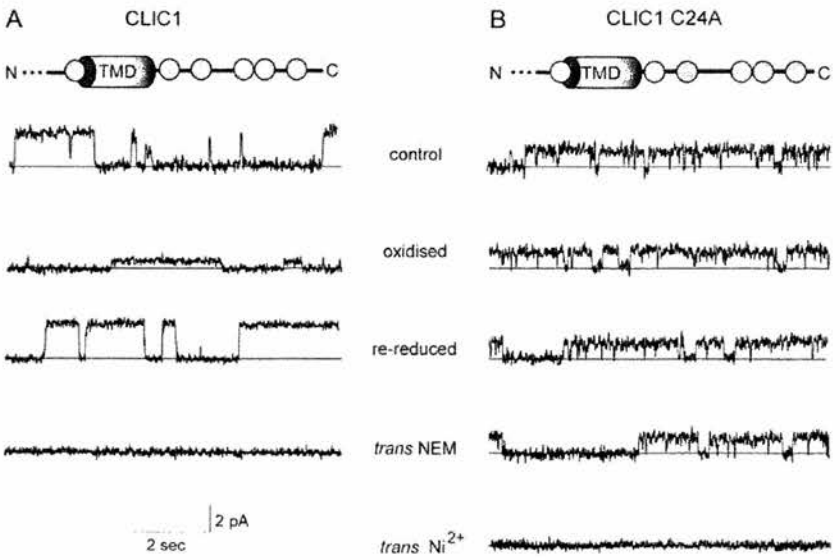

FIGURE 9 Comparison of CLIC1 and CLIC1 C24A currents. His-tagged CLIC1 and CLIC1 C24A reconstituted in 500 vs. 50 mM KCl containing 5 mM GSH and recorded at a HP of +100 mV. The cartoons (also see Fig. 7 *A*) summarize the locations of the cysteine residues, the position of the predicted TMD, and replacement of C24 by alanine (○). (*A*) CLIC1 single-channel currents responding to alterations in *trans* redox potential (−225 mV, −195 mV, and −225 mV, respectively) and block by 20 μM *trans* NEM. (*B*) CLIC1 C24A showing reduced overall conductance, insensitivity to the same changes in *trans* redox potential, and lack of block by 20 μM *trans* NEM. Note that 50 μM *trans* Ni^{2+} continues to inactivate the channel. In each recording, the solid lines indicate the closed current levels.

located in the *trans* chamber, corresponding to the extracellular or luminal side of the protein.

Experiments involving protease digestion (2) and antibodies targeted to the N- or C-terminus (7,8) are consistent with a single ~20-residue TMD near the N-terminus of membrane CLICs, just after the first of two cysteine-proline (CP) motifs common to many CLIC proteins, from *Xenopus* to higher organisms including mammals (28). Although the predicted TMD contains a tryptophan residue, which is atypical for a pore-lining region, this could be relevant for membrane (auto)insertion. In the *Caenorhabditis elegans* CLIC-like protein exc-4, substituting proline for a leucine residue in the middle of the predicted TMD, or truncating the domain, prevented membrane insertion (33). The presence of several potential cytosolic protein interaction and phosphorylation sites, from the predicted TMD all the way to the C-terminus (6), supports the idea that membrane CLICs contain just a single TMD, located near the (extracellular or *trans*) N-terminus, with the remainder of the protein in the cytosol. In this simple model for the membrane form of CLIC1, conducting channels must contain a minimum of four subunits, and in each subunit C24 is the only cysteine residue on the *trans* side of the membrane, in the CP motif just before the predicted TMD.

Implications for cellular CLIC1

Although C24 is very likely to be reduced in the cytosol, insertion of the residue into the lumen of certain intracellular organelles (e.g., the endoplasmic reticulum), or exposure to the oxidizing extracellular environment, could in principle result in disulphide bonds between neighboring subunits, if the residues approach closely enough. Our study is consistent with a simple functional model in which reversible disulphide bonds between neighboring subunits close or "block" the channel, provided the rate of reformation of free thiols is too fast to be resolved in our recordings. Oxidation would then also increase the apparent mean open (and closed) lifetimes, and although qualitatively this appeared to be the case, we could not collect enough events for statistical analysis. In a 2GSH/GSSG buffer, disulphide bond formation can be distinguished from the formation of glutathione mixed disulphides, because plots of relative reduced protein versus the [GSH]/[GSSG] ratio do not alter with [GSH] for the latter, as they do in our experiments. The model also explains the higher conductance of the channels in the presence of DTT ($E^0 = -312$ mV) compared to GSH, and the relatively low K_{ox} value (~25 mM) reflects the low stability of disulphide bonding in the protein compared to GSSG.

We tested the idea that C24 is the relevant redox- and NEM-sensitive residue in CLIC1 membrane subunits by replacing it with alanine. In the absence of structural data for the membrane proteins, we cannot of course exclude the possibility that CLIC1 C24A adopts an entirely new membrane conformation that not only relocates the original redox- and NEM-sensitive cysteine residue(s), but also forms an ion channel (with, rather surprisingly, the same selectivity). However, the simplest way to explain why CLIC1 C24A is insensitive to *trans* oxidation and functional covalent modification by *trans* NEM is that C24 and A24 are both on the *trans* side of the pore. In this location, C24 may form conformationally important extracellular (or intraorganellar) disulphide bonds between neighboring subunits, explaining the redox-sensitivity of the channels, and its location in or near the putative pore-forming region could explain why the single-channel conductance is modified when C24 is replaced by alanine (as in this study), and possibly eliminated altogether when replaced by serine (16). Further work to support and extend this model could include recordings at much enhanced resolution, replacement of the remaining CLIC1 cysteines (other than C24), and investigation of the potential role of the neighboring residue, P25.

5-HT_3 receptor channels appear to be gated by *cis-trans* isomerization of a proline residue linking two transmembrane helices at the entrance to the transmembrane pore (34). If P25, in the well-conserved (28) CLIC1 CP motif discussed earlier, has a role in the gating of CLIC1, a constraining disulphide bond might interfere with side-chain flipping, and lock the pore closed (but not, apparently, open). In conclusion, our channel model predicts that CLIC1, even if it inserts into membranes and assembles into a channel-competent form in an appropriate lipid region, will be poorly conducting at best if its N-terminus is inserted into an oxidizing microenvironment (e.g., the endoplasmic reticulum, or possibly a patch-pipette), or if it faces the outside of the cell. However, the channel will become functionally relevant (and easier to detect) as the extracytosolic environment is made reducing. These predictions can be tested in future work involving native and overexpressed CLIC1 (and CLIC1 C24A) in cells.

H.S. was supported by a University of Edinburgh College of Medicine and Veterinary Medicine Scholarship, and by the Overseas Research Students Award Scheme.

REFERENCES

1. Valenzuela, S. M., D. K. Martin, S. B. Por, J. M. Robbins, K. Warton, M. R. Bootcov, P. R. Schofield, T. J. Campbell, and S. N. Breit. 1997. Molecular cloning and expression of a chloride ion channel of cell nuclei. *J. Biol. Chem.* 272:12575–12582.
2. Duncan, R. R., P. K. Westwood, A. Boyd, and R. H. Ashley. 1997. Rat brain p64H1, expression of a new member of the p64 chloride channel protein family in endoplasmic reticulum. *J. Biol. Chem.* 272:23880–23886.
3. Harrop, S. J., M. Z. DeMaere, W. D. Fairlie, T. Reztsova, S. M. Valenzuela, M. Mazzanti, R. Tonini, M. R. Qiu, L. Jankova, K. Warton, A. R. Bauskin, W. M. Wu, S. Pankhurst, T. J. Campbell, S. N. Breit, and P. M. Curmi. 2001. Crystal structure of a soluble form of the intracellular chloride ion channel CLIC1 (NCC27) at 1.4-Å resolution. *J. Biol. Chem.* 276:44993–45000.
4. Cromer, B. A., C. J. Morton, P. G. Board, and M. W. Parker. 2002. From glutathione transferase to pore in a CLIC. *Eur. Biophys. J.* 31: 356–364.

5. Dulhunty, A., P. Gage, S. Curtis, G. Chelvanayagam, and P. Board. 2001. The glutathione transferase structural family includes a nuclear chloride channel and a ryanodine receptor calcium release channel modulator. *J. Biol. Chem.* 276:3319–3323.
6. Ashley, R. H. 2003. Challenging accepted ion channel biology: p64 and the CLIC family of putative intracellular anion channel proteins (Review). *Mol. Membr. Biol.* 20:1–11.
7. Tonini, R., A. Ferroni, S. M. Valenzuela, K. Warton, T. J. Campbell, S. N. Breit, and M. Mazzanti. 2000. Functional characterization of the NCC27 nuclear protein in stable transfected CHO-K1 cells. *FASEB J.* 14:1171–1178.
8. Proutski, I., N. Karoulias, and R. H. Ashley. 2002. Overexpressed chloride intracellular channel protein CLIC4 (p64H1) is an essential molecular component of novel plasma membrane anion channels. *Biochem. Biophys. Res. Commun.* 297:317–322.
9. Valenzuela, S. M., M. Mazzanti, R. Tonini, M. R. Qiu, K. Warton, E. A. Musgrove, T. J. Campbell, and S. N. Breit. 2000. The nuclear chloride ion channel NCC27 is involved in regulation of the cell cycle. *J. Physiol.* 529:541–552.
10. Suginta, W., N. Karoulias, A. Aitken, and R. H. Ashley. 2001. Chloride intracellular channel protein CLIC4 (p64H1) binds directly to brain dynamin I in a complex containing actin, tubulin and 14–3-3 isoforms. *Biochem. J.* 359:55–64.
11. Novarino, G., C. Fabrizi, R. Tonini, M. A. Denti, F. Malchiodi-Albedi, G. M. Lauro, B. Sacchetti, S. Paradisi, A. Ferroni, P. M. Curmi, S. N. Breit, and M. Mazzanti. 2004. Involvement of the intracellular ion channel CLIC1 in microglia-mediated beta-amyloid-induced neurotoxicity. *J. Neurosci.* 24:5322–5330.
12. Warton, K., R. Tonini, W. D. Fairlie, J. M. Matthews, S. M. Valenzuela, M. R. Qiu, W. M. Wu, S. Pankhurst, A. R. Bauskin, S. J. Harrop, T. J. Campbell, P. M. Curmi, S. N. Breit, and M. Mazzanti. 2002. Recombinant CLIC1 (NCC27) assembles in lipid bilayers via a pH-dependent two-state process to form chloride ion channels with identical characteristics to those observed in Chinese hamster ovary cells expressing CLIC1. *J. Biol. Chem.* 277:26003–26011.
13. Tulk, B. M., P. H. Schlesinger, S. A. Kapadia, and J. C. Edwards. 2000. CLIC-1 functions as a chloride channel when expressed and purified from bacteria. *J. Biol. Chem.* 275:26986–26993.
14. Tulk, B. M., S. Kapadia, and J. C. Edwards. 2002. CLIC1 inserts from the aqueous phase into phospholipid membranes, where it functions as an anion channel. *Am. J. Physiol. Cell Physiol.* 282:C1103–C1112.
15. Dulhunty, A. F., P. Pouliquin, M. Coggan, P. W. Gage, and P. G. Board. 2005. A recently identified member of the glutathione transferase structural family modifies cardiac RyR2 substate activity, coupled gating and activation by Ca^{2+} and ATP. *Biochem. J.* 390: 333–343.
16. Littler, D. R., S. J. Harrop, W. D. Fairlie, L. J. Brown, G. J. Pankhurst, S. Pankhurst, M. Z. DeMaere, T. J. Campbell, A. R. Bauskin, R. Tonini, M. Mazzanti, S. N. Breit, and P. M. Curmi. 2003. The intracellular chloride ion channel protein CLIC1 undergoes a redox-controlled structural transition. *J. Biol. Chem.* 279:9298–9305.
17. Miller, C. 1984. Ion channels in liposomes. *Annu. Rev. Physiol.* 46: 549–558.
18. Jez, J. M., J. L. Ferrer, M. E. Bowman, R. A. Dixon, and J. P. Noel. 2000. Dissection of malonyl-coenzyme A decarboxylation from polyketide formation in the reaction mechanism of a plant polyketide synthase. *Biochemistry.* 39:890–902.
19. Harroun, T. A., J. P. Bradshaw, and R. H. Ashley. 2001. Inhibitors can arrest the membrane activity of human islet amyloid polypeptide independently of amyloid formation. *FEBS Lett.* 507:200–204.
20. Hayman, K. A., T. S. Spurway, and R. H. Ashley. 1993. Single anion channels reconstituted from cardiac mitoplasts. *J. Membr. Biol.* 136: 181–190.
21. Brockman, H. 1999. Lipid monolayers: why use half a membrane to characterize protein-membrane interactions? *Curr. Opin. Struct. Biol.* 9:438–443.
22. Yellen, G. 1984. Ionic permeation and blockade in Ca^{2+}-activated K^+ channels of bovine chromaffin cells. *J. Gen. Physiol.* 84:157–186.
23. Palmer, M. 2004. Cholesterol and the activity of bacterial toxins. *FEMS Microbiol. Lett.* 238:281–289.
24. Olson, R., and E. Gouaux. 2005. Crystal structure of the *Vibrio cholerae* cytolysin (VCC) pro-toxin and its assembly into a heptameric transmembrane pore. *J. Mol. Biol.* 29:997–1016.
25. Howell, S., R. R. Duncan, and R. H. Ashley. 1996. Identification and characterisation of a homologue of p64 in rat tissues. *FEBS Lett.* 390: 207–210.
26. Clark, A. G., D. Murray, and R. H. Ashley. 1997. Single-channel properties of a rat brain endoplasmic reticulum anion channel. *Biophys. J.* 73:168–178.
27. Ashley, R. H. 1989. Activation and conductance properties of ryanodine-sensitive calcium channels from brain microsomal membranes incorporated into planar lipid bilayers. *J. Membr. Biol.* 111: 179–189.
28. Shorning, B. Y., D. B. Wilson, R. R. Meehan, and R. H. Ashley. 2003. Molecular cloning and developmental expression of two chloride intracellular channel (CLIC) genes in *Xenopus laevis*. *Dev. Genes Evol.* 213:514–518.
29. Redhead, C., S. K. Sullivan, C. Koseki, K. Fujiwara, and J. C. Edwards. 1997. Subcellular distribution and targeting of the intracellular chloride channel p64. *Mol. Biol. Cell.* 8:691–704.
30. Shanks, R. A., M. C. Larocca, M. Berryman, J. C. Edwards, T. Urushidani, J. Navarre, and J. R. Goldenring. 2002. AKAP350 at the Golgi apparatus. II. Association of AKAP350 with a novel chloride intracellular channel (CLIC) family member. *J. Biol. Chem.* 277:40973–40980.
31. Hayman, K. A., and R. H. Ashley. 1993. Structural features of a multisubstate cardiac mitoplast anion channel: inferences from single-channel recording. *J. Membr. Biol.* 136:191–197.
32. Hille, B. 1992. Ionic Channels of Excitable Membranes, 2nd ed. Sinauer Associates, Sunderland, MA. 374–389.
33. Berry, K. L., H. E. Bulow, D. H. Hall, and O. Hobert. 2003. A *C. elegans* CLIC-like protein required for intracellular tube formation and maintenance. *Science.* 302:2134–2137.
34. Lummis, S. C. R., D. L. Breene, L. W. Lee, H. A. Lester, R. W. Broadhurst, and D. A. Dougherty. 2005. *Cis-trans* isomerization at a proline opens the pore of a neurotransmitter-gated ion channel. *Nature.* 438:248–252.

Molecular Membrane Biology
2007, 1–12, PrEview article

informa
healthcare

CLIC4 (p64H1) and its putative transmembrane domain form poorly selective, redox-regulated ion channels

HARPREET SINGH & RICHARD H. ASHLEY

Biomedical Sciences, College of Medicine, University of Edinburgh, Edinburgh, UK

(Received 10 March 2006; and in revised form 3 July 2006)

Abstract
Despite being synthesized in the cytosol without a leader sequence, the soluble 253-residue mammalian protein CLIC4 (Chloride Intracellular Channel 4, or p64H1), a structural homologue of Ω-type glutathione-S-transferase, autoinserts into membranes to form an integral membrane protein with ion channel activity. A predicted transmembrane domain (TMD) near the N-terminus of CLIC4 could mediate membrane insertion, and contribute to oligomeric pores, with minimal reorganization of the soluble protein structure. We tested this idea by reconstituting recombinant CLIC4 in planar bilayers containing phosphatidyethanolamine, phosphatidylserine and cholesterol, recording ion channels with a maximum conductance of ~15 pS in KCl under both oxidizing and reducing conditions. The channels discriminated poorly between anions and cations, incompatible with the current "CLIC" nomenclature, and their conductance was modified by the *trans* (external or luminal) redox potential, as previously observed for CLIC1. We then reconstituted a truncated version of the protein, limited to the first 61 residues containing the predicted TMD. This included a single *trans* cysteine residue in the putative pore-forming subunits, at the external entrance to the pore. The truncated protein formed non-selective channels with a reduced conductance, but they retained their *trans*-redox sensitivity, and could still be blocked or inactivated by *trans* (not *cis*) thiol-reative dithiobisnitrobenzoic acid. We suggest that oligomers containing the putative TMD are essential components of the CLIC4 pore. However, the pore is inherently non-selective, and any ionic selectivity in CLIC4 (and other membrane CLICs) may be attributable to other regions of the protein, including the channel vestibules.

Keywords: *Anion channel, p64, planar bilayer, redox potential*

Introduction

Chloride Intracellular Channel (CLIC) proteins are unique among putative eukaryotic ion channels in being able to assume both soluble and membrane forms. CLICs also bypass the conventional secretory pathway, and "autoinsert" directly into membranes [1,2]. The proteins are related to p64, a putative anion channel purified from bovine kidney by drug affinity chromatography in pioneering work by Al-Awqati and his colleagues [3] before being cloned [4] and characterized in considerable detail (e.g. [5]). However, it has yet to be established (by single-channel recording) that p64 alone is sufficient to form an ion channel, in contrast to the best-studied CLIC protein, CLIC1 [6].

The first CLIC protein to be discovered, rat brain CLIC4 (p64H1, or p64 homologue 1), known in mouse as mitochondrial or mtCLIC [7], was identified and cloned by homology to p64 [8,9] as a potential candidate for an intracellular anion channel previously shown to be co-localized with rat brain ryanodine-sensitive calcium-release channels [10]. CLIC4 isologues are now known to be very widespread, and the proteins are highly conserved in vertebrates ranging from fish to mammals [11]. The structure of a soluble form of human CLIC4 (crystallized with a short random C-terminal extension) is similar [12] to previously crystallized, soluble human CLIC1 [13], as anticipated by modelling CLIC4 onto CLIC1 [2]. Like CLIC1, soluble CLIC4 has an Ω-glutathione-S-transferase (GST) fold, but although Ω-GSTs and CLICs are structurally similar, and distantly related, they do not have overlapping functions. In particular, Ω-GSTs do not autoinsert into membranes and form ion channels [14], and CLIC proteins appear to have little or no enzymatic activity.

In addition to brain and kidney, *CLIC4* mRNA is also expressed in many other mammalian tissues including lung, liver, skeletal muscle, testis and skin

Correspondence: Richard H. Ashley, Biomedical Sciences, College of Medicine, University of Edinburgh, George Square, Edinburgh EH8 9XD, UK. Tel: +44(0) 131 650 3873. Fax: +44(0) 131 650 3711. E-mail: Richard.Ashley@ed.ac.uk

ISSN 0968-7688 print/ISSN 1464-5203 online
DOI: 10.1080/09687860600927907

[7,9]. A putative "cytoplasmic domain" containing most of the protein formed complexes involving brain actin, dynamin I, tubulin and 14-3-3 proteins [15], and cytoplasmic CLIC4 has been shown to co-localize with A-kinase anchoring proteins (AKAPs) in specific cellular microdomains, including centrosomes and the cortical actin cytoskeleton [16]. The much less abundant [15] membrane form of CLIC4 is an integral (not peripheral [9]) membrane protein localized to several intracellular organelles, including the endoplasmic reticulum and outer nuclear membrane [9], (inner) mitochondrial membranes [7], and the membranes of dense core secretory vesicles [17], caveolae and (possibly) the trans-Golgi network [18]. It has also been localized to the plasma membrane [18,19], especially near intercellular junctions [16].

CLIC4 levels are dynamically regulated, and increase with tumour necrosis factor-α and p53 signalling [7]. Interestingly, CLIC4 overexpression induces p53-mediated apoptosis associated with mitochondrial depolarisation, cytochrome C release and caspase activation [20]. Although it is not yet clear whether this involves the soluble or membrane form of the protein, or both, possible implication of a putative mitochondrial ion channel in apoptosis could clearly be very significant. It is however notable that some cells, especially mammalian cells, express many different CLIC proteins, suggesting that some or all of their functions may be redundant. For example, transgenic mice lacking CLIC1 appear to be essentially normal apart from increased weight, splenomegaly and mild thrombocythaemia [21].

In contrast to CLIC1, relatively little is known about CLIC4-associated ion channels. Although the incorporation of microsomal membrane vesicles containing recombinant CLIC4 into planar lipid bilayers gave rise to novel anion channel activity of 10–50 pS [9], this could have been due to the activation of unidentified endogenous channels, especially since another CLIC, CLIC2, has been shown to be a channel modulator rather than an ion channel itself [22]. CLIC4 (possibly with the short C-terminal extension required for crystallisation) gave rise to channel activity in "tip-dip" bilayers [12], but the conductance of the channel was unclear (reported as both 31 pS and 57 pS). Novel ion channels specifically shown to contain FLAG-tagged CLIC4 have also been recorded by patch-clamping the plasma membrane of cells overexpressing the protein [19]. In the presence of large cations (to limit endogenous cation currents), the conductance of individual CLIC4 channels appeared to be very low, of the order of 1 pS. Currents through CLIC1 are now known to be regulated by the external redox potential [23], and if CLIC4 shows a similar mechanism, this may help to explain the very small single-channel currents observed by patch-clamping. Also, as discussed later, the use of large cations may have further reduced the CLIC4 currents.

We set out to investigate the single channel properties of CLIC4 under various redox conditions, because in contrast to a previous report [12], the protein can form channels under both reducing and non-reducing conditions, like CLIC1 [23]. We then tested a simple model for the transmembrane topology of CLIC4 that can be extrapolated to CLIC1 and other membrane CLICs, by reconstituting a truncated protein containing the N terminus of CLIC4 and its single putative transmembrane domain (TMD). We also determined whether CLIC4 is sensitive to the *trans* (extracellular or luminal) redox potential in the presence of a glutathione buffer, like CLIC1 [23], and whether a critical cysteine residue on the *trans* side of membrane CLIC4 subunits, corresponding to the GSH-binding "G-site" of Ω-GSTs, mediates this unusual effect.

Materials and methods

Expression and purification of CLIC4

We cloned rat brain *CLIC4* (*p64H1*, [9]) into pHis8, a modified pET vector encoding an N-terminal octa-His tag and a thrombin cleavage site [24], and inserted a stop codon into one clone by "Quik-Change" PCR to truncate the expressed protein at CLIC4 position 61. The inserts were verified by DNA sequencing (MWG Biotech), and fusion proteins were expressed in *E. coli* BL21 (DE3) cells and recovered from cell lysates by Ni^{2+}-NTA affinity chromatography, with yields for the soluble thrombin-cleaved full-length and truncated proteins of 4.0 ± 0.50 mg/l and 2.0 ± 0.65 mg/l (means $\pm$ SD, $n = 15$ or 3), respectively (determined by the Lowry method using appropriate standards). The preparations were analysed by SDS-PAGE and gel-exclusion FPLC using Superdex 200 (by methods detailed in [25]), and protein aliquots (which had at no stage been exposed to detergents) were stored for up to 3 months at -70°C in the presence of 5 mM DTT. The masses of proteins subjected to gel-exclusion FPLC were determined from a plot of log(Mr) vs. K_{av} (the corrected partition coefficient):

$$K_{av} = (V_e - V_o)/(V_t - V_o)$$

where V_e, V_o and V_t represent the elution volume, the void volume and the packed bed volume, respectively.

Channel incorporation into planar lipid bilayers

Planar bilayers were prepared at room temperature (20°C) using lipids selected from: palmitoyl-oleoyl phosphatidylcholine (POPC), PO-phosphatidylethanolamine (POPE), PO-phosphatidylserine (POPS) and cholesterol (all from Avanti, AL, USA), as detailed in the Results section. Briefly, the lipids were suspended in n-decane (25 μg total lipid/μl), and films were cast across a 0.3 mm hole in a polystyrene partition separating two chambers. The chambers, designated *cis* and *trans*, contained 50 mM KCl with 10 mM Tris-HCl (pH 7.4) and 1 mM DTT, unless otherwise specified, and were connected by agar salt bridges to the headstage input or ground, respectively, of an Axopatch 200-B amplifier, minimising and offsetting liquid junction potentials as previously described [26]. After the lipid film had thinned spontaneously to form a planar bilayer, monitored by measuring a relatively abrupt increase in membrane capacitance from <50 pF to >200 pF, the *cis* chamber was clamped at various holding potentials (HPs) relative to the *trans* chamber, and up to 25 ng/ml purified protein was stirred into the same chamber, followed by small aliquots of 5 M KCl to raise the KCl concentration to 500 mM. Transmembrane currents appeared within 10 min of adding the (full-length) protein, and were digitally recorded. Thereafter, the contents of the chambers were changed by perfusion (at least 10 volumes) as required.

Single-channel analysis

Single-channel currents (labelled following the standard electrophysiological convention, i.e., positive currents represent net cation flux from *cis* to *trans*), were low-pass filtered (8-pole, Bessel type response) at 50 Hz or 25 Hz and analysed with pClamp8 (Axon Instruments) and pStat (SPSS), using amplitude histograms as previously described [23] to measure channel amplitudes and open probabilities (Po). Salt concentrations were converted to activities using standard tables, and (relative) anion permeabilities (P) were calculated under equilibrium conditions using the Nernst equation:

$$P_{\text{anion}}/P_{\text{Cl}} = \text{a[Cl]}_{cis}/\text{a[anion]}_{trans} \times \exp(-\text{zFEr/RT})$$

where a is the activity coefficient of the relevant salt, Er is the reversal or equilibrium potential, and z, F, R and T have their usual significance. Relative anion vs. cation permeabilities (selectivities) were calculated from the following form of the Goldman-Hodgkin-Katz (GHK) voltage equation:

$$P_{\text{anion}}/P_{\text{cation}} = \{\text{n} \times \exp(\text{Er/k})\} - 1/\{\text{n} - \exp(\text{Er/k})\}$$

where n is the *cis*/*trans* salt activity ratio and k = RT/zF (26 mV).

Results

CLIC4 ion channels in fully-reducing conditions

CLIC4 recordings had an inconsistent appearance in experiments using POPC or equimolar POPE and POPS, but like CLIC1 [23], the protein formed highly consistent channels in 80/83 bilayers containing POPE, POPS and cholesterol, 4:1:1 mol/mol, respectively, in the presence of 1 mM DTT, 5 mM GSH or 100 μM H_2O_2. In the latter case, the protein was also exposed to 100 μM H_2O_2 for 5–10 min. before incorporation. Channel activity appeared more rapidly at an acidic *cis* pH of 5.5. However, these recordings were very noisy, and low pH conditions were not pursued further. No channel-like events were seen during prolonged (up to 30 min.) observation of control bilayers in the absence of added protein (15 experiments).

Figure 1A shows examples of recordings obtained in 1 mM DTT, representing "fully-reducing" conditions. The slope conductance of the main open state in a *cis:trans* gradient of 500:50 mM KCl with 1 mM DTT in both chambers was 10.3 ± 1.0 pS (mean $\pm$ SD, $n = 15$), calculated (by linear regression) from the linear region of the I/V plot (-100 mV to $+70$ mV) (Figure 1B). We noted several substates, including the prominent ~25% substate shown here. The reversal potential of the main open state was -12.2 ± 3.3 mV (mean + SD, $n = 15$) (Figure 1B), corresponding to a mean Cl^-/K^+ selectivity of 0.54 ± 0.09, i.e., a poorly selective or even mildly cation-selective channel. The Er for the ~25% substate was similar, and we observed direct transitions to and from both states (inset in Figure 2B). The main open state conductance was ohmic in symmetrical KCl solutions (e.g., inset I/Vs in Figure 2), but showed a complicated dependence on KCl activity (Figure 2, main panel). Up to ~ 350 mM, the relationship could be described as the sum of a hyperbolic and a linear component, but the maximum single-channel conductance was 13.8 ± 0.60 pS (mean $\pm$ SD, $n = 5$), and it declined at higher KCl activities, consistent with self-block.

We measured relative anion permeabilities at equilibrium under biionic conditions in the presence of 1 mM DTT by perfusing 50 mM KCl (corrected for activity) into the *cis* chamber, and different potassium salts with the same activity into the *trans* chamber. Relative anion permeabilities calculated from the equilibrium potential were the same for 5 test anions compared to Cl^- (set to 1.0): SCN^- (0.97 ± 0.11); NO_3^- (1.1 ± 0.50); I^- (1.1 ± 0.96);

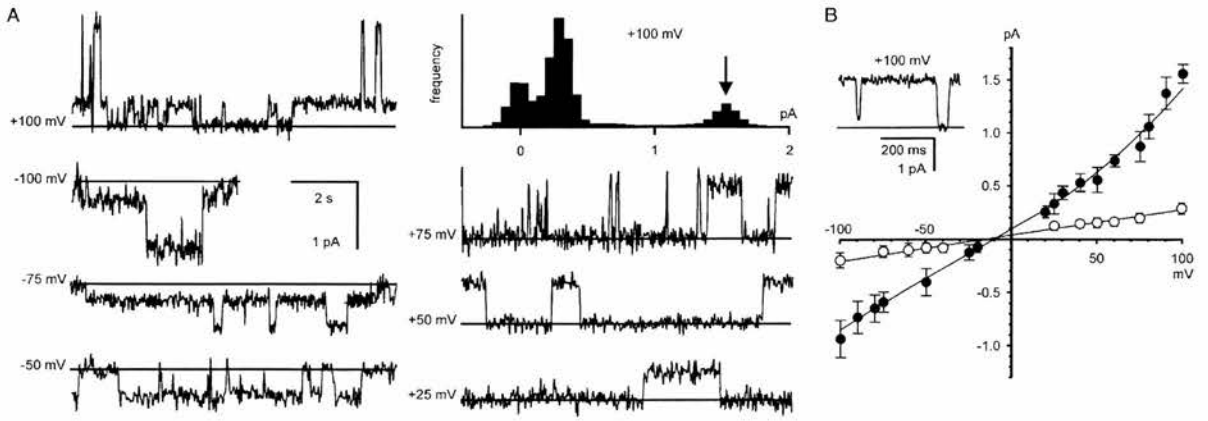

Figure 1. Bilayer reconstitution of CLIC4 in the presence of 1 mM DTT. Part A shows examples of recordings at selected holding potentials, with solid lines to indicate the closed levels, and an example of an all-points amplitude histogram from 30 sec of the +100 mV recording (the arrow indicates the maximum open level). Part B summarizes the I/V relationship of the main open level and a ~25% substate, from 15 independent experiments with 500 mM KCl *cis* vs. 50 mM KCl *trans*. The bars indicate ±1 SD, and the line was fitted by eye (see text for linear regression analysis). The inset shows examples of direct transitions between the ~25% substate, the main open level and the closed level, on an expanded time scale.

Br^- (1.3±0.50); F^- (1.4±0.95). The values in parentheses are the mean±SD for 4 independent comparisons in each case, and as expected they are not significantly different ($p > 0.5$). Single-channel currents were also obtained in 500 mM:50 mM *cis* vs. *trans* TrisCl (pH 7.4) in the presence of 1 mM DTT (Figure 3A). As shown in Figure 3B, the conductance was reduced to 2.6±0.43 pS (mean± SD, $n=7$), but the reversal potential was +11± 6.1 mV (mean±SD, $n=7$), giving a mean Cl^-/ $Tris^+$ selectivity of 1.8±0.51 (not corrected for activities). The difference in relative anion vs. cation selectivity compared to KCl is highly significant ($p < 0.001$).

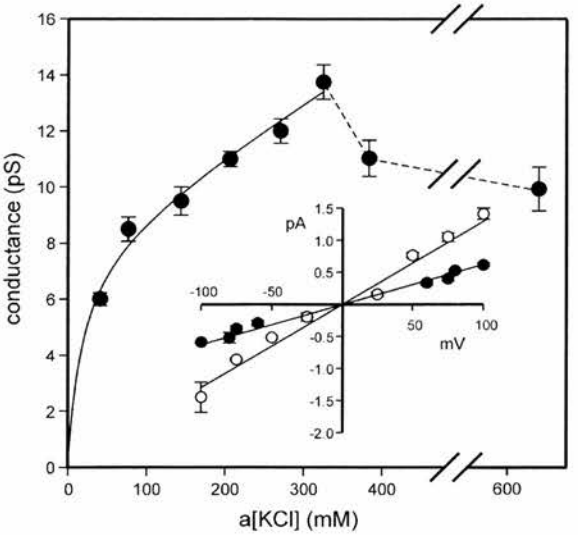

Figure 2. Conductance/activity relationship of CLIC4. The data in the main panel (shown as means±SD from 5 independent experiments) were fitted (by least squares) to the sum of a hyperbolic component with a g_{max} of 8.2 pS and a "K_m" of 19.1 mM plus a non-saturating linear component of 0.017 pS per mM KCl. The relationship breaks down at KCl activities >325 mM (as shown by the dotted lines – note the break in the plot between 400–600 mM KCl). The inset I/V relationships provide examples of the I/V data used to calculate the conductance at low (40 mM, closed circles) and high (325 mM, open circles) activities (points are means±SD, $n=5$, lines fitted by linear regression).

CLIC4 ion channels in other redox conditions

H_2O_2-oxidized CLIC4 channels were reconstituted in the presence of 100 μM H_2O_2 ("fully-oxidizing" conditions). Ion channels (Figure 4A) appeared more rapidly compared to the reduced protein, and had a slope conductance of 8.9±1.1 pS (mean±SD, $n=5$) in a *cis:trans* gradient of 500:50 mM KCl, measured (by linear regression) over the linear part of the I/V plot between −100 mV and +25 mV (Figure 4B). This value was indistinguishable from the conductance of channels reconstituted in the presence of DTT ($p > 0.5$). The oxidized channels displayed several substates, and the reversal potential of the main open state was +6.5±6.6 mV (mean± SD, $n=5$) under fully oxidizing conditions, corresponding to mildly anion-selective channels with a mean Cl^-/K^+ selectivity of 1.4±0.48.

Channels were also obtained in a *cis:trans* gradient of 500:50 mM KCl from (non pre-oxidized) CLIC4 in 5 mM glutathione, corresponding to "physiological" redox conditions [23], e.g., Figure 5. The single-channel currents had higher amplitudes at positive holding potentials (i.e., they were outwardly-rectifying, if *cis* is equivalent to the cell

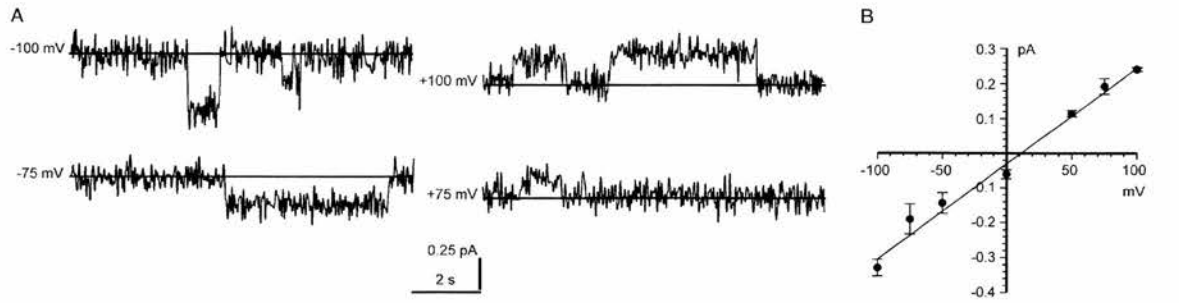

Figure 3. CLIC4 currents in Tris-HCl (pH 7.4). Examples of CLIC4 currents (part A) and a combined I/V relationship from several independent experiments (part B, means ± 1 SD, $n = 7$) in the presence of 1 mM DTT with 500 mM TrisCl *cis* vs. 50 mM TrisCl *trans*. The line was fitted by linear regression.

cytosol), and the maximum slope conductance (with 5 mM GSH/0.5 mM GSSG *cis* and *trans*) was 14.8 ± 1.6 pS (mean ± SD, $n = 5$, calculated by linear regression between −25 mV and +100 mV). The reversal potential of +8.8 ± 4.0 mV (mean ± SD, $n = 5$) (Figure 5B) corresponded to a mean Cl^-/K^+ selectivity of 1.5 ± 0.27. As previously observed for CLIC1 [23], the apparent single-channel slope conductance was modulated by the *trans* redox potential when this was manipulated in a GSH buffer. Sequential additions of GSSG to the *cis* chamber had no effect, but sequential additions of GSSG to the *trans* chamber (e.g., to give [GSH]/[GSSG] ratios of 2:1 or 1:1, as shown in Figure 5A), markedly decreased the apparent single-channel currents. This could be reversed by reverting to a redox potential of −225 mV (5 mM GSH with 0.5 mM GSSG) in the *trans* chamber (also shown in Figure 5A).

Like CLIC1 [23], channel recordings in GSH buffers were less noisy, and contained fewer substates, than recordings under fully-reducing or fully-oxidizing conditions (i.e., in the presence of DTT or H_2O_2, respectively). The excess channel noise we observed in the absence of a glutathione buffer was largely attributable to short-lived or poorly-resolved substates, possibly suggesting that fully-oxidised or fully-reduced membrane CLICs failed to adopt a single, optimally-folded conformation. Consistent with this idea, replacing the *cis* glutathione buffer with 1 mM DTT appeared to induce substates following channel incorporation (e.g., Figure 5C).

Single-channel properties of the putative TMD of CLIC4

As shown in Figure 6, the truncated protein, comprising the first 61 residues of CLIC4 (predicted Mr 6,800), including the N-terminus and the putative TMD [2,11], showed appropriate mobilities on SDS-PAGE, and appropriate retention times during gel-exclusion FPLC (consistent with a monomeric solution, like the full-length protein, which is shown for comparison). We reconstituted truncated CLIC4 into bilayers of the same composition as before (POPE, POPS and cholesterol, 4:1:1 mol/

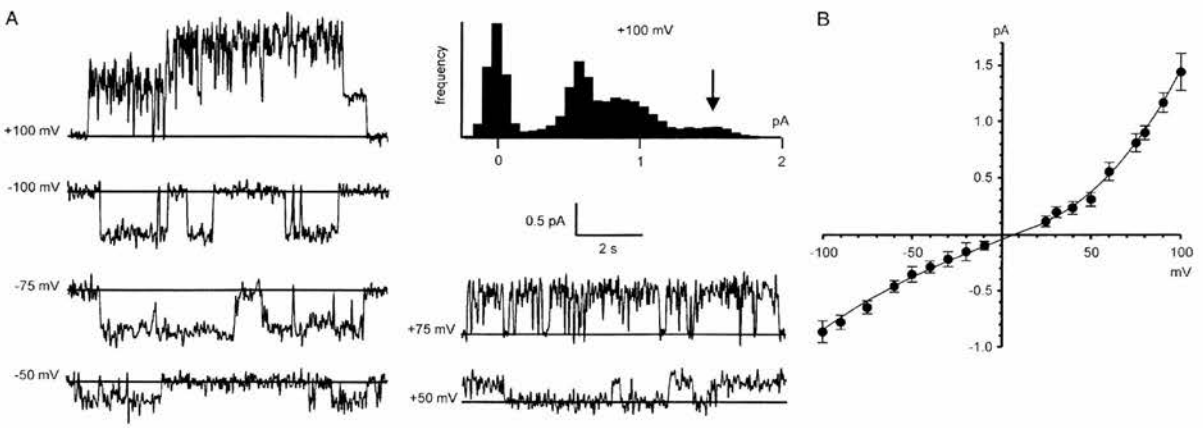

Figure 4. Bilayer reconstitution of CLIC4 in the presence of 100 μM H_2O_2. Part A shows examples of recordings at selected holding potentials, and an example of an all-points amplitude histogram from 30 sec of the +100 mV recording (the arrow indicates the maximum open level). Part B summarizes the I/V relationship obtained from 5 independent experiments (means ± 1 SD, $n = 5$). The line was fitted by eye (see text for linear regression analysis). All the data were obtained with 500 mM KCl *cis* vs. 50 mM KCl *trans*.

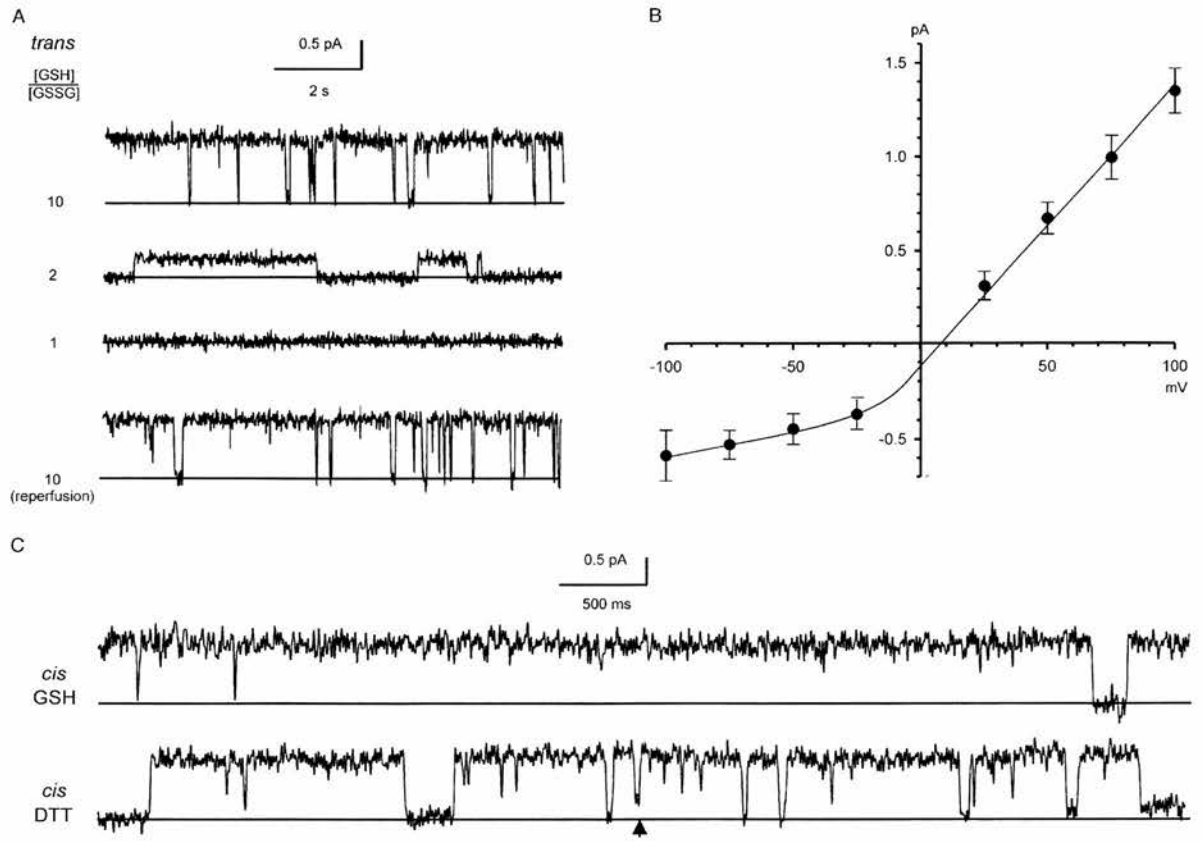

Figure 5. Bilayer reconstitution of CLIC4 in glutathione buffers. Part A shows recordings in 5 mM GSH (*cis* and *trans*), with GSSG added sequentially to the *trans* chamber to give the indicated GSH/GSSG ratios. Part B shows a combined I/V relationship from 5 independent experiments (means $\pm$SD) with 5 mM GSH/0.5 mm GSSG both *cis* and *trans* The line was fitted by eye (see text for results of linear regression analysis). The traces in part C (underfiltered, and on an expanded time scale), illustrate the appearance of substates (best-resolved where indicated by the arrowhead) immediately after replacing the *cis* glutathione buffer (5 mM GSH/0.5 mM GSSG) with 1 mM DTT by perfusion. All the data were obtained with 500 mM KCl *cis* vs. 50 mM KCl *trans*, and the recordings were carried out at a HP of + 100 mV.

mol, respectively) but it formed channels less readily, often taking 20–40 min. compared to less than 10 min for the full-length protein. However, once channels had appeared in the bilayer, "single-channel" recordings were highly consistent between experiments, typically showing infrequent low-amplitude currents of $\sim$0.5 pA at a HP or +100 mV. In some experiments we also observed occasional, large-amplitude currents of up to $\sim$1.5 pA at the same HP, especially in the presence of H_2O_2, including 3 independent experiments using only peak II fractions after FPLC of the truncated protein (Figure 6).

Figure 7A compares the appearance of channels formed by the truncated protein under the different oxidizing and reducing conditions described earlier (all at +100 mV), and Figure 7B summarizes their I/V relationships in a *cis:trans* gradient of 500:50 mM KCl. Currents through the truncated protein remained sensitive to the *trans* (but not the *cis*) redox potential, like the full-length protein (Figure 7A). Overall, the conductances and anion vs. cation selectivities of the truncated protein were very similar in the presence of 1 mM DTT, or 5 mM GSH with 0.5 mM GSSG. From an analysis of several independent experiments, the single-channel slope conductances, calculated by linear regression between +25 mV and +100 mV, were 5.5 $\pm$ 0.58 pS and 4.8 $\pm$ 0.61 pS (both means $\pm$SD, n = 5), respectively, for the two different conditions. The values are not significantly different ($p > 0.5$). The relative anion vs. cation selectivities of the truncated proteins, determined from equilibrium potentials measured under the same conditions, were 1.1 $\pm$ 0.27 and 1.0 $\pm$ 0.45, respectively (both means $\pm$SD, n = 5). Again, these values are indistinguishable ($p > 0.5$), and in Figure 7B all the points are fitted to a single line for both conditions.

As noted earlier, pre-oxidized truncated proteins reconstituted in the presence of 100 μM H_2O_2

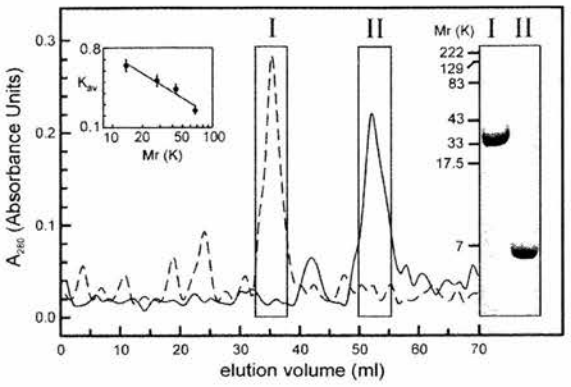

Figure 6. FPLC and SDS-PAGE analysis of full-length and truncated CLIC4. The main panel shows typical gel-exclusion FPLC profiles for full-length (FL) and truncated (TR) proteins in the presence of 5 mM DTT (dashed and solid lines, respectively, shown on the same plot for comparison). Fractions from the boxed peaks (I and II, respectively) were collected and concentrated, and subjected to reducing 10% (w/v) SDS-PAGE and Coomassie-stained as shown. FL and TR proteins show Mr values of ~30 K and ~6–7 K, respectively. The FPLC analysis reveals similar values (V_t was 70 ml, V_o was 4.5 ml, and the K_{av} values for the FL and TR proteins are 0.73 and 0.47, respectively). The column was calibrated (inset plot) with: RNase A (13.7 K), pGEX vector GST (26 K), ovalbumin (43 K) and albumin (67 K).

formed infrequent channels of both "low" and "high" conductance. The former had a slope conductance of 3.8 ± 0.53 pS (mean $\pm$ SD, $n = 5$) measured over the same interval (+25 mV to +100 mV), and a relative anion vs. cation selectivity of 1.2 ± 0.98 (mean $\pm$ SD, $n = 5$). Although these values are not significantly different from those found for the truncated protein in the presence of DTT or glutathione buffers ($p > 0.5$), the experimental points (Figure 7B, open circles) do not appear to align well with the corresponding data obtained using DTT or a glutathione buffer.

Orientation of membrane CLIC4

We previously investigated the bilayer orientation of CLIC1 containing an intact N-terminal His tag by attempting to block or inhibit the channel with 50 μM histidine-reactive Ni^{2+} from the *cis* and *trans* sides in turn, but in similar experiments with CLIC4 the metal ion left some channels unaffected, possibly because the N-terminal region before the putative TMD of CLIC4 is longer and more flexible. As an alternative, we deployed cysteine-specific reagents, also used previously, because the cysteine residues in CLIC4 are located asymmetrically with respect to the putative TMD, just as they are in CLIC1 [2]. As shown later (Figure 9), CLIC4 C35 lies in a cysteine-proline motif on the N-terminal side of the TMD, immediately before the postulated pore entrance. The three remaining cysteines in CLIC4 lie on the other side of the TMD, much further into the primary sequence. C35 is the only cysteine residue in the truncated from of CLIC4.

In contrast to similar experiments with CLIC1 [23], 20 μM NEM had no effect from either side of the bilayer. However, 0.2 mM 5,5′-dithiobis-(2-nitrobenzoic acid) (DTNB) blocked (or inactivated) CLIC4 channels from the *trans* side, but not the *cis* side (e.g., Figure 8). This applied equally to both full-length CLIC4 and the truncated protein (6/6 experiments in each case), and the effect was quantified by measuring the probability of a given channel being open (Po) over successive periods of 60 sec for each condition. The mean Po for full-length and truncated channels exposed to

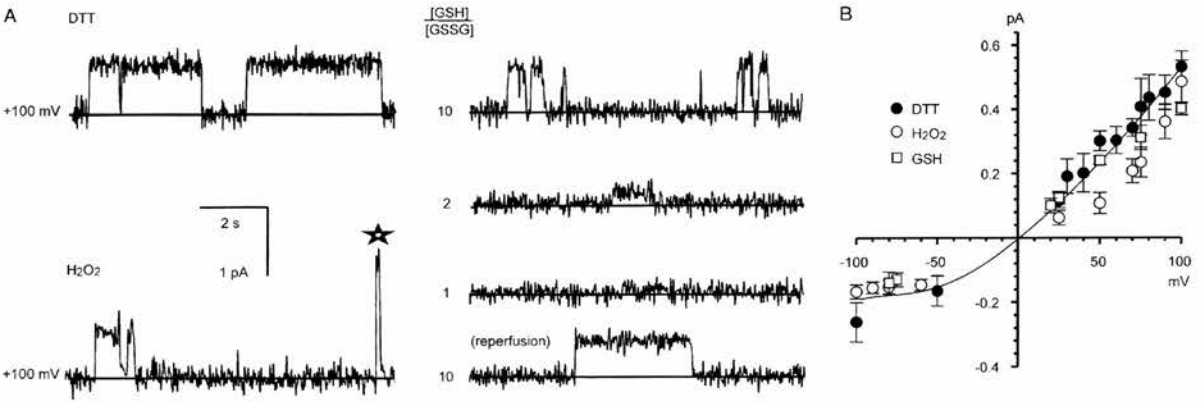

Figure 7. Bilayer reconstitution of truncated CLIC4. Part A compares the appearance of channels at +100 mV in the presence of either 1 mM DTT, 100 μM H_2O_2 (with a star to indicate an unusual large-amplitude opening, see text), or the indicated GSH/GSSG ratios (with [GSH] set to 5 mM), all in a *cis*:*trans* gradient of 500:50 mM KCl. Part B summarizes the corresponding I/V relationships in the presence of 1 mM DTT (closed circles), 100 μM H_2O_2 (open circles) and a 10:1 GSH/GSSG buffer (open squares) (means $\pm$ 1 SD for 5 independent experiments in each case). The line was fitted by eye (see text for results of linear regression analysis).

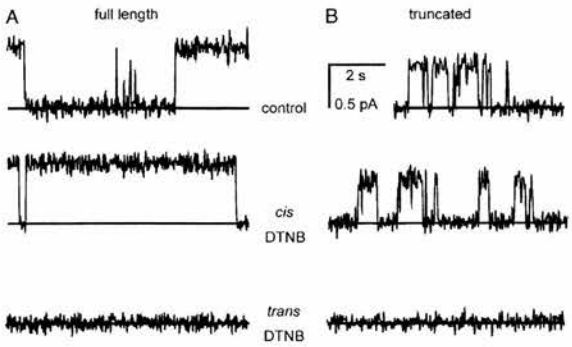

Figure 8. Inhibition of CLIC4 currents by DTNB. Parts A and B show examples of CLIC4 currents from full-length and truncated proteins, respectively, at +100 mV, obtained in the presence of 5 mM GSH (with 500 mM KCl *cis* vs. 50 mM KCl *trans*) before removing the GSH by perfusion with fresh GSH-free solutions. In each case, 0.2 mM DTNB had no effect from the *cis* side, but abolished channel activity when added from the *trans* side. See text for full statistical analysis.

5 mM GSH was 0.63 ± 0.21 and 0.52 ± 0.35, respectively (means $\pm$ SD, $n = 6$). After removing *cis* GSH by perfusion and adding 0.2 mM *cis* DTNB, the Po values were 0.65 ± 0.26 and 0.53 ± 0.34, respectively (means $\pm$ SD, $n = 6$). Following a similar procedure to add 0.2 mM *trans* DTNB, the mean Po values were reduced to 0.05 ± 0.03 and 0.04 ± 0.03, respectively (means $\pm$ SD, $n = 6$).

Although the differences between the mean Po values for control and *trans* DTNB differed significantly, the differences in Po between control and *cis* DTNB, and between control and *trans* DTNB, were also analysed channel by channel by paired *t*-tests, because of the relatively large variation in control Po from channel to channel. This showed no significant difference between control and *cis* DTNB for both full-length and truncated CLIC4 ($p > 0.5$), but significant differences between control and *trans* DTNB in each case ($p < 0.002$ and $p < 0.02$, respectively).

Discussion

Channel activity of CLIC proteins

Despite their structural similarities, Ω-GSTs and CLICs have very distinct functions. In particular, Ω-GSTs remain soluble and have no ion channel activity [14]. However, they are unusual compared to other GSTs in having weak GSH-dependent thioltransferase activities [28]. It has been speculated that this could involve thiol transfer between GSH bound at the G-site (containing the first cysteine residue in the primary sequence), and S-thiolated substrates (including proteins) in an adjacent ligand-binding site (the H-site). In contrast, CLICs appear to have little or no enzymatic activity, but CLIC1 can autoinsert into membranes and form novel ion channels [6]. CLIC proteins contain a single predicted TMD near the N-terminus, which is notable by its absence in Ω-GSTs [2]. In every mammalian CLIC protein, this putative TMD is preceded by an Ω-GST-like "G-site" cysteine residue, in a cysteine-proline motif.

The suggestion that an entire class of soluble eukaryotic proteins, including several mammalian proteins, can bypass the secretory pathway and autoinsert into membranes without any specific insertion machinery, remains highly controversial. In addition, there has been substantial disagreement concerning even the basic properties of the ion channels associated with CLIC1 (the best studied protein) [6,23,29–35]. This includes disagreement over whether the protein can insert into membranes in both oxidized and reduced forms [23], or whether it can only insert as an oxidized protein containing an intrachain disulphide bond [34]. However, the importance of specific membrane lipids, and the sensitivity of reduced membrane CLIC1 to external (or luminal) oxidation, could help to explain many previous inconsistencies. We suggested that membrane CLIC1 oligomers are oxidised and reduced by thiol-disulphide exchange involving GSH, GSSG and external or luminal "G-site"-like subunit cysteines, equivalent to the G-site in Ω-type GSTs. This in turn could regulate channel gating and the overall ion flux through CLIC1 [23]. Thus, channel function may depend on the external (or luminal) redox conditions, which are often poorly-controlled in experiments.

Like CLIC1, proper functional reconstitution of CLIC4 (distinct from simple protein autoinsertion, as shown previously for CLIC1 [23]) required a specific lipid mixture (PE/PS/cholesterol, 4:1:1 mol/mol). Although other, untested, lipid mixtures may also be effective, the presence of cholesterol recalls the specific role of the sterol in cytolysin channel insertion or assembly [36,37], and intracellular membranes contain a similar amount of the free sterol [38]. Alternatively, given that cholesterol and the inverted-cone shaped phospholipid PE are both associated with "curvature stress" in planar membranes, they may promote channel assembly or activity by a physical role similar to the activation of membrane-associated protein kinase C [39].

Channel formation by full-length CLIC4

CLIC4 contains 4 cysteine residues [9] and we reconstituted the membrane protein under a wide range of oxidizing and reducing conditions, including DTT (with a standard redox potential of −330 mV, for "fully-reducing" conditions), GSH/

GSSG (providing "physiological" redox potentials between −225 mV and −195 mV at a pH of 7.4), and 100 μM H_2O_2 ("fully-oxidising" conditions). The channels had a similar maximum conductance of ~15 pS in a *cis* vs. *trans* gradient of 500 mM: 50 mM KCl, but were noisier and displayed more substates in DTT and H_2O_2 compared to GSH. We speculated that the protein only folds optimally under physiological redox conditions. The single-channel conductance/activity relationship contained both hyperbolic and linear components at a[KCl] values up to ~350 mM (in 1 mM DTT), with a paradoxical reduction in conductance above 350 mM, consistent with a multi-ion conduction mechanism (i.e., more than one ion at a time in the selectivity filter).

CLIC4 is poorly-selective between anions and cations, inconsistent with the widely-adopted "CLIC" nomenclature proposed by [18] and [40]. It may be necessary to re-evaluate CLIC proteins, especially CLIC4, as "chloride" channels, if they behave like non-selective channels. This could be due to a wide pore lacking specific ion-binding sites. However, a maximum conductance of ~15 pS in KCl is inconsistent with a wide water-filled pore (as found for example in bacterial porins). Franciolini and Nonner [41,42] noted similar paradoxical behaviour in neuronal "background" Cl^- channels, and suggested that anions and cations crossed the membrane at least partly as counter ions. Based on similar ideas, if the putative pore lining of CLIC4 contains rings of arginine or lysine residues (as suggested in Figure 9), transient binding of permeant anions could provide an opportunity for counter ions (e.g., K^+) to cross the membrane without encountering a prohibitive positive charge.

In a scheme like this, ion permeation requires the presence of anions, and they must be sufficiently small to penetrate the pore. Large, impermeant anions would prevent the passage of both anions and cations (regardless of the latter's size), whereas large, relatively impermeant cations would not prevent all ion permeation, but would make the channel more anion-selective. Consistent with this idea, we noted enhanced anion vs. cation selectivity in the presence of the relatively large cation $Tris^+$ compared to K^+. We also noted that CLIC4 was unable to discriminate between a range of different anions, again consistent with the idea that the pore itself is poorly-selective. However, CLIC1 is slightly but measurably more anion-selective than CLIC4 [23], so if the putative pore-lining is not responsible for this difference (and the sequences are very similar, as shown in Figure 9, suggesting in passing that detailed site-directed mutagenesis studies of putative TMD/pore-lining residues may not be very productive), could other parts of the protein be important for selectivity?

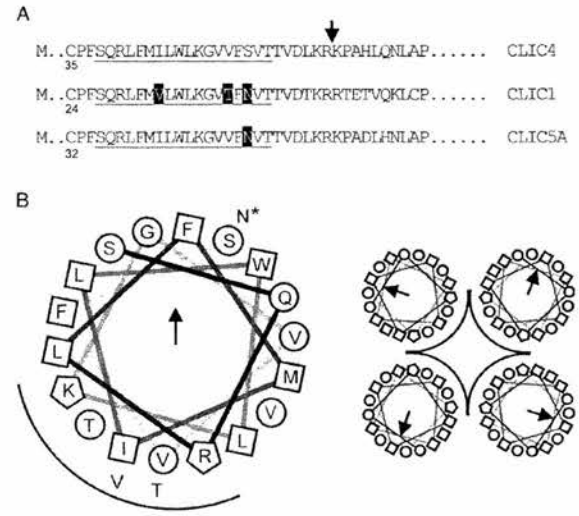

Figure 9. Organization of the putative CLIC TMD. Part A: selected regions of 3 CLICs aligned at the putative 18-residue TMD (underlined). The first cysteine residue in each sequence is numbered, and differences within the TMD are highlighted (rat and human CLIC4 are identical in this region). CLIC4 was truncated where indicated. Part B is a helical wheel projection of the TMD from N to C (D. Armstrong and R. Zidovetzki, http://rzlab.ucr.edu/scripts/wheel/wheel.cgi) with a "tetrameric pore" cartoon. Squares, circles and polygons indicate relatively hydrophobic or hydrophilic residues, or residues with positively charged side chains, respectively. The arrow and the arc indicate the direction of the hydrophobic moment, and suggested pore-lining residues, respectively. The alternative residues in CLIC1 (all 3) and CLIC5A (starred residue only) are also shown.

We also noted enhanced anion vs. cation selectivity in fully-oxidized CLIC4 (exposed to 100 μM H_2O_2) compared to the fully-reduced channel, although the channel remains essentially very poorly-selective. Oxidation of soluble CLIC1 induces a completely new protein conformation involving intrachain disulphide bond formation and non-covalent association into dimers [34], but a similar mechanism has been ruled out for CLIC4 [12], so we speculate that following membrane insertion the pore-lining regions of CLIC4 remain the same irrespective of oxidation or reduction. Instead, we suggest that the difference in selectivity observed here could be due to changes in the charged surface of the protein, away from the putative TMD, that affect the channel vestibule(s) or entrance(s). This suggestion is consistent with experiments involving truncated CLIC4.

Channel formation by truncated CLIC4

Several lines of evidence support the idea that membrane CLICs have a single TMD. Sequence alignments and hydrophobicity plots (e.g., [2,11])

strongly predict a single TMD near the N-terminus, following the first cysteine residue in CLIC1 and CLIC4. This predicted TMD is very obviously absent in Ω-GSTs [2], and it contains a tryptophan residue that could promote membrane autoinsertion. The presence of a single TMD is supported by the positioning of the N- and C-termini of CLIC1 on opposite sides of the membrane [32], by protease digestion studies on membrane CLIC4 [9], by truncation, mutagenesis and membrane localisation studies of the worm protein exc-4 [27,43], and by the presence of potential (and functional) protein interaction sites throughout the "cytosolic" region of, especially, CLIC4 [15]. Based on these findings, we suggest that CLIC4 (and CLIC1) channels are likely to be oligomers comprising at least 4 subunits.

We explored the possibility that a truncated version of CLIC4, comprising the N-terminus and the putative TMD, including a single remaining cysteine residue just before the putative TMD, could form functional ion channels in planar bilayers. Although channel formation proceeded less rapidly, the truncated protein formed ion channels with consistent appearances from experiment to experiment, with a reduced conductance compared to the full-length protein. This reduction is consistent with the idea that the missing parts of the protein form charged channel vestibules that "concentrate" permeant ions near the entrance to the pore [44]. Channels formed from the truncated protein were non-selective, regardless of redox conditions, again consistent with the idea that the missing extramembranous regions of the protein, rather than specific ion binding sites in the pore, confer the (poor) ionic selectivity of full-length CLIC4. Overall, we suggest that under partially- or fully-reducing conditions, despite the absence of much of the protein, including all the potential "cytosolic" domains, the truncated subunits continue to associate (by non-covalent interactions) to form a functional pore.

The truncated protein also formed functional pores under fully-oxidizing conditions, although pore formation occurred much less frequently. Under these conditions, two conductances were recorded, one slightly less than the pores formed under reducing conditions, and another whose conductance was substantially higher. The oxidized proteins presumably insert into bilayers as preformed disulphide-linked dimers, and then associate with other similar dimers in the membrane to form functional channels. However, *trans*-oxidized CLIC4 is normally poorly-conducting (see below), so we speculate that these pores must be assembled from a relatively large number of pre-linked dimers in order to produce a patent pore, compared to fewer pairs of monomers for the reduced protein. Occasional even larger assemblies could explain the infrequent high conductances we observed.

Orientation and redox-regulation of membrane CLIC4

CLIC1 inserted into bilayers with a well-defined orientation, with its N-terminus facing the *trans* ("extracellular" or "luminal") side of the membrane [23]. The same topology was expected for CLIC4, especially given that all the protein interaction sites known to be located between the putative TMD and the C-terminus [27] are cystosolic. This orientation places the first cysteine residue in membrane CLIC monomers in the *trans* chamber, immediately before the predicted TMD. Consistent with this orientation, CLIC4 was sensitive to the *trans* redox potential in glutathione buffers (as discussed below). However, in contrast to CLIC1, NEM had no effect on CLIC4, suggesting that in this case NEM may not have been able to react covalently with the relevant residue, or the reaction had no functional consequences. In contrast, DTNB inhibited the channel, and it only acted from the *trans* side. We speculate that the pore-associated cysteines in CLIC4 oligomers, equivalent to the "G-site" cysteine in Ω-GSTs that forms mixed disulphides with GSH [1], can react with DTNB to form mixed disulphides that block the channel pore or interfere with channel opening.

The maximum slope conductance of full-length CLIC4 showed a substantial and reversible dependence on the *trans* redox potential in glutathione buffers. This is similar to the behaviour of CLIC1, which was analysed in detail [23] and attributed to reversible disulphide bond formation involving pairs of subunits in the presence of GSH and GSSG. The "smooth" reduction in single-channel currents was consistent with rapid reduction and oxidation of the relevant thiol groups in the presence of the glutathione buffer system, at rates too fast to be resolved under the filtering conditions used. The requirement for relatively heavy filtering of CLIC channels in planar bilayers, and their relative long-lived open and closed times, precludes any meaningful channel gating analysis, because recordings would have to be very long in order to collect enough events. Truncated CLIC4 retained its sensitivity to the *trans* redox potential in glutathione buffers, strongly supporting the idea that the effect is mediated by C35, which is the only cysteine left in the truncated protein.

The sensitivity of the channels to extracellular (or luminal) redox conditions could have significant effects on the amplitude of CLIC4 currents recorded *in vitro* (e.g., [9]) and *in vivo* (e.g., [19]), making it difficult to compare recordings unless the *trans*

redox potential is well controlled. In addition, our selectivity data and their interpretation suggest that large cations (e.g., $Tris^+$) may have a dual effect – to reduce single-channel currents (especially with very large cations), and also make the channels more anion-selective. The anion vs. cation selectivities of both CLIC1 and CLIC4 may therefore be "artificially" improved in the presence of relatively large cations like N-methyl-D-glucamine$^+$, often used in patch-clamp experiments to reduce endogenous cation currents.

Conclusion

Our results suggest that mammalian membrane CLIC4 forms poorly-selective, oligomeric ion channels modulated by luminal (or external) GSH-dependent transthiolation. Its redox-sensitivity may shed more light on the role of CLIC4 in apoptosis [20], and at this stage it would be very helpful to establish the stoichiometry of the channel (the tetramer in Figure 9 is entirely speculative), and confirm the topology of its subunits. However, even if CLIC4 monomers contain just a single TMD, other parts of the protein may still contribute in unanticipated ways to the ion channel pore. In common with other transporters, a full understanding of ion permeation through membrane CLICs, and channel regulation by oxidation, awaits detailed structural analysis. As an added complication, it will be especially important to obtain membrane structures relevant to functional channels, with predictable electrophysiological properties, as opposed to the structures of proteins that insert into membranes without forming specific ion channels [23].

Acknowledgements

HS was supported by a University of Edinburgh College of Medicine and Veterinary Medicine Scholarship, and by the Overseas Research Students Award Scheme.

References

[1] Cromer BA, Morton CJ, Board PG, Parker MW. From glutathione transferase to pore in a CLIC. Eur Biophys J 2002;31:356–364.

[2] Ashley RH. Challenging accepted ion channel biology: p64 and the CLIC family of putative intracellular anion channel proteins (Review). Mol Membr Biol 2003;20:1–11.

[3] Landry DW, Akabas MH, Redhead C, Edelman A, Cragoe EJ, Al-Awqati Q. Purification and reconstitution of chloride channels from kidney and trachea. Science 1989;244:1469–1472.

[4] Landry D, Sullivan S, Nicolaides M, Redhead C, Edelman A, Field M, Al-Awqati Q, Edwards J. Molecular cloning and characterization of p64, a chloride channel protein from kidney microsomes. J Biol Chem 1993;268:14948–14955.

[5] Redhead C, Sullivan SK, Koseki C, Fujiwara K, Edwards JC. Subcellular distribution and targeting of the intracellular chloride channel p64. Mol Biol Cell 1997;8:691–704.

[6] Warton K, Tonini R, Fairlie WD, Matthews JM, Valenzuela SM, Qiu MR, Wu WM, Pankhurst S, Bauskin AR, Harrop SJ, Campbell TJ, Curmi PM, Breit SN, Mazzanti M. Recombinant CLIC1 (NCC27) assembles in lipid bilayers via a pH-dependent two-state process to form chloride ion channels with identical characteristics to those observed in Chinese hamster ovary cells expressing CLIC1. J Biol Chem 2002;277:26003–26011.

[7] Fernandez-Salas E, Sagar M, Cheng C, Yuspa SH, Weinberg WC. p53 and tumor necrosis factor alpha regulate the expression of a mitochondrial chloride channel protein. J Biol Chem 1999;274:36488–36497.

[8] Howell S, Duncan RR, Ashley RH. Identification and characterisation of a homologue of p64 in rat tissues. FEBS Lett 1996;390:207–210.

[9] Duncan RR, Westwood PK, Boyd A, Ashley RH. Rat brain p64H1, expression of a new member of the p64 chloride channel protein family in endoplasmic reticulum. J Biol Chem 1997;272:23880–23886.

[10] Ashley RH. Activation and conductance properties of ryanodine-sensitive calcium channels from brain microsomal membranes incorporated into planar lipid bilayers. J Membr Biol 1989;111:179–189.

[11] Shorning BY, Wilson DB, Meehan RR, Ashley RH. Molecular cloning and developmental expression of two Chloride Intracellular Channel (CLIC) genes in *Xenopus laevis*. Dev Genes Evol 2003;213:514–518.

[12] Littler DR, Assaad NN, Harrop SJ, Brown LJ, Pankhurst GJ, Luciani P, Aguilar MI, Mazzanti M, Berryman MA, Breit SN, Curmi PM. Crystal structure of the soluble form of the redox-regulated chloride ion channel protein CLIC4. FEBS J 2005;272:4996–5007.

[13] Harrop SJ, DeMaere MZ, Fairlie WD, Reztsova T, Valenzuela SM, Mazzanti M, Tonini R, Qiu MR, Jankova L, Warton K, Bauskin AR, Wu WM, Pankhurst S, Campbell TJ, Breit SN, Curmi PM. Crystal structure of a soluble form of the intracellular chloride ion channel CLIC1 (NCC27) at 1.4-Å resolution. J Biol Chem 2001;276:44993–45000.

[14] Dulhunty A, Gage P, Curtis S, Chelvanayagam G, Board P. The glutathione transferase structural family includes a nuclear chloride channel and a ryanodine receptor/calcium release channel modulator. J Biol Chem 2001;276:3319–3323.

[15] Suginta W, Karoulias N, Aitken A, Ashley RH. Chloride intracellular channel protein CLIC4 (p64H1) binds directly to brain dynamin I in a complex containing actin, tubulin and 14-3-3 isoforms. Biochem J 2001;359:55–64.

[16] Berryman MA, Goldenring JR. CLIC4 is enriched at cell-cell junctions and colocalizes with AKAP350 at the centrosome and midbody of cultured mammalian cells. Cell Motil Cytoskel 2003;56:159–172.

[17] Chuang JZ, Milner TA, Zhu M, Sung CH. A 29 kDa intracellular chloride channel p64H1 is associated with large dense-core vesicles in rat hippocampal neurons. J Neurosci 1999;19:2919–2928.

[18] Edwards JC. A novel p64-related Cl^- channel: subcellular distribution and nephron segment-specific expression. Am J Physiol 1999;276:F398–F408.

[19] Proutski I, Karoulias N, Ashley RH. Overexpressed Chloride Intracellular Channel protein CLIC4 (p64H1) is an essential molecular component of novel plasma membrane anion channels. Biochem Biophy Res Comm 2002;297:317–322.

[20] Fernandez-Salas E, Suh KS, Speransky VV, Bowers WL, Levy JM, Adams T, Pathak KR, Edwards LE, Hayes DD,

Cheng C, Steven AC, Weinberg WC, Yuspa SH. mtCLIC/CLIC4, an organellular chloride channel protein, is increased by DNA damage and participates in the apoptotic response to p53. Mol Cell Biol 2002;22:3610–3620.

[21] Qiu M. Functional and molecular aspects of ion channels in macrophages. PhD Thesis, University of New South Wales, Sydney, Australia; 2003.

[22] Dulhunty AF, Pouliquin P, Coggan M, Gage PW, Board PG. A recently identified member of the glutathione transferase structural family modifies cardiac RyR2 substate activity, coupled gating and activation by Ca^{2+} and ATP. Biochem J 2005;390:333–343.

[23] Singh H, Ashley RH. Redox regulation of CLIC1 by cysteine residues associated with the putative channel pore. Biophys J 2006;90:1628–1638.

[24] Jez JM, Ferrer JL, Bowman ME, Dixon RA, Noel JP. Dissection of malonyl-coenzyme A decarboxylation from polyketide formation in the reaction mechanism of a plant polyketide synthase. Biochem 2000;39:890–902.

[25] Findlay HE, McClafferty H, Ashley RH. Surface expression, single-channel analysis and membrane topology of recombinant *Chlamydia trachomatis* Major Outer Membrane Protein. BMC Microbiol 2005;5:5.

[26] Hayman KA, Spurway TS, Ashley RH. Single anion channels reconstituted from cardiac mitoplasts. J Membr Biol 1993;136:181–190.

[27] Berry KL, Bulow HE, Hall DH, Hobert O. A *C. elegans* CLIC-like protein required for intracellular tube formation and maintenance. Science 2003;302:2134–2137.

[28] Board PG, Coggan M, Chelvanayagam G, Easteal S, Jermiin LS, Schulte GK, Danley DE, Hoth LR, Griffor MC, Kamath AV, Rosner MH, Chrunyk BA, Perregaux DE, Gabel CA, Geoghegan KF, Pandit J. Identification, characterization, and crystal structure of the omega class glutathione transferases. J Biol Chem 2000;275:24798–24806.

[29] Valenzuela SM, Martin DK, Por SB, Robbins JM, Warton K, Bootcov MR, Schofield PR, Campbell TJ, Breit SN. Molecular cloning and expression of a chloride ion channel of cell nuclei. J Biol Chem 1997;272:12575–12582.

[30] Tulk BM, Schlesinger PH, Kapadia SA, Edwards JC. CLIC-1 functions as a chloride channel when expressed and purified from bacteria. J Biol Chem 2000;275:26986–26993.

[31] Valenzuela SM, Mazzanti M, Tonini R, Qiu MR, Warton K, Musgrove EA, Campbell TJ, Breit SN. The nuclear chloride ion channel NCC27 is involved in regulation of the cell cycle. J Physiol 2000;529:541–552.

[32] Tonini R, Ferroni A, Valenzuela SM, Warton K, Campbell TJ, Breit SN, Mazzanti M. Functional characterization of the NCC27 nuclear protein in stable transfected CHO-K1 cells. FASEB J 2000;14:1171–1178.

[33] Tulk BM, Kapadia S, Edwards JC. CLIC1 inserts from the aqueous phase into phospholipid membranes, where it functions as an anion channel. Am J Physiol 2002;282:C1103–C1112.

[34] Littler DR, Harrop SJ, Fairlie WD, Brown LJ, Pankhurst GJ, Pankhurst S, DeMaere MZ, Campbell TJ, Bauskin AR, Tonini R, Mazzanti M, Breit SN, Curmi PM. The intracellular chloride ion channel protein CLIC1 undergoes a redox-controlled structural transition. J Biol Chem 2004;279:9298–9305.

[35] Novarino G, Fabrizi C, Tonini R, Denti MA, Malchiodi-Albedi F, Lauro GM, Sacchetti B, Paradisi S, Ferroni A, Curmi PM, Breit SN, Mazzanti M. Involvement of the intracellular ion channel CLIC1 in microglia-mediated beta-amyloid-induced neurotoxicity. J Neurosci 2004;24:5322–5330.

[36] Ramachandran R, Tweten RK, Johnson AE. Membrane-dependent conformational changes initiate cholesterol-dependent cytolysin oligomerization and intersubunit beta-strand alignment. Nat Struct Mol Biol 2004;11:697–705.

[37] Tweten RK, Parker MW, Johnson AE. The cholesterol-dependent cytolysins. Curr Top Microbiol Immunol 2001;257:15–33.

[38] van Meer G. Lipids of the Golgi membrane. Trends Cell Biol 1998;8:29–33.

[39] Ho C, Slater SJ, Stagliano B, Stubbs CD. The C1 domain of protein kinase C as a lipid bilayer surface sensing module. Biochem 2001;40:10334–10341.

[40] Heiss NS, Poustka A. Genomic structure of a novel chloride channel gene, CLIC2, in Xq28. Genomics 1997;45:224–228.

[41] Franciolini F, Nonner W. Anion-cation interactions in the pore of neuronal background chloride channels. J Gen Physiol 1994;104:711–723.

[42] Franciolini F, Nonner W. A multi-ion permeation mechanism in neuronal background chloride channels. J Gen Physiol 1994;104:725–746.

[43] Berry K, Hobert O. Mapping functional domains of Chloride Intracellular Channel (CLIC) proteins *in vivo*. J Mol Biol 2006;359:1316–1333.

[44] Brelidze TI, Niu X, Magleby KL. A ring of eight conserved negatively charged amino acids doubles the conductance of BK channels and prevents inward rectification. Proc Natl Acad Sci USA 2003;100:9017–9022.